

# A new species of rake-legged mite, *Caeculus cassiopeiae* (Prostigmata, Caeculidae), from Canada and a systematic analysis of its genus

Jared Bernard<sup>1,2</sup>, Lisa M. Lumley<sup>1</sup>, Matthias Buck<sup>1</sup>, Tyler P. Cobb<sup>1</sup>

**1** *Invertebrate Zoology, Royal Alberta Museum, 9810 103A Avenue NW, Edmonton, Alberta T5J 0G2, Canada* **2** *Plant & Environmental Protection Sciences, University of Hawaii-Mānoa, 3050 Maile Way, Honolulu, HI 96822, USA*

Corresponding author: Jared Bernard ([bernardj@hawaii.edu](mailto:bernardj@hawaii.edu))

---

Academic editor: V. Pesic | Received 24 November 2019 | Accepted 2 March 2020 | Published 13 April 2020

---

<http://zoobank.org/1BB22C60-3A79-43E1-A591-C92EAC8B430F>

---

**Citation:** Bernard J, Lumley LM, Buck M, Cobb TP (2020) A new species of rake-legged mite, *Caeculus cassiopeiae* (Prostigmata, Caeculidae), from Canada and a systematic analysis of its genus. ZooKeys 926: 1–23. <https://doi.org/10.3897/zookeys.926.48741>

---

## Abstract

The genus *Caeculus* Dufour (Prostigmata, Caeculidae) contains 19 previously described species, most of which are found in North America, and for which no comprehensive phylogenetic treatment exists. Here, one new species from Alberta, Canada, is described: *Caeculus cassiopeiae* Bernard & Lumley, **sp. nov.**, and another caeculid known to be present in Canada is documented. The new species is characterized within the genus with a character state matrix, from which an updated key is produced. A systematic analysis of all 20 species based on morphological and geographical distribution traits obtained from literature represents the first phylogenetic review of the genus.

## Keywords

Acari, character state matrix, comparative morphology, phylogeny, Trombidiformes

## Introduction

The Caeculidae contains 108 previously described species of large (750–3000 µm) prostigmatic mites in seven genera distributed worldwide, with 19 species in the genus *Caeculus* Dufour (Walter et al. 2009; Taylor et al. 2013; Mangová et al. 2014; Ott and

Ott 2014; Taylor 2014; Fuangarworn and Butcher 2015; Rivas et al. 2016; Per et al. 2017; Porta et al. 2019). Employing the spiniform setae on legs I for which they are called rake-legged mites, caeculids are ambush predators of small arthropods including collembolans (Otto 1993). They do so camouflaged against rocky or sandy substrates in arid environments (Coineau 1974). Other than morphological reviews by Vitzthum (1933), Grandjean (1944), and Coineau (1974), a dichotomous key by Franz (1952), and original species descriptions, Caeculidae have not been widely collected or studied. Hence, a phylogenetic assessment of *Caeculus* has not yet been attempted.

In July 2014, we collected two specimens in yellow pan traps in Medicine Hat, Alberta, Canada. They represent a new species, *Caeculus cassiopeiae* sp. nov., described below. This record increases the number of known Canadian caeculids to two species. Evert E. Lindquist (Canadian National Collection, Ottawa, Ontario, Canada) collected the other species in Alberta's Writing-on-Stone Provincial Park in 1978, and the same species in Alberta's Waterton Lakes National Park in 1980, which are the only previously known collections from Canada and are deposited in the CNCI. He identified this species only to *Caeculus* and did not publish it, but herein we identify it as *C. cremnicolus* Enns. The only published record of caeculoids in Canada is by Lindquist et al. (1979), who listed at least one unidentified caeculid species in southern inland British Columbia based on personal communication with Valin G. Marshall (Canadian Forest Service, Victoria, British Columbia, Canada), but without collection or further identification information. Although Lindquist et al. (1979) estimated the potential discovery of 2 additional undetected species based on records in the United States, the updated catalogue of Canadian Acari still lists only one previously recorded caeculid species (Beaulieu et al. 2019).

We constructed a character state matrix to compare *C. cassiopeiae* sp. nov. to the descriptions of all other known species of *Caeculus*. In the absence of molecular data, we used the matrix as a phenotypic platform for a phylogenetic analysis of the genus, which illuminates the congeners most closely related to the new species, and provides a springboard for further assessment of the genus.

## Materials and methods

On 27 July 2014 in Medicine Hat, Alberta, Canada, we collected two female caeculid specimens in yellow pan traps filled with soapy water (Marshall et al. 1994), which for two days were placed on both the arid SW slope of a coulee (glacially formed from sandstone and clay) and on the adjacent plain dominated by non-native crested wheat grass (*Agropyron cristatum* (L.) Gaertner) and alfalfa (*Medicago sativa* L.). We revisited the same locality on June 26, 2017 and using a paintbrush collected additional specimens, which were found only on open, exposed soil surfaces of the arid SW slope during the hottest part of the day (13:45–15:30,  $\geq 32$  °C). The soil surfaces had a thin hardened crust, possibly created by drying after rainfall.

According to the Köppen-Geiger climate classification system, Medicine Hat is a cold semi-arid steppe (*BSk*) (Peel et al. 2007) with a mean annual precipitation of

322.6 mm and a mean annual temperature of 6.1 °C (NCDIA 2017). Based on geological maps of the region (Berg and McPherson 2005) and the presence of well-rounded gravel and fine-grained sediment, the surficial geology is consistent with Quaternary alluvium. Medicine Hat furthermore has brown chernozem soil by the Canadian classification (Fuller 2010; NSBD 2017), synonymous with ustic mollisol in the USDA soil taxonomy (Haynes 1998).

After photographing the specimens collected in 2014 with a K2 DistaMax long-distance microscope (Infinity Photo-Optical, Boulder, Colorado, USA), we stored one in 95% ethyl alcohol (EtOH) and cleared the other in 85% lactic acid (Thermo Fisher Scientific, Waltham, Massachusetts, USA) and dissected it before mounting on a slide in a solution of 1.66 g polyvinyl alcohol, 10 mL lactic acid, 1 mL glycerol, and 10 mL distilled water (produced by Bioquip, Rancho Dominguez, California, USA) for analysis under dissection and compound microscopes, both of which contributed to creating the free-hand illustrations. With the 2017 specimens, we kept two alive for observation and stored the remainder in 95% EtOH.

In describing the idiosomal morphology of the new species, we followed the terminology outlined by Coineau (1974), which is based on the model of idiosomal divisions by Grandjean (1969) and other aspects of caeculid morphology described by Grandjean (1944). Notation for setae follows Coineau (1964, 1967a, b, 1969, 1974). As described by Coineau (1964), the eponymous characteristic of rake-legged mites is their elongated thickened spiniform leg setae, which are known as “rake” setae and are labelled as such herein.

To compare our specimens to other congeners using established criteria, we mined morphological and geographical distribution data from all known publications on *Caeculus* to construct a standard categorical character state matrix of the female of 23 taxa in Mesquite version 3.2 (Maddison and Maddison 2017), including all 20 species of *Caeculus* and three species of *Neocaeculus* Coineau (Table 1). We incorporated additional chaetotactic data into the matrix for *C. echinipes* Dufour from Jacot (1936), and for both it and *C. americanus* Banks from Coineau (1974). The resulting matrix includes mostly characters that are clearly described and/or illustrated in the species descriptions. Missing data are denoted with a “?” and uncertainty between states is characterized with a “/”, following the notation used by Maddison and Maddison (2017). In rare circumstances we inferred characters that were consistently mentioned in the descriptions. For instance, because Mulaik (1945) noted tarsal bothridial setae for some species but not for others, we reasoned that he would mention the trait if present; thus if illustrations or text did not include a trait that had been described in other species by the same author, we treated the trait as absent. The matrix did not include information on ecology or internal anatomy because this was lacking in publications.

We conducted a parsimony analysis of these phenotypes with PAUP\* version 4.0β10 (Swofford 2000), which involved a heuristic search with a tree-bisection-reconstruction branch-swapping algorithm for 5000 replicates. If the maximum branch length was zero, we set branches to collapse. The setation of *N. imperfectus* Taylor, Gunawardene & Kinnear resembles that described by Coineau (1974) as the holotrichous setal complement of Caeculidae, so we designated this species as the

**Table 1.** Standard categorical character state matrix for *Caeculus* females, as well as three outgroup taxa, used for cladistic analysis. Polymorphism is denoted by “&”, uncertainty by “/”, missing data by “?” and inapplicable data by “-”. “+” signifies a size character not included in phylogenetic assessment.

Taxon	1	2	3	4	5	6	7	8	9	10	11	12	13	14	15	16	17	18	19	20	21	22	23	24	25	
<i>Caeculus americanus</i> Banks, 1899	2	2	1	2	0	0	0	0	1	0	0	1	1	0	0	1	0&1&2	0&1	0&1&2	0&1	1&2	0&1	?	?	?	
<i>Caeculus aeneus</i> Mulaik, 1945	1	1	0	1	0	0	0	0	1	0	0	1	1	1	1	1	2	0	2	0	0	0	1	?	3&4	3
<i>Caeculus calceolus</i> Mulaik, 1945	2	0/1	0	1	0	0	0	0	0	0	0	0	0	0	0	1	1	1	0	0	0	0	1	?	3	3
<i>Caeculus cassiponae</i> Bernard & Lumley, sp. nov.	3	2	0&1	2	0	0	0	0	1	1	0&1	0&1	1	0&1	1	1	2	0&1	2	1	1	1	1	6	4	2
<i>Caeculus clavatus</i> Banks, 1905	1	1	?	?	0	0	?	?	?	?	?	?	?	?	?	1	?	?	?	?	?	?	?	?	?	?
<i>Caeculus crennicolus</i> Enns, 1958	3	1	1	2	0	0	0	0	0&1	0	1	1&2	1	0&1	0	1	1&2	0&1	2	1	0	1	2	4	2	2
<i>Caeculus crosleyi</i> Hagan, 1985	1	1	1	3	0	0	0	1	1	0	1	0	2	1&2	1	3	0	5	0	0	0	1	0	4	3	3
<i>Caeculus domtheae</i> Mulaik, 1945	2	3	0	0	0	0	0	0	0	0	0	0	0	0	1	1	0	2	0	0	0	0	?	?	?	?
<i>Caeculus echinipes</i> Dufour, 1832	0	1	1	2	0	0	0	0&1	0	0&1	0&1	1	1	0&1	1	1&2	0&1	3	0	1	0	4	3	2	3	2
<i>Caeculus gertschi</i> Mulaik, 1945	2	1	1	1	0	0	0	0	0	0	0	0	0	0	1	1	1	2	0	0	0	1	5	2	3	2
<i>Caeculus harvii</i> Mulaik & Allred, 1954	2	1	2	1	0	0	0	0	0	0	0	0	0	0	1	1	0	1	1	1	1	1	?	?	?	?
<i>Caeculus hypopachus</i> Mulaik, 1945	2	1	0	1	1	0	0	0	0	0	0	0	0	0	1	1	1	1	0	0	0	0	?	?	?	?
<i>Caeculus janatae</i> Higgins & Mulaik, 1957	2	1	1	1	0	0	0	0	0	0	0	0	1	0	0	1	1	0&1	2	0	0	1	5	2&3&4&5	2&3	2
<i>Caeculus kernulus</i> Mulaik, 1945	2	0	0	1	0	1	0	0	0	0	0	0	0	0	1	0	2	0	2	1	1	0	?	?	?	?
<i>Caeculus kwanzi</i> Coineau, 1974	4	1	1	2	0	0	0	1	0	1	1	1	1	1	1	1	2	0	4	1	0	1	4	3	2	2
<i>Caeculus lewisi</i> McDaniel & Boc, 1990	3	3	0	2	0	0	0	0	0&1	0&1	0	0&1	0	0	0&1	1	1&2	0&1	3	1	0	1	5	3&4	2	2
<i>Caeculus mariae</i> Higgins & Mulaik, 1957	4	1	1	1	0	0	0	1	0	1	0	1	1	1	0	1	1	0	2	0	0	1	?	?	?	?
<i>Caeculus pettiti</i> Nevin, 1943	1	1	1	1	0	0	0	0	0&1	0&1	0	0&1	1&2	1	1&2	0	3	0&1	2&3	0&1	0	1	5	4	2	2
<i>Caeculus tipus</i> Mulaik, 1945	2	2	0&1	1&2	0	0	0	0	1	0	0&1	0&1	1	0	1	1	1&2	0&1	0&1&2&3	0&1	0	1	1	0&1&2	2	2
<i>Caeculus valentinus</i> Mulaik, 1945	2	2	0&1	2	0	0	0	0	2	0	0	1	1	0	1	2	0	1	1	0	1	0	1	?	3	3
<i>Neocaculus imperfectus</i> Taylor et al., 2013	5	1	1	0	0	0	0	0	0	0	0	0	0	0	0	0	1	0	0	0	0	1	3	3	1	1
<i>Neocaculus kimmeae</i> Taylor, 2014	5	1	1	0	1	0	0	0	0	0	0	0	0	0	0	0	1	0	1	1	1	1	3	2	1	1
<i>Neocaculus nudomates</i> Taylor, 2014	5	1	1	0	0	0	0	0	0	0	0	0	0	0	0	0	1	1	0	0	1	1	4	3	2	2

Table 1. Continued.

Taxon	26	27	28	29	30	31	32	33	34	35	36	37	38	39	40	41	42	43	44	45	46	47	48	49	50	51†
<i>Caeculus americanus</i> Banks, 1899	?	?	1	0	?	0	0	0	0/1	2	0/1	3	2	?	2	0	3	?	?	?	?	1	0	0	1	2
<i>Caeculus archeri</i> Mulaik, 1945	?	?	0	0	0	0	0	0	0	2	1	1	3	0	?	0	?	0	0	1	1	0	0	0	1	2
<i>Caeculus calachius</i> Mulaik, 1945	?	?	0	0	0	0	0	?	1	3	1	2	2	?	0	0	3	0	0	0	1	0	0	0	1	2
<i>Caeculus castiopeiae</i> sp. nov. Bernard & Lumley	1	1	2	0	1&2	0	0	0	1	2	1	3	4	0	3	0	2&3	0	0	1	1	0	0	0	1	2
<i>Caeculus clavatus</i> Banks, 1905	?	?	0	0	2	1	0	1	0	1	1	1	2	0	?	0	?	?	?	?	?	0	0	0	1	1
<i>Caeculus crennicolus</i> Enns, 1958	0	0	0	0	0	0	0	0	1	1	1	0	1&2	0	3	0	0	0	0	1	1	1	0	0	1	2&3
<i>Caeculus crosleyi</i> Hagan, 1985	1	0	0	0	0&1	0	0	0	0	1	1	0	1/2	0	3	0	0	1	1	1	1	1	0	0	1	0
<i>Caeculus dorothae</i> Mulaik, 1945	?	?	2	0	3	0	0	0	?	2	?	4	5	?	3	0	3	0	0	0	0	0	0	1	0	1&2
<i>Caeculus echinipes</i> Dufour, 1832	0	0	0	0	0	0	0	0	1	2	2	1	3	0	1	0	?	1	1	1	1	1	0	0	1	3
<i>Caeculus gerschi</i> Mulaik, 1945	1	0	1	1	1	0	0	?	2	?	2	?	?	?	1	0	1	0/1	0/1	0/1	0/1	0	0	0	1	1
<i>Caeculus hardyi</i> Mulaik & Allred, 1954	?	0	1	0	0	0	0	0	0	1	0	1	0	1	?	0	?	0	0	0	0	0	0	0	1	1&2
<i>Caeculus hypopachus</i> Mulaik, 1945	?	0	1	1	1	0	0	?	1	?	?	2	?	?	?	0	?	0	0	0	0	1	0	0	1	1
<i>Caeculus janetae</i> Higgins & Mulaik, 1957	1	0	0	0	1	0	0	0	0	3	0	4	0	0	?	0	?	0	0	0	0	0	0	0	1	1&2
<i>Caeculus kernulus</i> Mulaik, 1945	?	0	0	0	2	0	0	0	0	2	0	1	3	0	1	1	0	0	0	1	1	1	0	0	1	1
<i>Caeculus kranzsi</i> Coineau, 1974	0	0	?	0	?	?	?	?	?	?	?	?	?	?	?	0	?	?	?	?	?	?	0	0	0	3
<i>Caeculus lewisi</i> McDaniel & Boc, 1990	2	1	2	0	1&2	0	0	0	0	2	0&1	2&3	3&4	0	0	0	1&2	0	0	1	1	1	0	0	0	1&2
<i>Caeculus mariae</i> Higgins & Mulaik, 1957	?	0	0	0	0	0	0	?	1	?	1	?	?	2	2	0	0	0	0	0	0	0	0	0	1	0
<i>Caeculus pettiti</i> Nevin, 1943	2	1	2	0	0	0	0	0	0	1	1	1	3	0	3	0	0	0	0	0	0	1	0	0	1	2
<i>Caeculus ripus</i> Mulaik, 1945	1	0	1	0	1	0	0	0	1	1	2	4	3	2	0	2	0	2	0	1	1	0	0	0	1	2
<i>Caeculus valentini</i> Mulaik, 1945	?	0	2	0	2	0	0	?	2	4	3	4	?	2	0	2	0	2	0	1	1	0	0	0	1	2
<i>Neoaeculus imperfectus</i> Taylor et al., 2013	2	0	0	1	4	0	-	-	1	2	3	1	3	0	2	1	3	0	0	1	1	0	0	1	0	1
<i>Neoaeculus kimmeae</i> Taylor, 2014	1	0	3	0	5	1	-	-	0	1&2	1	1	4	0	2	0	2	0	0	1	1	0	0	1	0	1
<i>Neoaeculus nudonates</i> Taylor, 2014	1	0	0	0	1	1	-	-	1	1	1	0	2	0	1	0	0	0	0	1	1	1	0	1	0	0

**Table 2.** Character states of *Caeculus* species (females) used for morphological comparison and cladistic analysis. Row number aligns to column number in Table 1. A setal pair refers to two setae in symmetry on either side of the mid-sagittal plane. An excluded seta is denoted by “excl.” Size character is excluded from analysis.

Character	States
1. Distribution	0 = Old World, 1 = SE North America, 2 = SW North America, 3 = N Central North America, 4 = NW North America, 5 = Western Australia
2. Aspidosomal Pa setae	0 = absent, 1 = 1 pair, 2 = 2 pairs, 3 = 3 pairs
3. Aspidosomal Pm setae	0 = absent, 1 = 1 pair, 2 = 2 pairs
4. Aspidosomal Pp setae	0 = 1 pair, 1 = 2 pairs, 2 = 3 pairs, 3 = 5 pairs
5. Anterior margin of aspidosoma acuminate	0 = no, 1 = yes
6. Anterior margin of aspidosoma notched	0 = no, 1 = yes
7. Centrodorsal opisthosoma a setae (excl. as)	0 = 1 pair, 1 = 2 pairs
8. Unpaired medial as seta present	0 = no, 1 = yes
9. Centrodorsal opisthosoma b setae (excl. bs)	0 = 1 pair, 1 = 2 pairs, 2 = 3 pairs
10. Unpaired medial bs seta present	0 = no, 1 = yes
11. Centrodorsal opisthosoma c setae (excl. cs)	0 = 1 pair, 1 = 2 pairs
12. Unpaired medial cs seta present	0 = no, 1 = yes
13. Laterodorsal opisthosoma a setae	0 = 1 seta, 1 = 2 setae, 2 = 3 setae
14. Laterodorsal opisthosoma b setae	0 = 1 seta, 1 = 2 setae, 2 = 3 setae
15. Laterodorsal opisthosoma c setae	0 = 1 seta, 1 = 2 setae, 2 = 3 setae
16. Mediodorsal opisthosomal sclerites fused	0 = no, 1 = yes
17. Mediodorsal opisthosoma d setae (excl. ds)	0 = 1 pair, 1 = 2 pairs, 2 = 3 pairs, 3 = 4 pairs
18. Unpaired medial ds seta present	0 = no, 1 = yes
19. Posterior opisthosomal e setae (excl. es)	0 = 1 pair, 1 = 2 pairs, 2 = 3 pairs, 3 = 4 pairs, 4 = 5 pairs, 5 = 8 pairs
20. Unpaired medial es seta present	0 = no, 1 = yes
21. Pluriposterior sclerite h setae (excl. hs)	0 = absent, 1 = 1 pair, 2 = 2 pairs
22. Unpaired medial hs seta present	0 = no, 1 = yes
23. Aggenital + ventral sclerite setae	0 = 2 pairs, 1 = 4 pairs, 2 = 6 pairs, 3 = 8 pairs, 4 = 9 pairs, 5 = 10 pairs, 6 = 12 pairs
24. Progenital valve setae	0 = 3 pairs, 1 = 4 pairs, 2 = 5 pairs, 3 = 6 pairs, 4 = 7 pairs, 5 = 8 pairs
25. Adanal setae	0 = absent, 1 = 1 pair, 2 = 2 pairs, 3 = 3 pairs
26. Pseudanal Ps setae	0 = 2 pairs, 1 = 3 pairs, 2 = 4 pairs
27. Unpaired medial seta posterior to anus	0 = no, 1 = yes
28. Trochanter I anterolateral setae	0 = 1 seta, 1 = 2 setae, 2 = 3 setae, 3 = 4 setae
29. Trochanter I anterolateral setal shape	0 = clavate, 1 = spiniform
30. Posterior/dorsal trochanter I setae	0 = 1 seta, 1 = 2 setae, 2 = 3 setae, 3 = 4 setae, 4 = 5 setae, 5 = 8 setae
31. Basifemur I anteroventral rake setal shape	0 = spiniform, 1 = subclavate
32. Telofemur I anteroventral rake setae	0 = 1 seta, 1 = 2 setae
33. Telofemur I anteroventral rake setal shape	0 = spiniform, 1 = subclavate
34. Femur I posteroventral rake setae	0 = absent, 1 = 1 seta
35. Genu I anteroventral rake/spiniform setae	0 = 1 seta, 1 = 2 setae, 2 = 3 setae, 3 = 5 setae
36. Genu I posteroventral rake setae	0 = absent, 1 = 1 seta, 2 = 2 setae, 3 = 3 setae, 4 = 4 setae
37. Tibia I anteroventral rake/spiniform setae	0 = 2 setae, 1 = 3 setae, 2 = 4 setae, 3 = 5 setae, 4 = 6 setae
38. Tibia I posteroventral rake/spiniform setae	0 = absent, 1 = 1 seta, 2 = 2 setae, 3 = 3 setae, 4 = 4 setae, 5 = 5 setae
39. Tarsus I anterior rake-like setae	0 = absent, 1 = 3 setae, 2 = 4 setae, 3 = 5 setae
40. Trochanter III anterolateral setae	0 = absent, 1 = 1 seta, 2 = 2 setae, 3 = 3 setae
41. Trochanter III anterolateral setal shape	0 = clavate, 1 = spiniform
42. Posterior/dorsal trochanter III setae	0 = 1 seta, 1 = 2 setae, 2 = 3 setae, 3 = 4 setae
43. Bothridial bt seta on tarsus I	0 = no, 1 = yes
44. Bothridial bt seta on tarsus II	0 = no, 1 = yes
45. Bothridial bt seta on tarsus III	0 = no, 1 = yes
46. Bothridial bt seta on tarsus IV	0 = no, 1 = yes
47. Dark sclerites on dorsal idiosoma in adults	0 = no, 1 = yes
48. Body encrusted with cemented particles	0 = no, 1 = yes
49. Tarsal claws unequal in size	0 = no, 1 = yes
50. Aspidosoma projecting anteriorly over gnathosoma in lateral view	0 = no, 1 = yes
51. Body length (mm)	0 = ≤ 0.90, 1 = 0.91 – 1.29, 2 = 1.30 – 1.59, 3 = 1.60 – 2.00

outgroup (but not the other *Neocaeculus* species) for our phylogenetic analysis. Note that the ingroup of this study includes only species currently in the genus *Caeculus* and excludes those that have been reassigned to other genera (reviewed in Taylor et al. 2013). We visualized the majority consensus tree with FigTree 1.4.3 (Rambaut 2012).

### Repositories (see Zhang 2018 for abbreviations)

**CNCI** Canadian National Collection of Insects, Arachnids and Nematodes, Ottawa, Ontario, Canada;

**PMAE** Royal Alberta Museum (formerly Provincial Museum of Alberta) Invertebrate Zoology Collection, Edmonton, Alberta, Canada.

### Abbreviations of morphological characters

<b>AD</b>	adanal sclerite;	<b>IW</b>	idiosomal width;
<b>AG</b>	aggenital sclerite;	<b>PA</b>	palp;
<b>CH</b>	chelicera;	<b>PG</b>	progenital valve;
<b>IL</b>	idiosomal length;	<b>PS</b>	pseudanal sclerite.

### *Caeculus cassiopeiae* Bernard & Lumley, sp. nov.

<http://zoobank.org/BC876F53-B89C-4AEA-ABC7-EA8CA18B7F91>

Figures 1–4

**Material examined. Holotype.** CANADA • 1 ♀; Alberta, Medicine Hat, near Gas City Campground; 50°2.23'N, 110°43.56'W; elev. ca 700 m; 26–27 Jul. 2014; M. Buck leg.; yellow pan traps; arid SW slope and adjacent disturbed plain of *Agropyron cristatum* and *Medicago sativa*; det. J. Bernard and L. Lumley, 30 Aug. 2016; cleared in 85% lactic acid, dissected, and slide-mounted; PMAE M00019466.

**Paratype.** CANADA • 1 ♀; *ibid.*; stored in 95% EtOH; PMAE M00030967.

**Other material.** CANADA • 8 ♀♀; *ibid.*; 26 Jun. 2017; L. Lumley leg.; collected with paintbrush; hard dry soil surface; det. L. Lumley; stored in 95% EtOH; PMAE M00030972 to M00030979.

**Diagnosis.** The five *b* setae on the centrodorsal opisthosoma are arranged in an M, three pairs of *Pp* setae are aligned on the posterior third of the aspidosoma, and trochanter III has three setae along anterolateral surface.

**Female description** ( $N = 2$ , all measurements in micrometres,  $\mu\text{m}$ ).

**Idiosoma dorsum** (Figs 1–3). 1380–1592 = idiosomal length (*IL*); 1.920 × longer than greatest width (at level of posterior margin of mediodorsal opisthosomal sclerites) (718–829 = *IW*). Sclerites tawny with pale ridges, ochre to raw sienna between sclerites, translucent white setae (Fig. 1A). All clavate idiosomal setae barbed (Fig. 2C).

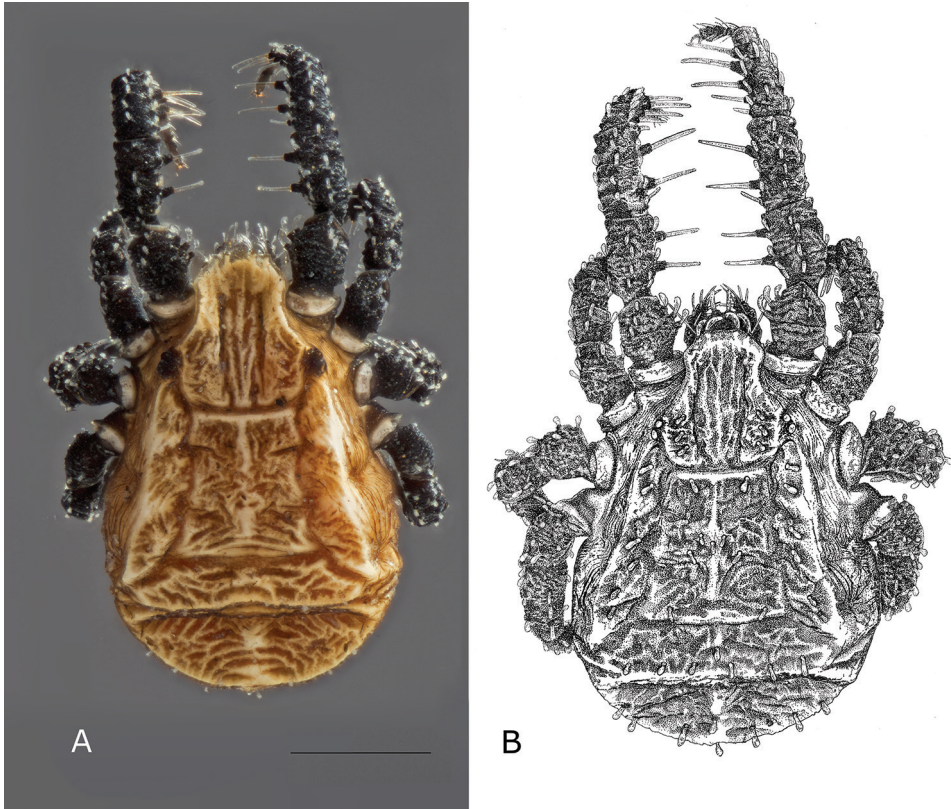


**Figure 1.** *Caeculus cassiopeiae* sp. nov., female **A** micrograph showing coloration **B** habitus illustrating cerotegument texture. Scale bar: 0.5 mm.

Rostral region with dark brown anteriorly projecting naso bearing one pair elongated clavate setae *Po* (74–94,  $\sim 0.054 \times IL$ ), one median eye immediately inferior to base of naso (Fig. 3A), one pair long, thickened attenuate bothridial seta *bo* (162–188,  $\sim 0.118 \times IL$ ) with barbed distal end (Fig. 3C), each inserted in anterolaterally projecting bothridium posterolaterad to median eye. Aspidosoma length 485–560 ( $0.352 \times IL$ ), width 425–491 ( $0.592 \times IW$ ) anterior to eyes, posterior margin of sclerite 309–357 ( $0.430 \times IW$ ); pronounced furrow along length of medial axis containing three or four shallow longitudinal reticulated ridges, anterior furrow width 135–157 ( $\sim 0.189 \times IW$ ), posterior furrow width 102–118 ( $\sim 0.142 \times IW$ ), posterior furrow depth 35–41 ( $\sim 0.050 \times IW$ ); two pairs procurved clavate *Pa* setae on anterior margin; none or one pair clavate *Pm* setae near corners of anterior margin; three pairs clavate *Pp* setae medial to eyes on posterior lateral margins, aligned parallel to mid-sagittal plane; area around eyes dark, posterior eyes  $1.077 \times$  diameter of anterior eyes (Fig. 2A), holotype with diminutive fourth *Pp* seta anterior to other three on right side. Centrodorsal opisthosomal sclerite trapezoidal, length 425–490 ( $0.308 \times IL$ ), posterior margin 477–552 ( $0.665 \times IW$ ); one pair clavate *a1* setae near anterior margin of sclerite midway between mid-sagittal

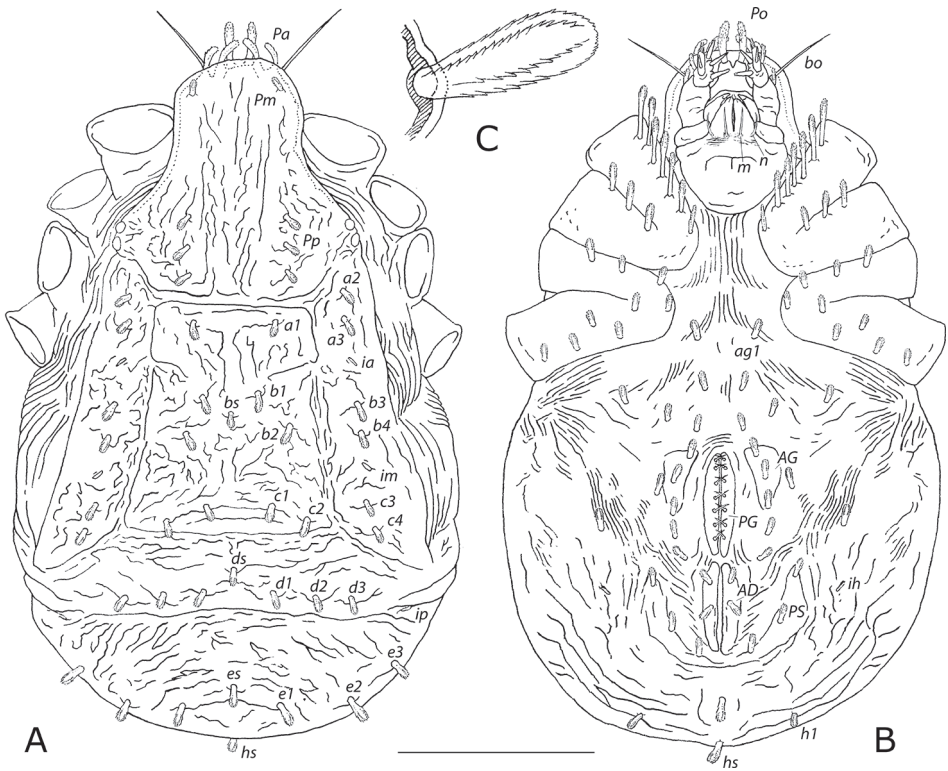


**Figure 2.** *Caeculus cassiopeiae* sp. nov., female idiosoma **A** dorsum **B** venter; *PG*, progenital valve; *AG*, aggenital sclerite; *AD*, adanal sclerite; *PS*, pseudanal sclerite **C** detail of *bs* seta, exemplifying typical clavate idiosomal seta. Scale bar: 0.5 mm (**A**, **B**).

plane and lateral margins; 2.5 pairs clavate *b* setae: *b1* pair anterior to mid-transverse plane and third of distance between mid-sagittal plane and lateral margins, *b2* pair posterior to mid-transverse plane and midway between mid-sagittal plane and lateral margins, one unpaired median *bs* seta present between anterior and posterior pairs, the five setae together forming M-shape; one or two pairs clavate *c* setae along posterior margin (sometimes *c1*, always *c2*) (Fig. 2A). Laterodorsal opisthosomal sclerites each bearing five or six clavate setae in tandem, two (*a2* and *a3*) near anterior margin, one or two *b* setae at middle of sclerite (always *b3*, sometimes *b4*), and two *c* setae near posterior margin (*c3* and *c4*); lyrifissure *ia* between *a3* and *b3*; lyrifissure *im* between *b4* and *c3* (Fig. 2A). Mediodorsal opisthosomal sclerites fused, bearing clavate *d1*, *d2*, and *d3* setal pairs, with or without unpaired median clavate *ds* seta slightly anterior to these; posterior opisthosomal sclerite length  $0.161 \times IL$ , bearing clavate *e1*, *e2*, and *e3* setal pairs and unpaired clavate *es* seta slightly anterior to these; lyrifissure *ip* near lateral margin between mediodorsal and posterior opisthosomal sclerites (Fig. 2A). Pluriposterior accessory sclerite bearing three clavate setae, including one unpaired median clavate *hs* seta (Fig. 2B).

***Idiosoma venter*** (Fig. 2B). Epimeres black to dark brown, cerotegument tawny, progenital valves dark sienna, aggenital sclerites raw sienna, adanal sclerites brown ochre, pseudanal sclerites raw sienna, translucent white setae. Epimeral setal formula (I–IV) 7-3-4-5. Epimeres I and II fused, anterior margin of epimere I bearing seven clavate setae, most proximal seta slightly less expanded than others and setae get progressively longer distally, distalmost  $\sim 76\text{--}120$  ( $\sim 0.071 \times IL$ ), epimere II with three clavate setae along anterior margin; epimeres III and IV fused (separate from I + II), epimere III with three clavate setae along anterior margin and one clavate seta midway along proximal margin, epimere IV with one clavate seta at anteroproximal margin, one clavate seta on midline a third epimeral length from proximal margin, and three clavate setae along posterior margin (Fig. 2B). Progenital valves (*PG*) each with seven smooth acuminate simple setae; aggenital sclerites (*AG*) each with three clavate setae; surrounding ventral cuticle bearing nine pairs of clavate setae, including pair *ag1* between epimeres IV (Fig. 2B). Adanal sclerites (*AD*) each bearing two clavate setae; pseudanal sclerites (*PS*) each with three clavate setae; one unpaired medial clavate seta posterior to anus; lyrifissure *ih* laterad to anterior pseudanal sclerite (Fig. 2B).

***Gnathosoma*** (Figs 2B, 3A, B). Palps black, chelicerae dark brown, subcapitulum black to dark sienna, translucent white setae. All clavate setae barbed, all simple setae smooth. Palps (*PA*) five-segmented, setal formula, trochanter-tarsus, solenidia  $\omega$  and eupathidia  $\zeta$  in brackets: 0-2-1-5-10( $1\omega+1\zeta$ ); trochanter without setae; femur bearing two dorsal clavate setae midway along length, with proximal seta a third length of distal seta; genu bearing longest subclavate seta on tubercle at distal laterodorsal margin; tibia bearing five setae: one proximal anteroventral barbed spiniform seta, one laterodorsal spiniform seta with barbed distal end, one proximal dorsal elongated clavate seta, one distal dorsal barbed spiniform seta, and one posterolateral clavate seta (Fig. 3A); well-developed tarsus (Fig. 3B) bearing three dorsal smooth acuminate spiniform setae, one elongated spiniform seta with barbed distal end midway on ventral surface, one elongated barbed subclavate seta midway along posterolateral surface slightly distal to a minute solenidion  $\omega$  recessed in large receptacle, one anterolateral smooth acuminate spiniform seta a third tarsal distance from distal end, one short smooth acuminate seta at distal posteroventral margin, two simple setae at distal end, and one eupathidium  $\zeta$  posterior to one minute smooth spiniform seta at distal ventral margin. Chelicerae (*CH*) each with fixed digit regressed to lobe and movable digit uncinata (Fig. 3A). Subcapitulum bearing two pairs of simple adoral *or* setae (Fig. 3A) and two pairs of elongated thickened acuminate simple hypostomal setae *m* and *n* along base of hypostome, *m* medial to and slightly longer ( $53\text{--}63$ ,  $\sim 0.039 \times IL$ ) than *n* (Fig. 2B).

***Legs*** (Fig. 4). Black with translucent white setae. All clavate setae barbed, all rake/spiniform setae smooth. Formulae of leg setae (including rake setae), trochanter-tarsus, tarsal bothridial setae *bt*, solenidia  $\varphi/\omega$ , eupathidia  $\zeta$ , microseta  $\varkappa$ , and famulus  $\varepsilon$  in brackets: leg I 5/6-8+3( $1\zeta$ )-21( $2\zeta$ )-22( $1\varphi+1\zeta+1\varkappa$ )-12( $1\omega+5\zeta+1\varepsilon$ ); leg II 5-10+4-16-17( $1\varphi$ )-14( $1\omega+1\varepsilon$ ); leg III 7-5+2( $2\zeta$ )-9( $1\zeta$ )-15( $1\varphi+1\zeta$ )-9( $1bt+1\zeta$ ); leg IV 7-2( $1\zeta$ )+3( $2\zeta$ )-9( $1\zeta$ )-13( $2\zeta$ )-13( $1bt+1\omega$ ). Leg I length 1301-1502 ( $\sim 0.943 \times IL$ ; Fig. 4A); trochanter I bearing three procurved clavate setae on tubercles along ante-

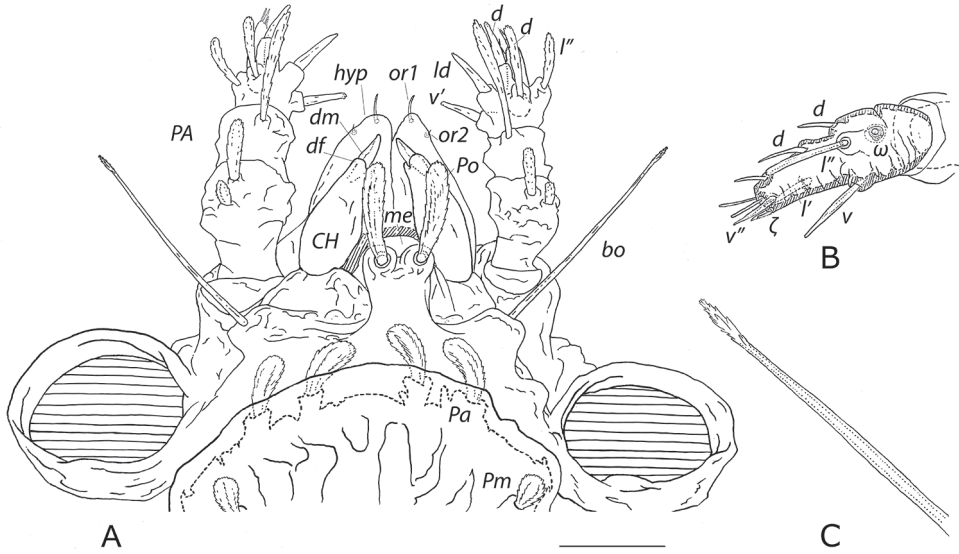


**Figure 3.** *Caeculus cassiopeiae* sp. nov., female **A** anterodorsal view of rostrum and gnathosoma **B** detail of palp tarsus **C** detail of distal bothridial seta. Abbreviations: *CH*, chelicera; *PA*, palp; *bo*, bothridial seta; *d*, dorsal; *df*, reduced fixed cheliceral digit; *dm*, movable cheliceral digit;  $\zeta$ , eupathidium; *hyp*, hypostome; *l''*, posterolateral; *ld*, laterodorsal; *me*, median eye; *Po*, naso seta;  $\omega$ , solenidium; *v'*, anteroventral; *v*, ventral; *v''*, posteroventral. Scale bar: 0.1 mm (**A**).

rolateral margin, two or three dorsal clavate setae; basifemur I with one rake seta on anteroventral margin and one rake seta on posteroventral surface; telofemur I with one rake seta on anteroventral margin and one eupathidium  $\zeta$  a third the length from distal end on posteroventral margin; genu I with two anteroventral rake setae, one elongated anteroventral subclavate seta near proximal margin aligned with rake setae, three anterolateral clavate setae, one short anterolateral eupathidium  $\zeta$  near distal margin, five clavate dorsal setae, five posterolateral setae with middle seta elongated subclavate and remainder clavate, one short eupathidium  $\zeta$  near distal posterolateral margin, five posteroventral setae with most proximal clavate, followed by one rake seta and three elongated subclavate setae; tibia I with four anteroventral rake setae, one elongated spiniform seta near proximal anteroventral margin in line with rake setae, four anterolateral clavate setae, five clavate dorsal setae, four posterolateral clavate setae, three posteroventral rake setae, and one spiniform seta on posteroventral surface proximad to rake setae, and the following three near distal anterolateral margin, most distal to least: one microseta  $\kappa''$ , one recessed solenidium  $\varphi$  in large receptacle, and one eupathidium  $\zeta$ ; tarsus I bearing four spiniform setae along each anterolateral, posterolateral, and posteroventral margins, one recessed solenidium  $\omega$  in large receptacle situated a third the tarsal length from distal end on dorsal surface (Fig. 4E), one famulus  $\varepsilon$  midway along anteroventral surface, and eupathidia  $\zeta$  at the following locations: proximal dorsal surface, midway along posterolateral margin, a tenth the tarsal length

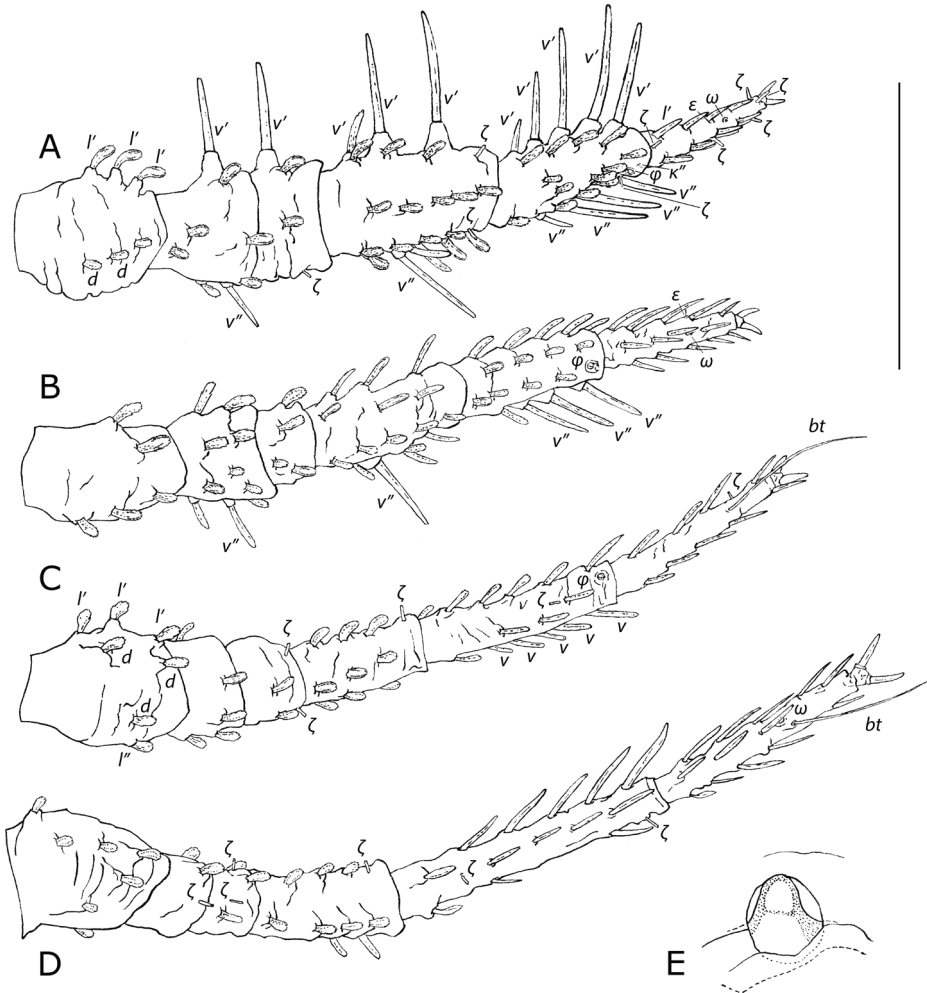


**Figure 4.** *Caeculus cassiopeiae* sp. nov., female **A–D** dorsal view of legs I–IV **E** detail of solenidium  $\omega$  on tarsus I. Scale bar: 0.5 mm (**A–D**). Abbreviations:  $\varepsilon$ , famulus;  $\zeta$ , eupathidium;  $x$ , microseta;  $\varphi$ , tibial solenidium;  $\omega$ , tarsal solenidium; *bt*, tarsal bothridial seta; *d*, dorsal; *l'*, anterolateral; *l''*, posterolateral; *v*, anteroventral; *v'*, ventral; *v''*, posteroventral.

from distal end on posteroventral margin, at distal anteroventral margin, and at distal anterolateral margin. Remaining clavate setation for leg I as in Fig. 4A. Chaetotaxy of other legs as in Fig. 4B–D. Basifemur II with one elongated barbed subclavate seta midway along posteroventral surface; genu II with one rake seta a third the distance along posteroventral surface; tibia II with three posteroventral rake setae, one dorsal solenidium  $\varphi$  near distal margin; tarsus II bearing one recessed solenidium  $\omega$  in large receptacle a third length from distal end on dorsal surface, slightly distal to one anteroventral famulus  $\varepsilon$  (Fig. 4B). Trochanter III with three anterolateral clavate setae and

two or three dorsal clavate setae; tibia III with one solenidion  $\varphi$  near distal margin on dorsal surface (Fig. 4C). Tarsi III and IV each with one elongated smooth slender bothridial seta  $bt$  a quarter of the length from distal margin on dorsal surface ( $125\text{--}145$  [ $-0.091 \times IL$ ] on tarsus III;  $143\text{--}166$  [ $-0.104 \times IL$ ] on tarsus IV); tarsus IV with one solenidion  $\omega$  a third the length from distal end on dorsal surface (Fig. 4C, D). Tarsal claws on all legs equal in size.

**Male** and immatures unknown.

**Etymology.** The  $b$  setal arrangement on the centrodorsal opisthosoma resembles the five-star constellation named for Cassiopeia, the vain wife of King Cepheus in Greek mythology. The constellation is also known as the “Celestial M” given its orientation to the horizon when it ascends in the night sky on its arc around Polaris, and is known as the “Celestial W” as it sets. Cassiopeia’s rise is most observable in the evenings during northern autumns. The genitive epithet abides by Articles 11.9.1.3 and 31.1.2 of the International Code of Zoological Nomenclature, and hence means “Cassiopeia’s rake-legged mite.”

**Ethology.** We observed individuals both walking and motionless with legs I positioned in a raptorial manner above the soil surface. A captive individual consumed a prostigmatan we collected from the same exposed soil.

### *Caeculus cremnicolus* Enns, 1958

Figure 5

**Material examined.** CANADA • 2 ♀♀, 1 deutonymph, 1 tritonymph; Alberta, Waterton Lakes National Park; 29 Jul. 1980; E.E. Lindquist leg.; under rocks in canyon bottom; det. J. Bernard, 4 Mar. 2015; slide-mounted; CNCI • 1 ♀, 2 deutonymphs, 1 tritonymph; Alberta, Writing-on-Stone Provincial Park; 12 Aug. 1978; E.E. Lindquist leg.; under rocks in hoodoo area [hoodoo = rock column formed by soft sediment eroding under harder sediment]; det. J. Bernard, 4 Mar. 2015; slide-mounted; CNCI.

**Previously known localities.** USA – Arkansas, Buffalo National River, Boen Gulf and Steel Creek; Petit Jean State Park (Skvarla et al. 2013) – Missouri, Baskett Wildlife Research and Education Area, Devil’s Backbone; Easley; Wilton (holotype) (Enns 1958).

**Diagnosis.** Distinguished by its unfused mediodorsal opisthosomal sclerites, by its dark sclerites in adult mites, and by three barbed clavate  $b$  setae on the centrodorsal opisthosoma arranged in a triangle.

### Phylogenetic analysis

The character state matrix contains 51 characters (Table 2), of which 27 are binary and the remainder occur in multiple states. The first 50 characters contributed to the phylogenetic analysis, and the last is a body length character that we retained only to



**Figure 5.** *Caeculus cremnicolus*, female. Micrograph of dorsal idiosoma, collected and slide mounted in 1978 by E.E. Lindquist. Scale bar: 0.5 mm.

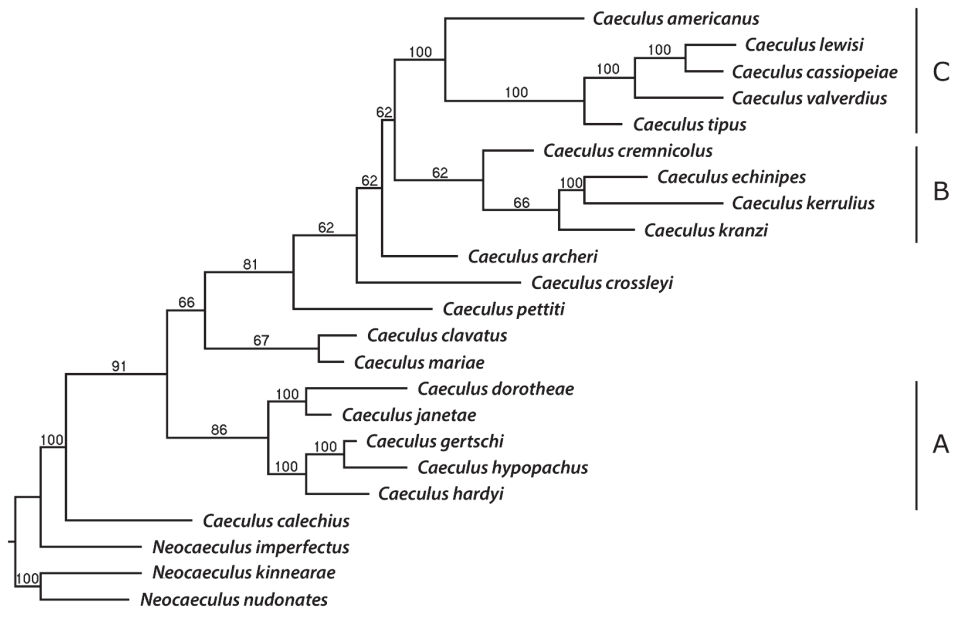


**Figure 6.** Phylogenetic 50% majority-rule consensus tree of *Caeculus* species based on character state matrix. Bootstrap values for 5000 replicates are above branches. Scale bar: 6.0 substitutions per phenotypic character.

improve the utility of the matrix as an identification tool but not used in the phylogeny. Among the characters used for phylogenetics, 88% were parsimony-informative. PAUP\* assessed  $5.659 \times 10^9$  arrangements in 5000 replicates for the cladistic analysis, generating a 50% majority-rule consensus tree from 722 retained trees (Fig. 6). The parsimony score of the best tree was 199.

The phylogeny reveals three morphological clades, termed A, B, and C (Fig. 6). *Caeculus calechius* Mulaik is basal within the genus; this taxon and a few other species fall out independently from the clades. Clade A characterizes *C. dorotheae* Mulaik as sister to *C. janetae* Higgins & Mulaik (100%), and *C. gertschi* Mulaik sister to *C. hypopachus* Mulaik (100%). Despite lower branch support for the B clade, there is high support for *C. kerrulius* Mulaik being sister to *C. echinipes* (100%). Sister to clade B is the strongly supported C clade, which represents *C. lewisi* McDaniel & Boe as sister to *C. cassiopeiae* sp. nov. (100%), and this pair is sister to *C. valverdius* Mulaik (100%).

## Discussion

### Taxonomy

Although *Caeculus cassiopeiae* sp. nov. is morphologically most similar to *C. lewisi* McDaniel & Boe and *C. valverdius* Mulaik, several noteworthy differences exist (Table 1). The dichotomous key below lists six traits that distinguish the new species from *C. lewisi*. Additionally, following Franz (1952) and McDaniel and Boe (1990), the new species keys to *C. valverdius*, yet several traits separate them as well: (i) *C. valverdius* bears six *b* setae on the centrodorsal opisthosomal sclerite, but five *b* setae are arranged in an M-shape in the new species; (ii) each laterodorsal opisthosomal sclerite has a single *c* seta in *C. valverdius* whereas the new species has two *c* setae; (iii) the posterior opisthosomal sclerite has five *e* setae in *C. valverdius* whereas the new species has seven; (iv) *C. valverdius* has six setae on each progenital valve whereas the new species has seven; (v) the adanal sclerites each have three setae in *C. valverdius* and two in the new species; (vi) genu I bears a single posteroventral rake seta in the new species whereas *C. valverdius* has four; and (vii) *C. valverdius* has two anterolateral setae on the proximal half of trochanter III, but the new species has three that are more evenly distributed along the length.

### Phylogenetic analysis

A few apomorphies denote the relationships within clade A; *C. dorotheae* and *C. janetae* both have six anteroventral rake setae on tibia I, which is a unique character. *Caeculus gertschi* and *C. hypopachus* each bear four rake setae in that location, a character shared with some members of clade B. Of the species in clade A, most are not recorded

as having tarsal bothridial setae *bt*, which occur in most other *Caeculus* as well as in the outgroups, indicating possible plesiomorphy for the rest of the genus. One exception is *C. gertschi* (Mulaik 1945). *Caeculus pettiti* Nevin and *C. mariae* Higgins & Mulaik also lack this trait, possibly resulting from homoplasy.

Aside from *C. krantzi* Coineau, the members of clade B exhibit dark dorsal idiosomal sclerites in adults, although this trait may be homoplastic as it recurs sporadically in the other clades and some taxa not in clades.

All members of the C clade possess five anteroventral rake setae on tibia I, except *C. tipus* Mulaik, which has four. However, McDaniel and Boe (1990) also describe a male and a nymph *C. lewisi* with four rake setae in this position. The species of clade C furthermore have four posteroventral rake setae on tibia I, although there are two such rake setae on *C. americanus*, basal in the clade. Rake seta number is regarded as more stable than other traits (Coineau 1974), so the above traits may be autapomorphies for the clade. Another potential apomorphy for clade C is two or three pairs of aspidosomal *Pa* setae, although Mulaik (1945) also describes *C. dorothae* with three pairs of *Pa*. All other congeners and all outgroup taxa have a single pair of *Pa* setae, which likely describes the ancestral state for the genus. Additionally, clade C species all have four to six centrodorsal opisthosomal *b* setae, also present in *C. crossleyi* Hagan and *C. pettiti*, so this may represent synapomorphy. The scarcity of autapomorphies in the topology likely reflects the variable nature of many traits in Caeculidae (Grandjean 1944; Coineau 1974).

### Key to adult *Caeculus* species (females)

- 1 Aspidosoma with 0 or 1 pair of *Pa* setae on anterior margin, or if more *Pa* setae then only 1 pair of *Pp* setae near posterior margin..... **2**
- Aspidosoma with  $\geq 2$  pairs of *Pa* setae on anterior margin, and  $\geq 2$  pairs of *Pp* setae near posterior margin..... **16**
- 2 Centrodorsal opisthosomal sclerite with 1 pair of setae at each the anterior margin (*a*), middle (*b*), and posterior margin (*c*), and with no unpaired medial setae; each laterodorsal opisthosomal sclerite with 1–2 *a* setae near the anterior margin, 1 *b* seta at middle, and 1 *c* seta near posterior margin; femoral segments of leg I with spiniform (never subclavate) rake setae..... **3**
- Not with above combination of characters ..... **8**
- 3 Trochanter I with 1 seta on both anterolateral and posterior/dorsal surfaces..... ***C. calechius* Mulaik**
- Trochanter I with > 1 seta on anterolateral surface, or if 1 anterolateral seta, then with 2 posterodorsal setae ..... **4**
- 4 Tibia I with 6 anteroventral rake/spiniform setae ..... **5**
- Tibia I with fewer anteroventral rake/spiniform setae ..... **6**

- 5 Trochanter I with 1 anterolateral seta; genu I with 5 anteroventral rake/spiniform setae; body not coated with cemented debris ..... *C. janetae* Higgins & Mulaik
- Trochanter I with 3 anterolateral setae; genu I with 3 anteroventral rake/spiniform setae; body encrusted with cemented particles ..... *C. dorotheae* Mulaik
- 6 Tibia I with 3 anteroventral rake/spiniform setae; trochanter I anterolateral setae are clavate ..... *C. bardyi* Mulaik & Allred
- Tibia I with 4 anteroventral rake/spiniform setae; trochanter I anterolateral setae are spiniform ..... 7
- 7 Anterior margin of aspidosoma acuminate; dark idiosomal sclerites ..... *C. hypopachus* Mulaik
- Anterior margin of aspidosoma not acuminate; pale idiosomal sclerites ..... *C. gertschi* Mulaik
- 8 Body length  $\leq 0.90$  mm ..... 9
- Body length  $> 0.90$  mm ..... 10
- 9 Elongated bothridial setae on each tarsus; tibia I with 2 anteroventral rake/spiniform setae; dark idiosomal sclerites ..... *C. crossleyi* Hagan
- No elongated bothridial setae on any tarsus; tibia I with 3 anteroventral rake/spiniform setae; pale idiosomal sclerites ..... *C. mariae* Higgins & Mulaik
- 10 Basi- and telofemur I with subclavate rake setae ..... *C. clavatus* Banks
- Basi- and telofemur I with spiniform rake setae ..... 11
- 11 Mediodorsal opisthosomal sclerite with 8–9 setae ..... *C. pettiti* Nevin
- Mediodorsal opisthosomal sclerite with fewer setae ..... 12
- 12 Pale idiosomal sclerites ..... 13
- Dark idiosomal sclerites ..... 14
- 13 Posterior opisthosomal sclerite with 6 setae ..... *C. archeri* Mulaik
- Posterior opisthosomal sclerite with 11 setae ..... *C. krantzi* Coineau
- 14 Tibia I with 2 anteroventral rake/spiniform setae; trochanter III with 3 anterolateral setae; pluriposterior sclerite with 1 unpaired medial *h* seta ..... *C. cremnicolus* Enns (Fig. 5)
- Tibia I with 3 anteroventral rake/spiniform setae; trochanter III with 1 anterolateral seta; pluriposterior sclerite with 1 pair of *h* setae and no unpaired medial seta ..... 15
- 15 Aspidosomal anterior margin notched and lacking *Pa* setae; anterolateral surface of trochanter III with 1 spiniform seta; mediodorsal opisthosomal sclerites not fused; elongated bothridial setae on tarsi III and IV ..... *C. kerrulius* Mulaik
- Aspidosomal anterior margin not notched and bearing 1 pair of *Pa* setae; anterolateral surface of trochanter III with 1 clavate seta; mediodorsal opisthosomal sclerites fused; elongated bothridial setae present on all tarsi ..... *C. echinipes* Dufour
- 16 Dark idiosomal sclerites; tibia I with 2 posteroventral rake/spiniform setae ..... *C. americanus* Banks
- Pale idiosomal sclerites; tibia I with 4 posteroventral rake/spiniform setae ..... 17

- 17 Trochanter I with 2 anterolateral setae; progenital valves each with  $\leq 5$  setae.....  
 ..... ***C. tipus* Mulaik**
- Trochanter I with 3 anterolateral setae; progenital valves with more setae..... **18**
- 18 Genu I with 4 posteroventral rake setae; adanal sclerites each with 3 setae.....  
 ..... ***C. valverdius* Mulaik**
- Genu I with 0 or 1 posteroventral rake seta; adanal sclerites each with 2 setae .... **19**
- 19 Aspidosomal anterior margin with 2 pairs of *Pa* setae; basifemur I with 1 poster-  
 oventral rake seta; trochanter III with 3 anterolateral setae; centrodorsal opistho-  
 somal sclerite with 5 *b* setae arranged in an “M”; laterodorsal opisthosomal scler-  
 ite with 2 *a* setae; posterior opisthosomal sclerite with 7 setae .....  
 ..... ***C. cassiopeiae* Bernard & Lumley, sp. nov. (Figs 1–4)**
- Aspidosomal anterior margin with 3 pairs of *Pa* setae; basifemur I without poster-  
 oventral rake setae; trochanter III without anterolateral setae; centrodorsal  
 opisthosomal sclerite with 3–4 *b* setae; laterodorsal opisthosomal sclerite with 1 *a*  
 seta; posterior opisthosomal sclerite with 9 setae ..... ***C. lewisi* McDaniel & Boe**

### Geographical distribution

The complete distribution ranges for the taxa described above are unknown, but the new find of *C. cassiopeiae* sp. nov. is 2074 km from the nearest recorded occurrence of *C. valverdius* in Los Lunas, New Mexico (Mulaik and Allred 1954), and 805 km from the record of *C. lewisi* near Newell, South Dakota (McDaniel and Boe 1990). A comparison of climates reveals that Los Lunas has a mean annual precipitation of 249.7 mm and a mean annual temperature of 13.45 °C for the 1981–2010 period, whereas data for Newell are 447 mm and 8.2 °C respectively (NCEI 2017). This gives Los Lunas a Köppen-Geiger climate classification of cold semi-arid steppe (*BSk*) like Medicine Hat, whereas Newell has a humid continental climate (*Dfa*) (Peel et al. 2007). The soil in both Los Lunas and Newell is brown chernozem/calcaric aridisol (NRCS 2017, NSBD 2017), somewhat similar to the brown chernozem/ustic mollisol soil at Medicine Hat. These data show that although the new species is morphologically distinct from *C. lewisi* and *C. valverdius*, it shares climatic preferences with *C. valverdius*, and has a comparable soil habitat with both *C. lewisi* and *C. valverdius*.

The Albertan *C. cremnicolus* are 1911 km from the closest published location in Easley, Missouri (Enns 1958). The localities in Missouri have a humid subtropical climate (*Cfa*) by the Köppen-Geiger system, but the climates in the Alberta locations are incongruent; Writing-on-Stone Provincial Park is classed as cold semi-arid (*BSk*) yet Waterton Lakes National Park is continental subarctic (*Dfc*) (Peel et al. 2007). Soils among these sites are also variable. Along the Missouri River, sites have soils classified as gleyed regosol/fluvent entisol, and at Devil’s Backbone the soil is gray brown luvisol/udalfic alfisol (NRCS 2017). In Canada, the soil at Writing-on-Stone Provincial Park is a regosol/fluvent entisol similar to Missouri, but Waterton

Lakes National Park has substrate that is classed as dystic brunisol/crypteceptisol (NSBD 2017). These disparate abiotic conditions indicate that *C. cremnicolus* is a habitat generalist.

As the localities for *C. cremnicolus* and *C. cassiopeiae* sp. nov. are 126 km apart and in the same climate, their ranges could potentially overlap if *C. cremnicolus* can inhabit the soil at Medicine Hat. These species are nevertheless in separate clades (Fig. 6), signifying multiple introductions of the family into Canada. Such a pattern of introductions may be attributable to postglacial changes in biome distributions, which enabled fragmented xeric populations to expand northward from arid refugia after the last glacial maximum 18,000 years ago (Riddle and Hafner 2006; Graham et al. 2013). This possibility is intriguing considering that at the time Medicine Hat was near the southern limit of the Laurentide Ice Sheet, and by 14,000 years ago it was the first area in Canada freed of the ice as it became semi-arid grassland (Dyke 2005). Likewise, Thaler et al. (1993) described a new locality of *Microcaeculus austriacus* in Austria that was ~440 km from its known locations in the easternmost extent of the Alps, and alluded to postglacial warming as a possible explanation for the scattered distribution.

Our phylogenetic analysis suggests that the common ancestor of *Caeculus* inhabited southwestern North America, based on the known locations for *C. calechius* and Clade A (the most basal clade). The other clades also contain representatives from the North American southwest as well as those from other areas, and there is a diversity of locations represented by the taxa that are not in clades. *Caeculus echinipes* is the only species of *Caeculus* described to date from Europe. The results suggest that the ancestor of *C. echinipes* spread to Europe from North America. Further work to include molecular data would be helpful to clarify the weaker branch support shown in the topology.

## Conclusions

Our description of *Caeculus cassiopeiae* sp. nov. elevates the number of known Canadian caeculids to two. Based on a maximum parsimony analysis of a character state matrix for all members of the genus, it is most closely related to *C. lewisi*. The phylogeny also suggests multiple introductions of caeculids into Canada, and that the origin of the genus is the American southwest. Further collection of caeculids in North America is required to determine to what extent ranges overlap, examine ecology or additional morphological traits (e.g., minute sensory structures) that were not described in previously published taxonomic accounts, and to enable genetic analysis. Population studies can further describe the degree of intraspecific variation and clarify species boundaries. Our phylogeny provides the first analysis of the genus, which can be useful for future systematic studies that integrate taxonomy and genetics to develop a better understanding of the genus *Caeculus* and its family.

## Acknowledgements

We thank Christopher Taylor at Curtin University in Perth, Australia for his insight. We are indebted to Frédéric Beaulieu and Wayne Knee at CNCI for providing Evert Lindquist's specimens for examination. We are also grateful to Chris Jass at the Royal Alberta Museum in Edmonton, Alberta for his knowledge on surficial geology of the type location. For her astute suggestions, we are beholden to Anne Baker at the Natural History Museum in London.

## References

- Banks N (1899) An American species of the genus *Caeculus*. Proceedings of the Entomological Society of Washington 4: 221–222. <https://www.biodiversitylibrary.org/item/19516#page/229/mode/1up>
- Banks N (1905) Descriptions of some new mites. Proceedings of the Entomological Society of Washington 7: 133–142. <https://doi.org/10.5962/bhl.part.8752>
- Beaulieu F, Knee W, Nowell V, Schwarzfeld M, Lindo Z, Behan-Pelletier VM, Lumley L, Young MR, Smith I, Proctor HC, Mironov SV, Galloway TD, Walter DE, Lindquist EE (2019) Acari of Canada. In: Langor DW, Sheffield CS (Eds) The Biota of Canada – A Biodiversity Assessment, Part 1: the Terrestrial Arthropods. ZooKeys 819: 77–168. <https://doi.org/10.3897/zookeys.819.28307>
- Berg TE, McPherson RA (2005) Surficial Geology Medicine Hat, Alberta, NTS 72L. Alberta Geological Survey. [https://ags.aer.ca/publications/MAP\\_142.html](https://ags.aer.ca/publications/MAP_142.html)
- Coineau Y (1964) Contribution à l'étude des Caeculidae. Première série. Développement postlarvaire de *Allocaeculus catalanus* Franz 1954. Deuxième partie. La chétotaxie des pattes. Acarologia 6: 47–72. <https://www1.montpellier.inra.fr/CBGP/acarologia/article.php?id=3836>
- Coineau Y (1967a) Contribution à l'étude des Caeculidae. Troisième série. Développement postlarvaire de *Neocaeculus luxtoni* n. gen., n. sp. Acarologia 9: 55–75. <https://www1.montpellier.inra.fr/CBGP/acarologia/article.php?id=3637>
- Coineau Y (1967b) Contribution à l'étude des Caeculidae IV. *Procaeculus bryani* Jacot, 1936 (Acariens, Prostigmatés). Pacific Insects 9: 709–720. [http://hbs.bishopmuseum.org/pi/pdf/9\(4\)-709.pdf](http://hbs.bishopmuseum.org/pi/pdf/9(4)-709.pdf)
- Coineau Y (1969) Contribution à l'étude des Caeculidae. Cinquième série. *Procaeculus aitkeni*, une nouvelle espèce de Trinidad, B.W.I. Revue d'Ecologie et de Biologie du Sol 6: 53–67. <https://eurekamag.com/research/022/272/022272490.php>
- Coineau Y (1974) Éléments pour une monographie morphologique, écologique et biologique des Caeculidae (Acariens). Mémoires du Muséum National d'Histoire Naturelle, Série A, Zoologie 81: 1–299. <https://www.biodiversitylibrary.org/page/57792659>
- Dufour L (1832) Description et figure du *Caeculus echinipes*, Arachnide nouvelle. Annales des Sciences Naturelles 25: 289–296. <https://doi.org/10.5962/bhl.part.19204>

- Dyke AS (2005) Late Quaternary vegetation history of northern North America based on pollen, macrofossil, and faunal remains. *Géographie Physique et Quaternaire* 59: 211–262. <https://doi.org/10.7202/014755ar>
- Enns WR (1958) A new species of rake-legged mite from Missouri (Acarina, Caeculidae). *Journal of Kansas Entomological Society* 31: 107–113. <https://www.jstor.org/stable/25082279>
- Franz H (1952) Revision der Caeculidae Berlese 1883 (Acari). *Bonner Zoologische Beiträge* 3: 91–124. <https://www.biodiversitylibrary.org/page/44716813#page/105/mode/1up>
- Fuangarworn M, Butcher BA (2015) *Neocaeculus orientalis* sp. nov. (Acari, Trombidiformes, Caeculidae) from Thailand. *Zootaxa* 4048: 251–268. <https://doi.org/10.11646/zootaxa.4048.2.6>
- Fuller L (2010) Chernozemic soils of the prairie region of Western Canada. *Prairie Soils and Crops* 3: 37–45. <https://prairiesoilsandcrops.ca/articles/volume-3-6-screen.pdf>
- Graham MR, Jaeger JR, Prendini L, Riddle BR (2013) Phylogeography of the Arizona hairy scorpion (*Hadrurus arizonensis*) supports a model of biotic assembly in the Mojave Desert and adds a new Pleistocene refugium. *Journal of Biogeography* 40: 1298–1312. <https://doi.org/10.1111/jbi.12079>
- Grandjean F (1944) Observations sur les Acariens du genre *Caeculus*. *Archives des Sciences Physiques et Naturelles, 5ème période* 26: 33–46. <http://doi.org/10.5169/seals-742677>
- Grandjean F (1969) Stases. Actinopiline. Rappel de ma classification des Acariens en 3 groupes majeurs. Terminologie en soma. *Acarologia* 11: 796–827. <https://www1.montpellier.inra.fr/CBGP/acarologia/article.php?id=3467>
- Hagan DV (1985) *Caeculus crossleyi* n. sp. (Acari: Caeculidae) from granite outcrops in Georgia, U.S.A. *International Journal of Acarology* 58: 241–245. <https://doi.org/10.2307/1936920>
- Haynes RH (1998) Chapter 16: correlation of Canadian soil taxonomy with other systems. In: Haynes RH, Cavers PB, Herzberg G, Ingold KU, Kaufmann W, Lecours M, Lewis WH, Milligan LP, Scudder GGE, Taylor EW, Dancik BP (Eds) *The Canadian System of Soil Classification* (3<sup>rd</sup> edn.). Ottawa, National Research Council of Canada, 153–156. ISBN: 978-0660174044
- Higgins HG, Mulaik SB (1957a) A new *Caeculus* from Oregon (Acarina: Caeculidae). *Great Basin Naturalist* 17: 27–29. <https://doi.org/10.5962/bhl.part.6226>
- Higgins HG, Mulaik SB (1957b) Another *Caeculus* from southwestern United States (Acarina Caeculidae). *Texas Journal of Science* 9: 267–269.
- Jacot AP (1936) Some rake-legged mites of the family Cheyletidae. *Journal of the New York Entomological Society* 44: 17–30. <https://www.biodiversitylibrary.org/item/205823#page/31/mode/1up>
- Lindquist EE, Ainscough BD, Clulow FV, Funk RC, Marshall VG, Nesbitt HHJ, OConnor BM, Smith IM, Wilkinson PR (1979) Acari. In: Danks HV (Ed.) *Canada and its insect fauna. Memoirs of the Entomological Society of Canada* 111 (Supplement 108): 252–290. <https://doi.org/10.4039/entm111108252-1>
- Maddison WP, Maddison DR (2017) Mesquite: a modular system for evolutionary analysis. Version 3.2. <http://mesquiteproject.org>

- Mangová B, Krumpál M, Luptáček P (2014) *Allocaeculus sandbergensis* sp. n. (Acari: Caeculidae), a new prostigmatid mite from Slovakia. *Biologia* 69 (Section Zoology): 214–218. <https://doi.org/10.2478/s11756-013-0303-2>
- Marshall SA, Anderson RS, Roughley RE, Behan-Pelletier V, Danks HV (1994) Terrestrial arthropod biodiversity: planning a study and recommended sampling techniques. *Bulletin of the Entomological Society of Canada* 26 (Supplement): 1–33. <https://esc-sec.ca/wp/wp-content/uploads/2017/03/Bulletin-volume26-number1-Mar1994-supplement-Terrestrial-arthropod-biodiversity.pdf>
- McDaniel B, Boe A (1990) A new species and distribution record for the genus *Caeculus* Dufour (Acari: Caeculidae) from South Dakota. *Proceedings of the Entomological Society of Washington* 92: 716–724. <https://www.biodiversitylibrary.org/page/26238311#page/734/mode/1up>
- Mulaik S (1945) New mites in the family Caeculidae. *Bulletin of the University of Utah* 35: 1–23. <https://collections.lib.utah.edu/ark:/87278/s6m6242g>
- Mulaik S, Allred DM (1954) New species and distribution records of the genus *Caeculus* in North America (Acarina, Caeculidae). *Proceedings of the Entomological Society of Washington* 56: 27–40. <https://www.biodiversitylibrary.org/item/54777#page/401/mode/1up>
- NCDIA Canadian Climate Normals (1981–2010) National Climate Data and Information Archive, Environment and Climate Change Canada. [http://climate.weather.gc.ca/climate\\_normals/results\\_1981\\_2010\\_e.html?stnID=1641&autofwd=1](http://climate.weather.gc.ca/climate_normals/results_1981_2010_e.html?stnID=1641&autofwd=1) [accessed 6 March 2020]
- NCEI (1981–2010) US Climate Normals. National Centers for Environmental Information, National Oceanic and Atmospheric Administration. <https://www.ncdc.noaa.gov/data-access/land-based-station-data/land-based-datasets/climate-normals/1981-2010-normals-data> [accessed 6 March 2020]
- Nevin FR (1943) *Caeculus pettiti*, a new species of mite from Virginia. *Annals of the Entomological Society of America* 36: 389–393. <https://doi.org/10.1093/acesa/36.3.389>
- NRCS (2020) Soil Survey. Natural Resources Conservation Service, US Department of Agriculture. <http://www.nrcs.usda.gov/wps/portal/nrcs/main/soils/survey/> [accessed 6 March 2020]
- NSBD (2020) Soils of Canada. National Soil Database, Agriculture and Agri-Food Canada. <http://www.agr.gc.ca/atlas/soil> [accessed 6 March 2020]
- Ott AP, Ott R (2014) A new species of *Andocaeculus* (Acari, Caeculidae) from the Pampa biome, southern Brazil. *Iheringia, Série Zoologia* 104: 355–363. <https://doi.org/10.1590/1678-476620141043355363>
- Otto JC (1993) A new species of *Microcaeculus* from Australia (Acarina: Caeculidae), with notes on its biology and behaviour. *International Journal of Acarology* 19: 3–13. <https://doi.org/10.1080/01647959308683533>
- Peel MC, Finlayson BL, McMahon TA (2007) Updated world map of the Köppen-Geiger climate classification. *Hydrology and Earth System Sciences* 11: 1633–1644. <https://doi.org/10.5194/hess-11-1633-2007>
- Per S, Doğan S, Zeytun E, Ayyıldız N (2017) Description of a new rake legged mite of the genus *Allocaeculus* (Acariformes: Caeculidae) from Turkey with description of variation in dorsal setation. *Acarologia* 57: 369–382. <https://doi.org/10.1051/acarologia/20164162>

- Porta AO, Proud DN, Franchi E, Porto W, Epele MB, Michalik P (2019) The first record of caeculid mites from the Cretaceous amber of Myanmar with notes on the phylogeny of the family. *Zootaxa* 4647: 23–43. <https://doi.org/10.11646/zootaxa.4647.1.5>
- Rambaut A (2012) FigTree 1.4.3. <http://tree.bio.ed.ac.uk/software/figtree>
- Riddle BR, Hafner DJ (2006) A step-wise approach to integrating phylogeographic and phylogenetic biogeographic perspectives on the history of a core North American warm deserts biota. *Journal of Arid Environments* 66: 435–461. <https://doi.org/10.1016/j.jaridenv.2006.01.014>
- Rivas G, Serrano-Sánchez L, Vega FJ (2016) First record of *Procaeculus* (Acari: Caeculidae) in Miocene amber from Chiapas, Mexico. *Boletín de la Sociedad Geológica Mexicana* 68: 87–92. <https://doi.org/10.18268/BSGM2016v68n1a10>
- Skvarla MJ, Fisher JR, Dowling APG (2013) On some mites (Acari: Prostigmata) from the Interior Highlands: descriptions of the male, immature stages, and female reproductive system of *Pseudocheylus americanus* (Ewing, 1909) and some new state records for Arkansas. *Zootaxa* 3641: 401–419. <https://doi.org/10.11646/zootaxa.3641.4.7>
- Swofford DL (2000) PAUP\* Version 4.0β10, Phylogenetic Analysis using Parsimony (\*and other methods). Sinauer Associates, Sunderland.
- Taylor CK (2014) Two further *Neocaeculus* species (Acari: Prostigmata: Caeculidae) from Barrow Island, Western Australia. *Acarologia* 54: 347–358. <https://doi.org/10.1051/acarologia/20142136>
- Taylor CK, Gunawardene NR, Kinnear A (2013) A new species of *Neocaeculus* (Acari: Prostigmata: Caeculidae) from Barrow Island, Western Australia, with a checklist of world Caeculidae. *Acarologia* 53: 439–452. <https://doi.org/10.1051/acarologia/20132105>
- Thaler K, Knoflach B, Meyer E (1993) Fragmenta Faunistica Tirolensia–X (Arachnida, Acari: Caeculidae; Myriapoda: Diplopoda; Insecta, Nematocera: Limoniidae, Sciaridae). *Berichte des Naturwissenschaftlich-medizinischen Verein Innsbruck* 80: 311–325. [https://www.zobodat.at/pdf/BERI\\_80\\_0311-0325.pdf](https://www.zobodat.at/pdf/BERI_80_0311-0325.pdf)
- Vitzthum HG (1933) Die larvenformen der gattung *Caeculus* Dufour. *Zoologischer Anzeiger* 105: 85–92.
- Walter DE, Lindquist EE, Smith IM, Cook DR, Krantz GW (2009) Order Trombidiformes. In: Krantz GW, Walter DE (Eds) *A Manual of Acarology* (3<sup>rd</sup> edn.). Lubbock, Texas Tech University Press, 233–420. ISBN: 978-0896726208
- Zhang Z-Q (2018) Repositories for mite and tick specimens: acronyms and their nomenclature. *Systematic and Applied Acarology* 23: 2432–2446. <https://doi.org/10.11158/saa.23.12.12>



# Review of the *Bobekia*-group (Braconidae, Alysiinae, Alysiini), with description of a new genus and a new subgenus

Ruo-Nan Zhang<sup>1</sup>, Cornelis van Achterberg<sup>1,2</sup>, Xiao-Xia Tian<sup>1</sup>, Jiang-Li Tan<sup>1</sup>

**1** Shaanxi Key Laboratory for Animal Conservation/Key Laboratory of Resource Biology and Biotechnology in Western China, Ministry of Education, College of Life Sciences, Northwest University, Xi'an 710069, China

**2** State Key Laboratory of Rice Biology and Ministry of Agriculture Key Lab of Agricultural Entomology, Institute of Insect Sciences, Zhejiang University, Hangzhou 310058, China

Corresponding author: Jiang-Li Tan ([tanjl@nwu.edu.cn](mailto:tanjl@nwu.edu.cn))

---

Academic editor: J. Fernandez-Triana | Received 12 October 2019 | Accepted 30 January 2020 | Published 13 April 2020

---

<http://zoobank.org/54572214-9175-41F1-83D1-9A8AD5F633E7>

---

**Citation:** Zhang R-N, van Achterberg C, Tian X-X, Tan J-L (2020) Review of the *Bobekia*-group (Braconidae, Alysiinae, Alysiini), with description of a new genus and a new subgenus. ZooKeys 926: 25–51. <https://doi.org/10.3897/zookeys.926.47270>

---

## Abstract

The world genera of the *Bobekia*-group of Alysiini (Braconidae: Alysiinae) are reviewed and keyed. A new genus (*Neodiasta* **gen. nov.**) is proposed for *Phasmidiasta ecuadorensis* Fischer, 2006, from Ecuador. One new subgenus (*Parabobekoides* **subg. nov.**; type species *Separatatus (Parabobekoides) yinshani* **sp. nov.** from NW China) is described and illustrated. *Neosymphanes* Belokobylskij, 1998 is a new synonym of *Bobekia* Niezabitowski, 1910 (**syn. nov.**).

## Keywords

*Bobekia*, *Bobekoides*, *Hoalysia*, *Hylcalosia*, key, *Neodiasta*, new species, new genera, *Parabobekoides*, *Phasmidiasta*, *Sennot*, *Separatatus*, world revision

## Introduction

The group of alysiine genera with sculptured second metasomal tergite, distinct dorsope in the first metasomal tergite, and a closed first subdiscal cell of the fore wing (here defined as the *Bobekia*-group of the Alysiinae, Braconidae) is comprised of eight

genera worldwide, with *Phasmalysia* Tobias, 1971, as a ninth borderline genus. The lack of comprehensive keys has confused several researchers and resulted in associating Chinese species with Afrotropical genera (Wharton 2002; Zheng et al. 2013). The recent series of papers on this group (Zheng et al. 2013, 2017, 2018; Belokobylskij 2015; Yao et al. 2018a, b, 2019) and the discovery in Shaanxi (NW China) of a new species with conspicuous sexual dimorphism seems the right moment to give a revised key to all genera of this group worldwide; to describe a new genus, a new subgenus, and one new species; and to report the sexual dimorphism present in the new species.

The biology is unknown within most genera, but at least some species are putatively parasitoids of xylophilous fly larvae, because their cocoons have been found in the galleries of scilytine beetles (Wharton 1980; Belokobylskij 1998). Others seem to parasitize presumably more easily accessible hosts such as mining larvae of Agromyzidae and Muscidae (see note under *Bobekia* Niezabitowski).

## Material and methods

The specimens were collected in Malaise traps in an abandoned garden in the village of Shangluo (NW China: Shaanxi, Luonan) and directly preserved in 70% alcohol; they were later chemically treated with a mixture of 96% xylene + alcohol and amylacetate (AXA-method; van Achterberg 2009) before card-pointing. For identification of the subfamily Alysiinae, see van Achterberg (1990, 1993); for identification of the genera of Chinese Alysiini, see Zhu et al. (2017); for references, see Yu et al. (2016).

The type species of all genera were examined for the key, except for *Senwot* Wharton, which was included using information from existing literature. Morphological terminology follows van Achterberg (1988, 1993), including the abbreviations for wing venation. Measurements are taken as indicated by van Achterberg (1988): for the length and the width of a body part the maximum length and width is taken, unless otherwise indicated. The length of the mesosoma was measured from the anterior border of the mesoscutum to the apex of the propodeum and of the first tergite from the posterior border of the adductor to the medio-posterior margin of the tergite.

Observations and descriptions were made with an Opto-Edu A230903 stereomicroscope and a fluorescent lamp. Photographic images were made with the Keyence VHX-5000 digital microscope. The following acronyms are used for the depositories: **AEI** – American Entomological Institute, Utah State University (Logan); **BZL** – Biologiezentrum - Oberösterreichisches Landesmuseum (Linz); **CNC** – Canadian National Collection of Insects (Ottawa); **FAFU** – Fujian Agricultural and Forestry University (Fuzhou); **MNHN** – Muséum National d'Histoire Naturelle (Paris); **NWUX** – Department of Life Sciences, Northwest University (Xi'an); **PAN** – Muzeum i Instytut Zoologii Polskiej Akademii Nauk (Warsaw); **RMNH** – Naturalis Biodiversity Center (Leiden); **ZIL** – Zoological Institute (Lund); **ZMB** – Museum für Naturkunde (Berlin).

**Key to the world genera of the *Bobekia*-group**

- 1 Second metasomal tergite distinctly sculptured basally (Figs 9, 21, 27), dorsope distinctly developed (Figs 9, 27, 96) and first subdiscal cell of fore wing closed distally (Figs 5, 20, 36); mandible without oblique ventral carina (Figs 15, 41, 74, but present in *Phasmidiasta*; Figs 102, 103); mandible often with 4 teeth or lobes (Figs 15, 17, 41, 71); pronope present and usually medium-sized to rather large (Figs 8, 46, 116); *Bobekia*-group ..... **2**
- Either second tergite smooth basally or dorsope absent or first subdiscal cell of fore wing open distally; oblique ventral carina of mandible often present and mandible usually with 3 teeth; pronope variable ..... **other genera of Alysiini**
- 2 Vein r of fore wing issued at basal 0.2–0.4 of pterostigma (Fig. 107); pterostigma parallel-sided (Fig. 107); first (= dorsal) tooth much wider than third (= ventral) tooth and dorso-apically with small to medium-sized, tooth-shaped protuberance; vein CU1b of fore wing distinctly longer than vein 3-CU1 or 3-CU1 absent, first subdiscal cell narrow and vein CU1a at level of vein CU1 (Fig. 107); vein M+CU of hind wing 0.7–1.0× as long as vein 1-M (Fig. 107); [face distinctly convex in type species, less so in Asian spp. (Fig. 111); upper valve of ovipositor convex and with small nodus (Fig. 114); clypeus triangular and acute; Afrotropical species have pterostigma more elongate than Asian spp.]; Afrotropical, Oriental ..... ***Senwot Wharton, 1983***
- Vein r of fore wing issued medially from pterostigma or behind it (Figs 1, 5, 17, 20, 79, 92); pterostigma triangular or elliptical (Figs 1, 17, 40, 65), but parallel-sided or nearly so in *Neodiasta* (Fig. 79); first tooth of mandible similar to other teeth (Figs 14, 25, 39, 57), if much larger then without dorso-apical protuberance (Fig. 41, but present in *Hylcalosia ruficeps*; Fig. 71); vein CU1b of fore wing distinctly shorter than vein 3-CU1, first subdiscal cell moderately wide and vein CU1a distinctly below level of vein CU1 (Figs 5, 20, 36, 97); vein M+CU of hind wing at least 1.2× as long as vein 1-M (Figs 6, 20, 53, 65, 92), but shorter than vein 1-M in *Neodiasta* (Fig. 80) ..... **3**
- 3 Clypeus acute ventrally, triangular (Fig. 43,); first tooth of mandible very wide and lobe-shaped protruding dorsally and apically and third tooth much smaller (Figs 41, 42, 71, 74); upper valve of ovipositor enlarged and enclosing the small lower valve; third tergite sculptured in non-Afrotropical species; head often more square in dorsal view (i.e., head length longer relative to head width; Figs 47, 67); [mandible large and ventrally sinuate, with a more or less protruding small lobe (“fourth tooth”); vein 2-SR of fore wing curved basally and longer than vein 3-SR] ..... **4**
- Clypeus obtuse ventrally, semicircular (Figs 12, 18, 24); upper valve of ovipositor cylindrical or depressed (*Parabobekoides*: Fig. 2; unknown of *Hovalysia* and *Neodiasta* type species); third tergite smooth; head length shorter relative to head width in dorsal view (Figs 8, 28, 55, 88, 94) ..... **5**

- 4 Vein r-m of fore wing distinctly oblique, angle with vein 2-M acute (Fig. 40); anterior tentorial pits distinctly impressed (Fig. 43); fourth to sixth metasomal tergites of ♀ largely exposed (Fig. 50); third tergite smooth (Fig. 51); Afrotropical ..... **Bobekoides van Achterberg, 1998**
- Vein r-m of fore wing vertical or slightly oblique, angle with vein 2-M about rectangular (Fig. 65); anterior tentorial pits hardly impressed (Fig. 70); fourth and following tergites largely retracted of ♀ (cf. Fig. 78); third metasomal tergite sculptured (Fig. 66); [third antennal segment nearly always distinctly widened, 1.4–2.0× wider than fourth segment (except in *H. loasensis*) and usually distinctly shorter than fourth segment: Fig. 73]; Eastern Palearctic, Oriental.... **Hylcalosia Fischer, 1967**
- 5 Vein SR1 of fore wing slightly longer than vein 3-SR (Fig. 79); vein M+CU of hind wing shorter than vein 1-M (Fig. 80); pterostigma parallel-sided or narrow elliptical (Fig. 79); Neotropical ..... **Neodiasta van Achterberg, gen. nov.**
- Vein SR1 of fore wing much longer than vein 3-SR (Figs 5, 20, 26, 53); vein M+CU of hind wing at least 1.2 × as long as vein 1-M (Figs 6, 20, 26, 92); pterostigma moderately wide elliptical or triangular (Figs 5, 26, 92) ..... **6**
- 6 Vein r issued near middle of pterostigma (Fig. 53); veins r, 1-SR and 1-M of fore wing of ♂ widened (Fig. 53); precoxal sulcus nearly horizontal (Fig. 64); clypeus 2.5–3.0 × wider than high (Fig. 58); [metanotum obtuse dorsally]; Afrotropical... ..... **Hovalysia Granger, 1949**
- Vein r issued behind middle of pterostigma (Figs 1, 17); veins r, 1-SR and 1-M of fore wing of ♂ slender (Fig. 20); precoxal sulcus oblique (Figs 7, 17) or absent; clypeus 2.0–2.5 × wider than high (Figs 12, 98, 121)..... **7**
- 7 Precoxal sulcus absent (Fig. 102); in lateral view medial part of face distinctly protruding dorsally in front of antennal socket and its dorsal half nearly straight in profile (Fig. 102; Fig. 110.8 in Belokobylskij 1998); mandible straight ventrally, without fourth protuberance and hardly widened dorsally (Figs 102, 103; fig. 110.11 in Belokobylskij 1998); Holarctic..... **Phasmidiasta Wharton, 1980**
- Precoxal sulcus present, usually wide and oblique (Figs 7, 17, 38, 125); in lateral view medial part of face normal, less protruding and its dorsal half evenly curved in profile (Figs 1, 14, 38, 125); mandible sinuate ventrally, with fourth protuberance more or less developed and widened dorsally (Figs 15, 17, 25, 32, 39, 117, 120) ..... **8**
- 8 Mandible comparatively slender, and its first tooth less protruding dorsally (Fig. 39); metanotum distinctly protruding in lateral view (Fig. 38); third antennal segment about as long as fourth segment (Fig. 34); [♂ has according to fig. 109.18 in Belokobylskij (1998) pterostigma modified, but vein r short, approx. 0.3× width of pterostigma]; Palearctic, Afrotropical..... **Bobekia Niezabitowski, 1910**
- Mandible robust (Figs 1, 14, 17, 125), its first tooth distinctly protruding dorsally (Figs 14, 16, 117); metanotum hardly or not protruding dorsally (Figs 1, 7, 125); third antennal segment shorter than fourth segment (Figs 10, 22, 123), but sometimes only slightly so; [♂ has modified pterostigma, but vein r medium-sized, approx. 0.7× width of pterostigma: Figs 17, 20]; Oriental, Eastern Palearctic; genus *Separatatus* Chen & Wu, 1994 ..... **9**

- 9 Base of vein 1-R1 of fore wing widened, more so in ♂♂ than in ♀♀ (Figs 1, 5, 17, 20); setose part of ovipositor sheath 1.5–1.6× longer than metasoma and 0.6–0.7× as long as fore wing (Fig. 1); upper valve of ovipositor flattened dorsally; hind femur 4.4–5.3× longer than wide (Figs 1, 17); propodeal areola reduced anteriorly (Figs 9, 21) .....**subgenus *Parabobekoides* van Achterberg & Tan, subg. nov.**
- Base of vein 1-R1 of fore wing narrow (♀: Fig. 115; ♂ unknown); setose part of ovipositor sheath 0.8–1.0× longer than metasoma and 0.3–0.4 × as long as fore wing (Fig. 125); upper valve of ovipositor (at least in type species) normal, convex dorsally; hind femur 2.7–3.5× longer than wide (Fig. 119); propodeal areola complete anteriorly (Fig. 116), except in *S. malaysiae* ....**subgenus *Separatatus* Chen & Wu, 1994**

**Notes.** *Phasmalsysia* Tobias, 1971 (type species: *Phasmalsysia zinovjevi* Tobias, 1971, from S. Russia [examined]) might belong to the *Bobekia* group, but it is excluded here because of the uniquely shaped mandible (first tooth extremely enlarged and lobe-shaped, with curved carina present on first and third tooth and mandible consisting mainly of two large lobes (if viewed with full sight on the first tooth) because of the deep medio-apical incision). The type species has the third antennal segment slender, and the second tergite only superficially sculptured. The Nearctic *P. borealis* Wharton, 1980, has the second tergite more sculptured, but is also characterized by an aberrantly shaped mandible.

## Taxonomy

### ***Separatatus* Chen & Wu, 1994**

Figs 1–25, 115–126

*Separatatus* Chen & Wu, 1994: 132; Zhu et al. 2017: 69–72; Yao et al. 2018a: 187–188. Type species (by monotypy): *Separatatus carinatus* Chen & Wu, 1994 [holotype (FAFU) examined].

*Phasmidiasta* sensu Fischer 2006: 628–631 (p.p.).

*Hovalysia* sensu Wharton 2002: 79 (figs 124–127).

*Bobekoides* sensu Zheng et al. 2013: 143–146 (p.p.).

**Notes.** A small Oriental and East Palearctic genus in terms of species richness; hosts are unknown for all species. Species of *Separatatus* can be identified with the key by Yao et al. (2018a), and those of *Parabobekoides* with the key below.

### **Subgenus *Parabobekoides* van Achterberg & Tan, subg. nov.**

<http://zoobank.org/79C99F4A-C69C-4B45-97BF-FC1C800C3412>

**Type species.** *Separatatus (Parabobekoides) yinshani* Zhang & van Achterberg, sp. nov. Gender: masculine.

**Diagnosis.** Propodeal areola reduced anteriorly (Figs 8, 9, 21); setose part of ovipositor sheath distinctly longer than metasoma and 0.6–0.7× as long as fore wing (Fig. 1); upper valve of ovipositor flattened apically (Fig. 2). Superficially, the new subgenus is very similar to *Bobekoides* van Achterberg and shares the derived shape of the upper valve of the ovipositor, but differs by the semicircular clypeus (Fig. 12; acute and triangular in *Bobekoides*), vein r-m of the fore wing nearly straight and angle with vein 2-M about 90° (Figs 1, 5, 17, 20; distinctly inclivous and angle distinctly less than 90° in *Bobekoides*), the transverse head in dorsal view (Fig. 8; more square in *Bobekoides*), the basally widened and more or less differentiated vein 1-R1 (narrow and not differentiated in *Bobekoides*), the distinct sexual dimorphism of the fore wing venation (Fig. 20; absent in *Bobekoides*), the posteriorly wide propodeal areola (Fig. 21; narrow in *Bobekoides*) and the mandible less massively enlarged dorsally, its dorsal tooth somewhat wider than second (= middle) tooth (Fig. 15; strongly enlarged dorsally, dorsal tooth much wider than second tooth in *Bobekoides*).

**Distribution.** China (Hubei, Shaanxi).

**Etymology.** “Para” is Greek for “beside, near, by” and the generic name *Bobekoides*, because it is similar to this genus.

#### Key to species of subgenus *Parabobekoides* nov.

- 1 Antenna of ♀ with ca 47 segments and 1.7× longer than fore wing; face transversely rugose laterally; mesoscutum largely blackish brown; striae of second tergite partly distinctly oblique..... **S. (*P.*) *sinicus* (Zheng, Chen & Yang, 2013)**
- Antenna of ♀ with 31–33 segments and 1.3–1.4× longer than fore wing (of ♂ up to 1.5×); face smooth laterally, remainder largely superficially rugulose (Figs 12, 18); mesoscutum yellowish brown; striae of second tergite largely longitudinal or nearly so (Figs 9, 21).....**S. (*P.*) *yinshani* Zhang & van Achterberg, sp. nov.**

#### Discussion

Zheng et al. (2013) reported *Bobekoides sinicus* Zheng, Chen & Yang, 2013 from Central China (Hubei). This was the first time that a species of *Bobekoides* van Achterberg, 1998 was reported from outside Africa. Zhu et al. (2017) included this species in the genus *Separatatus* Chen & Wu, 1994, because it has an obtuse clypeus as in the type species of *Separatatus*. In *Bobekoides*, the clypeus is acute and triangular (Fig. 43).

In 2017 a series of a similar species was collected at Luonan (Qinling Mountains, Shaanxi, NW China) in which males have the venation modified (Figs 17, 20) in comparison to females. The venation is also modified in the male of the type species of *Hoalysia* Granger, 1949, known only from the Afrotropical region, of which the female is unknown. Wharton (2002) reported the occurrence of *Hoalysia* in China (Taiwan), but the lack of females did not allow for a proper inclusion in the key by

Zhu et al. (2017), and it was left out pending the availability female specimens. Fischer (1999) described *Hoivalysia cruciata* from South Africa based on one female specimen, but he did not indicate the shape of the ovipositor. The series from Luonan include females with normal (= slender) veins 3-SR and 2-M, vein 2-SR about as long as vein 3-SR, with a modified upper valve of the ovipositor, and vein r 0.6× width of pterostigma (Fig. 5). The males have the basal part of vein 1-R1 wider than in females, veins 3-SR and 2-M widened, vein 2-SR distinctly shorter than vein 3-SR, and vein r about 0.7× as wide as the pterostigma (Fig. 20). Inclusion in *Hoivalysia* is a possibility, but is problematic because the Chinese specimens have the first mandibular tooth wide, lobe-shaped, and strongly protuberant both dorsally and apically (rectangular, not protruding apically and hardly so dorsally in *Hoivalysia*); the males have a different pattern of widened veins (e.g., veins 1-SR, 1-M, and r are widened in *Hoivalysia* and slender in Chinese males); and vein CU1b of the fore wing is shorter than vein 3-CU1 (as long as vein 3-CU1 in *Hoivalysia*).

***Separatatus (Parabobekoides) yinshani* Zhang & van Achterberg, sp. nov.**

<http://zoobank.org/AB358A9B-BE34-418B-A823-6A3320D4A49C>

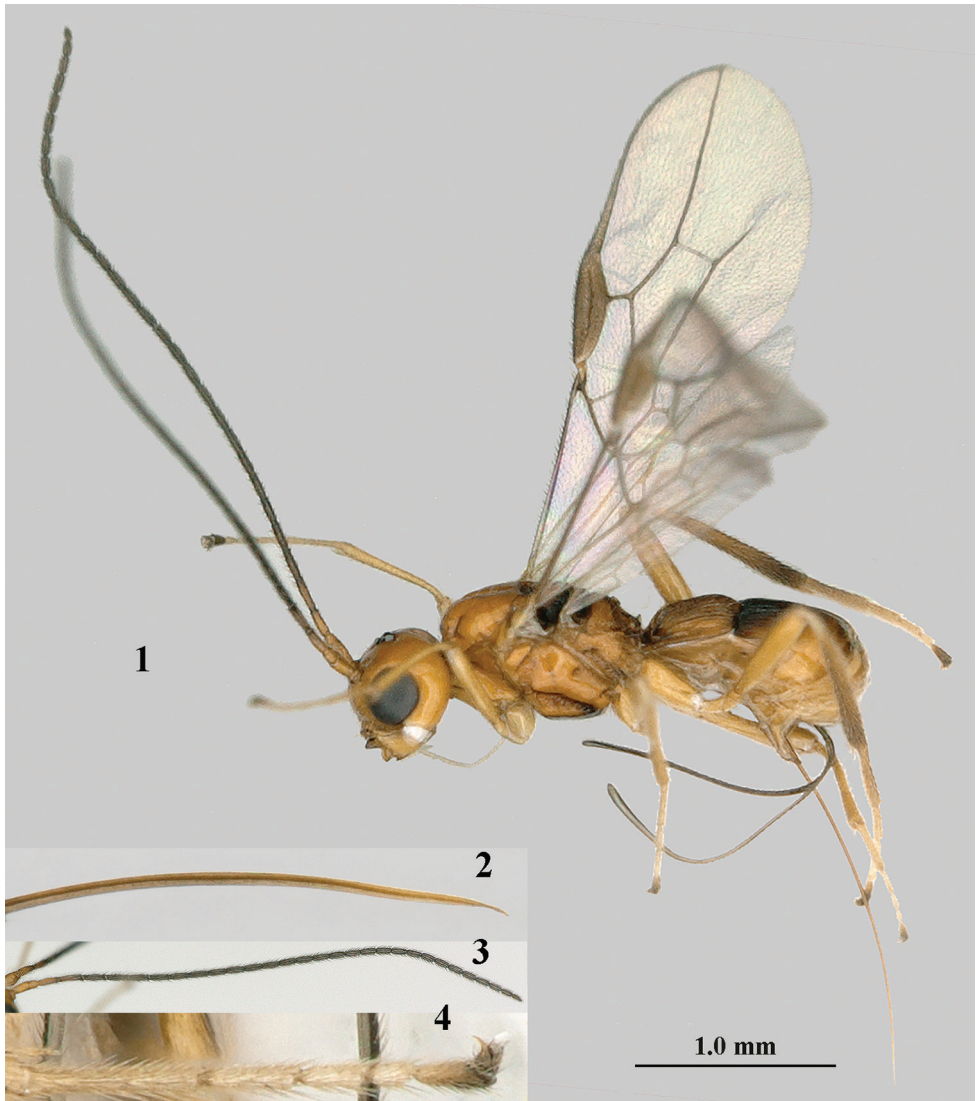
Figs 1–25

**Type material. Holotype:** ♀ (NWUX), “NW. China: Shaanxi, Luonan, Shangluo, 34.03N, 110.10E, 9.vii.–9.ix.2017, alt. 1006 m, B[lack] Mal[aise] trap, Tan Jiangli, NWUX”. **Paratypes:** 5 ♂ + 1 ♀ (NWUX, RMNH), same data.

**Diagnosis.** Antenna of ♀ with 31–33 segments and 1.3–1.4× longer than fore wing; face smooth laterally and remainder largely superficially rugulose (Figs 12, 18, 24); mesoscutum yellowish brown; vein r of fore wing 0.3 × as long as vein 3-SR and 0.5–0.6 (♀) – 0.7 (♂) × width of pterostigma (Figs 1, 5, 17, 20); striae of second tergite largely longitudinal or nearly so (Figs 9, 21); setose part of ovipositor sheath approx. 0.7× as long as fore wing and nearly twice as long as hind tibia (Fig. 1).

**Description.** Holotype, ♀, length of body 2.6 mm, of fore wing 2.8 mm.

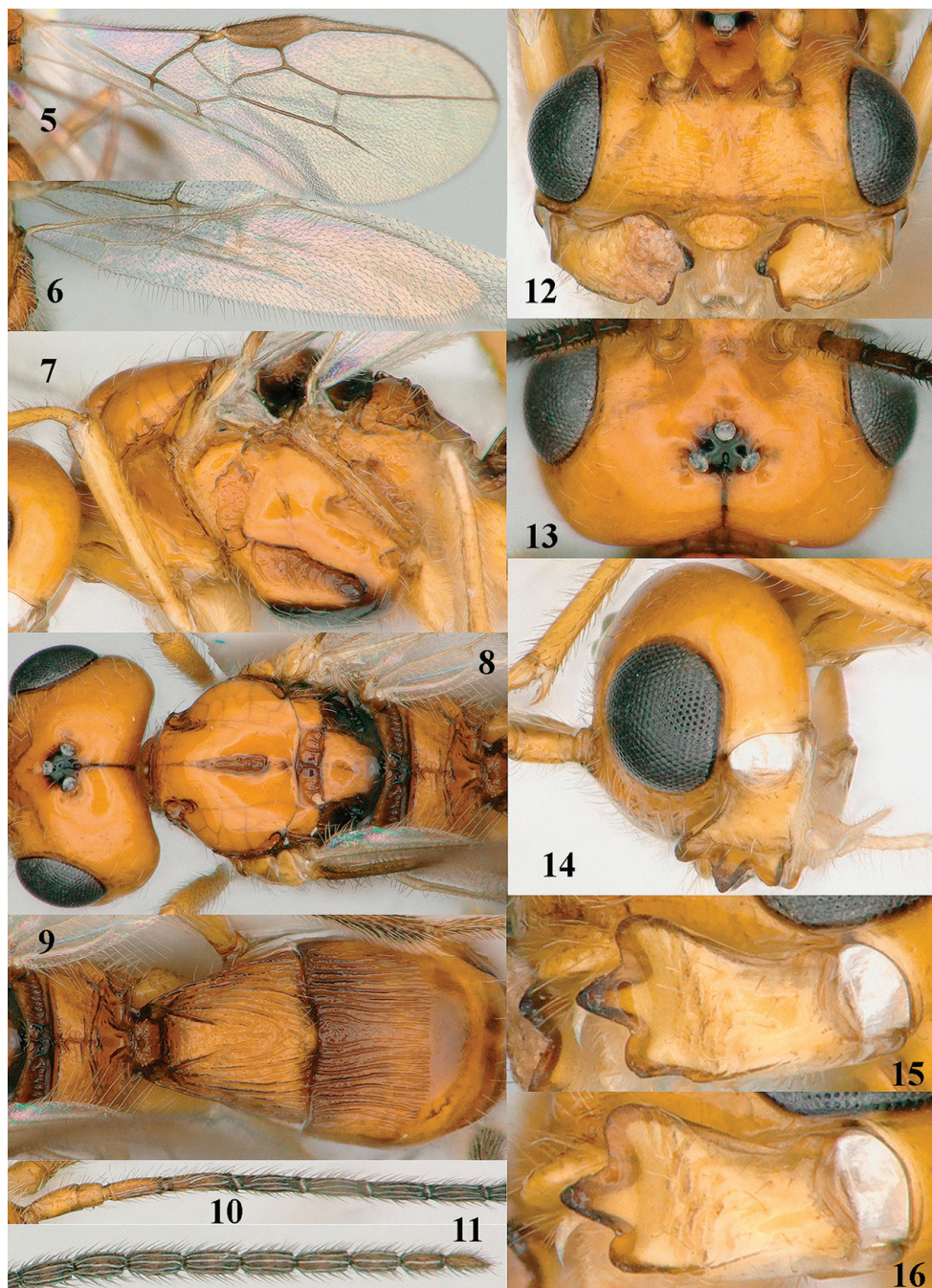
**Head:** Moderately transverse and shiny, slightly concave posteriorly (Fig. 8), width of head 1.8× its lateral length; antenna with 31 segments and 1.4× longer than fore wing, segments with long bristly setae, third segment 0.8× as long as fourth segment and 1.3× wider than fourth segment in lateral view, length of third, fourth and penultimate segments 2.4, 4.0 and 2.8× their width, respectively (Figs 10, 11); length of maxillary palp 1.3× height of head; eye in dorsal view 1.5× as long as temple (Fig. 8); frons depressed in front of anterior ocellus and with shallow reversed V-shaped depression anteriorly (Fig. 13); vertex convex and very sparsely setose; OOL: diameter of ocellus: POL = 15:4:5; face 2.1× wider than high, largely smooth laterally and dorsally, superficially rugulose medially but with longitudinal convex median area smooth (Fig. 12); clypeus 2.2× wider than high, protruding, semicircular and nearly truncate medio-ventrally (Fig. 12); malar space virtually absent; mandible moderately widened dorsally and ventrally sinuate, dorsal tooth large and lobe-shaped, similar to ventral



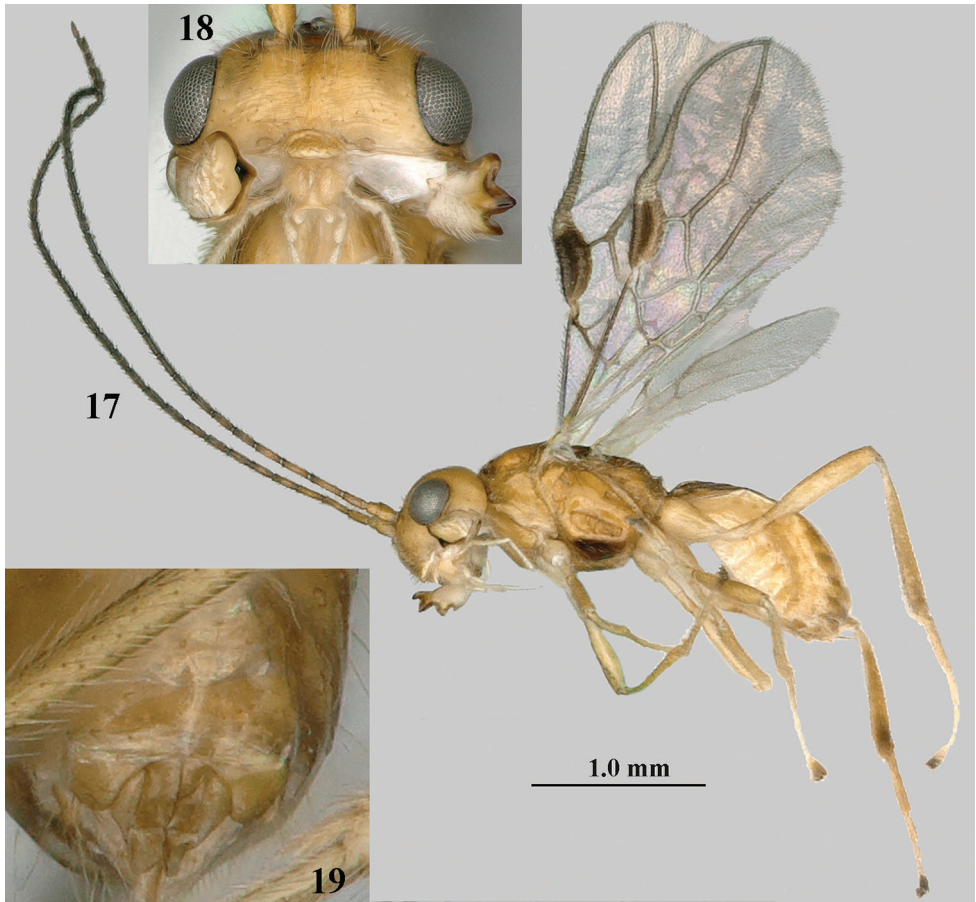
**Figures 1–4.** *Separatatus yinshani* Zhang & van Achterberg, sp. nov., ♀, holotype **1** habitus, lateral aspect **2** apex of ovipositor, lateral aspect **3** antenna **4** middle tarsus and outer claw, lateral aspect.

tooth and with minute ventral protuberance, middle tooth curved and robust; medial length of mandible  $1.5\times$  its maximum width (Figs 14–16).

**Mesosoma:** Length of mesosoma  $1.5\times$  its height; mesoscutum with lateral carina in front of tegulum distinct (Fig. 7); pronotal sides smooth except for oblique carina anteriorly; epicnemial area widely depressed and partly crenulate (Fig. 7); precoxal sulcus very wide, oblique, coarsely crenulate, up to anterior depression but absent posteriorly (except short depression above middle coxa; Fig. 7); remainder of mesopleuron smooth and largely glabrous; pleural sulcus narrowly crenulate; episternal scrobe medium-sized



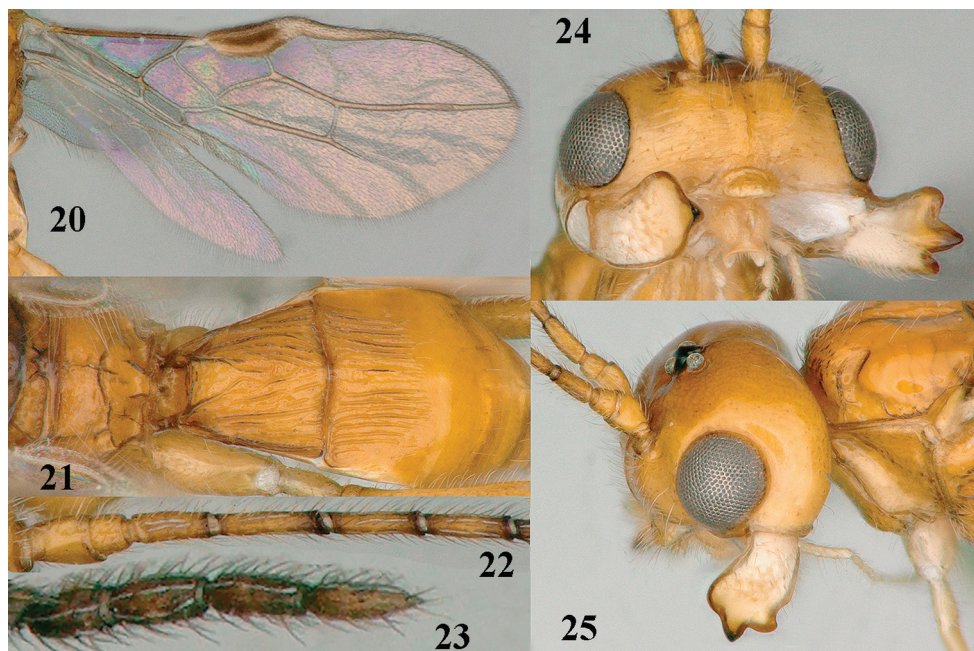
**Figures 5–16.** *Separatatus yinshani* Zhang & van Achterberg sp. nov., ♀, holotype **5** fore wing **6** hind wing **7** mesosoma, lateral aspect **8** head and mesosoma, dorsal aspect **9** propodeum, first–third metasomal tergites, dorsal aspect **10** basal antennal segments **11** apical antennal segments **12** head, anterior aspect **13** head, dorsal aspect **14** head, lateral aspect **15** mandible, full view of third tooth **16** mandible, full view of first tooth.



**Figures 17–19.** *Separatatus yinshani* Zhang & van Achterberg sp. nov., ♂, paratype **17** habitus, lateral aspect **18** head, anterior aspect **19** genitalia, ventral aspect.

and oblique; metapleuron largely smooth but with some coarse carinae posteriorly, with long setae and rather small pit anteriorly; pronope medium-sized compared to length of pronotum and nearly round (Fig. 8); notauli crenulate and wide, but only anteriorly impressed on disc; medio-posterior depression of mesoscutum long and deep, finely crenulate and up to level of notauli (Fig. 8); mesoscutum strongly shiny and smooth, with some setae anteriorly and posteriorly of notauli; scutellar sulcus deep and wide, with 5 carinae and 3× wider than its maximum length; scutellum rather convex and smooth, sparsely setose (Fig. 8); metanotum hardly protruding medio-posteriorly and only anterior half with median carina; medio-longitudinal carina of propodeum medium-sized, connected to (partly double) curved carina and areola incomplete, only posteriorly with pair of curved carinae and laterally crenulate, remainder largely smooth (Figs 8, 9).

**Wings** (Figs 1, 5, 6): Pterostigma elliptical, rather swollen, apically differentiated from widened basal part of 1-R1; vein r 0.6× width of pterostigma; r: 3-SR:SR1 = 5:19:52;



**Figures 20–25.** *Separatatus yinshani* Zhang & van Achterberg sp. nov., ♂, paratype **20** wings **21** propodeum, first–third metasomal tergites, dorsal aspect **22** basal antennal segments **23** apical antennal segments **24** head, anterior aspect **25** head, lateral aspect.

SR1 straight and 2-SR curved posteriorly; cu-a subinterstitial, short; 3-CU1 much longer than CU1b; 2-SR: 3-SR: r-m = 19:19:11; m-cu postfurcal, strongly converging to 1-M posteriorly; first subdiscal cell 2.7× as long as wide; M+CU1 largely sclerotized. Hind wing: M+CU: 1-M: 1r-m = 23:17:10; m-cu faintly indicated.

**Legs:** Hind coxa smooth; tarsal claws rather robust and shorter than arolium (Fig. 4); length of femur, tibia and basitarsus of hind leg 5.3, 11.2 and 4.4 × their width, respectively; hind leg rather conspicuously setose.

**Metasoma:** Length of first tergite equal to its apical width, its surface largely coarsely longitudinally striate (but striae partly converging posteriorly), its dorsal carinae widely separated (Fig. 9); dorsope distinct, medium-sized (Fig. 9); second tergite entirely coarsely longitudinally striate; third tergite smooth and in lateral view distinctly convex (Fig. 1); setose part of ovipositor sheath with rather short and dense setae, 0.61× as long as fore wing (total visible sheath (including glabrous band-shaped part) 0.68×), 1.5× metasoma, 3.2× first tergite and 1.7× as long as hind tibia; hypopygium acute apically and weakly sclerotized.

**Colour:** Brownish yellow; mandible, palpi, tegulum, humeral plate and legs (but hind tibia (except basally) and tarsus infuscate) pale yellowish or ivory; antenna (except 3 basal segments), mesosternum largely, scutellum laterally and posteriorly and ovipositor sheath dark brown; pterostigma (except pale yellowish apex) and most veins brown; second and third tergites slightly darkened; wing membrane subhyaline.

**Variation:** The wing venation of males show distinct sexual dimorphism (Figs 17, 20), the pterostigma is enlarged and apically distinctly differentiated from the strongly widened basal part of vein 1-R1. Additionally, veins 3-SR, 2-M, and SR1 of fore wing are widened. The body length of females is 2.5–3.0 mm and, of males, 2.6–2.8 mm; the length of the fore wing of females is 2.8–3.0 mm and, of males, 2.7–3.0 mm; the antennal segments of females is 31(1), 33(1) and, of males, 29(1), 31(2), 32(1), and 33(1); the antenna is 1.3–1.5× as long as the fore wing. The setose part of the ovipositor sheath is 0.61–0.63× as long as the fore wing. The mesosternum is brownish yellow or largely dark brown, and up to basal third of the antenna may be brownish yellow or brown.

**Etymology.** Named after the father of one of the co-authors (RNZ) in recognition of his support for many years.

### ***Bobekia* Niezabitowski, 1910**

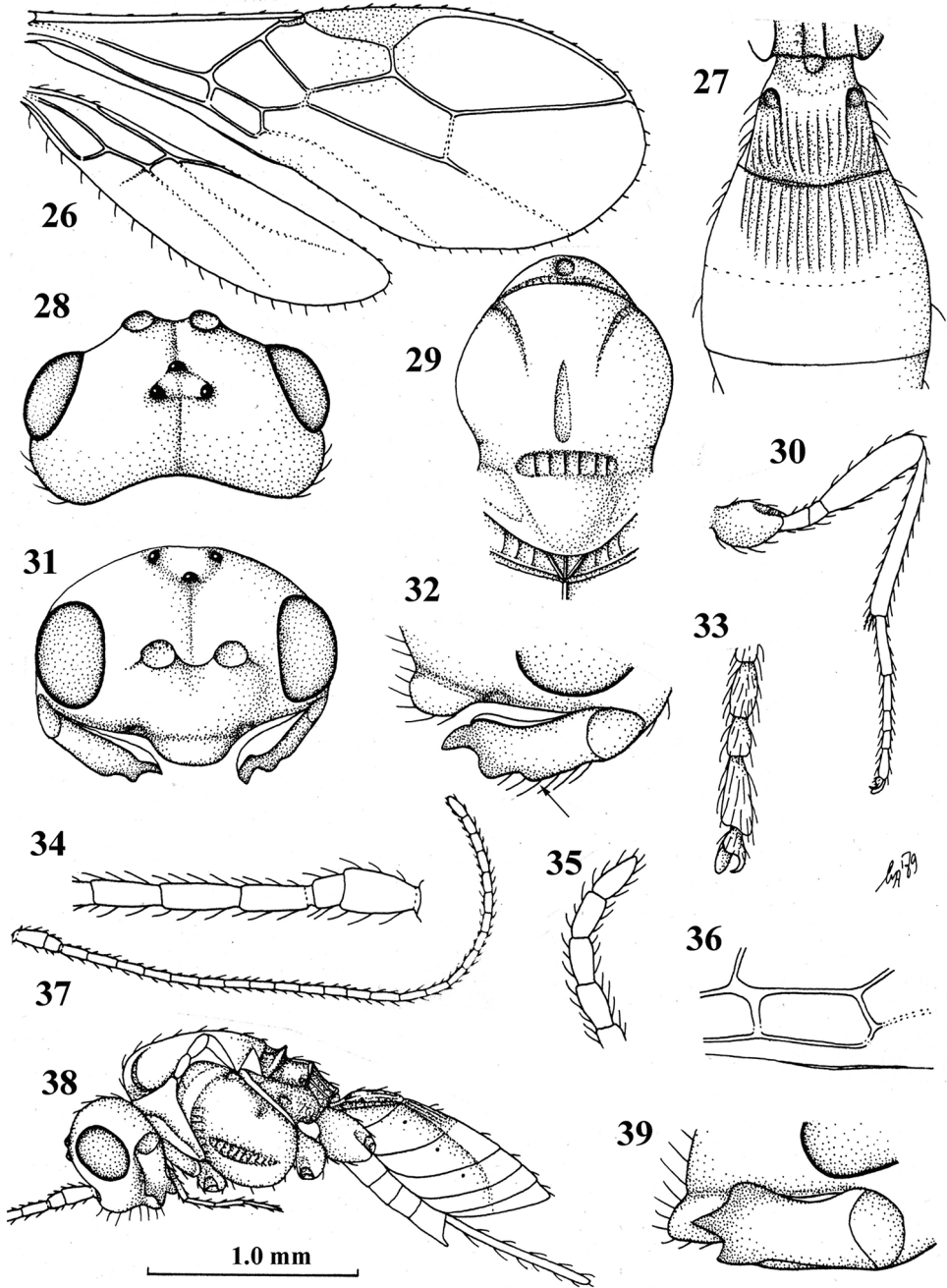
Figs 26–39

*Bobekia* Niezabitowski, 1910: 102; Fischer 1971: 137–139 (as synonym of *Symphanes* Foerster, 1863); Shenefelt 1974: 1020 (id.); Wharton 1980: 68 (id.); van Achterberg 1998: 106 (as valid genus). Type species: *Bobekia montana* Niezabitowski, 1910, designated by Shenefelt (1974) (= *Alysia striolata* Thomson, 1895; synonymized by Fischer (1974)) [holotype (PAN) examined].

*Neosymphanes* Belokobylskij, 1998: 294 (as subgenus of *Symphanes* Foerster, 1863). Type species (by original designation): *Alysia striolata* Thomson, 1895 [holotype (ZIL) examined]. Syn. nov.

**Notes.** A small genus with species from the Palaearctic and Afrotropical regions of which the type species and only named Palaearctic species has been reared from Agromyzidae (Yu et al. 2016). One of us (CvA) has seen Afrotropical specimens (RMNH) reared from mining Muscidae (*Atherigona* sp.). Unfortunately, host specimens were not retained and no additional data exists on how the specimens were reared.

As indicated by van Achterberg (1998), the genus *Symphanes* Foerster, 1863, is morphologically heterogeneous and does not belong to the *Bobekia*-group. Also, *Bobekia* is a separate genus from *Symphanes*. *Symphanes* is excluded because of the absence of a distinct dorsople in the first metasomal tergite (distinctly developed in *Bobekia*), tarsal claws angulate (evenly curved in *Bobekia*), first subdiscal cell of fore wing narrowly open (closed in *Bobekia*), and third antennal segment slightly longer than fourth segment (slightly shorter in *Bobekia*). *Neosymphanes* is a junior synonym of *Bobekia* because they share the same type species, *Bobekia montana* Niezabitowski, 1910, which was synonymized with *Alysia striolata* Thomson, 1895 by Fischer (1974). The differences between the types of *B. montana* and *A. striolata* are minimal: the ovipositor sheath is more retracted in *A. striolata* and vein 3-CU1 of the fore wing is distinctly longer than CU1b in *B. montana* (Fig. 36) and about equal in *A. striolata*.



**Figures 26–39.** *Bobekia montana* Niezabitowski, ♀, holotype **26** wings **27** first–third metasomal tergites, dorsal aspect **28** head, dorsal aspect **29** mesosoma, dorsal aspect **30** hind leg **31** head, anterior aspect **32** mandible, full view of third tooth (fourth tooth arrowed) **33** outer hind claw, lateral aspect **34** basal antennal segments **35** apical antennal segment **36** detail of first subdiscal cell of fore wing **37** antenna **38** habitus, lateral aspect **39** mandible, full view of first tooth.

***Bobekoides* van Achterberg, 1998**

Figs 40–52

*Bobekoides* van Achterberg, 1998: 105; Zheng et al. 2013: 143. Type species (by original designation): *Bobekoides fulvus* van Achterberg, 1998 [holotype (ZIL) examined].

**Notes.** A genus with a few species in the Afrotropical region. The biology is unknown. See van Achterberg (1998) for a key to species; see *Separatatus* for the Chinese species.

***Hoalysia* Granger, 1949**

Figs 53–64

*Hoalysia* Granger, 1949: 400; Shenefelt 1974: 992; Fischer 1993: 609–611, 1999: 9–10. Type species (by monotypy); *Hoalysia seyrigi* Granger, 1949 [holotype (MNHN) examined].

**Notes.** The main characters are the medial position of vein r at the pterostigma and the aberrant venation of the fore wing in males (Fig. 53), which is unknown in other genera. Only two Afrotropical species are known. For their identification, see the key by Fischer (1999). So far, no males are known in China with similar venation, but Chinese male *Separatatus* with aberrant venation (Figs 17, 20) are known. Therefore, Wharton's (2002) reference to Taiwanese specimens with widened veins probably refers to a species of *Separatatus*. The biology is unknown.

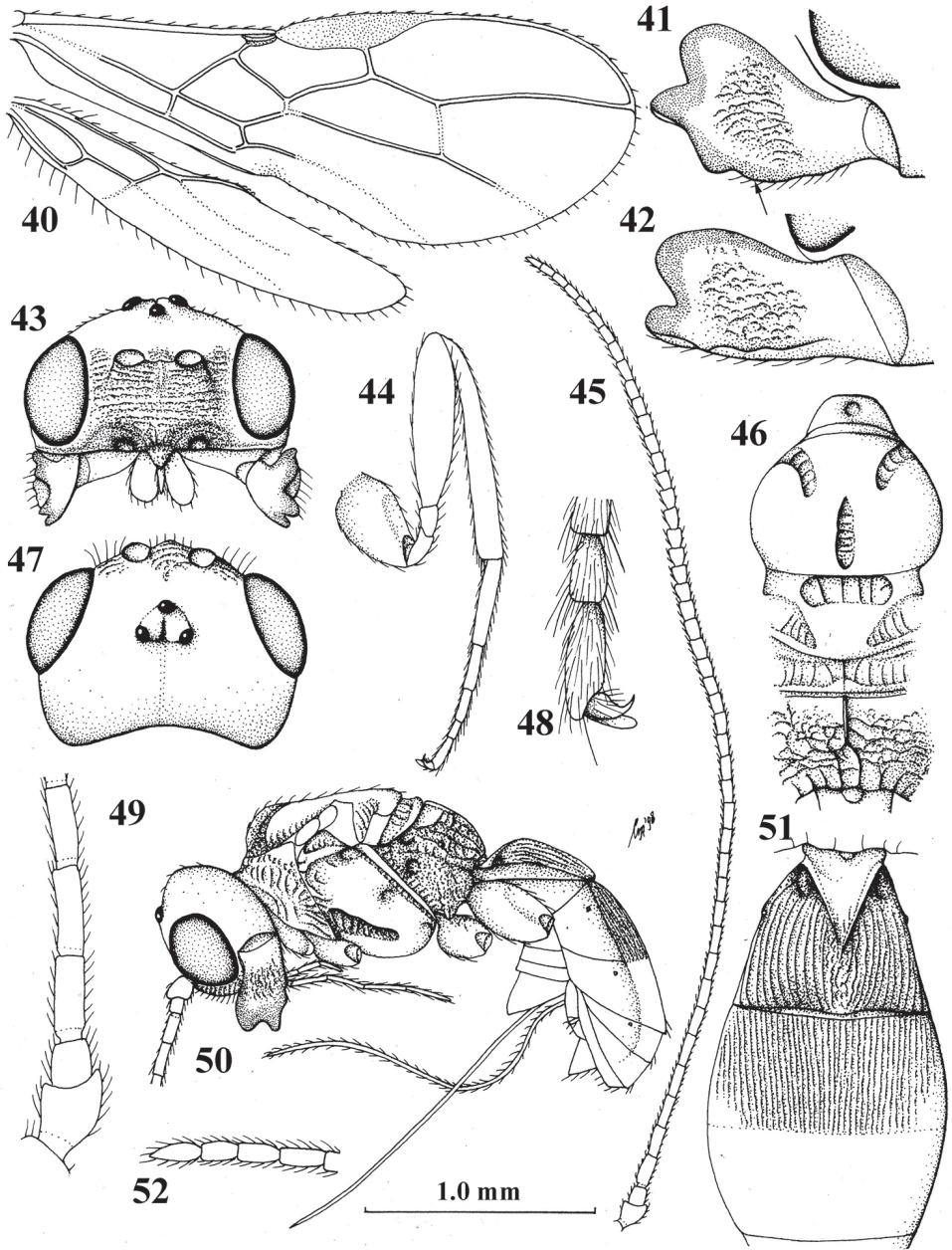
***Hylcalosia* Fischer, 1967**

Figs 65–78

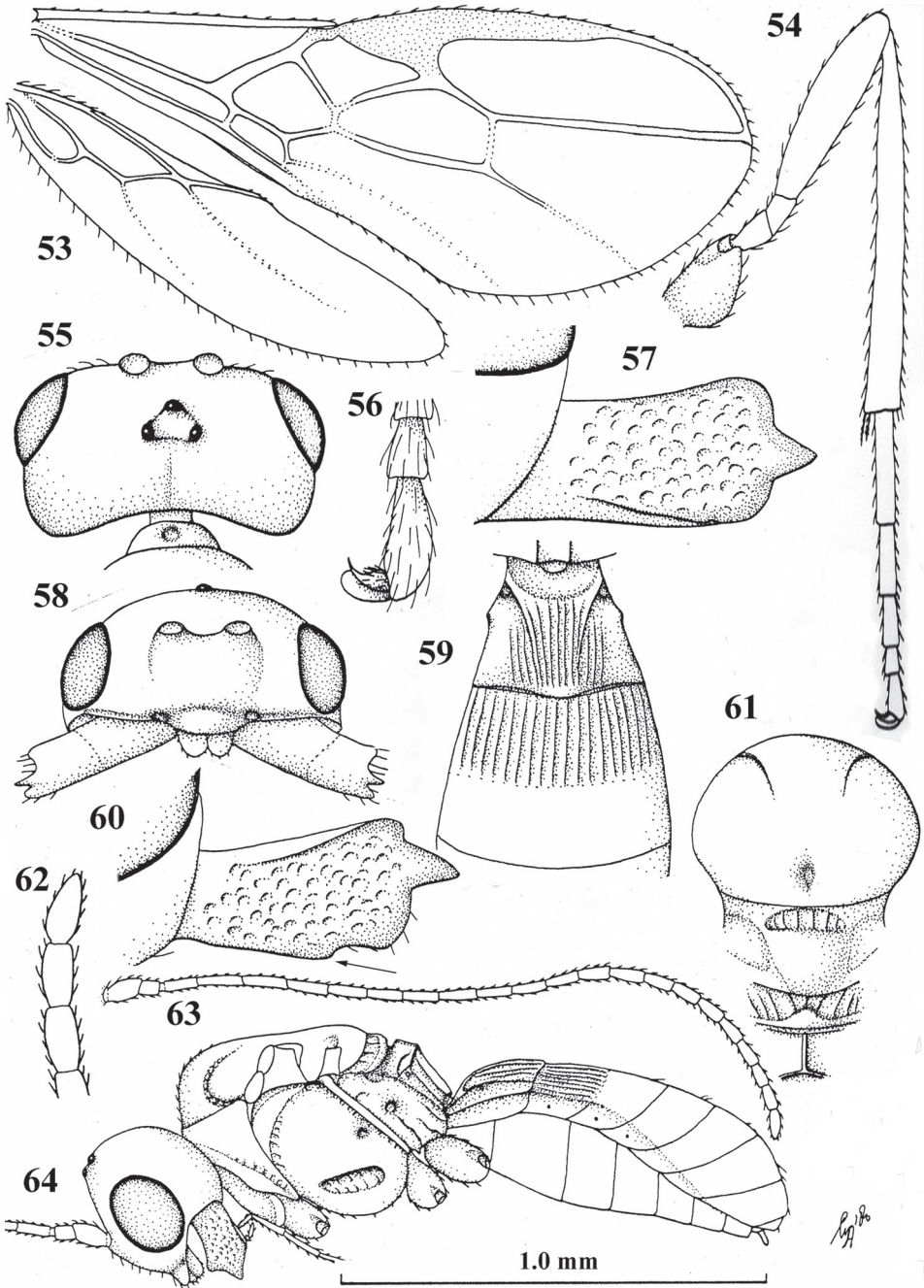
*Holcalysia* Cameron 1910: 6; Shenefelt 1974: 993. Type species (by monotypy): *Holcalysia ruficeps* Cameron, 1910 [holotype (ZMB) examined].

*Hylcalosia* Fischer, 1967: 125 (replacement name for *Holcalysia* Cameron, 1910 (not Cameron 1905), 2008: 718–722; Shenefelt 1974: 993; van Achterberg 1983: 81; Belokobylskij 1992: 143, 1998: 297, 2015: 530; Chen and Wu 1994: 85; Papp 1994: 139–142; Wharton 2002: 23; Zheng et al. 2012: 454; Zhu et al. 2017: 63–64, 2018: 548; Yao et al. 2019: 4. Type species (by monotypy): *Holcalysia ruficeps* Cameron, 1910 [holotype (ZMB) examined].

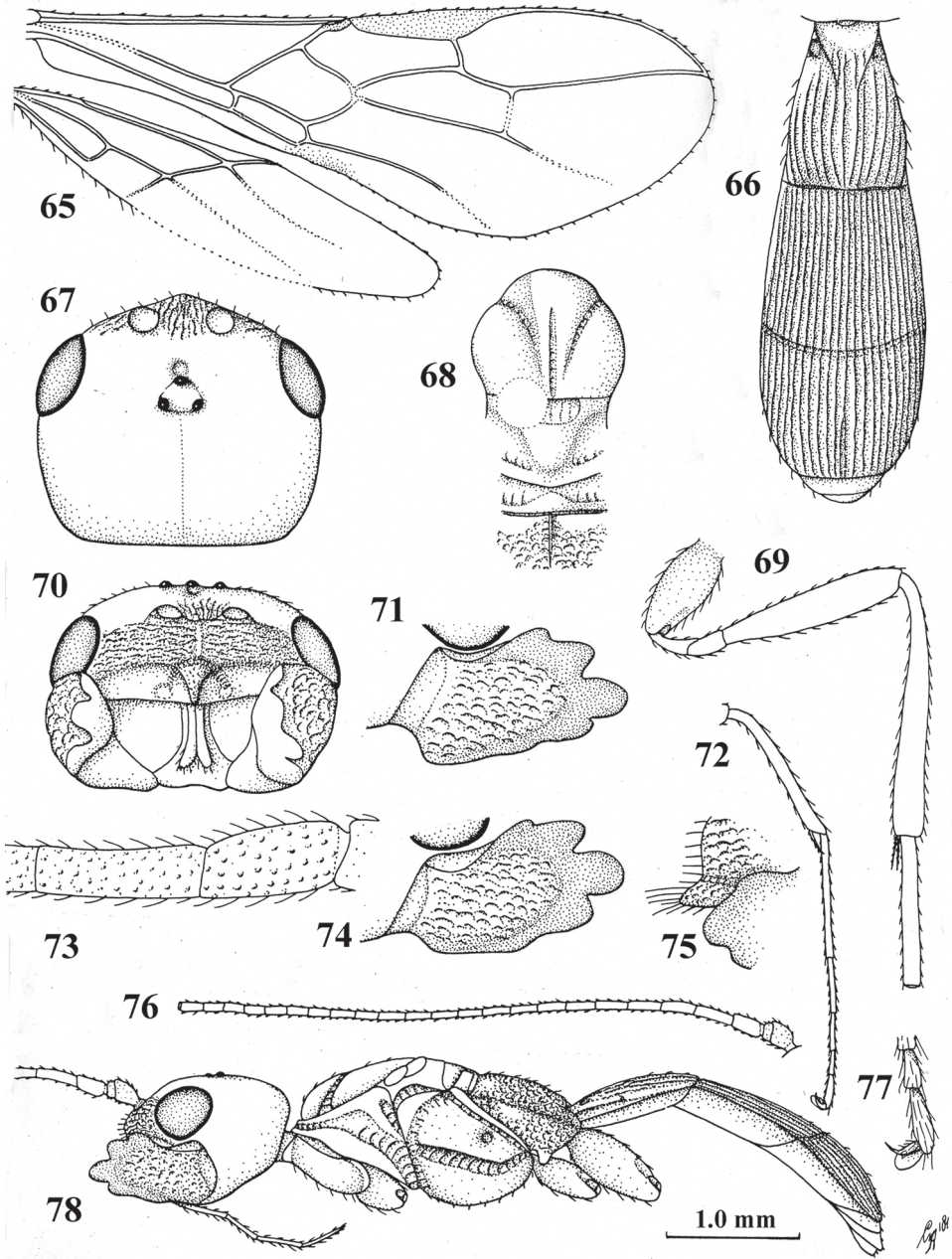
**Notes.** A rather small Palaearctic and Oriental genus, of which the biology is unknown. Wharton (2002) included it in his generic key for Australia, suggesting its occurrence in the Australasian region. *Hylcalosia* species show several apomorphic character states



**Figures 40–52.** *Bobekoides fulvus* van Achterberg, ♀, holotype **40** wings **41** mandible, full view of third tooth (fourth tooth arrowed) **42** mandible, full view of first tooth **43** head, anterior aspect **44** hind leg **45** antenna **46** mesosoma, dorsal aspect **47** head, dorsal aspect **48** outer hind claw, lateral aspect **49** basal antennal segments **50** habitus, lateral aspect **51** first–third metasomal tergites, dorsal aspect **52** apical antennal segments.



**Figures 53–64.** *Hovalysia seyrigi* Granger, ♂, holotype **53** wings **54** hind leg **55** head, dorsal aspect **56** outer hind claw, lateral aspect **57** mandible, full view of first tooth **58** head, anterior aspect **59** first–third metasomal tergites, dorsal aspect **60** mandible, full view of third tooth (fourth tooth arrowed) **61** mesosoma, dorsal aspect **62** apical antennal segments **63** antenna **64** habitus, lateral aspect.



**Figures 65–78.** *Hylcalosia ruficeps* (Cameron), ♂, holotype **65** wings **66** first–third metasomal tergites, dorsal aspect **67** head, dorsal aspect **68** mesosoma, dorsal aspect **69** hind leg **70** head, anterior aspect **71** mandible, full view of first tooth **72** fore tibia and tarsus **73** basal antennal segments **74** mandible, full view of third and fourth teeth **75** clypeus lateral aspect **76** antenna **77** outer fore claw, lateral aspect **78** habitus, lateral aspect.

within the *Bobekia*-group, as expressed by the shape of the clypeus, mandible (especially in the type species; Fig. 74), and metasoma (more or less carapace-like; Fig. 78). Identification keys to species were given by Zhu et al. (2018) and Yao et al. (2019).

***Neodiasta van Achterberg, gen. nov.***

<http://zoobank.org/10A95EB9-7224-4CF3-A65A-A96C9E69A499>

Figs 79–91

**Type species.** *Phasmidiasta ecuadorensis* Fischer, 2006.

**Diagnosis.** Third antennal segment shorter than fourth segment and slender (Fig. 91); mandible strongly widened apically, with minute ventral lobe and no oblique ventral carina, with 3 large teeth, middle tooth much smaller than upper tooth, upper tooth without dorso-apical protuberance, ventral margin straight but near third lobe-shaped tooth with minute lobe (Figs 85, 90); clypeus obtuse ventrally, semicircular (Figs 85, 87, 90); face normally convex and not protruding medially (Figs 87, 89); pronope deep and medium-sized (Fig. 88); precoxal sulcus wide and coarsely crenulate medially; vein 2-SR of fore wing straight posteriorly (Fig. 79); vein r of fore wing issued behind medially from pterostigma and pterostigma parallel-sided to narrow elliptical (Fig. 79); vein CU1b of fore wing distinctly shorter than vein 3-CU1 and vein CU1a distinctly below level of vein CU1 (Fig. 79); first subdiscal cell of fore wing closed distally and moderately wide (Fig. 79); vein M+CU of hind wing distinctly shorter than vein 1-M (Fig. 80); first metasomal tergite with distinct dorsope; second tergite distinctly striate basally (Fig. 83) and third tergite smooth; shape of ovipositor and length of ovipositor sheath unknown (only ♂ known).

**Distribution.** Neotropical (one species).

**Notes.** The biology of the only known specimen (the male holotype from Ecuador) is unknown. The type species does not fit in *Phasmidiasta* because the precoxal sulcus is present and coarsely crenulate (absent in *Phasmidiasta*), the face is medially not protruding (distinctly protruding in *Phasmidiasta*), vein SR1 of the fore wing about as long as vein 3-SR (about 4× as long in *Phasmidiasta*), vein M+CU of the hind wing is distinctly shorter than vein 1-M (longer than vein 1-M in *Phasmidiasta*), mandible without oblique carina connected to third tooth (present in *Phasmidiasta*), and the pterostigma is parallel-sided to narrowly elliptical (moderately widely elliptical to triangular in *Phasmidiasta*).

**Etymology.** Name derived from a combination of “neo” (Greek for “new”) and the generic name *Phasmidiasta*, because it occurs in the Neotropical region and was formerly included in *Phasmidiasta*. Gender: feminine.

***Neodiasta ecuadorensis* (Fischer, 2006) comb. nov.**

Figs 79–91

*Phasmidiasta ecuadorensis* Fischer, 2006: 628–629.

**Type material. Holotype:** ♂ (BZL), “Ecuador: Tungurahua prov., Banos, 14.ii.2002, 1500 m, M. Halada”, “♂ **Holotype:** *Phasmidiasta ecuadorensis* sp. nov., M. Fischer, det. 2005”.

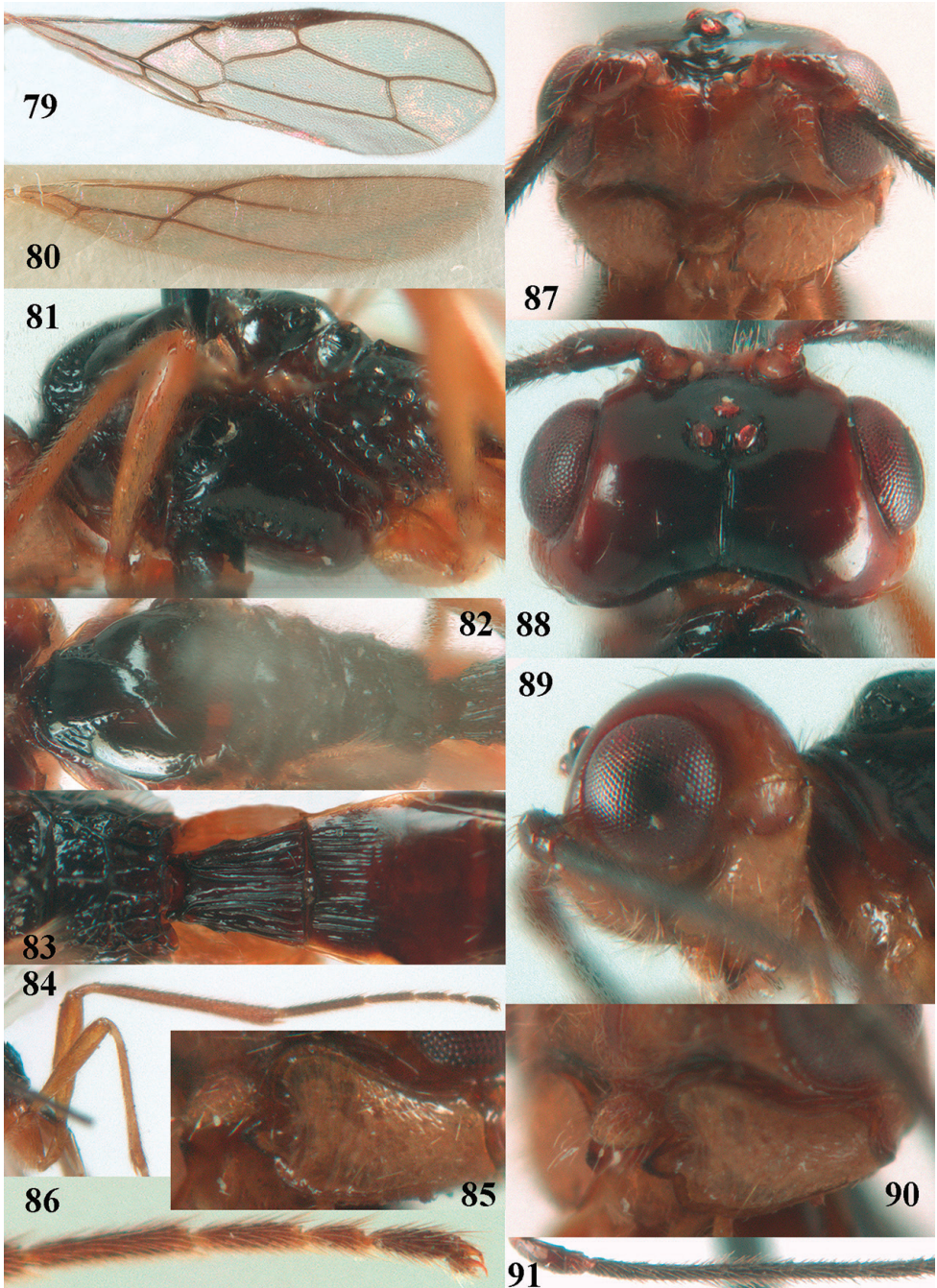
**Diagnosis.** See genus diagnosis.

**Description.** Holotype, ♂, length of body 4.3 mm, of fore wing 4.3 mm.

**Head:** Head moderately transverse and shiny, concave posteriorly (Fig. 88), width of head 1.8× its lateral length; antenna incomplete, 27 segments remaining and segments with long bristly setae, third segment 0.8× as long as fourth segment and 1.2× wider than fourth segment in lateral view, length of third and fourth segments 2.7 and 4.2× their width, respectively (Fig. 91); length of maxillary palp 1.8× height of head; eye in dorsal view 1.6× as long as temple (Fig. 88); frons largely flat in front of anterior ocellus and only behind antennal sockets with narrow depression (Fig. 88); vertex convex and very sparsely setose; OOL: diameter of ocellus: POL= 9:2:2; face 2.4 × wider than high, largely striate laterally, largely smooth medio-dorsally, moderately convex and with longitudinal convex median area (Fig. 87); clypeus 1.3× wider than high, protruding, semicircular and nearly truncate medio-ventrally (Fig. 87); malar space virtually absent; mandible strongly widened dorsally and ventrally straight, but near third lobe-shaped tooth with minute lobe, dorsal tooth large and lobe-shaped, larger than similar ventral tooth, middle (= second) tooth curved, small compared to first tooth and robust; medial length of mandible 1.6× its maximum width (Figs 85, 90).

**Mesosoma:** Length of mesosoma 1.6× its height; mesoscutum with lateral carina in front of tegulae distinct and crenulate; pronotal sides shiny and smooth but oblique groove crenulate anteriorly and sparsely crenulate posteriorly; epicnemial area depressed anteriorly and partly crenulate (Fig. 81); precoxal sulcus very wide, oblique, coarsely crenulate, but posterior 0.3 absent (except short depression above middle coxa; Fig. 81); remainder of mesopleuron smooth and largely glabrous except ventrally; pleural sulcus finely crenulate; episternal scrobe medium-sized and oblique; metapleuron largely smooth but with some rugae medially, with some long setae and deep pit anteriorly; mesosternal sulcus finely crenulate; pronope medium-sized (compared to length of pronotum in dorsal view), deep and nearly round (Fig. 88); notauli distinctly crenulate and wide, but posteriorly narrow and nearly smooth; medio-posterior depression of mesoscutum long and deep, smooth and up to level of notauli (Fig. 82); mesoscutum strongly shiny and smooth, largely glabrous; scutellar sulcus deep and wide, with one carina, narrowed medially and 2.4× wider than its maximum length; scutellar disc weakly convex (but posteriorly rather bulging), largely glabrous and smooth (Fig. 81); metanotum hardly protruding and only anterior half with median carina; medio-longitudinal carina of propodeum coarse and only on anterior face of propodeum, connected to complete parallel-sided areola, posterior face smooth between carinae and dorsally crenulate-rugose except smooth anterior area (Figs 81–83).

**Wings** (Figs 79, 80). Pterostigma very narrow elliptical (nearly parallel-sided), apically hardly differentiated from 1-R1 and vein r issued slightly behind middle of pterostigma; vein r 0.8× width of pterostigma; r:3-SR:SR1 = 5:31:31; SR1 and 2-SR straight; cu-a just postfurcal; 3-CU1 much longer than CU1b; 2-SR:3-SR:r-m = 25:31:14; m-cu far postfurcal, converging to 1-M posteriorly; first subdiscal cell 4.3×



**Figures 79–91.** *Neodiasta ecuadorensis* (Fischer), ♂, holotype **79** fore wing **80** hind wing **81** mesosoma, lateral aspect **82** mesosoma, dorsal aspect **83** propodeum, first–third metasomal tergites, dorsal aspect **84** hind leg **85** mandible, full view of first tooth **86** outer hind claw **87** head, anterior aspect **88** head, dorsal aspect **89** head, lateral aspect **90** mandible, full view of third tooth **91** basal antennal segments.

as long as wide; M+CU1 largely sclerotized. Hind wing: M+CU:1-M:1r-m = 34:45:16; m-cu distinct, curved and unsclerotized.

**Legs:** Hind coxa rugose dorsally and remainder largely smooth; tarsal claws rather slender, evenly curved and longer than arolium (Fig. 86); length of femur, tibia and basitarsus of hind leg 5.7, 12.0, and 9.6× their width, respectively; hind leg densely setose; hind tarsus slender (Fig. 86) and slightly longer than tibia.

**Metasoma:** Length of first tergite 1.1× its apical width, its surface coarsely longitudinally costate-striate, its dorsal carinae converging and meeting submedially (Fig. 83); dorsope deep and medium-sized (Fig. 83); basal 0.7 of second tergite entirely coarsely longitudinally striate; remainder of metasoma smooth; third tergite in lateral view flat.

**Colour:** Black or blackish brown; mandible, palpi, clypeus and second tergite laterally pale yellowish; legs (but hind tibia and all tarsi infuscate or dark brown), tegulae and basal half of metasoma ventrally brownish yellow; apical half of metasoma dark brown ventrally; face yellowish brown; propleuron posteriorly, orbita and temple reddish brown; pterostigma, second and third tergites dark brown and most veins brown; wing membrane subhyaline.

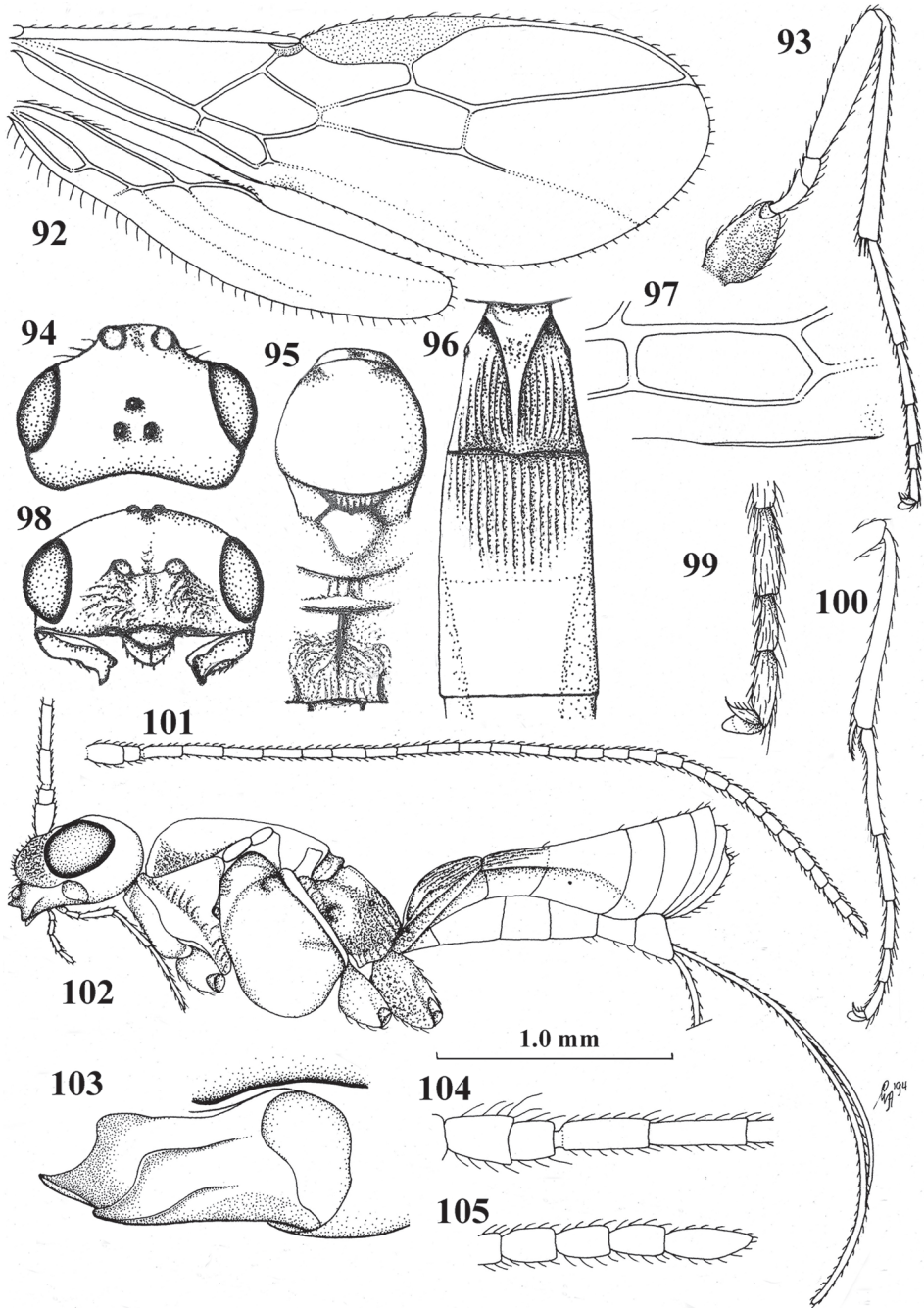
### ***Phasmidiasta* Wharton, 1980**

Figs 92–105

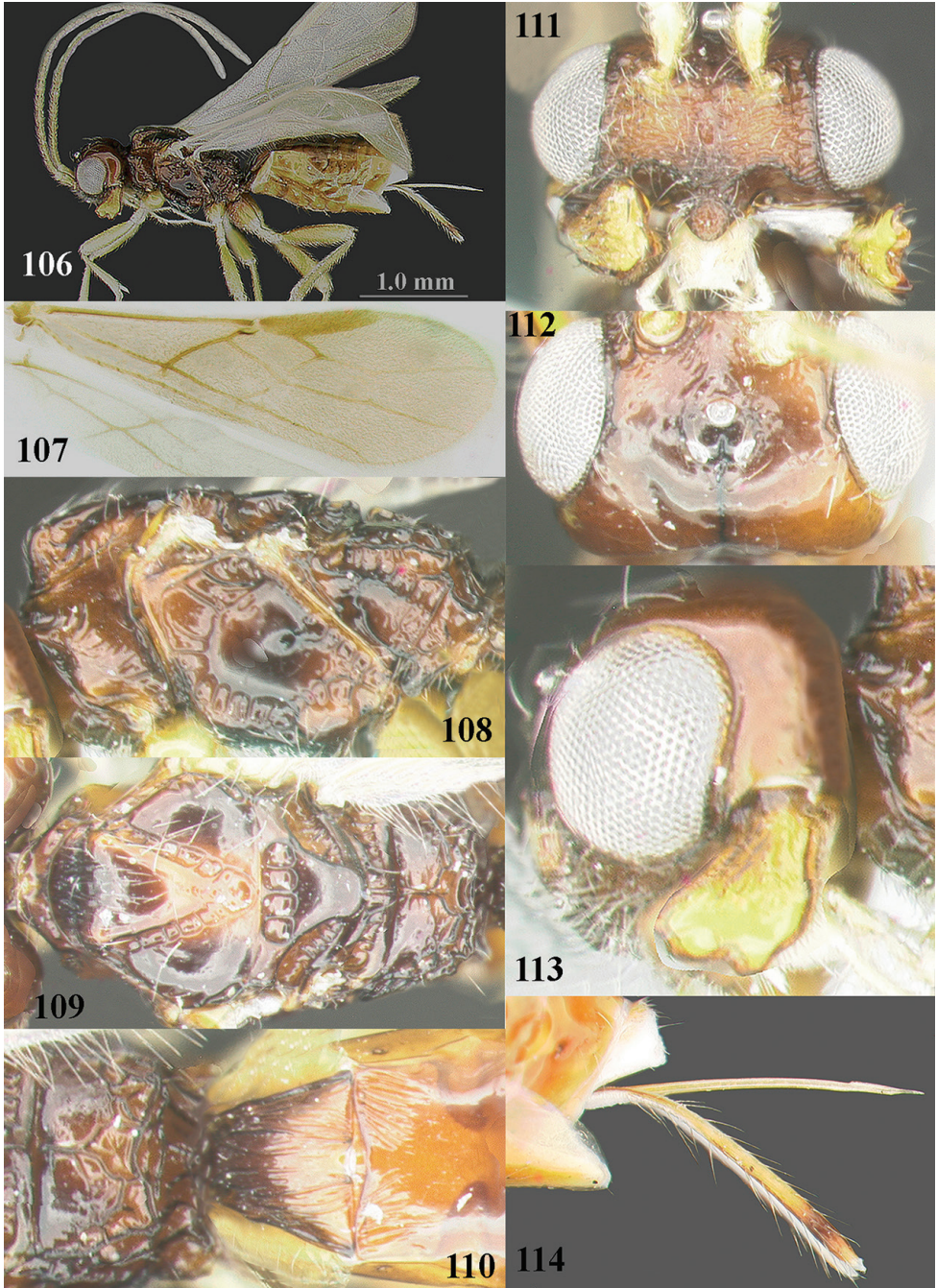
*Phasmidiasta* Wharton, 1980: 63; Belokobylskij 1998: 169, 294–296; Fischer 2006: 628. Type species (by original designation): *Phasmidiasta lia* Wharton, 1980 [holotype (CNC) examined].

**Notes.** The biology of this Holarctic genus is uncertain. It is likely a parasitoid of xylophilous fly larvae (Wharton 1980). Only two species are known: *P. effecta* Belokobylskij, 1998, occurs in the Eastern Palaearctic region (reared from a cocoon in a bark beetle gallery (Belokobylskij 1998) and the type species in the Nearctic region. The Neotropical *P. ecuadorensis* Fischer, 2006, does not belong in *Phasmidiasta* and is transferred to *Neodiasta* van Achterberg, gen. nov. (see above) and *P. malaysiae* Fischer, 2006, was transferred to *Separatatus* by Yao et al. (2018a). The species remaining in *Phasmidiasta* are very similar and may be separated as follows:

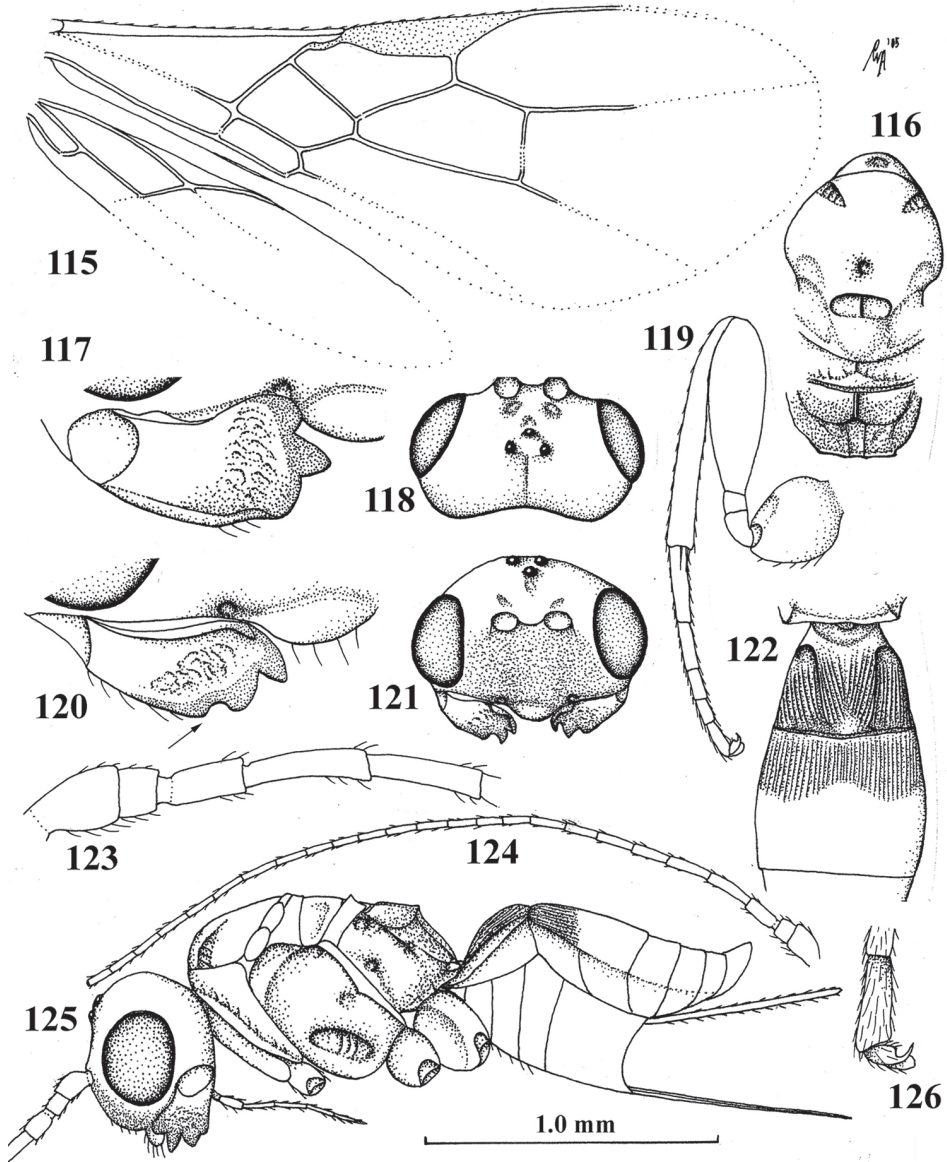
- 1 Scutellar sulcus laterally connected to posteriorly diverging and narrow oblique grooves (Fig. 95); ovipositor sheath 1.4–1.5× as long as metasoma and 0.6–0.7× as long as fore wing (Fig. 102); first metasomal tergite 1.2–1.4× as long as its apical width (Fig. 96); Nearctic (Canada) ..... ***P. lia* Wharton, 1980**
- Scutellar sulcus transverse, without narrow oblique grooves laterally; ovipositor sheath 1.1 × as long as metasoma and 0.7 × as long as fore wing; first tergite 1.5× as long as its apical width; Eastern Palaearctic (Far East Russia) ..... ***P. effecta* Belokobylskij, 1998**



**Figures 92–105.** *Phasmalsia lia* Wharton, ♀, holotype **92** wings **93** hind leg **94** head, dorsal aspect **95** mesosoma, dorsal aspect **96** first–third metasomal tergites, dorsal aspect **97** first subdiscal cell of fore wing **98** head, anterior aspect **99** outer hind claw, lateral aspect **100** fore tibia and tarsus lateral aspect **101** antenna **102** habitus, lateral aspect **103** mandible, full view of first tooth **104** basal antennal segments **105** apical antennal segments.



**Figures 106–114.** *Senwot yinxianggaoae* Yao, ♀, holotype **106** habitus, lateral aspect **107** wings **108** mesosoma, lateral aspect **109** mesosoma, dorsal aspect **110** propodeum, first–third metasomal tergites, dorsal aspect **111** head, anterior aspect **112** head, dorsal aspect **113** head, lateral aspect **114** ovipositor and its sheath, lateral aspect. Photos: J-L Yao.



**Figures 115–126.** *Separatatus carinatus* Chen & Wu, ♀, holotype **115** wings **116** mesosoma, dorsal aspect **117** mandible, full view of first tooth **118** head, dorsal aspect **119** hind leg **120** mandible, full view of third tooth (fourth tooth arrowed) **121** head, anterior aspect **122** first–third metasomal tergites, dorsal aspect **123** basal antennal segments **124** antenna **125** habitus, lateral aspect **126** outer hind claw, lateral aspect.

### ***Senwot* Wharton, 1983**

Figs 106–114

*Senwot* Wharton, 1983: 277–279; Fischer 1991: 31 (redescription). Type species (by original designation): *Senwot africanus* Wharton, 1983 [holotype (AEI) was unavailable].

**Notes.** A small genus of Afrotropical and Oriental species with unknown biology. The four species can be identified with the key by Yao et al. (2018b). Morphologically similar to *Bobekoides* and *Hylcalosia*, as shown by the shape of the mandible and clypeus, the genus differs mainly by the parallel-sided and more or less elongated pterostigma (in Asian spp. less than in African spp.).

## Acknowledgements

We wish to thank Dr Martin Schwarz (BZL) for the loan of the holotype of *Phasmidiasta ecuadorensis*, Dr Jun-li Yao (Fuzhou) for allowing us to use her photos of *Senwot yinxianggaoae*, and Dr Sergey Belokobylskij (St Petersburg) for additional information on *Phasmidiasta effecta*. The research was supported jointly by the National Natural Science Foundation of China (NSFC, No. 31201732, 31572300, 31872263), and the Agricultural Sci-Tech Innovation Programme of Xi'an Science and Technology Bureau (no. 201806116YF04NC12-1).

## References

- Belokobylskij SA (1992) Finding of the genus *Hylcalosia* (Hymenoptera, Braconidae, Alysiinae) of the USSR and descriptions of two new species from the south of the Far East. *Zoologicheskii Zhurnal* 71(5): 143–149. [translation: *Entomological Review* 71(9): 142–147]
- Belokobylskij SA (1998) 9. Alysiinae (Alysiini). In: Ler PA (Ed.) *Opredelitel Nasekomykh Dal'nego Vostoka Rossii* (T. IV). *Setchatokryloobraznye, Skorpionnitsy, Pereponchatokrylye*. Pt 3. Dal'nauka, Vladivostok, 163–298.
- Belokobylskij SA (2015) The genus *Hylcalosia* Fischer, 1967 (Hymenoptera: Braconidae: Alysiinae) of the Russian Far East. *Zootaxa* 4040(5): 530–542. <https://doi.org/10.11646/zootaxa.4040.5.2>
- Cameron P (1910) On some Asiatic species of the Braconid subfamilies Rhogadinae, Agathinae, and Macrocentrinae and of the Alysiidae. *Wiener Entomologische Zeitschrift* 29: 1–10. <https://doi.org/10.5962/bhl.part.23337>
- Chen J-H, Wu Z-S (1994) [The Alysiini of China: (Hymenoptera: Braconidae: Alysiinae).] China Agricultural Press, Fuzhou, 218 pp. [in Chinese, with English summary]
- Fischer M (1967) Seltene Alysiinae aus verschiedenen Erdteilen. *Annalen des Naturhistorischen Museums in Wien* 70: 109–138.
- Fischer M (1971) Untersuchungen über die europäischen Alysiini mit besonderer Berücksichtigung der Fauna Niederösterreichs (Hymenoptera, Braconidae). *Polskie Pismo Entomologiczne* 41: 19–160.
- Fischer M (1974) Studien an Alysiinen-Typen (Hymenoptera, Braconidae, Alysiinae). *Zeitschrift der Arbeitsgemeinschaft Österreichischer Entomologen* 25: 47–51.
- Fischer M (1993) Neubeschreibungen und Wiederbeschreibungen von Kieferwespen (Hym., Braconidae, Alysiinae: Tribus Alysiini) der Alten Welt. *Linzer biologische Beiträge* 25(2): 593–647.

- Fischer M (1999) Einiges über Kieferwespen (Hymenoptera, Braconidae, Alysiiinae). Linzer biologische Beiträge 31(1): 5–56.
- Fischer M (2006) Neue Kieferwespen aus der Sammlung des Biologiezentrums des Oberösterreichischen Landesmuseums in Linz und Mitteilungen über andere Arten (Hymenoptera, Braconidae, Alysiiinae). Linzer biologische Beiträge 38(1): 605–651.
- Fischer M (2008) Über die Gattungen *Idiasta* Foerster, *Aphaereta* Foerster und *Hylcalosia* Fischer (Hymenoptera, Braconidae, Alysiiinae). Linzer biologische Beiträge 40(1): 703–734.
- Niezabitowski EL (1910) Materyaly do fauny Brakonidow Polski. Braconidae, zebrane w Galicyi. Sprawozdania Akademii Umiejetnosci w Krakowie 44: 47–106.
- Papp J (1994) Braconidae (Hymenoptera) from Korea, XV. Acta Zoologica Academiae Scientiarum Hungaricae 40(2): 133–156.
- Shenefelt RD (1974) Hymenopterorum Catalogus (nova editio Braconidae 7. Alysiiinae, 7: 937–1113.
- van Achterberg C (1983) A revision of the genus *Hylcalosia* Fischer (Hymenoptera: Braconidae, Alysiiinae). Zoologische Mededelingen Leiden 57(8): 81–90.
- van Achterberg C (1988) Revision of the subfamily Blacinae Foerster (Hymenoptera, Braconidae). Zoologische Verhandelingen Leiden 249: 1–324.
- van Achterberg C (1998) *Bobekoides* gen. nov. (Hymenoptera: Braconidae: Alysiiinae) from South Africa. Zoologische Mededelingen Leiden 72(9): 105–111.
- van Achterberg C (1990) Illustrated key to the subfamilies of the Holarctic Braconidae (Hymenoptera: Ichneumonoidea). Zoologische Mededelingen Leiden 64: 1–20.
- van Achterberg C (1993) Illustrated key to the subfamilies of the Braconidae (Hymenoptera: Ichneumonoidea). Zoologische Verhandelingen Leiden 283: 1–189.
- van Achterberg C (2009) Can Townes type Malaise traps be improved? Some recent developments. Entomologische Berichten Amsterdam 69: 129–135.
- Wharton RA (1980) Review of the Nearctic Alysiiini (Hymenoptera, Braconidae) with discussion of generic relationships within the tribe. University of California Publications in Entomology 88: 1–112.
- Wharton RA (2002) Revision of the Australian Alysiiini (Hymenoptera: Braconidae). Invertebrate Systematics 16(1): 7–105. <https://doi.org/10.1071/IT01012>
- Yao J-L, van Achterberg C, Sharkey MJ, Chen J-H (2018a) *Separatatus* Chen & Wu (Hymenoptera: Braconidae: Alysiiinae) newly recorded from Thailand, with description of one new species and one new combination. Zootaxa 4433(1): 187–194. <https://doi.org/10.11646/zootaxa.4433.1.12>
- Yao J-L, van Achterberg C, Sharkey MJ, Chapman EG, Chen J-H (2018b) *Senwot* Wharton, a new genus for the Oriental region with description of two new species from Thailand (Hymenoptera: Braconidae: Alysiiinae). Journal of Asia-Pacific Entomology 22(1): 103–109. <https://doi.org/10.1016/j.aspen.2018.12.001>
- Yao J-L, van Achterberg C, Sharkey MJ, Chapman EG, Chen J-H (2019) Five species and a genus new for Thailand, with description of five new species of *Hylcalosia* Fischer (Hymenoptera: Braconidae: Alysiiinae). Insect Systematics & Evolution. <https://doi.org/10.1163/1876312X-00002303>
- Yu DSK, van Achterberg C, Horstmann K (2016) Taxapad 2016, Ichneumonoidea 2015. Database on flash-drive. Ottawa. <http://www.taxapad.com>

- Zheng M-L, Chen J-H, Yang J-Q (2013) The discovery of the genus *Bobekoides* van Achterberg (Hymenoptera, Braconidae) in China, with description of one new species. *Acta Zootaxonomica Sinica* 38(1): 143–146.
- Zhu J-C, van Achterberg C, Chen X-X (2017) An illustrated key to the genera and subgenera of the Alysiini from China (Hymenoptera, Braconidae, Alysiinae). *ZooKeys* 722: 37–79. <https://doi.org/10.3897/zookeys.722.14799>
- Zhu J-C, van Achterberg C, Chen X-X (2018) Review of the genus *Hylcalosia* Fischer (Hymenoptera, Braconidae, Alysiinae), with description of four new species from China. *Zootaxa* 4462(4): 547–565. <https://doi.org/10.11646/zootaxa.4462.4.7>



# Redescriptions of two parasitoids, *Metapelma beijingense* Yang (Hymenoptera, Eupelmidae) and *Spathius ochus* Nixon (Hymenoptera, Braconidae), parasitizing *Coraebus cavifrons* Descarpentries & Villiers (Coleoptera, Buprestidae) in China with keys to genera or species groups

Liang Ming Cao<sup>1</sup>, Cornelis van Achterberg<sup>2</sup>, Yan Long Tang<sup>3</sup>, Zhong Qi Yang<sup>1</sup>,  
Xiao Yi Wang<sup>1</sup>, Tian Wen Cao<sup>4</sup>

**1** The Key Laboratory of Forest Protection of National Forestry and Grassland Administration, Research Institute of Forest Ecology, Environment and Protection, Chinese Academy of Forestry, Beijing 100091, China **2** State Key Laboratory of Rice Biology, Ministry of Agriculture Key Lab of Agricultural Biology of Crop Pathogens and Insects, and Institute of Insect Sciences, Zhejiang University, Hangzhou 310058, China **3** Laboratory of Regional Characteristic for Conservation and Utilization of Plant Resource in Chishui River Basin, College of Biology and Agriculture, Zunyi Normal University, Zunyi, 563002, China **4** Shanxi Insect Herbarium, Institute of Plant Protection, Shanxi Academy of Agricultural Sciences, Taiyuan 030031, China

Corresponding author: Liang Ming Cao ([caolm1206@126.com](mailto:caolm1206@126.com))

Academic editor: A. Köhler | Received 22 November 2019 | Accepted 24 February 2020 | Published 13 April 2020

<http://zoobank.org/5A4CA4BA-59C1-4114-9370-F15834AB6476>

**Citation:** Cao LM, van Achterberg C, Tang YL, Yang ZQ, Wang XY, Cao TW (2020) Redescriptions of two parasitoids, *Metapelma beijingense* Yang (Hymenoptera, Eupelmidae) and *Spathius ochus* Nixon (Hymenoptera, Braconidae), parasitizing *Coraebus cavifrons* Descarpentries & Villiers (Coleoptera, Buprestidae) in China with keys to genera or species groups. ZooKeys 926: 53–72. <https://doi.org/10.3897/zookeys.926.48688>

## Abstract

Two parasitoids, *Metapelma beijingense* Yang (Hymenoptera, Eupelmidae) and *Spathius ochus* Nixon (Hymenoptera, Braconidae) are redescribed and illustrated. Both were reared from *Coraebus cavifrons* Descarpentries & Villiers (Coleoptera, Buprestidae) boring in *Symplocos stellaris* Brand (Symplocaceae). *Metapelma beijingense* is a solitary parasitoid with a parasitism rate of about 13.5% and *S. ochus* is a gregarious parasitoid with a parasitism rate of about 21.2%. A revised key to Oriental and Palaearctic species of *Metapelma* Westwood and a key to the species of the *Spathius labdacus*-group are provided.

## Keywords

*Coraebus*, natural enemy, synparasitism, *Symplocos stellaris*, woodborer

## Introduction

*Symplocos stellaris* Brand (Symplocaceae) is common landscape ornamental tree in South China. It is popular for its beautiful clusters of small white flowers in the spring. In addition, the wood is made into kitchen tools, furniture, etc., the seed oil is used to make soap, and the leaves and roots are used in traditional Chinese medicine. During recent investigations of woodborer biodiversity and their natural enemies in Guizhou Province, South China, we found a beautiful but little-known beetle, *Coraebus cavifrons* Descarpentries & Villiers (Coleoptera, Buprestidae) (Fig. 1D), which feeds on this tree and can cause serious damage (Fig. 1A). According to our investigation, this pest infests healthy trees rather than stressed trees. It bores into the main trunk making long longitudinal galleries (Fig. 1C). In the worst observed instance, the whole trunk was crowded with galleries bored by dozens of individual larvae (Fig. 1B). The pupal chambers are constructed about 5–10 mm under the bark in the xylem and close each other. The shape of pupal chamber is elongate-oblong. The young pupa is yellow but turns blue before emergence.

*Coraebus cavifrons* was described based on one female from Tonkin, northern Vietnam (Descarpentries and Villiers 1967), and nothing new has been reported about it except for the occurrence records by Bellamy (2008) in several provinces of southern China (Zhejiang, Fujian, Guangdong, Hainan, Sichuan). Here, we newly report this species from Zunyi City in Guizhou Province, and, more importantly, for the first time we report *Symplocos stellaris* as its host plant.

During our investigations on the biology of *C. cavifrons*, two parasitoid species belonging to different families of Hymenoptera were discovered parasitizing the buprestid larvae.

One of the parasitoid species belongs to *Metapelma* Westwood (Eupelmidae). Members of this genus are solitary parasitoids, with one larva parasitizing a single host larva (Yang 1996). Prior to this study, 38 valid species were reported (Noyes 2019), including 11 species from the Oriental region, five species from the Palearctic region (including one extinct species from Baltic amber), 13 species from the Afrotropical region, six species from the Australian region, two species from the Nearctic region, and one species from the Neotropical region. In the Palearctic region, Yang (1996) described two species parasitizing bark beetles in Beijing, China. The specimens found on *C. cavifrons* belong to *M. beijingense* Yang despite some minor differences with the original description by Yang (1996). The detailed redescription is given below, including the observed variation.

The second discovered parasitoid belongs to *Spathius* Nees (Braconidae), which is a huge cosmopolitan genus of the subfamily Doryctinae. The genus includes about 425 described species, of which 299 are known from the Oriental region and 91 from the Palearctic region (Nixon 1943; Belokobylskij 2003; Chen and Shi 2004; Belokobylskij and Maeto 2009; Tang et al. 2015; Yu et al. 2016). Nixon (1943) tried to arrange the species in almost 40 species groups to facilitate identification. Our specimens belong to the *S. labdacus* species-group in the sense of Nixon (1943). Prior to this study, eight species have been included in this group, including three species occurring in China.

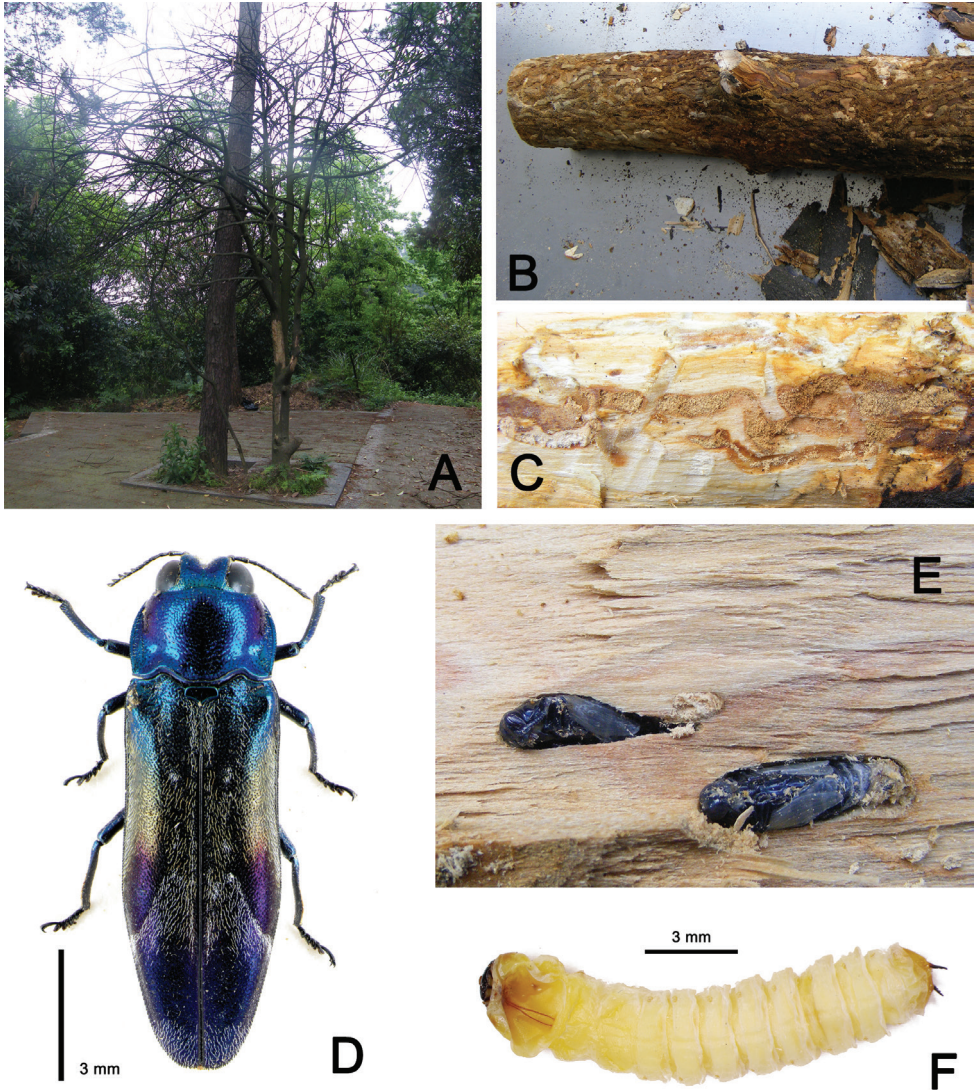


**Figure 1.** **A** Tree (*Symplocos stellaris* Brand) damaged by *Coraeus cavifrons* Descarpentries & Villiers **B** trunk damaged by *C. cavifrons* Descarpentries & Villiers **C** gallery of larvae **D** adult of *C. cavifrons* Descarpentries & Villiers **E** pupal chamber **F** larva of *C. cavifrons* Descarpentries & Villiers.

## Material and methods

### Survey site

Material was collected in Zunyi City, Guizhou Province, 27°41'54.91"N, 106°54'40.29"E, South China. The collection area was a small hilly, public park planted with various trees, such as *Camphora officinarum* (Lauraceae), *Osmanthus fragrans* (Oleaceae), *Magnolia liliflora* (Magnoliaceae), and *Symplocos stellaris*, which, although not the main tree, was still numerous.

## Survey methods

Dying *Symplocos* trees were cut down and cleaned of all small branches because borers are only present in the tree trunk. The trunks were cut into logs of 50 cm length. Each log was dissected and all parasitized hosts were collected and reared individually in vials (with diameter 12 mm and length 50 mm) in the laboratory at 25 °C and 65%–85% humidity. After the parasitoids emerged, they were collected, killed, and glued to triangle cards for taxonomic study. Some newly killed specimens were used for imaging. The parasitism rates were based on the number of beetles found in these dissected logs.

## Identification and photography

The parasitoid specimens were examined with a Nikon SMZ1500 stereomicroscope, and redescription of the parasitoids is based on naturally dried specimens. Photographs of fresh specimens of all the species were taken with a UV-C Optical Totally focused System (Beijing United Vision Technology Co. Ltd.) mounted on an Olympus CX31 microscope. Terminology follows Nixon (1943), van Achterberg (1993) (*Spathius*), and Gibson (2009) (*Metapelma*). Measurements were obtained using a calibrated micrometer. Specimens are deposited in Insect Museum, Chinese Academy of Forestry, Beijing, China, except for three specimens of *S. ochus* deposited in Naturalis Biodiversity Center, Leiden, the Netherlands, and two specimens of *S. ochus* deposited in Shanxi Insect Herbarium, Institute of Plant Protection, Shanxi Academy of Agricultural Sciences, Taiyuan, China. Abbreviations used in descriptions are as in Belokobylskij and Maeto (2009): POL = postocellar line, OD = ocellar diameter, OOL = ocellar-ocular line.

## Species determination and development of keys

The identification of *Metapelma beijingense* is based on the key provided by Narendran et al. (2013), the original description of *M. beijingense* (Yang 1996) and its type series. According to personal communication with Dr Gary Gibson (Agriculture and Agri-Food Canada, Canadian National Collection of Insects and Arachnids) the main morphological differences between the types and the reared specimens belong to intra-specific variation. We describe the Guizhou population to distinguish it from the holotype (Beijing population) and to facilitate future research on this species. The Guizhou population may be in the process of speciation considering the distinct differences. The key to Oriental and Palearctic species of *Metapelma* provided is based on Narendran et al. (2013), to which *M. beijingense*, *M. zhangii* Yang, and *M. nobilis* (Förster) have been added. The inclusion of the latter species is based on the original description and additional published information only (Yang 1996).

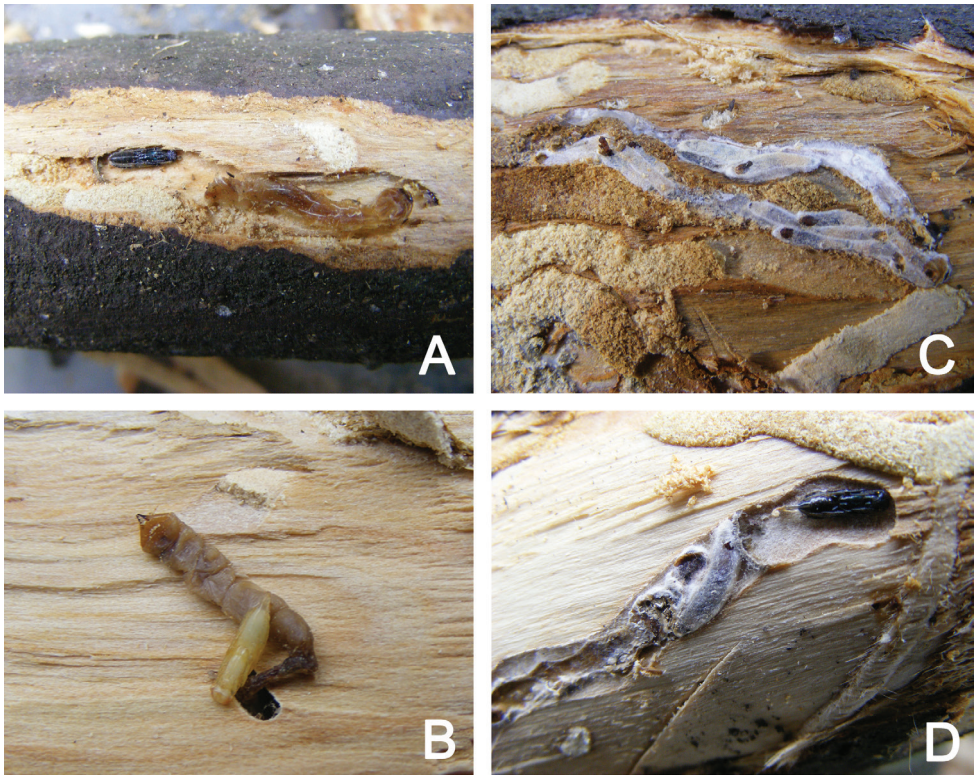


**Figure 2.** **A** A mature pupa of *Metapelma beijingense* Yang, near the buprestid larva **B** a new pupa of *M. beijingense* Yang, with the buprestid larva **C** empty cocoons of *Spathius ochus* Nixon **D** pupa of *M. beijingense* Yang and cocoons of *S. ochus* Nixon showing synparasitism.

*Spathius ochus* Nixon was identified based on Nixon's (1943) original description, Chao's (1957) redescription, and the keys by Belokobylskij and Maeto (2009) and Tang et al. (2015). The key to species of the *Spathius labdacus*-group provided here is based on Belokobylskij and Maeto (2009) and Tang et al. (2015), plus original descriptions and collected specimens.

## Taxonomy

### *Metapelma* Westwood, 1868

**Main history of Oriental and Palaeartic species.** Westwood (1835) established *Metapelma* with *M. spectabile* Westwood as the type species from North America. Förster (1856) subsequently described *Halidea* based on *H. nobilis* from Germany, but Ashmead (1896) synonymized *Halidea* under *Metapelma* (see Gibson 1989 for further remarks on generic synonymy).

Until now, 15 valid extant species of *Metapelma* from the Oriental and Palaearctic regions are known, namely *M. albisquamulatum* Enderlein from the Philippines, *M. beijingense* from China, *M. compressipes* Cameron from Malaysia, *M. gloriosum* Westwood from the Philippines, *M. kokkaricum* Narendranand & Abhilash from India, *M. mesandamna* Mani & Kaul from India, *M. nobilis* (Förster) from Germany, *M. obscuratum* Westwood from India, *M. pacificum* Nikolskaya from Russia, *M. periyaricum* Narendranand & Mohana from India, *M. rufimanum* Westwood from Malaysia (Sarawak), *M. strychnocola* Mani & Kaul from India, *M. taprobanae* Westwood from Sri Lanka, *M. tenuicrus* Gahan from the Philippines, and *M. zhangyi* Yang from China.

**Recognition.** *Metapelma* is one of four extant genera described for Neanastatinae (Eupelmidae). The genus is differentiated from the other three genera using the keys by Gibson (1995, 2009), but individuals can be recognized uniquely by the following combination of characters: head lenticular with short scrobe above each torulus but scrobes not united into a common scrobal depression (Fig. 3C); antenna 13-segmented with flagellum composed of longer than wide anellus, seven funicular segments, and 3-segmented clava (Fig. 3D); scutellum entire, not divided longitudinally (Fig. 3E); mesopleuron with upper and lower mesepimeron differentiated posteriorly behind acropleuron (Fig. 4A, B); hind tibia usually conspicuously compressed and widened apically (Fig. 3A).

### *Metapelma beijingense* Yang, 1996

Figures 3–5

*Metapelma beijingense* Yang 1996: 236.

**Material.** Holotype, ♀, China, Beijing, Xishan Experimental Forest Farm, 7.viii.1989, Yang Zhong Qi leg., from apricot trunk, deposited in Insect Museum, Chinese Academy of Forestry, Beijing, China; 6♀♀, 1♂♂, China, Guizhou Province, Zunyi City, 27°41'54.91"N, 106°54'40.29"E, pupae collected 10.v.2015 from carcasses of *Coraebus cavifrons* Descarpentries & Villiers under bark of dead *Symplocos stellaris* Brand, emerged into adults 15–18.v.2015, Tang Yan Long.

**Redescription** (based on specimens from Guizhou; differences between Beijing and Guizhou populations are shown in the key below).

**Female.** Body length 5.3–5.9 mm; forewing length 3.1–3.2 mm (Fig. 3A).

**Color.** Body generally dark with metallic tints (Fig. 3A). In frontal view, head with lower half of frons and entire face, gena, and occiput bright metallic green, but upper half of frons and vertex with slight red tint (Fig. 3C). Propleuron, apical half of mesopleuron in lateral view with metallic green tint (Fig. 4A); V-shaped sulcus on mesonotum, apical half of axilla, metanotum bright metallic green (Fig. 3E), basal 1/3 of 1<sup>st</sup> gastral tergite in dorsal view (Figure 4C), and basal 2/3 of visible ovipositor sheath in lateral view with metallic green tint (Fig. 4B). Lateral stripe on metacoxa and tergites 2–5 in lateral view varies in color from base to apex in metallic red, golden

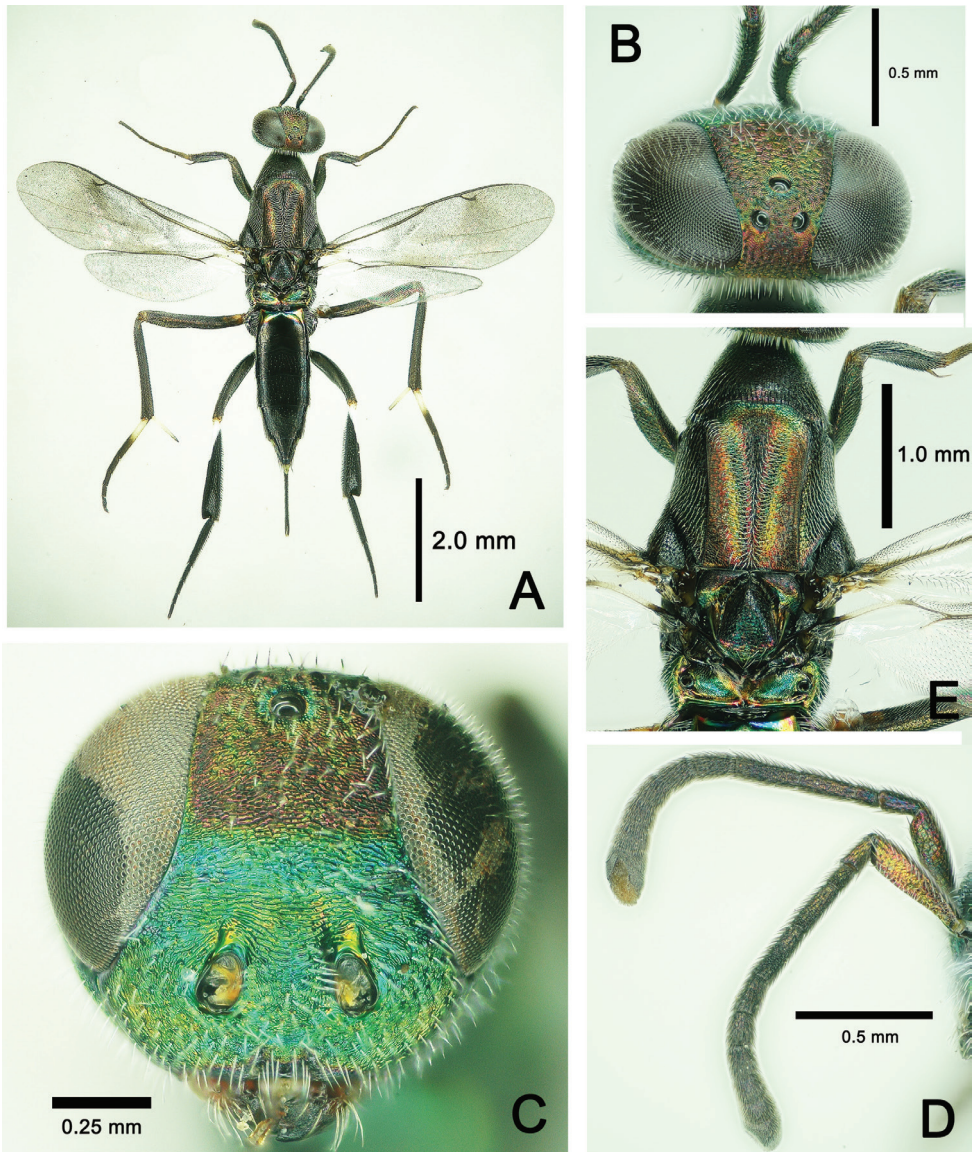


**Figure 3.** *Metapelma beijingense* Yang, ♀, China, Guizhou. **A** Habitus, dorsal aspect **B** head, dorsal aspect **C** head, anterior aspect **D** antennae, lateral aspect **E** mesosoma, dorsal aspect.

and green, successively (Fig. 4B). Apical spur and basal 1/2 of 1<sup>st</sup> tarsal segment of mid leg white to pale yellow. Basal 1/5 of mesofemur yellow to brown. Outer margin of metatibia with basal 0.3–0.4 length white (Fig. 4C). Fore wing subhyaline, infuscation paler posteriorly and extend beyond medial fold toward posterior margin, as well as along medial fold and along posterior margin of discal area basally; veins and setae dark brown; hind wing subhyaline (Fig. 4E).

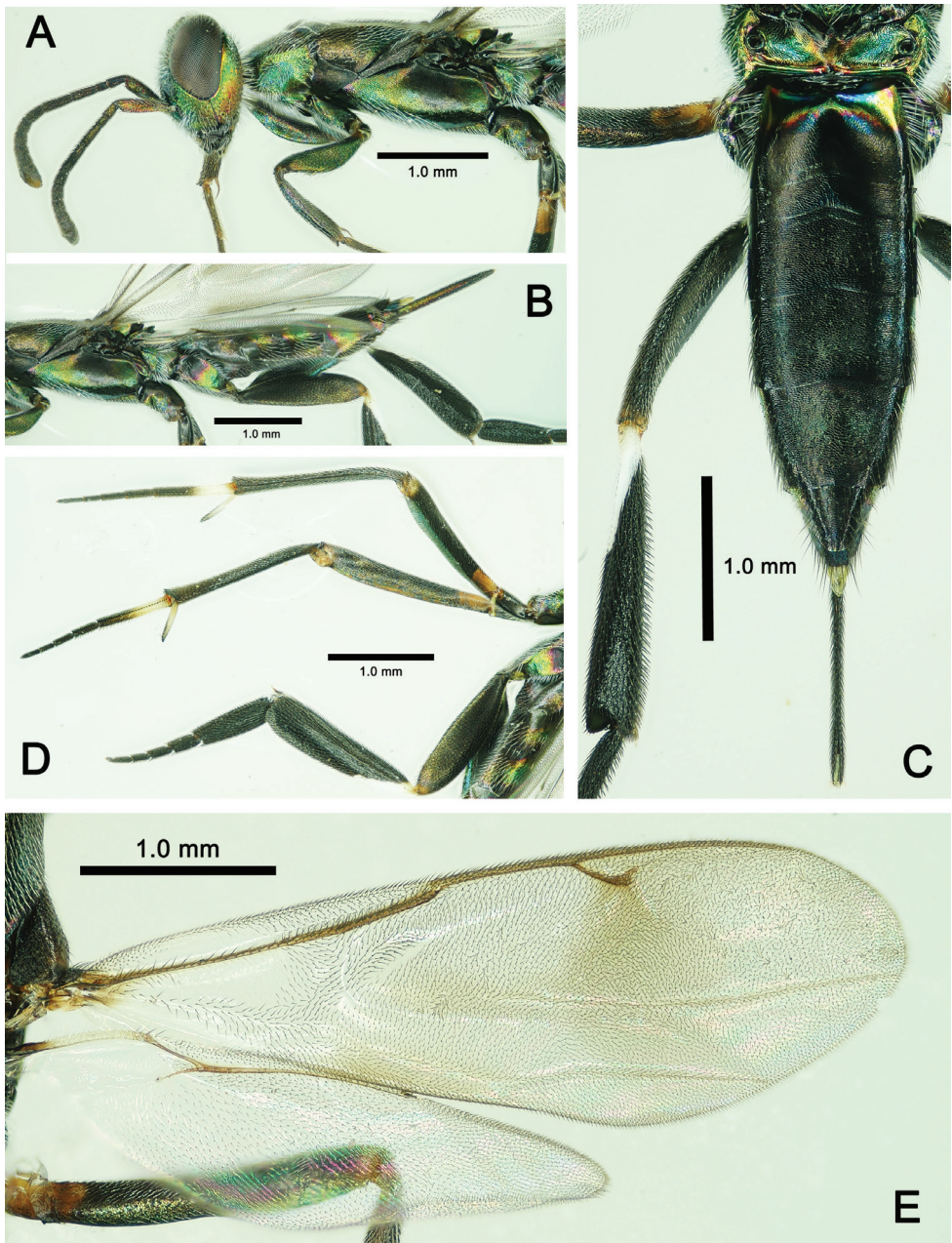


**Figure 4.** *Metapelma beijingense* Yang, ♀, China, Guizhou. **A** Head and mesosoma, lateral aspect **B** metasoma, lateral aspect, **C** metasoma, dorsal aspect **D** mid and hind legs, lateral aspect **E** wings.

**Head.** Head with sparse long white setae. In dorsal view, head width  $1.75\times$  its median length, eye occupy  $1/3$  of maximum width in dorsal view (Fig. 3B), pilose, nearly as long as head; ocelli small, POL: OD: OOL = 2: 3: 4. In frontal view, head as wide

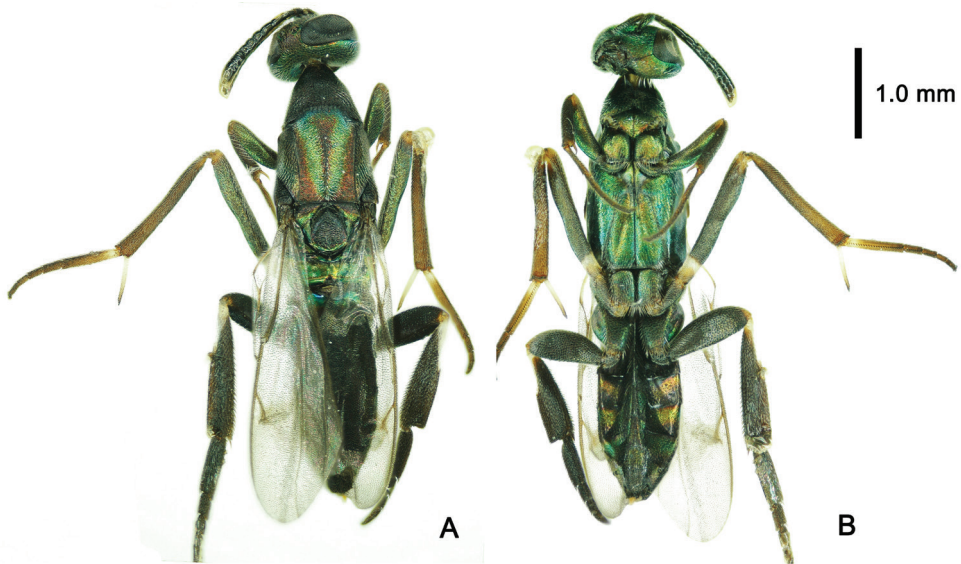


**Figure 5.** *Metapelma beijingense* Yang, ♂, China, Guizhou. **A** Habitus, dorsal aspect **B** habitus, ventral aspect.

as high; height of eye  $0.6\times$  and mandible width  $0.3\times$  head width; minimum width of frons  $1/3$  head width; face, gena, frons and vertex with tiny transverse strigate-rugose stripes. Scrobes short, no more than  $1/3$  length of scape. In lateral view, malar sulcus straight,  $1/2$  eye height. Mandibles bidentate (Figs 3B, C, 4A). Dorsal margin of torulus slightly above lower ocular line, but its ventral margin distinctly below it (Fig. 3C); antenna with a very short radicle, almost not evident; scape  $3.8\times$  its maximum width,  $3\times$  length of pedicel,  $4.7\times$  length of anellus, and  $2.2\times$  length of 1<sup>st</sup> funicular segment; pedicel  $0.8\times$  of length 1<sup>st</sup> funicular segment; 1<sup>st</sup> funicular segment  $0.9\times$  length of 2<sup>nd</sup> funicular segment (Fig. 3D).

**Mesosoma.** Mesosoma length  $2.4\times$  its maximum height. Pronotum and mesonotum with evenly distributed, dense, long white setae. Pronotum campaniform, length  $1/2$  of mesoscutum, with posterior margin incurved (Fig. 3E). Mesoscutum as long as broad, V-shaped notauli differentiate a convex anteromedial lobe; scutellar-axillar complex with deep oblique crenulate scutoscutellar sutures. Scutellum with an inverted Y-shaped longitudinal carina. Metanotum wide bilaterally and narrowest medially with a deep fossa, with posterior margin carinate. Medial length of propodeum twice length of medial length of metanotum and  $1/2$  length of scutellum, smooth without carinae, but posterior margin carinate; spiracle oval, large, situated at about half length at lateral margin of propodeum (Fig. 3E). In lateral view, mesopleuron entirely delicately reticulate, anterior lower margin with long setae, metapleuron shiny with dense setae (Fig. 4A).

**Legs.** Profemur curved,  $4.6\times$  as long as its maximum width and  $1.2\times$  length of tibia; tarsus  $1.6\times$  length of tibia, tibia with one spur  $0.4\times$  as long as basitarsus; relative lengths of protarsal segments 1–5 = 15: 10: 7: 6: 7. Mid leg: femur  $1.2\times$  length of

tibia; tarsus as long as tibia, relative lengths of segments 1–5 = 30: 9: 7: 5: 6 (Fig. 4D). Hind leg: femur 3.6× its maximum width, 0.9× length of metatibia 4.3× its maximum width, with two equally long spurs apical-ventrally, spurs 1/6 as long as basitarsus; dorsal margin of metatibia evenly curved; metatarsus as long as metatibia, relative lengths of segments 1–5 = 60: 20: 15: 12: 15. Metafemur, metatibia and metatarsal segments 1–3 compressed (Fig. 4D).

**Wings.** Fore wing extending beyond apex of metasoma to about middle of visible part of ovipositor sheath; basal cell bare but disc with dense setae except for slender, oblique bare band behind parastigma; submarginal vein 2.3× length of marginal vein, marginal vein 0.7× length of postmarginal vein and 2.25× length of stigmal vein; R fold and Cu fold visible. Hind wing about 0.8× as long as fore wing (Fig. 4E).

**Metasoma.** Metasoma sessile, 0.8× as long as head plus mesosoma combined; metasoma reticulate. Posterior margins of tergites 1–4 incurved medially; median length ratio of tergites 1–6 = 45: 20: 42: 49: 56: 35. Visible part of ovipositor sheath 0.5× length of metasoma, about 0.29× length of forewing, and 0.75× length of metatibia (Fig. 4B, C).

**Male.** Body length 5.0 mm, forewing 3.2 mm (Fig. 5A, B), otherwise similar to female.

**Remarks.** *Metapelma beijingense* is a solitary parasitoid with a parasitism rate of about 13.5%, based on seven individuals together with 34 buprestid pupae. The ratio of females to males is six.

### Key to Oriental and Palaearctic species of *Metapelma*\*

(Modified from Narendran et al. 2013)

- |   |  |                                     |
|---|--|-------------------------------------|
| 1 | Metatibia with a dorsal forked expansion (Mani et al. 1973: fig. 38E) .....  | <i>M. strychnocola</i> Mani & Kaul  |
| – | Dorsal margin of metatibia evenly curved (Fig. 4D).....  | 2                                   |
| 2 | Metatibia elongate, 5.75× wider than long.....   | <i>M. compressipes</i> Cameron      |
| – | Metatibia less than 5.0× wider than long .....   | 3                                   |
| 3 | Head metallic green with spot on vertex and two oval and anteriorly contiguous spots on middle of frons cupreous ..... | <i>M. albisquamulatum</i> Enderlein |
| – | Head without cupreous spots.....   | 4                                   |
| 4 | Metafemur totally black or black with apex white or yellow.....  | 10                                  |
| – | Metafemur with different color pattern.....  | 5                                   |
| 5 | Fore wing apex and adjoining area infuscated .....   | <i>M. gloriosum</i> Westwood        |
| – | Forewing apex subhyaline .....   | 6                                   |
| 6 | Metasoma red with a cupreous tint basally; mesosoma black.....   |                                     |
| – | .....  | <i>M. taprobanae</i> Westwood       |
| – | Metasoma and mesosoma partly or completely with different color pattern 7  |                                     |

\* *Metapelma pacificum* Nikolskayais excluded because of the lack of information.

- 7 Flagellum with 3<sup>rd</sup> funicular segment as long as 2<sup>nd</sup> segment; middle tibial spur as long as basal tarsal segment; metatibial lamellar width equal to hind tibial width ..... ***M. rufimanum* Westwood**
- Flagellum with 3<sup>rd</sup> funicular segment shorter than 2<sup>nd</sup> segment; mesotibial spur shorter than basal tarsal segment; width of metatibial lamella greater than width of metatibia ..... **8**
- 8 Head in anterior view with minimum distance between eyes 0.46× maximum distance between eyes; 2<sup>nd</sup> funicular segment 4.5× as long as 1<sup>st</sup> funicular segment ..... ***M. periyaricum* Narendran & Mohana**
- Head in anterior view with minimum distance between eyes less than 0.34× maximum distance between eyes; 2<sup>nd</sup> funicular segment 2.7–3.1× as long as 1<sup>st</sup> funicular segment ..... **9**
- 9 Malar space 0.2× height of eye; metasoma half as long as body; ovipositor sheath 0.9× as long as metasoma. ***M. kokkaricum* Narendran and Abhilash**
- Malar space 0.3× height of eye; metasoma 0.4× as long as body, ovipositor sheath as long as metasoma ..... ***M. mesandamna* Mani & Kaul**
- 10 Length of ovipositor sheath equal to combined length of mesosoma and metasoma and 0.7 × length of body ..... ***M. tenuicrus* Gahan**
- Length of ovipositor sheath less than half of metasoma and less than 1/3 length of body ..... **11**
- 11 Spur of mesotibia black ..... ***M. nobilis* (Förster)**
- Spur of mesotibia white or pale ..... **12**
- 12 Metafemur black with white tip; metatibia entirely white; visible part of ovipositor sheath as long as metasoma ..... ***M. obscuratum* Westwood**
- Metafemur entirely black, metatibia black with white base; visible part of ovipositor sheath less than 1/2 length of metasoma ..... **13**
- 13 Head between lateral ocelli with a longitudinal carina; metatibia with dorso-basal white stripe extending 1/2 length of tibia ..... ***M. zhangii* Yang**
- Head between lateral ocelli without a longitudinal carina; metatibia with dorso-basal white stripe extending 2/5 length of tibia; *M. beijingense*, s.l. ... **14**
- 14 Pedicel longer than 1<sup>st</sup> funiculus (15: 14); 1<sup>st</sup> funiculus 1.8× length of anellus; ovipositor sheath 0.37 × length of metasoma; 1<sup>st</sup> tergite 5.2× longer than 2<sup>nd</sup> tergite; body length 4 mm (Yang 1996: 237, figs 373, 374) ..... ***M. beijingense* Yang** (Beijing population; holotype)
- Pedicel shorter than 1<sup>st</sup> funiculus (12: 16); 1<sup>st</sup> funiculus 3.0× length of anellus; ovipositor sheath 0.49× length of metasoma; 1<sup>st</sup> tergite 2.3× longer than 2<sup>nd</sup> tergite; body length 5.8–6.6 mm (Figs 3A, D, 4C) ..... ***M. beijingense* Yang** (Guizhou population)

## *Spathius* Nees, 1818

### *Spathius labdacus*-group (sensu Nixon 1939)

**Main history of *S. labdacus*-group.** Nixon (1939) described the first species of this group, *S. labdacus* from Coimbatore in South India, with its host as the cotton stem weevil, *Pempheres affinis* (Faust). Nixon (1943) keyed the three described species of this group, with two new species, *S. tereus* Nixon from Philippines and *S. ochus* Nixon from Malaya and the Philippines. Chao (1957) redescribed *S. ochus* and synonymized *S. tereus* with *S. ochus*. Chao (1978) described *S. deplanatus* Chao and keyed *S. ochus* Nixon and *S. deplanatus* Chao. Belokobylskij (2003) included *S. alexandri* Belokobylskij, *S. polonicus* Niezabitowski, and *S. udaegae* Belokobylskij. Belokobylskij and Maeto (2009) reviewed and keyed Japanese species, described *S. parochus* Belokobylskij & Maeto and *S. tsukubaensis* Belokobylskij & Maeto. Tang et al. (2015) included and keyed *S. deplanatus*, *S. ochus*, and *S. parochus* as members of the *S. labdacus*-group in China.

The species group is now represented by eight valid species, namely *S. alexandri* Belokobylskij, *S. deplanatus* Chao, *S. labdacus* Nixon, *S. ochus* Nixon, *S. parochus* Belokobylskij & Maeto, *S. polonicus* Niezabitowski, *S. tsukubaensis* Belokobylskij & Maeto, and *S. udaegae* Belokobylskij.

**Recognition.** Body slightly depressed to distinctly depressed dorso-ventrally. Eyes obliquely placed, transverse diameter usually longer than length of temple. Gena smooth. Vertex, face, and temple usually sculptured. Pronotal carina free, distinct, prominent or sharp. Setae on mesoscutum sparse and erect, posteriorly mesoscutum always with raised rugosity. Propodeum elongate, medio-longitudinal carina 0.5–1.0× anterior fork of areola. Forewing strongly infuscated, subbasal cell distinctly constricted just beyond middle and crossed by a broad subhyaline fascia at its narrowest part, base of marginal cell with an oblong subhyaline spot, a broad subhyaline fascia from base of pterostigma to posterior margin of wing. Hind coxa simple, hind femur narrowed basally. First metasomal tergite densely rugulose with short rugulae, tergite 2+3 evenly shagreened all over. Ovipositor sheath less than, equal to or longer than metasoma.

### *Spathius ochus* Nixon, 1943

Figures 6–8

*Spathius ochus* Nixon 1943: 372; Chao 1957: 13; Shenefelt and Marsh 1976: 1410; Chao 1978: 180; Chen and Shi 2004: 150; Yuet et al. 2012; Tang et al. 2015: 79.

**Material.** 71♀♀, 5♂♂, China, Guizhou Province, Zunyi City, 27°41'54.91"N, 106°54'40.29"E, collected 10.v.2015 pupae from carcass of *Coraebus cavifrons* Descarpentries & Villiers under bark of dead *Symplocos stellaris* Brand, emerged into adults 15–20.v.2015, Tang Yan Long.

**Redescription. Female.** Body length 4.1–4.6 mm (Fig. 6A), forewing length 3.1–3.2 mm.

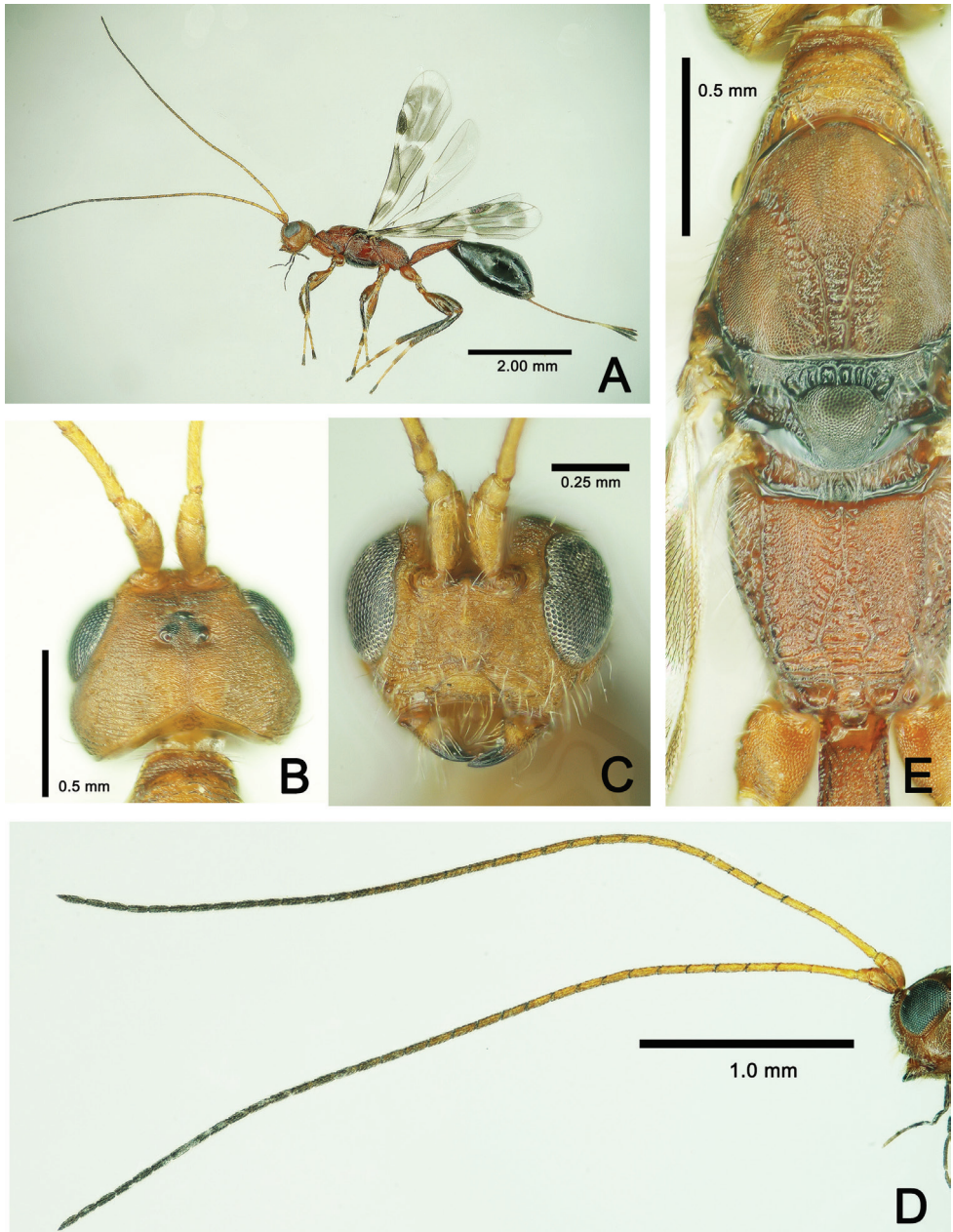


**Figure 6.** *Spathius ochus* Nixon, ♀, China, Guizhou. **A** Habitus, lateral aspect **B** head, dorsal aspect **C** head, anterior aspect **D** antennae, lateral aspect **E** mesosoma, dorsal aspect.

**Color.** Body generally brown (Fig. 6A). Head yellowish brown, basal half of antenna yellow, its apical half brown; pronotum, mesoscutum, propodeum, petiole and legs (except tarsi) dark brown; scutellum, axilla, metanotum, mesosternum, metasoma except first tergite, and telotarsus black; basal half of basitarsus white, and remainder

of tarsus yellow. Fore wing distinctly infusate, with several subhyaline spots and strips, apical 2/3 pterostigma dark brown, veins brown; hind wing subhyaline. Ovipositor sheath pale brown in basal 3/5, yellow in next 1/5 and dark 1/5 apically.

**Head.** Median length 0.8× of its width in dorsal view; with transverse striae. Length between posterior margin of lateral ocellus and occipital carina 1/2 of length of head in dorsal view; occipital carina distinct, median portion concave, reversed V-shaped; length of eye: length of temple in dorsal view = 11: 14 (Fig. 6B); eyes rather large (Fig. 7A); OOL: OD: POL = 3: 2: 1. Width of head 1.2× height in anterior view and width of face 1.1× height of eye; clypeus with transverse thin carina, face covered with sparse white setae; malar space 0.4× height of eye; height of clypeus 0.4× its width, exterior margin of clypeus slightly concave; length of maxillary palp 0.6× head width, 1.5× height of eye and 3.2× length of malar space; hypoclypeal depression deeply concave (Fig. 6C); antennae 36-segmented, scape 1/3 length of first flagellar segment, and 0.65× its maximum width; first flagellar segment 7.5× its maximum width, 1.3× as long as second segment; last antennal segment acute (Fig. 6D).

**Mesosoma.** Length of mesosoma 2.4–4.0× its height in lateral view; pronotal keel fine, weak, with fine posterior branches, mesoscutum distinctly roundly elevated above pronotum. In dorsal view pronotum with parallel longitudinal carina bilaterally, median length of mesoscutum equal to its maximum width; mesoscutum finely granulate; notauli deep and middle of mesoscutum with two parallel longitudinal carinae, between with six transverse carinae. Anterior 1/3 of mesopleuron near pronotum and tegula with short rugae and white setae, posterior 2/3 with scaly sculpture. Scutellum apical 2/3 of scutellum finely granulate; scutellar sulcus 0.3× as long as scutellum, with 7–9 longitudinal carinae and separated small depressions. Metanotum narrow, medially concave, with 9 or 10 longitudinal carinae, propodeum weakly oblique posteriorly, 1.2× longer than its apical width, 0.5× petiole, medio-longitudinal carina bifurcates at basal 1/3 of propodeum, posterior half of propodeum with irregular carinae (Figs 6E, 7B).

**Legs.** Fore femur 0.8× length of tibia and 3.6× its maximum width, fore tibia 6.5× longer than wide, outside with a row of spines and apex with comb of spines, ratio of fore tarsal segments I–V = 20: 10: 7: 5: 6; mid femur 0.7× length of tibia, ratio of mid tarsal segments I–V = 10: 6: 5: 4: 8; hind coxa simple, hind femur 2.5× longer than wide, 0.7× as long as hind tibia, ratio of hind tarsal segments I–V = 18: 9: 6: 4: 8.

**Wings.** Forewing 3.5× its width; pterostigma 3.5× its maximum width; 1–R1 1.25× pterostigma, r originate from middle of pterostigma; SR1 7.2× longer than r, straightly extending to wing margin; r nearly 1/4 of 2–SR, cu-a perpendicular to CU1, m–cu enters second submarginal cell; meeting point of 2–SR, 2–M and 2–SR+M weak, veins reduced; 1–SR+M straight, 1–SR 1/4 length of 1–M; M+CU1 distinctly curved, apical subbasal cell narrow and elongate, r–m unsclerotized, hardly invisible; 3–M and CU1a reaching wing margin. Length of hind wing 4.5× its width, m-cu and SR pigmented (Fig. 7E).

**Metasoma.** First tergite 3.5–3.9× longer than its maximum apical width in dorsal view, with regular longitudinal carinae; in lateral view first tergite slender and 1.5–1.7× as long as propodeum, spiracular tubercles located at basal third, laterally with erect

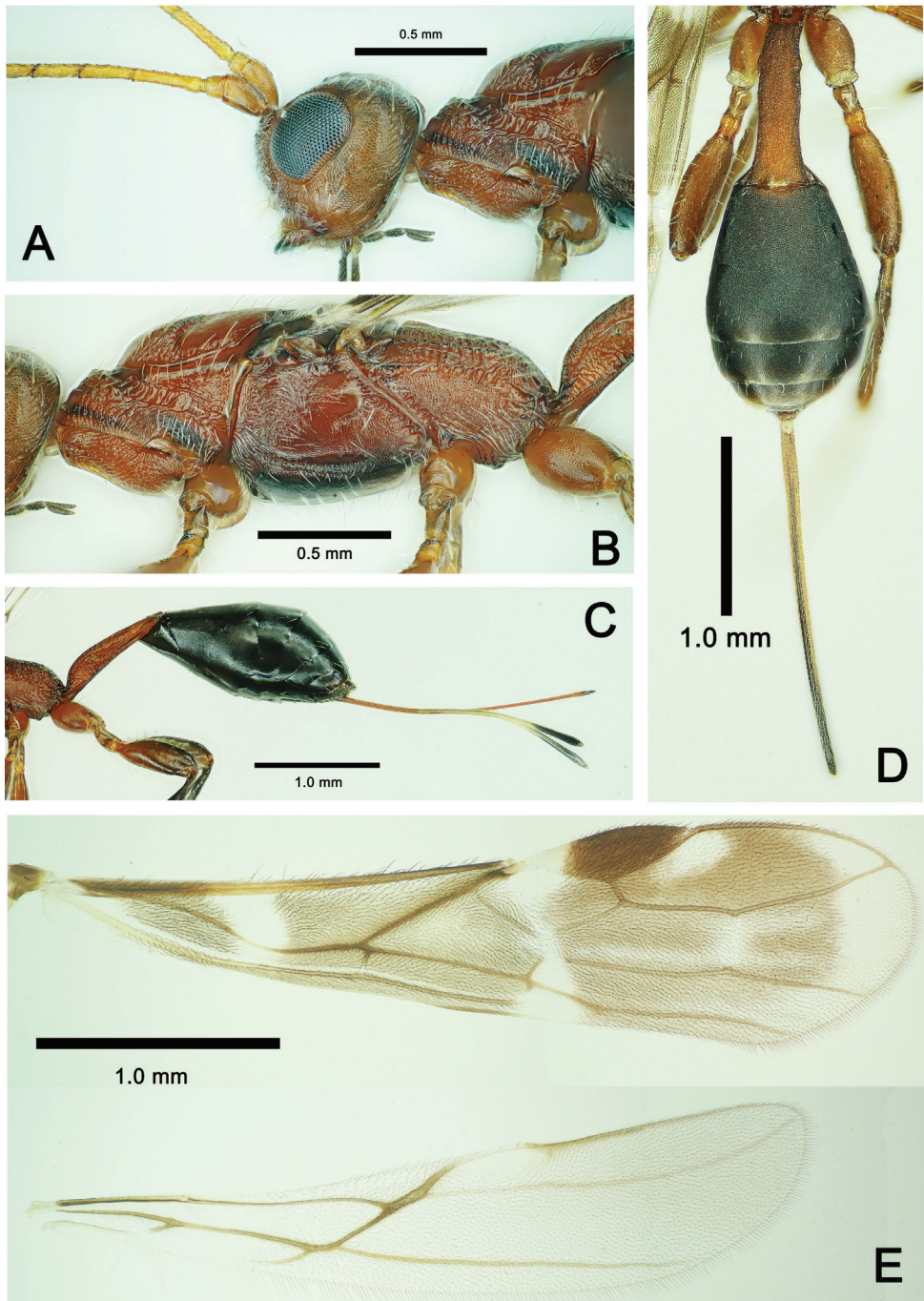


**Figure 7.** *Spathius ochus* Nixon, ♀, China, Guizhou. **A** Head, lateral aspect **B** metasoma, lateral aspect **C** metasoma, lateral aspect **D** metasoma, lateral aspect **E** wings.

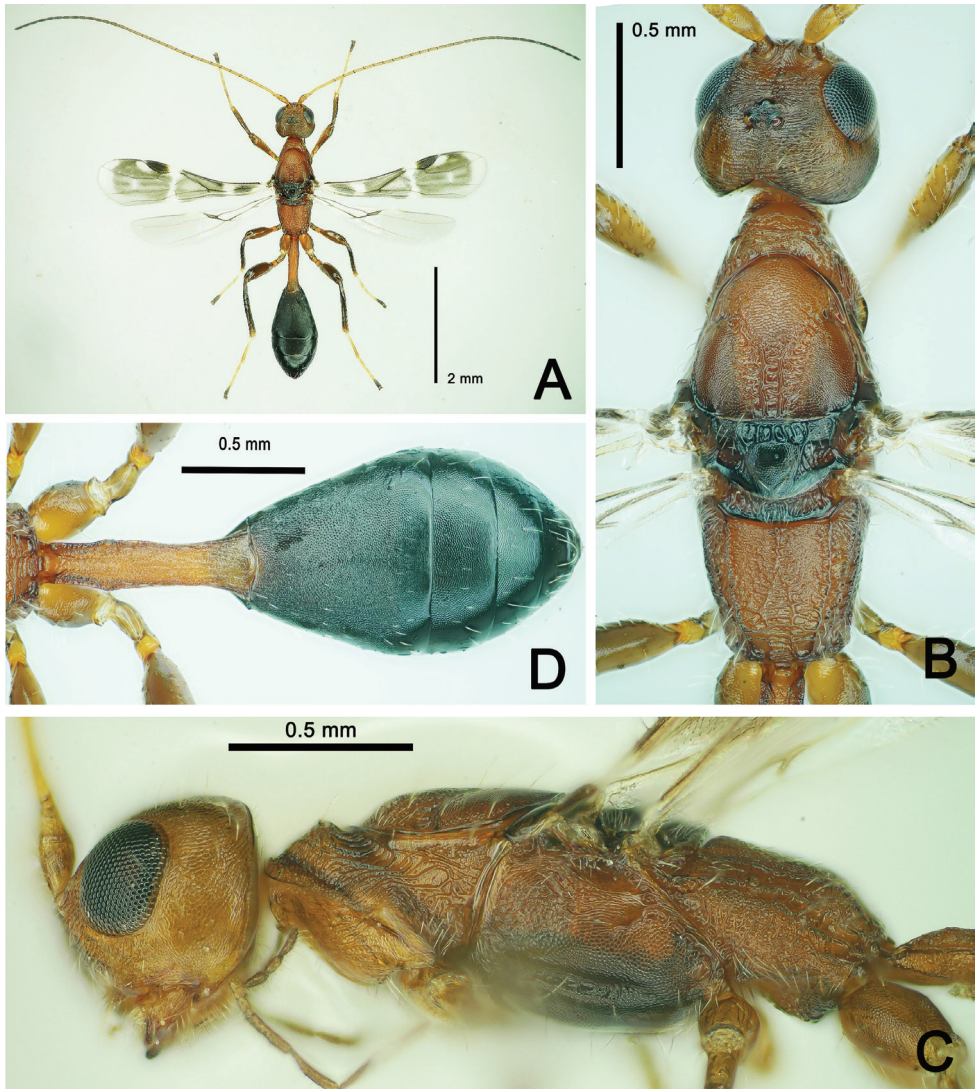


**Figure 8.** *Spathius ochus* Nixon, ♂, China, Guizhou. **A** Habitus, dorsal aspect **B** head and mesosoma, dorsal aspect **C** head and mesosoma, lateral aspect **D** metasoma, dorsal aspect.

white long setae; tergites 2–4 densely granulate; fifth and sixth tergites smooth. Length of visible setose part of ovipositor sheath 0.7–0.8× length of metasoma, 0.85× length of fore wing, and 0.6× length of body (Fig. 7C, D).

**Male.** Body length 4.0–4.2 mm, forewing 2.7 mm (Fig. 8), otherwise similar to female.

**Remarks.** The mesosoma is variably depressed; usually 2.4–2.9× longer than high, but in some specimens up to 3.7–4.0×. Obviously, this character is useless to separate *S. tereus* Nixon, 1943. Therefore, we agree with Chao (1957) that the latter cannot be separated. *Spathius ochus* is a gregarious koinobiont ectoparasitoid like most other

*Spathius*, each buprestid larva can feed 3–9 individuals. From one tree 11 borer larvae were parasitized by 42 individuals of *S. ochus*, together with seven borer larvae were parasitized by *M. beijingense* and 34 live buprestid pupae, resulting in a parasitism rate of about 21.2% for *S. ochus*. The sex ratio is about 14:1 (71 females to 5 males).

The very interesting phenomenon of synparasitism (Tobias 2007) is shown in Figure 2D; one individual of *M. beijingense* and four individuals of *S. ochus* were together parasitizing the same woodborer larva. Likely, these two ectoparasitoid species laid their eggs near the host at about the same time, and the larvae did not start fighting each other because the host was large enough to avoid severe food competition. Of course, this is only circumstantial evidence that is in need of corroboration.

The species is very similar to *S. parochus* Belokobylskij & Maeto and can be recognized with the key below.

### Key to species of *Spathius labdacus*-group

- 1 Mesosoma very strongly depressed, 4.0–6.0× longer than its maximum height and ovipositor sheath 0.3–0.4× as long as metasoma..... ***S. deplanatus* Chao**
- Mesosoma less depressed, 2.0–4.0× longer than its maximum height, if 3.5–4.0× (= *S. tereus* Nixon, 1943) then ovipositor sheath 0.6–0.8× as long as metasoma ..... **2**
- 2 Ovipositor sheath 0.5–0.8× as long as metasoma ..... **3**
- Ovipositor sheath as long as metasoma or longer ..... **5**
- 3 Ovipositor sheath 0.4–0.5× as long as metasoma; base of hind tibia pale; medio-longitudinal carina of propodeum 1.4–1.8× as long as anterior fork of areola..... ***S. tsukubaensis* Belokobylskij & Maeto**
- Ovipositor sheath 0.7–0.8× as long as metasoma; base of hind tibia dark brown; medio-longitudinal carina of propodeum 0.5–1.0× as long as anterior fork of areola..... **4**
- 4 First metasomal tergite 1.5× as long as propodeum (Fig. 7A), medio-longitudinal carina of propodeum about as long as anterior fork of areola (Fig. 6E) ..... ***S. ochus* Nixon**
- First tergite 1.6–1.8× as long as propodeum, medio-longitudinal carina of propodeum 0.5–0.7× length of anterior fork of areola ..... ***S. udaegae* Belokobylskij**
- 5 Ovipositor sheath about 1.8× as long as metasoma ..... ***S. alexandri* Belokobylskij**
- Ovipositor sheath less than 1.2× as long as metasoma ..... **6**
- 6 Pronotal keel sharp and protuberant ..... ***S. labdacus* Nixon**
- Pronotal keel fine and hardly protruding..... **7**
- 7 Length of first metasomal tergite about twice its maximum width ..... ***S. polonicus* Niezabitowski**
- Length of first tergite 3.0–3.3× its maximum width..... ***S. parochus* Belokobylskij & Maeto**

## Discussion

During the investigation, we found that the host *C. cavifrons* boring in *Symplocos stellaris* has only one generation per year in Zunyi, Guizhou Province. From the end of May to early June, this buprestid begins emerging and it will last for about 2 weeks. We chose 20–30 days before its emergence to cut and dissect logs when there are no emergence holes of parasitoids in the trunk. The best time for collecting these parasitoids proved to be the first week of May. We guess that both two parasitoids are at least oligophagous, because there are no *C. cavifrons* larvae available for laying eggs after their emergence. However, they may search for another host to lay their eggs. Both parasitoids seem to have two generations per year in Zunyi, but this needs to be further investigated.

Combined study of the stressed tree (host), the woodborers (pest), the parasitoids (natural enemies) and their relationships is interesting, and biological traits may be useful in their taxonomy. For the identification of *Metapelma beijingense* we used only morphological and biological evidence, but a molecular data analysis study with fresh material of the Beijing and Guizhou populations might be helpful for the identification and determination of the systematic status of these two populations.

## Acknowledgements

We sincerely thank Prof. Andreas Köhler (Laboratório de Entomologia, Universidade de Santa Cruz do Sul, Santa Cruz do Sul, Rio Grande do Sul, Brazil), Dr Mao-Ling Sheng (General Station of Forest Pest Management, National Forestry and Grassland Administration, Shenyang, China), Prof. Katja Seltsmann (University of California, Santa Barbara, California, USA), Prof. K. Sudheer (Systematic Entomology Laboratory, Department of Zoology, University of Calicut, Kerala, India), and the anonymous reviewer for their critical reading of and helpful comments on the manuscript. Cao is much indebted to Dr Gary A.P. Gibson (Agriculture and Agri-Food Canada, Canadian National Collection of Insects and Arachnids) for his most generous help on the manuscript with many valuable suggestions. This research was supported by the Science and Technology Project of Guizhou Province [2017]5202 and the Fundamental Research Funds for the Central Non-profit Research Institution of CAF (CAFYBB2018ZB001) and the key project of Science-technology basic condition platform from The Ministry of Science and Technology of the People's Republic of China (Grant No. 2005DKA21402).

## References

- Ashmead WH (1896) On the genera of Eupelminae. Proceedings of the Entomological Society of Washington 4: 4–20.
- Bellamy CL (2008) A world catalogue and bibliography of the jewel beetles (Coleoptera: Buprestoidea). Volume 3. Buprestinae: Pterobothrini through Agrilinae: Rhaeboscelina, Pensoft Series Faunistica No. 78. Pensoft Publishers, Sofia-Moscow, Russia, 1260–1931.

- Belokobylskij SA (1989) The Palaearctic species of braconide wasps of the genus *Spathius* Nees: *S. labdacus*, *S. urios* and *S. leucippus* species group (Hymenoptera, Braconidae, Doryctinae). Trudy Zoologicheskogo Instituta Akademii Nauk SSSR 188: 39–57.
- Belokobylskij SA (2003) The species of the genus *Spathius* Nees, 1818 (Hymenoptera: Braconidae: Doryctinae) not included in the monograph by Nixon (1943). Annales Zoologici 53 (3): 347–488.
- Belokobylskij SA, Maeto K (2009) Doryctinae (Hymenoptera, Braconidae) of Japan (Fauna Mundi. Vol. 1). Warszawska Drukarnia Naukowa, Warszawa, 806 pp. <https://doi.org/10.3161/067.058.0107>
- Cameron P (1909) Descriptions of three undescribed species of Chalcididae from Borneo. Deutsche Entomologische Zeitschrift 1909: 205–207. <https://doi.org/10.1002/mmnd.48019090203>
- Chao HF (1957) On south-eastern Chinese braconid-flies of the subfamily Spathinae (Braconidae). Transactions of the Fujian Agricultural College 4: 1–18.
- Chao HF (1978) A study on Chinese braconid wasps of the tribe Spathiini (Hymenoptera, Braconidae, Doryctinae). Acta Entomologica Sinica 21: 173–184.
- Chen JH, Shi QX (2004) Systematic studies on Doryctinae of China (Hymenoptera: Braconidae). Fujian Science and Technology Publishing House, Fujian, 274 pp.
- Descarpentries A, Villiers A (1967) Catalogue raisonné des Buprestidae d'Indochine. XIV. Coraebini (4e partie). Annales de la Société Entomologique de France 3: 471–492.
- Enderlein G (1912) Zur Kenntnis der Chalcididen Ceylons (Hym.). Entomologische Mitteilungen 1: 144–148. <https://doi.org/10.5962/bhl.part.25896>
- Förster A (1856) Hymenopterologische Studien. II. Heft. Chalcidiae und Proctotrupii, Aachen, 152 pp.
- Gahan AB (1925) A second lot of parasitic Hymenoptera from the Philippines. Philippine Journal of Science 27: 83–109.
- Gibson GAP (1989) Phylogeny and classification of Eupelmidae, with revision of the world genera of Calosotinae and Metapelmatinae (Hymenoptera: Chalcidoidea). Memoirs of the Entomological Society of Canada 149: 1–121. <https://doi.org/10.4039/entm121149fv>
- Gibson GAP (1995) Parasitic wasps of the subfamily Eupelminae (Hymenoptera: Chalcidoidea: Eupelmidae). Memoirs on Entomology International 5: 1–5 + 1–421.
- Gibson GAP (2009) Description of three new genera and four new species of Neanastatinae (Hymenoptera, Eupelmidae) from Baltic amber, with discussion of their relationships to extant taxa. In: Johnson N (Ed.) Advances in the systematics of Hymenoptera. Festschrift in honour of Lubomír Masner. ZooKeys 20: 175–214. <https://doi.org/10.3897/zookeys.20.161>
- Mani MS, Dubey OP, Kaul BK, Saraswat GG (1973) On some Chalcidoidea from India. Memoirs of the School of Entomology, St. John's College 2: 1–128.
- Narendran TC, Rajmohana K, Abhilash P, Bijoy C (2013) Taxonomic studies on some Chalcidoidea (Hymenoptera) associated with xylophagous beetle *Demonaxdecorus* Gahan (Coleoptera: Cerambycidae) from Kerala (India) with descriptions of five new species. Samagra 9 (26): 3–22.
- Nikolskaya M (1952) Chalcids of the fauna of the USSR (Chalcidoidea). Opredelitelipo Faune SSSR 44. Zoologicheskim Institutom Akademii Nauk SSSR, Moscow-Leningrad, 1–486.

- Nixon GEJ (1943) A revision of the Spathiinae of the old world (Hymenoptera, Braconidae). Transactions of the Royal Entomological Society of London 93(2): 173–495. <https://doi.org/10.1111/j.1365-2311.1943.tb00434.x>
- Nixon GEJ (1939) New species of Braconidae (Hymenoptera). Bulletin of Entomological Research 30: 119–128. <https://doi.org/10.1017/S0007485300004430>
- Noyes JS (2019) Universal Chalcidoidea Database. <https://www.nhm.ac.uk/our-science/data/chalcidoids> [Accessed on: 2019–7–8]
- Shenefelt RD, Marsh PM (1976) Braconidae 9. Doryctinae. In: van der Vecht J, Shenefelt RD (Eds) Hymenopterorum Catalogus (Nova Editio) 13. W. Junk's, Gravenhage, Netherlands, 1263–1424.
- Tang P, Belokobylskij SA, Chen XX (2015) *Spathius* Nees, 1818 (Hymenoptera: Braconidae, Doryctinae) from China with a key to species. Zootaxa 3960: 1–132. <https://doi.org/10.11646/zootaxa.3960.1.1>
- Tobias VI (2007) On some synonymical terms in the parasitology of entomophagous insects and on the terms parasitoid and carnivoroid. Entomological Review 87: 273–278. <https://doi.org/10.1134/S0013873807030049>
- van Achterberg C (1993) Illustrated key to the subfamilies of the Braconidae (Hymenoptera: Ichneumonoidea). Zoologische Verhandelingen 283: 1–189. <https://www.repository.naturalis.nl/document/150389>
- Westwood JO (1835) Characters of new genera and species of hymenopterous insects. Proceedings of the Zoological Society of London 3: 51–54, 68–72.
- Westwood JO (1868) Descriptions of new genera and species of Chalcididae. Proceedings of the Entomological Society of London 1868: 36.
- Westwood JO (1874) Thesaurus Entomologicus Oxoniensis; or, Illustrations of New, Rare, and Interesting Insects, for the Most Part Contained in the Collection Presented to the University of Oxford by the Rev. F.W. Hope. University of Oxford, Oxford, 150 pp. <https://doi.org/10.5962/bhl.title.14077>
- Yang ZQ (1996) Parasitic Wasps on Bark Beetles in China (Hymenoptera). Science Press, Beijing, 4 + 363 pp.
- Yu DS, van Achterberg C, Horstmann K (2016) Taxapad 2015: World Ichneumonoidea, taxonomy, biology, morphology and distribution. Taxapad Interactive Catalogue on Flash Drive. Nepean.

# On *Aethiopomyia* Malloch (Diptera, Muscidae) with the revision of the type specimens deposited in the Museum für Naturkunde, Berlin (Germany) with a key to species

Viviane Rodrigues de Sousa<sup>1</sup>, André Fontinelle Magalhães Pereira<sup>1</sup>,  
Márcia Souto Couri<sup>1,2</sup>

**1** Museu Nacional, Quinta da Boa Vista, São Cristóvão, Rio de Janeiro, 20.940–040, RJ, Brazil **2** Conselho Nacional de Desenvolvimento Científico e Tecnológico fellow, Brazil

Corresponding author: Viviane Rodrigues de Sousa ([sousavrodrigues@gmail.com](mailto:sousavrodrigues@gmail.com))

Academic editor: M. De Meyer | Received 9 December 2019 | Accepted 13 February 2020 | Published 13 April 2020

<http://zoobank.org/B8716F7E-70B0-440A-8508-0111DC5AE564>

**Citation:** de Sousa VR, Pereira AFM, Couri MS (2020) On *Aethiopomyia* Malloch (Diptera, Muscidae) with the revision of the type specimens deposited in the Museum für Naturkunde, Berlin (Germany) with a key to species. ZooKeys 926: 73–80. <https://doi.org/10.3897/zookeys.926.49210>

## Abstract

*Aethiopomyia* Malloch (Diptera, Muscidae) is a small genus with occurrence restricted to the Afrotropical region. Only five species are currently known in this genus: *A. patersoni* Zumpt, 1969, *A. williamsi* Snyder, 1951, *A. arguta* (Karsch, 1879), *A. steini* Curran, 1935, and *A. gigas* (Stein, 1906). All *Aethiopomyia* species are large, reaching up to 15 mm, as in *A. patersoni* and the most visible differences among them are based in the color pattern of the body. The species are mostly yellow, with a broad scutum and abdomen, males and females are dichoptic, the anepimeron is haired and they have stubby spines on the upper side of the palpi. Phylogenetically, *Aethiopomyia*, together with two other genera restricted to the Afrotropical region, *Alluaudinella* Giglio-Tos and *Ochromusca* Malloch, appear to form a monophyletic group, defined by the presence of the remarkably short stubby spines on the upper side of the palpi. Four species deposited in the Museum für Naturkunde, Berlin (Germany) were analyzed; three of them are types. Diagnosis for all species, colored illustrations, male dissections and illustrations and a key to separate them are presented herein.

## Keywords

Afrotropical, diversity, morphology, taxonomy

## Introduction

*Aethiopomyia* Malloch (Diptera, Muscidae) is a small genus restricted to the Afro-tropical region. It was proposed by Malloch (1921) with a differentiated diagnosis from the allied genus *Alluaudinella* Giglio-Tos. Both genera have a mostly yellow and broad scutum and abdomen, dichoptic males, anepimeron haired, and the presence of stubby spines on the upper side of the palpi which, according to Malloch (1921), readily separates the two genera from their nearest allies. In the differentiated diagnoses from *Alluaudinella*, Malloch (1921) mentioned the following characters of *Aethiopomyia*: propleuron hairy in center; proepisternum bare, prosternum hairy, metanotum with fine hairs on lateral elevation, vein  $R_{4+5}$  setulose at base below and above. *Spilogaster gigas* Stein was originally designated as the type-species.

In the phylogenetic analysis made by Couri and Carvalho (2003), these two genera, together with *Ochromusca* Malloch appear to form a monophyletic group, defined by the presence of remarkably short stubby spines on the upper side of the palpi. The larva of *Ochromusca* and *Alluaudinella* feed on dead snails, while the larval habits of *Aethiopomyia* are not known. According to Skidmore (1985) the final larval instar of *Aethiopomyia* closely resembles those of *Ochromusca*, *Alluaudinella*, *Synthesiomyia* Brauer & Bergenstamm, and *Muscina* Robineau-Desvoidy.

Five species are currently known in the genus. *Aethiopomyia patersoni* Zumpt, 1969 is restricted to Tanzania and *Aethiopomyia williamsi* Snyder, 1951 is recorded from Kenya, Malawi, and Tanzania. *Aethiopomyia arguta* (Karsch, 1879), *Aethiopomyia steini* Curran, 1935 and *Aethiopomyia gigas* (Stein, 1906) are more widespread in the Afrotropical region (Pont 1980). Zumpt (1969) published a key for the identification of the five species, mostly based on the color pattern of scutum and abdomen, together with taxonomic notes.

Diagnosis for all species, colored photographs, male dissections, illustrations, and a key to separate them are presented herein.

## Materials and methods

All examined material belongs to the Museum für Naturkunde, Berlin (Germany) and were examined during a scientific visit of MSC during the years 2018–2019. Four of the five species were analyzed, *A. williamsi* and types of *A. arguta*, *A. gigas*, and *A. patersoni*. For *A. steini* we used the characters in the original description.

Color photos were made using Auto-Montage. Complementary line drawings to the ones presented by Zumpt (1969) of the male terminalia of *A. arguta* were made, and male and female terminalia of *A. gigas* were dissected and illustrated.

The terminology follows that of Cumming and Wood (2017).

## Results

### Key to *Aethiopomyia* species

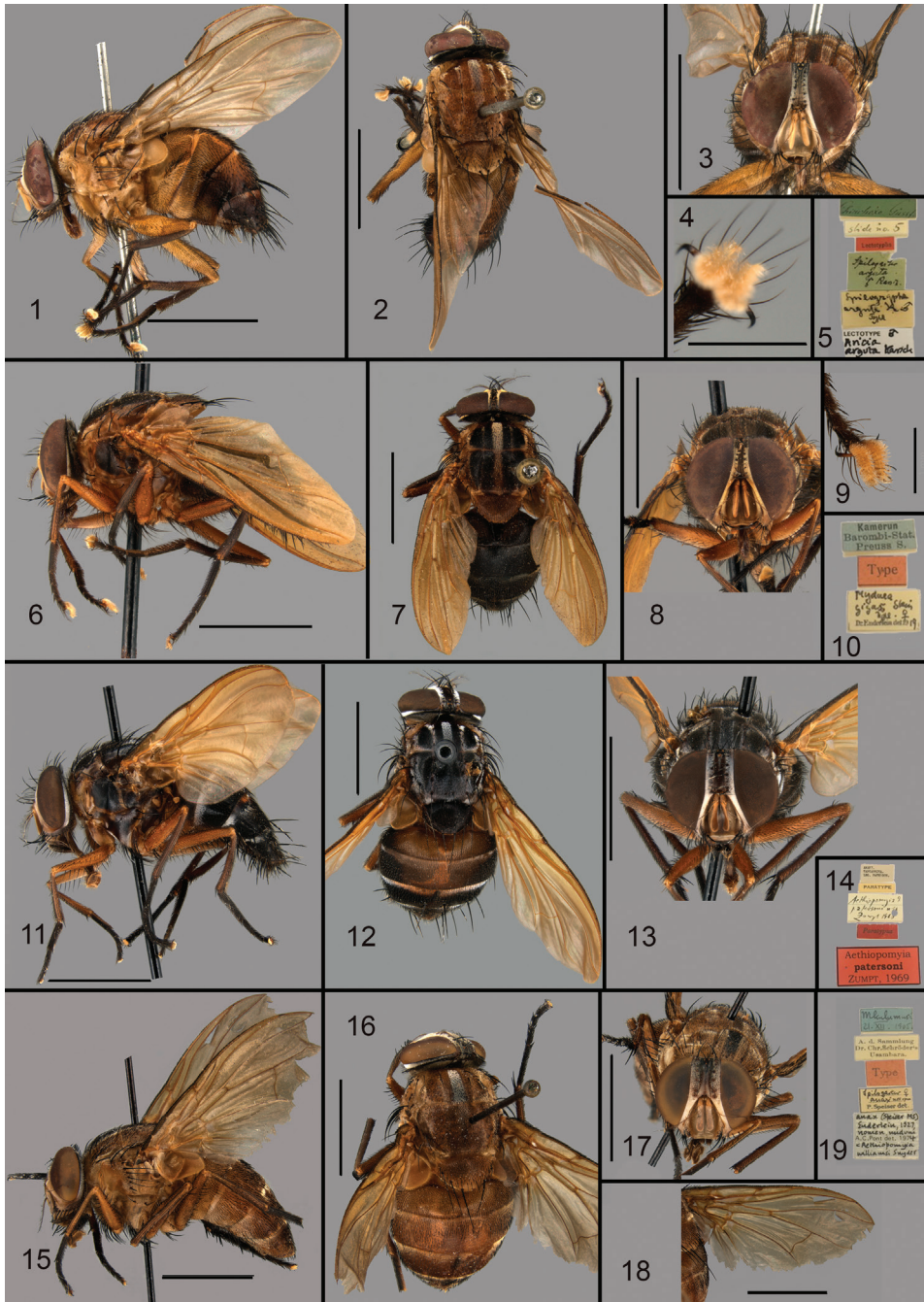
- 1 Palpus yellow (Fig. 8), abdomen almost all black with some grey pruinescence along the margins of the tergites (Fig. 7) [Sternite 5 quadrangular with 2 strong setae at middle (Fig. 21); cercal plate and surstyli as in Figs 22 and 23; aedeagus as in Figs 24 and 25] ..... *A. gigas* (Stein)
- Palpus reddish brown to brown, abdomen more reddish brown with tergites variable ..... 2
- 2 Calypters yellowish ..... 3
- Calypters yellowish with brown margin or fulvous brown ..... 4
- 3 Arista yellow (Fig. 3), femora yellow (Fig. 1), mid tibia with 2 posterior setae, abdomen reddish brown, tergites III–V with a median brown vitta, tergite IV brown laterally and tergite V broadly brown [aedeagus as in Fig. 20] ..... *A. arguta* (Karsch)
- Arista mostly brown, femora reddish, mid tibia with 4 or 5 posterior setae, third and fourth abdominal segments wholly black ..... *A. steini* (Curran)
- 4 Fronto-orbital plate silvery-white pruinose (Fig. 13), scutellum dark brown (Fig. 12) [abdominal sternites with strong setae] ..... *A. patersoni* Zumpt
- Fronto-orbital plate greyish brown (Fig. 17), scutellum light brown (Fig. 16) [abdominal basal sternites hairy, others with numerous long, ventrally directed setae in male] ..... *A. williamsi* (Snyder)

### *Aethiopomyia arguta* (Karsch, 1879)

Figures 1–5, 20

**Lectotype.** ♂; **paralectotype** ♂ (see Pont and Werner 2006: 23–24 for details)

**Diagnosis.** *Length of body.* 11.0–12.0 mm (♂). **Head.** ♂ frons narrow, with the same width of frontal triangle. Frons and fronto-orbital plate dark brown. Parafacial, face and gena reddish yellow. Ocellar setae short. Gena very thin. Pedicel, postpedicel and arista yellow. Postpedicel ca. 4 × as long as wide. Arista long; plumose. Palpus brown, filiform. **Thorax.** Scutum reddish yellow-brown, with 1–3 incomplete brown white dusted vittae presuturally. Dorsocentrals 2+4. Katepisternals 1+2. Anepimeron setulose. Katatergite setulose. Lower calypter broad, ca. 3 × as long as the upper one. Haltere yellow. Calypters yellowish. **Legs.** Femora yellow; tibiae and tarsi brown. Fore tibia without median seta. Mid tibia with two posterior setae in middle third. ♂. Hind tibia with two anterodorsal and two or three anteroventral very fine setae. Pulvilli long and very enlarged (Fig. 4). **Wing.** Uniformly smoky yellowish. Costal spine not distinct. **Abdomen.** Robust, reddish brown; tergites III–V with a median brown vitta;



**Figures 1–19.** 1–5 *Aethiopomyia arguta* (Karsch, 1879) lectotype ♂ of *Aricia arguta* Karsch: 1 lateral view 2 dorsal view 3 head frontal view 4 pulvilli 5 labels 6–10 *Aethiopomyia gigas* (Stein, 1906) syntype ♂: 6 lateral view 7 dorsal view 8 head frontal view 9 pulvilli 10 labels 11–14 *Aethiopomyia patersoni* Zumpt, 1969 Paratype ♀: 11 lateral view; 12 dorsal view 13 head frontal view 14 labels 15–19 *Aethiopomyia williamsi* (Snyder, 1951) ♀ of *Lophomala anax* Enderlein, 1927, nomen nudum: 15 lateral view 16 dorsal view 17 head frontal view 18 wing 19 labels. Scale bars: 5 mm (1–3, 5, 6–8, 10–19); 1 mm (4, 9).

tergite IV brown laterally and tergite V broadly brown. Rows of strong setae on margins of tergites IV and V and on disc of tergite V. Abdominal sternites with thin setae. Sternite 6 asymmetrical. **Terminalia.** Aedeagus as in Fig. 20.

**Note.** The species was keyed by Zumpt (1969). Cercal plate and surstylus as in Zumpt (1969: fig. 3). We present complementary drawings of the terminalia, that are in the same slide prepared by Zumpt (1969).

### *Aethiopomyia gigas* (Stein, 1906)

Figures 6–10, 21–30

**Syntypes.** 1 ♂, 2 ♀ (see Pont and Werner 2006: 51 for details)

**Diagnosis.** *Length of body.* 11.0–15.0 mm (♂♀). Similar to *A. arguta*, differing as follows: **Head.** Frons, fronto-orbital plate, parafacial, face, and gena reddish yellow, silver pruinose under certain lights. Palpus yellow. **Thorax.** Scutum ground color yellow, four broad black vittae laterally and one median white-silver pruinose vitta. Scutum laterally yellow, scutellum yellow. Pleurae mostly yellow; anepisternum and anepimeron mostly dark brown, Lower calypter broad, ca. 2.5 × as long as the upper one. Haltere yellow. Calypters yellowish with brown margins. **Legs.** Color and chaetotaxy as in *A. arguta*. **Abdomen.** Almost all black, with some grey pruinescence along the margins of the tergites, under certain lights. Abdominal sternites with strong setae. Sternite 5 quadrangular with two strong setae at middle (Fig. 21). **Terminalia** ♂. Cercal plate and surstylus as in Figs 22 and 23; aedeagus as in Figs 24 and 25. **Ovipositor** as in Figs 26 and 27; only two spermathecae found (Fig. 28). **Larva.** One big larva found in ♀ abdomen (Fig. 29); detail of spiracle as in Fig. 30. Cuthbertson (1938 in Skidmore 1985) recorded that the ♀ deposits a single late instar larva.

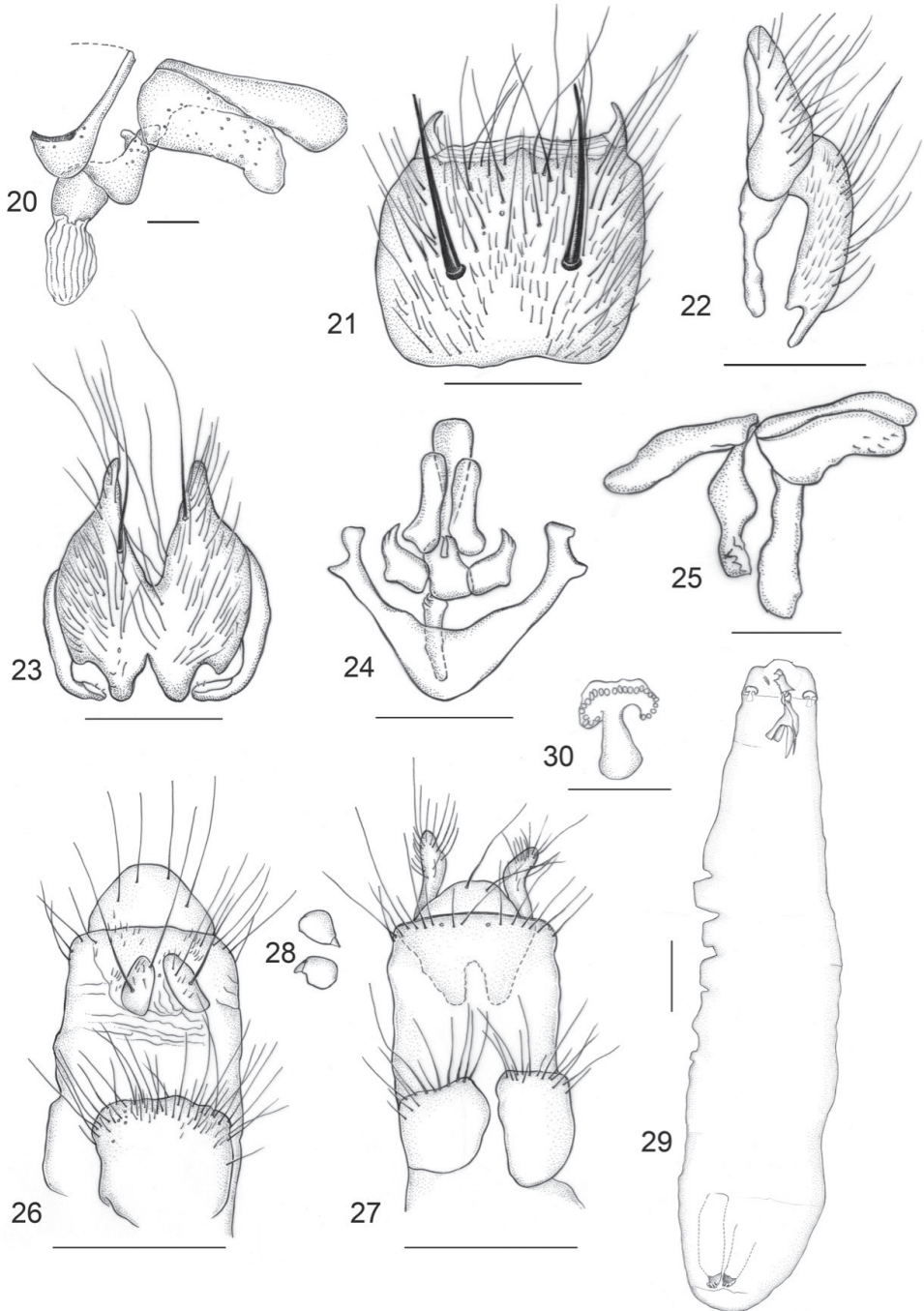
**Note.** The species was keyed by Zumpt (1969). One ♂ and one ♀ (not types) from Spanish Guinea were dissected and illustrated. ♂: Uellebg. Benitogbt. /15–31.i.07 / G. Tessmann S. G.; ♀: Alou Benitogbt/16–31.vii.06/ Tessmann S. G. Recently, O'Hara et al. (2013) transferred *Paleotachina* Townsend from Tachinidae to Muscidae and placed in synonymy with *Aethiopomyia* and *Paleotachina smithii* Townsend, type species of *Paleotachina*, was synonymized with *A. gigas*.

### *Aethiopomyia patersoni* Zumpt, 1969

Figures 11–14

**Paratypes.** 2 ♀ (see Pont and Werner 2006: 81 for details)

**Diagnosis.** *Length of body.* 11.0–14.0 mm (♀). Very similar to *A. gigas*, differing as follows: **Head.** Fronto-orbital plate silvery white pruinose. Palpus dark brown. **Thorax.** Scutum ground color brown, four broad black vittae laterally and one median white-silver pruinose vitta. Scutum laterally and scutellum dark brown. Pleurae dark brown, Lower calypter broad, ca. 3 × as long as the upper one. Haltere yellow. Calypters yellowish, the upper one with brown margin. **Legs.** Color and chaetotaxy as in



**Figures 20–30.** *Aethiopomyia arguta* (Karsch, 1879) **20** aedeagus lateral view. *Aethiopomyia gigas* (Stein, 1906) **21** Sternite 5 **22** cercal plate, lateral view **23** cercal plate, dorsal view **24** aedeagus dorsal view **25** aedeagus lateral view **26** ovipositor, dorsal view **27** ovipositor, ventral view **28** spermathecae **29** larva **30** detail of the anterior spiracle of larva. Scale bars: 0.2 mm **20–27, 29, 30**; 0.1 mm **20, 28**.

*A. arguta*. **Abdomen.** Tergites I–III almost reddish brown; tergites IV and V almost all black. Abdominal sternites with strong setae.

**Note.** The species was keyed Zumpt (1969). Cercal plate and surstylus as in Zumpt (1969: figs 1, 2). Only females seen.

### *Aethiopomyia steini* (Curran, 1935) (not seen)

**Diagnosis** (characters from Curran (1935) original description). Length of body. 9.5–11.5 mm. **Head.** black, face and lower third of frons reddish with silver-white pruinescence. Frontal vittae brownish; palpus reddish brown; antenna yellow and arista mostly brown. **Thorax.** scutum reddish, darker above, with an incomplete median vitta and the lateral margins whitish pruinose, posteriorly with reddish brown pruinescence, the two broad, shiny, ferruginous vittae more or less divided by a thin yellowish pruinose line in front of the suture. Haltere reddish yellow. **Legs.** Reddish, posterior, and middle tibiae more or less brown and tarsi black. Mid tibia with four or five posterior setae. **Abdomen.** basal two abdominal segments rusty reddish, the third and fourth black.

Female. Differs in frontal vitta reddish brown above; no orbitals; scutum with very poorly defined dark vittae, almost unicolorous.

Types. Holotype ♂; 3 paratypes ♂ (all from Eden, Cameroon); Allotype ♀ (Sierra Leone) (Zumpt 1969). Not seen.

**Note.** The species was keyed Zumpt (1969). According to Curran (1935) *A. steini* is very similar to *A. gigas*, differing by having the median vittae reddish and much finer setae on the sternite. Also differs from *A. arguta* by having the third and fourth abdominal segment wholly black.

### *Aethiopomyia williamsi* (Snyder, 1951)

Figures 15–19

**Material examined.** 2 ♀ of *Lophomala anax* Enderlein, 1927, nomen nudum (see Pont and Werner 2006: 20 for details)

**Diagnosis.** **Length of body.** 12.0–14.0 mm (♀) **Head.** Fronto-orbital plate greyish brown Palpus dark brown. **Thorax.** Scutum brownish yellow, with a median silvery grey vitta, more visible pre-suturally. Scutellum light brown, paler at tip. Calypters and halteres fulvous brown. **Legs.** Brownish yellow; tarsi dark brown. **Abdomen.** Brownish yellow with a dark dorsal median vitta on tergites IV and V. Abdominal basal sternites hairy, others with numerous long, ventrally directed setae in ♂ (from the original description; ♂ not seen).

**Note.** The species was keyed by Zumpt (1969). Zumpt (1969: 166) doubted if this species is specifically different from *A. arguta*, as, according to him, they differ only by the thicker setae on abdominal sternites in *A. williamsi*. More specimens must be examined to elucidate the specific status of the species.

## Acknowledgements

MSC is thankful to the ZMHU Diptera team for their support during a research visit to the collection and to “Conselho Nacional de Desenvolvimento Científico e Tecnológico” (CNPq, 202465/2018-7) an agency of the Brazilian Government fostering scientific and technological development, for a grant to visit and work with the collection of ZMHU. FAPERJ also supports the project (process nr. E-26/202.875/2017).

## References

- Couri MS, de Carvalho CJB (2003) Systematic relations among *Philornis* Meinert, *Passeromyia* Rodhain and Villeneuve and allied genera (Diptera, Muscidae). *Brazilian Journal of Biology* 63(2): 223–232. <https://doi.org/10.1590/S1519-69842003000200007>
- Cumming JM, Wood DM (2017) Adult Morphology and Terminology. In: Kirk-Spriggs AH, Sinclair BJ (Eds), *Manual of Afrotropical Diptera, Volume 1. Introductory chapters and keys to Diptera families. Suricata 4*. South American National Biodiversity Institute, Pretoria, 89–133.
- Curran CH (1935) African Muscidae – II. *American Museum Novitates* 776: 1–27.
- Malloch JR (1921) Exotic Muscaridae (Diptera) – II. *Annals and Magazine of Natural History* 9: 420–431. <https://doi.org/10.1080/00222932108632541>
- O’Hara E, Raper C, Pont, AC, Whitmore D (2013) Reassessment of *Paleotachina* Townsend and *Electrotachina* Townsend and their removal from the Tachinidae (Diptera). *ZooKeys* 361: 27–36. <https://doi.org/10.3897/zookeys.361.6448>
- Pont AC (1980) Family Muscidae. In: Crosskey RW (Ed.) *Catalogue of the Diptera of the Afrotropical Region*. British Museum (Natural History), London, 721–761.
- Pont AC, Werner D (2006) The types of Fanniidae and Muscidae (Diptera) in the Museum für Naturkunde, Humboldt-Universität zu Berlin, Germany. *Mitteilungen aus den Museum für Naturkunde in Berlin, Zoologische Reihe*. 82: 3–139. <https://doi.org/10.1002/mmz.200600001>
- Skidmore P (1985) *The biology of the Muscidae of the world*. Dr. W. Junk Publishers, Dordrecht, Boston, Lancaster, Series Entomologica 29: 14–550.
- Zumt F (1969) Notes on the genus *Aethiopomyia* Malloch (Diptera: Muscidae) with a new species from Tanzania. *Journal of the Entomological Society of Southern Africa* 32: 163–167.

# A new species of hagfish, *Eptatretus wandoensis* sp. nov. (Agnatha, Myxinidae), from the southwestern Sea of Korea

Young Sun Song<sup>1</sup>, Jin-Koo Kim<sup>1</sup>

<sup>1</sup> Department of Marine Biology, Pukyong National University, Busan, 48513, Korea

Corresponding author: Jin-Koo Kim ([taengko@hanmail.net](mailto:taengko@hanmail.net))

---

Academic editor: M.E. Bichuette | Received 24 November 2019 | Accepted 24 February 2020 | Published 13 April 2020

---

<http://zoobank.org/5E83DB40-3A11-442E-85F3-6C8DCCF487E4>

---

**Citation:** Song YS, Kim J-K (2020) A new species of hagfish, *Eptatretus wandoensis* sp. nov. (Agnatha, Myxinidae), from the southwestern Sea of Korea. *ZooKeys* 926: 81–94. <https://doi.org/10.3897/zookeys.926.48745>

---

## Abstract

Four specimens of the five-gilled white mid-dorsal line hagfish, *Eptatretus wandoensis* sp. nov. were recently collected from the southwestern Sea of Korea (Wando). This new species has five pairs of gill apertures, 14–18 prebranchial slime pores, 4 branchial slime pores, a dark brown back with a white mid-dorsal line and a white belly. These hagfish are similar to *Eptatretus burgeri* and *Eptatretus minor* in having a white mid-dorsal line, but can be readily distinguished by the numbers of gill apertures (5 vs. 6–7), gill pouches (5 vs. 6), and prebranchial slime pores (14–18 vs. > 18), as well as the body color (dark brown back vs. gray or brown pale). In terms of genetic differences, *Eptatretus wandoensis* could be clearly distinguished from *E. burgeri* (0.9% in 16S rRNA and 8.5% in cytochrome c oxidase subunit I sequences) and *E. minor* (4.5% and 13.9%).

## Keywords

mitochondrial DNA, morphology, myxinid, Myxiniformes, Northwest Pacific, taxonomy

## Introduction

Myxinidae (hagfishes) are currently classified into six genera and 81 species worldwide (Fernholm et al. 2013; Froese and Pauly 2019). They are characterized by an eel-like body shape and 1–16 pairs of gill apertures and gill pouches; however, they

have no jaws, eyes, or fins (Fernholm 1998). Recent research using morphological and molecular characteristics revealed that hagfishes comprise three subfamilies: Eptatretinae, Myxininae, and Rubicundinae (Fernholm et al. 2013). There have been several unresolved issues regarding the number of recognized genera in the subfamily Eptatretinae; however, its genera were recently reorganized taxonomically based on morphological and molecular data (Fernholm et al. 2013; Song 2019). Therefore, Eptatretinae currently includes a single genus, *Eptatretus*, which is characterized by the presence of more than two pairs of gill apertures; notably, *Eptatretus* is the most species-rich myxinid genus, currently comprising 51 valid species in the northwestern Pacific Ocean (e.g., Korea, Taiwan, and Japan) and coastal waters around Asia (e.g., China, Philippines, and Vietnam) (Froese and Pauly 2019). Surveys of the deep sea and other hard-to-reach areas using special-purpose submarines are increasingly revealing new or cryptic species worldwide (Fernholm and Quattrini 2008; Mincarone and Fernholm 2010; Zintzen et al. 2015). Based on examinations of both morphological and genetic characteristics of hagfish specimens from the southwestern Sea of Korea, we herein describe a new species, *Eptatretus wandoensis* sp. nov., and compare it with other members of the *Eptatretus* genus in around northeastern Asia.

## Materials and methods

We obtained four specimens (202.0–292.0 mm total length) from Yeoseo-ri, Wandogun in Korean waters in 2018, caught by fishing trapping and bought to the fish markets (Fig. 1). The specimens have been deposited in the Marine Fish Resource Bank of Korea (MFRBK) at Pukyong National University (PKU), Busan-si, Korea. We performed morphological and molecular analyses to clarify their taxonomic status, the former based on a total of 11 counts and 13 measurements. Morphological methods and terminology followed Fernholm and Hubbs (1981) and Wisner and McMillan (1988). Each body part was measured to the nearest 0.1 mm using digital Vernier calipers, and the data were converted to percentages of the total length (TL). We counted the numbers of anterior (outer) unicusps (AUC), posterior (inner) unicusps (PUC), multicusps (= fused cusps), and total cusps according to Fernholm (1998), using a stereomicroscope (SZX-16; Olympus, Tokyo, Japan). Images were analyzed using an image analyzer (Shinhan Active Measure; Shinhan Scientific Optics, Seoul, Korea), and features were sketched using a camera lucida (SZX-DA; Olympus). We examined the anatomical characters such as the arrangement between gill pouch (GP) and efferent branchial duct (EBD). The terminology of anatomical structures followed Mok and McMillan (2004): afferent branchial arteries (ABA), efferent branchial artery (EBA), ventral aorta (VA), medial section of ventral artery (MVA), and side branchial artery (SBA). We examined (and added to) the morphological description of nasal-sinus papillae following Mok (2001) and Zintzen et al. (2015).

To compare molecular characters, total genomic DNA was extracted from the muscle tissues using 10% Chelex 100 resin (Bio-Rad, Hercules, CA) and PCR was

then performed for mitochondrial DNA 16S ribosomal RNA (16S rRNA) and cytochrome c oxidase subunit I (COI), using an MJ Mini Thermal Cycler PTC-1148 (Bio-Rad) in mixtures consisting 1  $\mu$ L of genomic DNA, 2  $\mu$ L of 10 $\times$  PCR buffer, 1.6  $\mu$ L of 2.5 mM dNTPs, 0.5  $\mu$ L of each primer, 0.1  $\mu$ L of TaKaRa EX-*Taq* polymerase (TaKaRa Bio Inc., Kyoto, Japan), and distilled water to bring the final volume to 20  $\mu$ L. PCR products were amplified using universal primers: VF2-F (5'-TCA ACC AAC CAC AAA GAC ATT GGC AC-3') and FishR2-R (5'-ACT TCA GGG TGA CCG AAG AAT CAG AA-3') designed by Ward et al. (2005) and 16SAR-L (5'-CGC CTG TTT ATC AAA AAC AT-3') and 16SBR-H (5'-CCG GTC TGA ACT CAG ATC ACG T-3') designed by Ivanova et al. (2007). The PCR profiles for the COI and 16S rRNA region consisted of initial denaturation at 95 °C for 5 min, followed by 35 cycles of denaturation at 95 °C for 1 min, annealing at 54 °C for 1 min (annealing at 50 °C in 16S rRNA), extension at 72 °C for 1 min, and a final extension at 72 °C for 5 min. The PCR products were purified using a Davinch™ PCR Purification Kit (Davinch-K Co., Ltd., Seoul, Korea). The DNA was sequenced with an Applied Biosystems ABI 3730XL sequencer (Applied Biosystems, Foster City, CA) using an ABI PRISM BigDye Terminator Cycle Sequencing Ready Reaction Kit v3.1 (Applied Biosystems). We compared our molecular data with those of the mtDNA 16S rRNA and COI sequences from various hagfish species obtained from the National Center for Biotechnology Information. Sequences were aligned using ClustalW (Thompson et al. 1994) in BioEdit version 7 (Hall 1999). The genetic divergences were calculated using the Kimura 2-parameter (K2P) (Kimura 1980) model with Mega 6 (Tamura et al. 2013). Phylogenetic trees were constructed using the neighbor-joining (NJ) method (Saitou and Nei 1987) in Mega 6 (Tamura et al. 2013), with confidence assessed based on 1000 bootstrap replications. For molecular comparison, we further analyzed the COI and 16S rRNA sequences of the *Eptatretus* species, the other hagfish species obtained from the GenBank database. The new species sequences of each regions have been deposited with GenBank (PKU 62167, MT002683; PKU 62169, MT002684; PKU 62171, MT002685; PKU 62173, MT002686 in 16S rRNA, and PKU 62171, MT002967 in COI).

## Taxonomy

### *Eptatretus wandoensis* sp. nov.

<http://zoobank.org/9C6CA8CC-BC42-48E2-87EE-47702CC46D49>

Figures 1–5, Table 1

New English name: Five-gilled white mid-dorsal line hagfish; new Korean name:

Huin-jul-wae-meok-jang-eo

**Type locality.** The coast of Yeoseo-do (southwestern Sea of Korea): Yeoseo-ri, Cheongsan-myeon, Wando-gun, Jeollanam-do, Republic of Korea, 33°59'56.5"N, 126°53'57.0"E, caught by fishing traps, 60–80 m (Fig. 1).

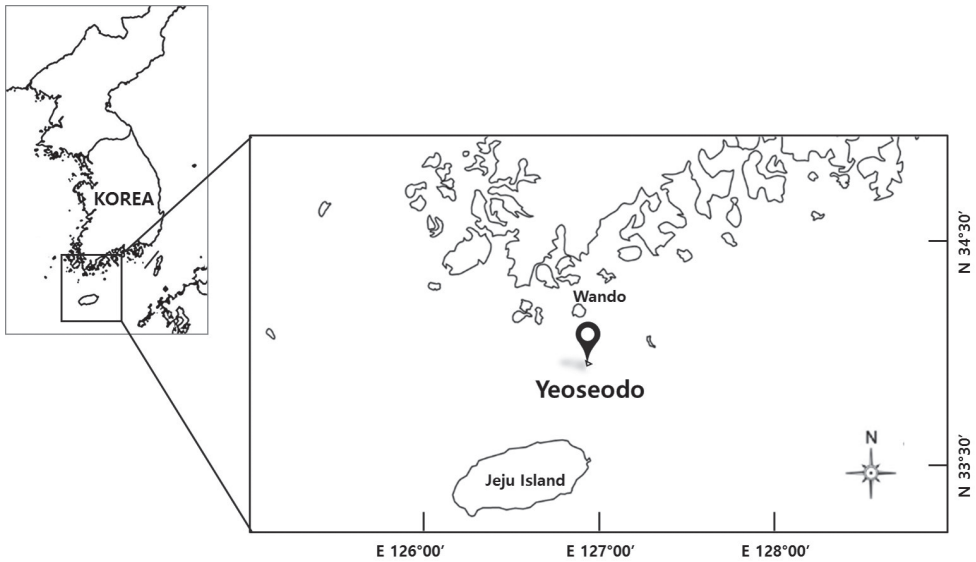


**Figure 1.** Sampling location of *Eptatretus wandoensis* sp. nov. in Korea.

**Holotype.** PKU 62167, 292.0 mm TL, Yeoseo-ri, Cheongsan-myeon, Wando-gun, Jeollanam-do, Republic of Korea, 33°59'56.5"N, 126°53'57.0"E, caught by fishing traps, 60–80 m, 26 Jun 2018.

**Paratypes.** PKU 62169 (1 specimen), 202.0 mm TL, Yeoseo-ri, Cheongsan-myeon, Wando-gun, Jeollanam-do, Republic of Korea, 33°59'56.5"N, 126°53'57.0"E, fishing trap, 60–80 m, 12 May 2018; PKU 62171, PKU 62173, 275.0–290.0 mm TL, Yeoseo-ri, Cheongsan-myeon, Wando-gun, Jeollanam-do, Republic of Korea, 33°59'56.5"N, 126°53'57.0"E, fishing trap, 60–80 m, 26 Jun 2018.

**Diagnosis.** Gill apertures, 5; eyespots, conspicuous; fused cusps, 3/2; total cusps, 40–43; 1 GP at end of dental muscle; total slime pores, 74–82 (prebranchial, 14–18; branchial, 4; trunk, 46–49; tail, 9–11); branchial length, 5.2%–6.2% of TL; pharyngocutaneous duct confluent with last gill aperture; ventral artery splitting at approximately 3–4 GP; dorsal region with dark brown body color, ventral region with white body color; white mid-dorsal line, conspicuous.

**Description.** Body elongated; laterally compressed at trunk and strongly compressed at tail (Fig. 2). Rostrum slightly blunt and round (Fig. 3A). Nasal-sinus papilla absent. Eyespots present (Fig. 3A). Pre-eyespots shorter than branchial region (4.4%–4.9% of TL). Three pairs of barbels on head: first (1.5%–1.6% of TL) and second barbels (1.6%–1.9% of TL) nearly equal in size; third barbel is longer (2.1%–2.3% of TL) and tips of third barbels extend at the mouth (Fig. 3B). Five pairs of GP and apertures; each gill aperture arranged regularly spaced in a straight line (Fig. 3C). Teeth row comb-like, consisting of two rows with tips sharp and curved rearward (Fig. 4A); in the outer row, 3 multicusps and 7–8 unicusps; in the inner row, 2 multicusps and 8–9 unicusps; total number of cusps, 40–43. Dental muscle thick and long, posterior tip of dental muscle located in first GP (Fig. 4B). Slime pores: prebranchial, 14–18;



**Figure 2.** Overall view of *Eptatretus wandoensis* sp. nov., **A** holotype, PKU 62167, 292.0 mm in total length (TL) **B** paratype, PKU 62169, 202.0 mm TL **C** paratype, PKU 62171, 290.0 mm TL **D** paratype, PKU 62173, 275.0 mm TL, photographed prior to preservation. Scale bars: 1 mm.

branchial, 4; trunk, 46–49; tail, 9–11; total, 74–82. Body proportions are as follows: prebranchial length, 24.4%–26.3% of TL; branchial length, 5.2%–6.2% of TL; trunk length, 54.9%–59.3% of TL; tail length, 12.8%–14.0% of TL; cutaneous duct, 7.6%–9.3% of TL; branchial duct (with ventral fin-fold), 6.9%–9.7% of TL; and branchial duct (alone), 5.6%–7.7% of TL (Table 1). Posterior-most EBD confluent with pharyngocutaneous duct on left side, forming a larger aperture (Fig. 4B). All efferent branchial ducts are equal in length. VA consists of two SBAs and one medial section, bifurcating at approximately the third or fourth GP. First through third pairs of ABAs, which cannot be regarded as branches of the VA, branch from SBAs; however, fourth and fifth ABAs on left and right branch from the medial section of the ventral artery (Fig. 4B). Ventral fin-fold weakly developed or vestigial, beginning approximately at middle of body and extending to cloaca (Fig. 3D). Caudal fin-fold weakly developed, beginning posterior cloaca and extending around tail to dorsal surface.

Coloration when fresh: Body uniformly dark brown or purplish dorsally and white ventrally; white mid-dorsal line conspicuous, beginning from the upper region of the first prebranchial slime pore to around the tail. Eyespots conspicuous; whole barbels (rarely the tip) pale, and pale around mouth. Each gill aperture and pharyngocutaneous duct aperture with white margin; most slime pores blackish (except for tail region), tail slime pores same as surrounding color. White around cloaca; ventral fin-fold with a white line along the ventral midline; posterior margin of caudal fin pale (Fig. 2).

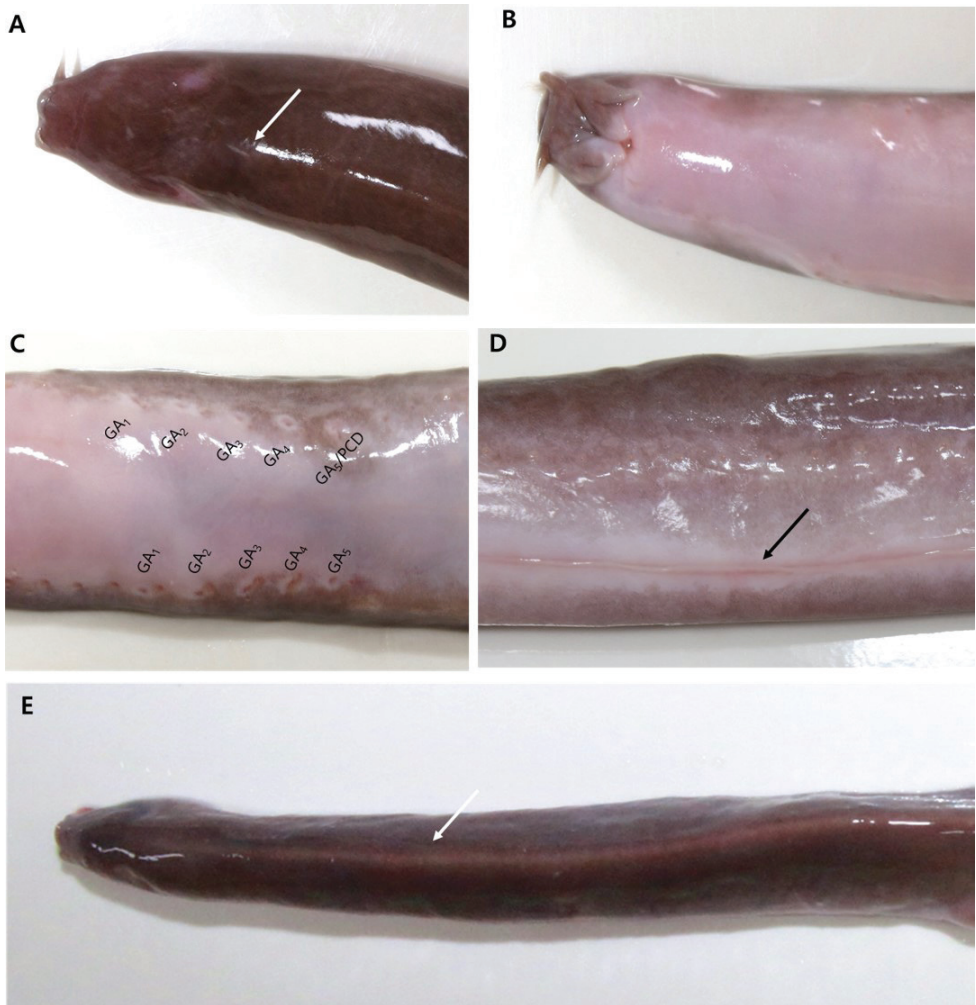


**Figure 3.** *Eptatretus wandoensis* sp. nov. PKU 62167, prior to preservation **A** head dorsal view, white arrow indicates a white mid-dorsal line **B** head ventral view **C** gill apertures (GA) and pharyngocutaneous duct (PCD), note the location of GA and PCD **D** ventral view of body, black arrow indicates the ventral fin-fold (VFF) **E** dorsal region of body with a white mid-dorsal line.

Coloration when preserved: Body brown to dark brown dorsally and murky white ventrally (more conspicuous than fresh specimen). Eyespots conspicuous; all slime pores surrounded by conspicuous white ring. Each gill aperture and pharyngocutaneous duct aperture conspicuous; ventral fin-fold pale; white mid-dorsal line inconspicuous.

**Distribution.** Southwestern Sea of Korea.

**Biology.** Attains a maximum TL of 292.0 mm (fresh specimen); this specimen is female, without mature eggs in the body cavity. A female specimen of 290.0 mm TL carries approximately 20 developing eggs, which have no terminal anchor filaments or hooks; each egg approximately 4–7 mm in diameter and 10–12 mm in length.

**Etymology.** The specific name, *wandoensis*, refers to the type locality, in Korea.

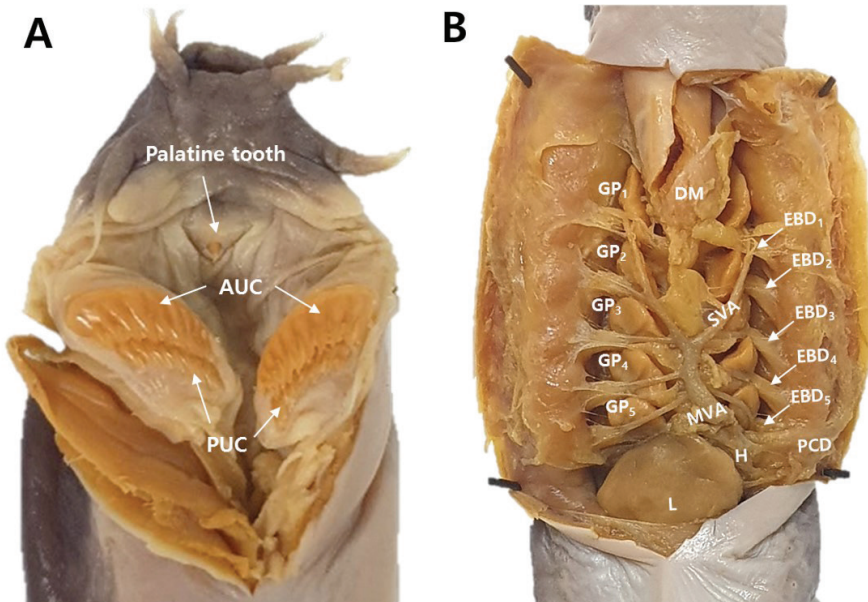


**Figure 4.** Anatomical morphology of *Eptatretus wandoensis* sp. nov. PKU 62167. **A** palatine tooth, anterior unicusps (AUC) and posterior unicusps (PUC) **B** branchial region dissected, gill pouches (GP), median ventral aorta (MVA), separated ventral aorta (SVA), efferent branchial duct (EBD), pharyngocutaneous duct (PCD), dental muscle (DM), liver (L), and heart (H).

### Morphological comparisons

*Eptatretus wandoensis* sp. nov. is most similar to *Eptatretus burgeri* (Girard, 1855) and *Eptatretus minor* Fernholm & Hubbs, 1981 due to the presence of a light mid-dorsal line, gill apertures regularly spaced in a straight line, and EBDs of equal length. These three species differ from each other in the number of gill apertures (5 for *E. wandoensis*, compared to 6 for *E. burgeri* and *E. minor*), body color (dark brown or purplish dorsally and white ventrally for *E. wandoensis*, compared to brown for *E. burgeri* and gray/brown pale for *E. minor*), prebranchial slime pores (14–18 for *E. wandoensis*, compared to 18–23 for *E. burgeri*), total slime pores (74–82 for *E. wandoensis*, compared to 81–92 for *E. burgeri*), ventral fin-fold (weakly developed for *E. wandoensis*, compared to well developed for *E. burgeri*), multicusps (3/2 for *E. wandoensis*, compared to 3/3 for *E. minor*), total cusps (40–43 for *E. wandoensis*, compared to 46–52 for *E. minor*) (Table 1), nasal-sinus papillae (absent for *E. wandoensis*, compared to paired for *E. minor*), and eyespots (present for *E. wandoensis*, compared to absent for *E. minor*). *Eptatretus wandoensis* sp. nov. can be distinguished from *Eptatretus cheni* (Shen & Tao, 1975), *Eptatretus nelsoni* (Kuo, Huang & Mok, 1994), and *Eptatretus yangi* (Teng, 1958) by the presence of regularly spaced gill apertures in a linear (vs. irregular and crowded for *E. cheni*, *E. nelsoni*, and *E. yangi*) arrangement; equal length of all EBDs (vs. length of first efferent branchial duct notably longer than that of the most posterior efferent branchial duct); 40–43 total cusps (vs. 50–53 for *E. cheni*; 32–40 for *E. nelsoni* and *E. yangi*); 4 branchial slime pores (vs. no branchial slime pores); prebranchial length, 24.4%–26.3% of TL (vs. more than 29.0%

**Table 1.** Morphometric and meristic measurements of *Eptatretus wandoensis* sp. nov., and congeneric species with five gill apertures (*E. cheni*, *E. nelsoni* and *E. yangi*) and white mid-dorsal line (*E. burgeri* and *E. minor*).

	<i>Eptatretus wandoensis</i> sp. nov.		<i>E. cheni</i> *	<i>E. nelsoni</i> *	<i>E. yangi</i> *	<i>E. burgeri</i> *	<i>E. minor</i> **
	Holotype	Paratypes (3)					
Gill aperture (GA)	5	5	5	5	5	6–7	6
Gill pouch (GP)	5	5	5	5	5	6	6
NSP	absent	absent	absent	absent	absent	absent	paired
<b>Cusps</b>							
MUC (multi)	3/2	3/2	3/3	3/2	3/2	3/2	3/3
AUC (outer)	7	7–8	9–11	5–8	5–8	6–8	8–11
PUC (inner)	8	8–9	9–10	5–8	6–9	7–9	8–10
Total Cusps	42	40–43	50–53	32–40	32–40	35–42	46–54
<b>Slime pores</b>							
Prebranchial	14	15–18	24–27	13–20	16–23	18–23	15–18
Branchial	4	4	0	0	0	4–5	4–6
Trunk	47	46–49	41–47	33–39	39–47	45–51	41–48
Tail	11	9–11	7–10	6–10	7–12	11–14	11–14
<b>Total pores</b>	76	74–82	75–81	57–67	68–79	81–92	74–82
<b>Length in % of TL</b>							
Prebranchial	24.7	24.4–26.3 (25.3)	33.3–35.5	30.5–32.6	29.2–32.0	25.2–29.6	20.1–25.9
Branchial	5.9	5.2–5.8 (5.5)	2.2–3.4	1.1–2.8	1.1–1.7	6.2–7.8	5.1–7.2
Trunk	56.5	54.9–59.3 (56.9)	45.9–50.8	49.5–52.6	53.2–54.9	47.6–55.0	50.6–55.9
Tail	13.4	12.8–14.0 (13.5)	13.2–16.7	15.0–18.0	12.2–15.6	13.2–17.0	13.9–18.3
Nostril to mouth	3.4	3.7–3.8 (3.8)	–	–	–	–	–
Nostril width	1.7	0.8–1.5 (1.2)	–	–	–	–	–
Nostril length	0.6	0.7–1.6 (1.1)	–	–	–	–	–
Mouth width	3.2	3.3–3.8 (3.6)	–	–	–	–	–
Pre-eyespot to nostril	4.9	4.4–5.2 (4.8)	–	–	–	–	–
<b>Depth in % of TL</b>							
w/VFF	7.5	6.9–9.7 (8.3)	8.1–9.0	15.0–15.5	6.9–10.4	4.7–8.5	7.1–11.4
Branchial region	6.3	5.6–7.7 (6.7)	–	–	–	–	–
Over caudal	7.8	7.6–9.3 (8.6)	7.6–10.2	8.9–10.1	6.5–10.0	5.1–8.5	5.3–11.6

\*McMillan and Wisner (2004), \*\*Fernholm and Hubbs (1981); Abbreviation: NSP (nasal-sinus papillae), MUC (multi-cusps), AUC (anterior unicusps), PUC (posterior unicusps), VFF (ventral fin-fold).

of TL); branchial length, 5.2%–5.9% of TL (vs. less than 3.4% of TL); trunk length, 54.9–59.3% of TL (vs. less than 54.9%); eyespots conspicuous (vs. inconspicuous), and dorsal dark brown and ventral white body color (vs. brownish-grey). In comparison to *Eptatretus* species occurring in Korean and Japanese waters, this new species is well distinguished from the three most common hagfishes, *Eptatretus atami* (Dean, 1904), *Eptatretus walkeri* (McMillan & Wisner, 2004), and *Eptatretus okinoseanus* (Dean, 1904) based on the difference of gill apertures (5 in *E. wandoensis* sp. nov. vs. 6 in *E. atami* and *E. walkeri* vs. 8 in *E. okinoseanus*), branchial slime pores (4, 0–1, 0, and 6–8), and a white mid-dorsal line (present, absent, absent, and absent) (Table 2).

**Table 2.** Comparison of meristic and proportional measurements among *Eptatretus* species occurring in Korean and Japanese waters.

Characters	<i>E. wandoensis</i> sp. nov.	<i>E. atami</i> *	<i>E. walkeri</i>	<i>E. okinoseanus</i> *
Gill aperture	5	6	6	8
Gill pouch	5	6	6	8
NSP	absent	absent	absent	absent
<b>Cusps</b>				
MUC	3/2	3/3	3/2	3/2
AUC	7–8	9–10	6–9	7–10
PUC	8–9	8–10	7–9	7–10
Total	40–43	47–52	36–44	40–49
<b>Slime pores</b>				
Prebranchial	14–18	12–19	15–22	13–17
Branchial	4	0–1	0	6–8
Trunk	46–49	43–47	40–48	54–61
Tail	9–11	9–12	8–13	10–14
<b>Total pores</b>	74–82	71–78	68–79	87–97
<b>Length in % of TL</b>				
Prebranchial	24.4–26.3	26.6–30.2	24.2–39.1	19.2–22.6
Branchial	5.2–5.9	1.3–4.2	2.0–3.8	6.2–9.2
Trunk	54.9–59.3	53.9–56.1	50.8–68.6	50.4–59.4
Tail	12.8–14.0	11.1–14.2	10.7–16.1	12.7–15.5
<b>Depth (mm)</b>				
w/VFF	6.9–9.7	8.1–9.0	5.0–11.1	5.7–8.1
Over caudal	7.6–9.3	7.4–8.8	6.3–11.4	6.2–9.0

\*McMillan and Wisner (2004); Abbreviation: NSP (nasal-sinus papillae), MUC (multicusps), AUC (anterior unicusps), PUC (posterior unicusps), VFF (ventral fin-fold).

## Genetic comparisons

Differences among mtDNA sequences obtained from the holotype and paratypes of *Eptatretus wandoensis* sp. nov. were consistent with species-level divergences in other hagfish species (Fernholm et al. 2013). The phylogenetic relationships of myxinid species, inferred from neighbor-joining trees, showed large genetic distances between similar hagfish species using mtDNA 16S rRNA (477 bp) and cytochrome c oxidase subunit I (COI) (466 bp) sequences. *Eptatretus wandoensis* sp. nov. is separated from other congeneric species by high genetic divergences of 0.9%–7.5% in 16S rRNA sequences and 4.9%–13.9% in COI sequences (Fig. 5). The respective genetic distances between this species and *E. burgeri* and *E. minor* were 0.9% and 4.5% in 16S rRNA sequences and 8.5% and 13.9% in COI sequences. In addition, phylogenetic analysis of 16S rRNA sequences showed that *E. wandoensis* sp. nov. is well separated from other five-gilled hagfishes (*E. cheni*, *E. nelsoni*, and *E. yangi*), with genetic differences of 7.5%, 1.4%, and 1.6%, respectively. *Eptatretus cheni* is located at a basal position of hagfishes and well nested in the *Eptatretus* clade.

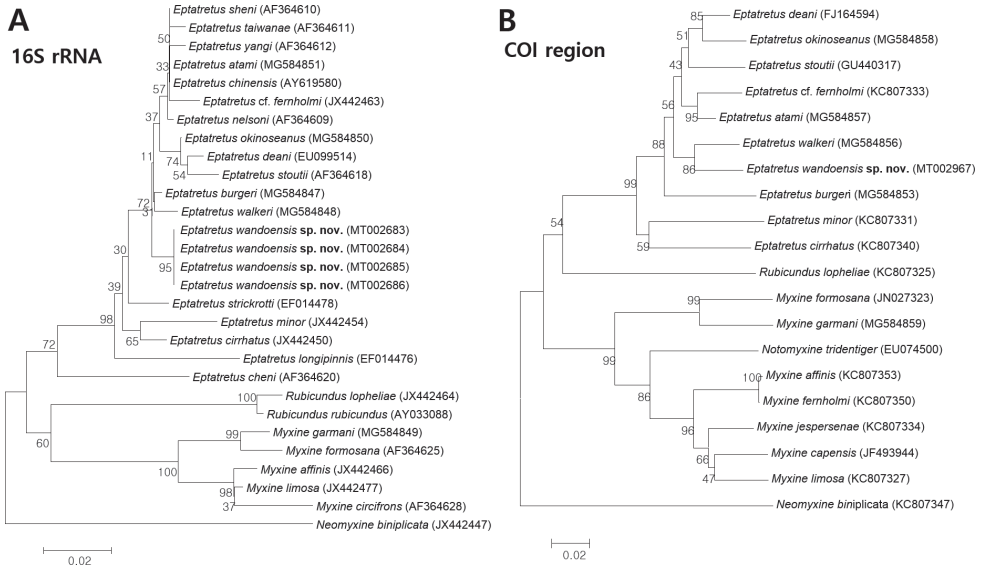


**Figure 5.** Phylogenetic tree of hagfishes based on mitochondrial DNA sequences, constructed with the Neighbor-joining (NJ) method using Kimura 2-parameter distances **A** mitochondrial DNA 16S rRNA sequences **B** mitochondrial DNA cytochrome c oxidase subunit I (COI) sequences. Numbers above tree branches are bootstrap values based on 1000 replicates. Scale bar represent nucleotide substitutions per site.

## Discussion

*Eptatretus wandoensis* sp. nov. is one of many new hagfish species recently discovered in the northwest Pacific Ocean. Thus far, six hagfish species with five gill apertures have been reported worldwide (McMillan and Wisner 2004; Kuo et al. 2010; Zintzen et al. 2015); most are included in the genus *Eptatretus* (Fernholm et al. 2013). However, three species have tubular nostrils and pink coloration; thus, they are regarded as *Rubicundus* species (Fernholm et al. 2013; Zintzen et al. 2015). This new species is the third member of the genus with a white mid-dorsal line, after *Eptatretus burgeri* and *E. minor* (Girard 1855; Fernholm and Hubbs 1981). This new species was initially confused with *E. burgeri* because it may have been considered a morphological variation of *E. burgeri*, due to the presence of five gill apertures. However, they are well distinguished by the body color, prebranchial slime pores, total slime pores, and ventral fin-fold. In addition, we found a female specimen with ripe eggs on June 26, 2018. Recent study revealed that the minimum mature size *Eptatretus burgeri* with ripe eggs is more than 500.0 mm TL (Song 2019); however, this female specimen was 290.0 mm TL. Recently, specific anatomical structures such as cusps, nasal-sinus papillae, and heart have been regarded as useful characters for clarifying interrelationship among hagfish (Mok 2001; Icardo et al. 2016a; Icardo et al. 2016b). Indeed, Mok (2001) suggested that the absence of nasal-sinus papillae may be an apomorphic character of most eptatretines. Interestingly, all three *Eptatretus* species have no nasal-sinus papillae (Song and Kim 2020), and so therefore well supports the hypothesis of Mok (2001). Phylogenetic trees indicated that the new species is sister-

group to *E. walkeri* (supported by CO1 gene), but *E. walkeri* becomes the sister-group of *E. burgeri* (supported by 16S rRNA gene). Naylor and Brown (1998) mentioned that genes yielding correct results might vary among data sets and thus this discordance might be influenced by stochastic error associated with a different number of species and data sets. Kawaguchi et al (2001) suggested that taxonomic sampling and comprehensive sequencing may clarify intra- and interrelationships of fish using mitochondrial data.

In terms of geographic distribution, *Eptatretus minor* occurs in the Gulf of Mexico and Atlantic Ocean, while *E. burgeri* coexists with this new species in the same region of coastal Korea. In the comparison of depths, *Eptatretus wandoensis* sp. nov. is collected from depths between 60 to 80 m, and *E. burgeri* is known as between 5 and 270 m, and *E. minor* is known as between 300 and 400 m (Fernholm and Hubbs 1981; Moller and Jones 2007; Knapp et al. 2011; Angulo and Moral-Flores 2016). Among them, *Eptatretus minor* is deeper than the other two species. Interestingly, most Korean hagfishes tend to be distributed in quite shallow waters (within 100 m water depth) (Song 2019; Song and Kim 2020). In a recent morphological and molecular taxonomic review of *Eptatretus atami* from the coast of Japan, the specimens with 3/2 multicusps from the western coast of Honshu were identified as *E. walkeri*, whereas eastern specimens with 3/3 multicusps matched *E. atami* (Kase et al. 2017; Kitano et al. 2019). Later, Song and Kim (2020) revealed for the first time the existence of *E. walkeri* previously misidentified as *E. atami* in Korea, and confirmed that three species are currently distributed in Korea.

## Acknowledgments

This research was supported by the Marine Biotechnology Program of the Korea Institute of Marine Science and Technology Promotion (KIMST) funded by the Ministry of Oceans and Fisheries (MOF) (No. 20170431).

## References

- Angulo A, Moral-Flores LF (2016) Hagfishes of Mexico and Central America: Annotated catalog and identification key, In: Orlov A, Beamish R (Eds) *Jawless fishes of the world*. Cambridge Scholars Publishing, 94–125.
- Dean B (1904) Notes on Japanese myxinoids. A new genus, *Paramyxine*, and a new species *Homea okinoseana*. Reference also to their eggs. *Journal of the College of Science, Imperial University, Tokyo*, 19: 1–23.
- Fernholm B (1998) Hagfish systematics. In: Jørgensen JM, Lomholt JP, Weber RE, Malte H (Eds) *Biology of Hagfishes*. Chapman & Hall, London, 33–44. [https://doi.org/10.1007/978-94-011-5834-3\\_3](https://doi.org/10.1007/978-94-011-5834-3_3)
- Fernholm B, Hubbs CL (1981) Western Atlantic hagfishes of the genus *Eptatretus* (Myxinidae) with description of two new species. *Fishery Bulletin* 79: 69–83.

- Fernholm B, Noren M, Kullander SO, Quattrini AM, Zintzen V, Roberts CD, Mok HK, Kuo CH (2013) Hagfish phylogeny and taxonomy, with description of the new genus *Rubicundus* (Craniata, Myxinidae). *Journal of Zoological Systematics and Evolutionary Research* 51(4): 296–307. <https://doi.org/10.1111/jzs.12035>
- Fernholm B, Quattrini AM (2008) A new species of hagfish (Myxinidae: *Eptatretus*) associated with deep-sea coral habitat in the western North Atlantic. *Copeia* 2008(1): 126–132. <https://doi.org/10.1643/CI-07-039>
- Froese R, Pauly D (Eds) (2019) FishBase. World Wide Web electronic publication. [www.fishbase.org](http://www.fishbase.org) [version (08/2019)]
- Girard CF (1855) Contributions to the fauna of Chile. Report to Lieut. James M. Gilliss, U. S. N., upon the fishes collected by the U. S. Naval Astronomical Expedition to the southern hemisphere during the years 1849-50-51-52. Washington, D.C. 1858, 2 vols. 42 pls. <https://doi.org/10.4000/quaternaire.5086>
- Hall TA (1999) BioEdit: a user-friendly biological sequence alignment editor and analysis program for Windows 95/98/NT. *Nucleic Acids Symposium Series* 41: 95–98. [https://doi.org/10.14601/Phytopathol\\_Mediterr-14998u1.29](https://doi.org/10.14601/Phytopathol_Mediterr-14998u1.29)
- Icardo JM, Colvee E, Schorno S, Lauriano ER, Fudge DS, Glover CN, Zaccone G (2016a) Morphological analysis of the hagfish heart. I. The ventricle, the arterial connection and the ventral aorta. *Journal of Morphology* 277: 326–340. <https://doi.org/10.1002/jmor.20498>
- Icardo JM, Colvee E, Schorno S, Lauriano ER, Fudge DS, Glover CN, Zaccone G (2016b) Morphological analysis of the hagfish heart. II. The venous pole and the pericardium. *Journal of Morphology* 277: 853–865. <https://doi.org/10.1002/jmor.20539>
- Ivanova NV, Zemlak TS, Hanner RH, Hebert PDN (2007) Universal primer cocktails for fish DNA barcoding. *Molecular Ecology Notes* 7: 554–548. <https://doi.org/10.1111/j.1471-8286.2007.01748.x>
- Kase M, Shimizu T, Kamino K, Umetsu K, Sugiyama H, Kitano T (2017) Brown hagfish from the northwest and east coasts of Honshu, Japan are genetically different. *Genes & Genetic Systems* 92: 197–203. <https://doi.org/10.1266/ggs.17-00004>
- Kawaguchi A, Miya M, Nishida M (2001) Complete mitochondrial DNA sequences of *Aulopus japonicas* (Teleostei: Aulopiformes), a basal Eurypterygii: longer DNA sequences and higher-level relationships. *Ichthyological Research* 48: 213–223. <https://doi.org/10.1007/s10228-001-8139-0>
- Kimura M (1980) A simple method for estimating evolutionary rate of base substitution through comparative studies of nucleotide sequences. *Journal of Molecular Evolution* 16: 111–120. <https://doi.org/10.1007/BF01731581>
- Kitano T, Sasaki K, Ichinoseki S, Umetsu K, Sugiyama H (2019) The Northern Brown Hagfish, *Eptatretus walkeri* (McMillan and Wisner, 2004) (Myxiniformes: Myxinidae), is Widely Distributed in Japanese Coastal Waters. *Asian Fisheries Science* 32: 29–38. <https://doi.org/10.33997/j.afs.2019.32.01.004>
- Knapp L, Mincarone MM, Harwell H, Polidoro B, Sanciangco J, Carreter K (2011) Conservation status of the world's hagfish species and the loss of phylogenetic diversity and ecosystem function. *Aquatic Conservation* 21: 401–411. <https://doi.org/10.1002/aqc.1202>

- Kuo CH, Huang KF, Mok HK (1994) Hagfishes of Taiwan (I): a taxonomic revision with description of four new *Paramyxine* species. *Zoological Studies* 33: 126–139.
- Kuo CH, Lee SC, Mok HK (2010) A New Species of Hagfish *Eptatretus rubicundus* (Myxiniidae: Myxiniiformes) from Taiwan, with Reference to Its Phylogenetic Position Based on Its Mitochondrial DNA Sequence. *Zoological Studies* 49: 855–864.
- McMillan CB, Wisner RL (2004) Review of the Hagfishes (Myxiniidae: Myxiniiformes) of the Northwestern Pacific Ocean, with Descriptions of Three New Species, *Eptatretus fernholmi*, *Paramyxine moki*, *P. walkeri*. *Zoological Studies* 43(1): 51–73.
- Mincarone MM, Fernholm B (2010) Review of the Australian hagfishes with description of two new species of *Eptatretus* (Myxiniidae). *Journal of Fish Biology* 77: 779–801. <http://doi.org/10.1111/j.1095-8649.2010.02661.x>
- Mincarone MM (2011) *Eptatretus burgeri*. The IUCN Red List of Threatened Species 2011: e.T196016A8992245. <https://doi.org/10.2305/IUCN.UK.2011-1.RLTS.T196016A8992245.en>
- Mok HK (2001) Nasal-sinus Papillae of Hagfishes and Their Taxonomic Implications. *Zoological Studies* 40(4): 355–364.
- Mok HK, McMillan CB (2004) Bifurcating Pattern of the Ventral Aorta and Distribution of the Branchial Arteries of Hagfishes (Myxiniiformes), with Notes on the Taxonomic Implications. *Zoological Studies* 43: 737–748.
- Moller PR, Jones WJ (2007) *Eptatretus strickrotti* n. sp. (Myxiniidae): First Hagfish Captured From a Hydrothermal Vent. *Biological Bulletin* 212(1): 55–66. <https://doi.org/10.2307/25066580>
- Naylor GJP, Brown WM (1998) Amphioxus mitochondrial DNA, chordate phylogeny, and the limits of inference based on comparisons of sequences. *Systematics Biology* 47: 61–76. <https://doi.org/10.1080/106351598261030>
- Saitou N, Nei M (1987) The Neighbor-Joining Method: A New Method for Reconstructing Phylogenetic Trees. *Molecular Biology and Evolution* 4: 406–425. <https://doi.org/10.1093/oxfordjournals.molbev.a040454>
- Shen SC, Tao HJ (1975) Systematic studies on the hagfish (Eptatretidae) in the adjacent waters around Taiwan with description of two new species. *Chinese Bioscience* 2: 65–80.
- Song YS (2019) Phylogeny and taxonomic revision of the family Myxiniidae (Myxiniiformes) in the Northwest Pacific, with population genetics of *Eptatretus burgeri*. Pukyong National University, 337 pp.
- Song YS, Kim JK (2020) Range expansion and redescription of the hagfish *Eptatretus burgeri* (Myxiniidae) from northeast Asia and its distribution from *E. atami*. *Journal of Asia Pacific Biodiversity* (In press). <https://doi.org/10.1016/j.japb.2020.01.003>
- Tamura K, Stecher G, Peterson D, Filipski A, Kumar S (2013) MEGA6: Molecular Evolutionary Genetics Analysis version 6.0. *Molecular Biology and Evolution* 30: 2725–2729. <https://doi.org/10.1093/molbev/mst197>
- Teng HT (1958) A new species of Cyclostomata from Taiwan. *Chinese Fisheries* 66: 3–6.
- Thompson JD, Higgins DG, Gibson TJ (1994) Clustal W: improving the sensitivity of progressive multiple sequence alignment through sequence weighting, position-specific gap

- penalties and weight matrix choice. *Nucleic Acids Research* 22: 4673–4680. [https://doi.org/10.1007/978-1-4020-6754-9\\_3188](https://doi.org/10.1007/978-1-4020-6754-9_3188)
- Ward RD, Zemlak TS, Innes BH, Last P, Hebert PDN (2005) DNA barcoding Australia's fish species. *Philosophical Transactions of the Royal Society Biological Sciences* 360: 1847–1857. <https://doi.org/10.1098/rstb.2005.1716>
- Wisner RL, McMillan CB (1988) A new species of hagfish, genus *Eptatretus* (Cyclostomata, Myxinidae), from the Pacific Ocean near Valparaiso, Chile, with new data on *E. bischoffi* and *E. polytrema*. *Transactions of the San Diego Society of Natural History* 21: 227–244. <https://doi.org/10.5962/bhl.part.24585>
- Zintzen V, Roberts CD, Shepherd L, Stewart AL, Struthers CD, Anderson MJ, Mcveagh M, Noren N, Fernholm B (2015) Review and phylogeny of the New Zealand hagfishes (Myxiniiformes: Myxinidae), with a description of three new species. *Zoological Journal of Linnean Society* 174: 363–393. <https://doi.org/10.1111/zoj.12239>

# Painted black: *Iguana melanoderma* (Reptilia, Squamata, Iguanidae) a new melanistic endemic species from Saba and Montserrat islands (Lesser Antilles)

Michel Breuil<sup>1</sup>, David Schikorski<sup>2</sup>, Barbara Vuillaume<sup>2</sup>, Ulrike Krauss<sup>3</sup>,  
Matthew N. Morton<sup>4</sup>, Elizabeth Corry<sup>4</sup>, Nicolas Bech<sup>5</sup>, Mišel Jelić<sup>6</sup>,  
Frédéric Grandjean<sup>5</sup>

**1** Muséum national d'Histoire naturelle, Laboratoire des Reptiles et Amphibiens, Bâtiment 30, 57, rue Cuvier, CP n° 30, 75231 Paris cedex 05, France **2** Laboratoire Labofarm-Genindexe, 4 rue Théodore Botrel, 22600 Loudéac, France **3** Maison du Soleil, Dauphin Road, La Borne, P O Box GM 1109, Saint Lucia **4** Durrell Wildlife Conservation Trust, Les Augres Manor, Trinity, Jersey JE3 5BP, UK **5** Laboratoire Écologie et Biologie des Interactions, équipe EES, UMR CNRS 6556, Université de Poitiers, 5 rue Albert Turpin, 86073 Poitiers Cedex 9, France **6** Entomological Department, Varaždin City Museum, Šetalište Josipa Jurja Strossmayera 3, 42000 Varaždin, Croatia

Corresponding author: Frédéric Grandjean ([frederic.grandjean@univ-poitiers.fr](mailto:frederic.grandjean@univ-poitiers.fr))

Academic editor: A. Bauer | Received 21 November 2019 | Accepted 28 February 2020 | Published 13 April 2020

<http://zoobank.org/E6D165DE-8C61-4CE1-A75A-56BE68389379>

**Citation:** Breuil M, Schikorski D, Vuillaume B, Krauss U, Morton MN, Corry E, Bech N, Jelić M, Grandjean F (2020) Painted black: *Iguana melanoderma* (Reptilia, Squamata, Iguanidae) a new melanistic endemic species from Saba and Montserrat islands (Lesser Antilles). ZooKeys 926: 95–131. <https://doi.org/10.3897/zookeys.926.48679>

## Abstract

The Lesser Antilles, in the Eastern Caribbean, is inhabited by three *Iguana* species: the Lesser Antillean iguana *Iguana delicatissima*, which is endemic to the northernmost islands of the Lesser Antilles, the introduced common iguana from South America, *Iguana iguana iguana*, represented also by the two newly described endemic subspecies *Iguana iguana sanctaluciae* from Saint Lucia and *Iguana iguana insularis* from Saint Vincent and the Grenadines, and Grenada, and the introduced *Iguana rhinolopha* from Central America. Drawing on both morphological and genetic data, this paper describes the *Iguana* populations from Saba and Montserrat as a new species, *Iguana melanoderma*. This species is recognized on the basis of the following combination of characteristics: private microsatellite alleles, unique mitochondrial ND4 haplotypes, a distinctive black spot between the eye and tympanum, a dorsal carpet pattern on juveniles and young adults, a darkening of body coloration with aging (except for the anterior part of the snout), a black dewlap, pink on the jowl, the high number of large tubercular nape scales, fewer than ten medium

sized–triangular dewlap spikes, high dorsal spikes, and lack of horns on the snout. This new melanistic taxon is threatened by unsustainable harvesting (including for the pet trade) and both competition and hybridization from escaped or released invasive alien iguanas (*I. iguana iguana* and *I. rhinolopha*) from South and Central America, respectively. The authors call for action to conserve *Iguana melanoderma* in Saba and Montserrat and for further research to investigate its relationship to other melanistic iguanas from the Virgin Islands and coastal islands of Venezuela.

### Keywords

Conservation Biology, *Iguana*, Lesser Antilles, microsatellites, mtDNA, new endemic species, phylogeny

## Introduction

In the 1960s, Lazell (1973) studied the morphological variation of the Common Green Iguana (*Iguana iguana*) and identified three groups of this species in the Lesser Antilles (Fig. 1). The populations from Saba, Montserrat, and St. Croix were characterized by having large tubercular nape scales, highly developed dorsal crest spikes, a carpet pattern in 10–30 percent of the populations, an increasing incidence of melanistic individuals, and the absence of horns on the snout [1]. Populations of the Guadeloupien Archipelago and Les Saintes were distinguished by having very weak tubercular nape scales, and a high incidence of unpatterned and of grey individuals [2]. The southern Lesser Antillean populations, from Saint Lucia, Saint Vincent, the Grenadines, and Grenada were in turn characterized by very weakly tubercular nape scales, grey or green individuals with dorsolateral bands and highly developed, hornlike, median snout scales [3]. Lazell (1973) thought that geographic variation was clinal and concluded that the Common Iguana in Les Saintes and Guadeloupe was autochthonous rather than introduced.

Breuil (2002, 2013, 2016), Breuil et al. (2010), and Vuillaume et al. (2015) demonstrated that the Common Green Iguana present in Guadeloupe came from French Guiana and that this species displaced the Lesser Antilles iguanas (*Iguana delicatissima*) from Les Saintes and Grande-Terre through competition and hybridization. The same phenomenon is underway in Basse-Terre and St. Barthélemy leading to the further decline of *Iguana delicatissima* (Vuillaume et al. 2015; Breuil 2013, 2016). Since these recent studies, hybridization between these two species is known to have occurred in Martinique, La Désirade (MB, unpublished results), and St. Eustatius (Van den Burg et al. 2018a; 2018b). Thus, a natural cline concerning, for example, the size of the tubercular nape scales as advocated by Lazell (1973), cannot exist with only two groups of iguanas naturally present.

Morphological studies of the St. Lucia Iguana, belonging to the third group of Lazell (1973), indicated this iguana population is very different from the horned iguana population from Central America (Breuil 2013, 2016). Breuil et al. (2019) showed with genetic (microsatellites, mtDNA) and morphological studies that this third group comprises two subspecies, *Iguana iguana sanctaluciae*, endemic to Saint Lucia and *I. iguana insularis*, endemic to the Grenadine Bank.



**Figure 1.** Geographical distribution of the three iguana groups identified by Lazell (1973) in the 1960s and new taxonomic proposition. In the 1960s, the invasive iguanas from South America (*Iguana iguana*) were only present in the îles des Saintes and Guadeloupe (Basse-Terre) and formed the Central Group. Now, alien iguanas are present and breed on every bank (van den Burg et al. 2018b). The southern group is now considered to support two subspecies *Iguana iguana insularis* and *Iguana iguana sanctaluciae* (Breuil et al. 2019). The northern group is considered here as a new species.

In Saba, the local iguana, the Saban Black Iguana is considered as a flagship species. In Montserrat, the local melanistic iguana does not receive special attention due to its putative exotic origin. The two flagship herp species for conservation on the island are the mountain chicken (*Leptodactylus fallax*) and the Galliwasp (*Diploglossus montiserrati*).

Melanistic iguanas phenotypically close to those of Saba-Montserrat also occur in the northern islands (St. Croix, St. Thomas: USA Virgin Islands, USVI) and also on the island of Margarita and other coastal islands such as Los Roques and La Banquilla (Venezuela) (Lazell 1973; van Buurt 2005). Thus, further detailed investigations are required to establish the relationships among all these melanistic iguanas. It is noteworthy that Stephen et al. (2013) used in their phylogeny a unique individual from Venezuela that was captured on the mainland (Cumana) near Margarita Island and that clustered with melanistic iguanas from Saba and Montserrat.

The extension of the range of the Common Green Iguana from Central America, considered by Breuil et al. (2019) as a species in its own right (*Iguana rhinolopha*), to Saint Maarten (Vuillaume et al. 2015) increases the probability that this invasive lineage will arrive on the Dutch island of Saba (Yokoyama 2012). Morphological studies (Breuil 2013, 2016) combined with genetic studies (Vuillaume et al. 2015) have shown that the Saba population has unique characteristics. Stephen et al. (2013) found that Montserrat and Saba iguanas share the same ND4 haplotype. Montserrat conservationists also need to be able to differentiate between endemic melanistic iguanas and potential invasive Common Iguanas from Central and South American lineages that are likely to invade other islands (Breuil 2013, 2016; Falcón et al. 2013; Van den Burg et al. 2018b). With the increase in trade and shipping in the Caribbean region and post-hurricane restoration activities, it is very likely that there will be new opportunities for invasive iguanas to colonize new islands inhabited by endemic lineages.

The paper aims to describe the common melanistic iguanas from the islands of Saba and Montserrat as a new taxon and to establish its relationships with other Common Green Iguanas. An outcome of this study will be the enabling of conservationists to accurately differentiate this endemic lineage from invasive iguanas and investigate its ecology and biology population on these two very small islands that are subject to a range of environmental disturbances including hurricanes, earthquakes and volcanic eruptions.

## Materials and methods

Morphological, molecular (i.e., mitochondrial and microsatellites markers) and biological data were used to compare the iguanas of Saba and Montserrat with *Iguana iguana* (South America), *Iguana rhinolopha* (Central America), and the two new subspecies *I. iguana insularis* and *I. iguana sanctaluciae* from southern Lesser Antilles (Breuil et al. 2019).

## Morphological analyses

The morphological traits used to identify iguanas are described in Breuil (2013; 2016). Most consist of meristic and qualitative characteristics recorded on wild iguanas in the field on the islands of Saba and Montserrat, which are easily recorded from digital photographs taken by the authors. We also examined specimens at the Museum of Comparative Zoology (MCZ) at Harvard University, USA, based on photographs taken by Joseph Martinez and Corentin Bochaton (Muséum national Histoire naturelle, Paris).

We also reviewed photographs of *Iguana* found on the Internet using the Google Images search engine for the islands of St. Croix, St. Thomas (US Virgin Islands), for the coastal islets of Venezuela and for the vicinity of Cumana (Venezuela), regions known to be inhabited by melanistic iguanas, in relation to published data. Leighton et al. (2016) advocated the use of Internet images for taxonomic research to study spatial patterns in phenotypic traits that are objective, binary and easy to score, regardless of the camera angle. We used only photographs that were georeferenced to allow valid comparisons with the morphological characteristics of this new taxon (Breuil et al. 2019).

## Molecular analyses

Collection and preparation of genetic material

Genomic DNA was isolated from 44 individuals from tissue, shed skin and/or blood samples using the QIAamp DNA Mini Kit (QIAGEN, Deutschland) and following the manufacturer's recommendations (Table 1).

## Mitochondrial DNA (ND4) and phylogenetic analysis

Fragments of the ND4 mitochondrial locus, encompassing the 3' end of the NADH dehydrogenase subunit 4 gene (ND4) and the tRNA genes histidine, serine and leucine (partial 5' end), were PCR-amplified using the primer pair and protocols of Malone et al. (2000). Sequence chromatograms were analyzed in SEQUENCHER (v5.3; Gene Codes Corp., Ann Arbor). The resulting ND4 sequences were aligned with GenBank sequences of iguanas from previous studies (Malone et al. 2000; Malone and Davis 2004; Stephen et al. 2013; Breuil et al. 2019). Sequence alignment was calculated using MAFFT (v7.18) (Katoh et al. 2005). For the ND4 analysis, the molecular data set included 21 iguanas (Table 1) from insular and continental origins.

The best nucleotide substitution model was chosen using JModelTest 2 (Darriba et al. 2012) under the Bayesian information criterion (BIC). Hierarchical relationships between individual ND4 genotypes/haplotypes were analysed using Maximum Likelihood (ML) and Maximum Parsimony (MP) tree reconstructions, and Median-Joining (MJ) haplo-

**Table 1.** Sampling and haplotype information. The effectives in the locality column correspond to the number of individuals studied for the microsatellites and the mitochondrial ND4 gene. The number in the ND4 column is the length of the sequence used in the analysis. SabaNP, Saba National Park. SBHNR, Saint Barthélemy Natural Reserve. DWCT, Durrell Wildlife Conservation Trust.

Locality/Status	Microsatellites	ND4	Collectors	GenBank
<b>Saba</b> ( <i>N</i> = 7/ <i>N</i> = 6)	SABA01	SABA01 (888)	SabaNP/SBHRN	MN590163
	SABA02	SABA02 (890)	SabaNP/SBHRN	MN590164
	SABA03	SABA03 (739)	SabaNP/SBHRN	
	SABA04	SABA04 (892)	SabaNP/SBHRN	MN590165
	SABA05	SABA05 (892)	SabaNP/SBHRN	MN590166
	SABA06	SABA06 (892)	SabaNP/SBHRN	MN590167
	SABA07	SABA07 (891)	SabaNP/SBHRN	MN590168
<b>Montserrat</b> ( <i>N</i> = 12/ <i>N</i> = 4)	IGU86		E. Corry DWCT	
	IGU87		E. Corry DWCT	
	IGU88	IGU88 (713)	E. Corry DWCT	MN590169
	IGU89	IGU89(711)	E. Corry DWCT	MN590170
	IGU90		E. Corry DWCT	
	IGU91		E. Corry DWCT	
	IGU92	IGU92(713)	E. Corry DWCT	MN590171
	IGU93	IGU93(713)	E. Corry DWCT	MN590172
	IGU94		E. Corry DWCT	
	IGU95		E. Corry DWCT	
	IGU96		E. Corry DWCT	
	IGU99		E. Corry DWCT	
<b>St. Lucia /End</b> ( <i>N</i> = 13/ <i>N</i> = 2)	IGU58	IGU63(779)	St. Lucia authors	MK687397
	IGU59		St. Lucia authors	
	IGU60		St. Lucia authors	
	IGU61		St. Lucia authors	
	IGU62		St. Lucia authors	
	IGU63	IGU63(737)	St. Lucia authors	MK687398
	IGU64		St. Lucia authors	
	IGU67		St. Lucia authors	
	IGU68		St. Lucia authors	
	IGU69		St. Lucia authors	
	IGU70		St. Lucia authors	
	IGU71		St. Lucia authors	
IGU72		St. Lucia authors		
<b>Grenadines/End</b> ( <i>N</i> = 4/ <i>N</i> = 4)	IGU73		J. Daltry/G. Gaymes	MK787400
	IGU75		J. Daltry/G. Gaymes	MK787401
	IGU76		J. Daltry/G. Gaymes	MK787403
	IGU77		J. Daltry/G. Gaymes	MK787404
<b>Guiana/auto</b> ( <i>N</i> = 7/ <i>N</i> = 4)	IGU78	IGU78 (702)	F. Catzefis (CNRS)	MK687405
	IGU79	IGU79 (593)	F. Catzefis (CNRS)	MK687406
	IGU80		F. Catzefis (CNRS)	
	IGU81		B. de Thoisy (Pasteur)	
	IGU82	IGU82 (712)	B. de Thoisy (Pasteur)	MK687407
	IGU83		B. de Thoisy (Pasteur)	
	IGU84	IGU84 (697)	B. de Thoisy (Pasteur)	MK687408
	IGU85		B. de Thoisy (Pasteur)	

type networks. The evolutionary history was inferred using the ML method based on the Hasegawa-Kishino-Yano model (Hasegawa et al. 1985). The initial trees for the heuristic search were obtained automatically by applying the Neighbor-Joining and BioNJ algorithms to a matrix of paired distances estimated using the Maximum Composite Likelihood (MCL) approach, then selecting the topology with the highest log likelihood value. A discrete Gamma distribution was used to model evolutionary rate differences between sites [5 categories (+G, parameter = 0.3079)]. The tree was drawn to scale, with branch lengths measured as the number of substitutions per site. The MP tree reconstruction was obtained using the Subtree-Pruning-Regrafting (SPR) algorithm (Nei and Kumar 2000) with a search level 1, in which the initial trees were obtained by random addition of sequences (10 replicates). Node supports for tree topologies obtained by ML and MP methods were calculated as percentages of replicate trees in which the associated taxa had clustered in the bootstrap test (1000 replicates). Node supports were indicated with bootstrap support (BS  $\geq 70$ ). ML and MP analyses were conducted in MEGA7 (Kumar et al. 2016). The MJ haplotype network (Bandelt et al. 1999) was constructed using PopART (Population Analysis with Reticulate Trees) v1.7 (Leigh and Bryant 2015) with the epsilon parameter set to zero.

### **Microsatellites analysis**

Analyses based on microsatellite molecular markers included 43 individuals of both insular and continental origins (Table 1). A panel of 16 microsatellite markers was used and amplified as described previously in Valette et al. (2013) and Vuillaume et al. (2015). Individuals were grouped into five populations according to their sampling localities (i.e., four islands: Montserrat, Saba, Saint Lucia and Grenadines as well as the continental population from French Guiana).

### **Genetic diversity**

We tested the departures from Hardy-Weinberg expectations and linkage disequilibria using exact tests (1200 permutations) as implemented in the *FSTAT* software ver. 2.9.3.2 (Goudet 2001). Significance levels were adjusted for multiple tests using Bonferroni's standard correction (Rice 1989). We calculated the genetic polymorphism at all loci for each population by computing the allelic richness ( $A_r$ ), the expected heterozygosity ( $H_e$ ) and  $F_{is}$  (Weir and Cockerham 1984) using *FSTAT* ver. 2.9.3.2 (Goudet 2001) with 1,200 permutations.

### **Genetic structure**

We calculated paired  $F_{st}$  values between populations (Weir and Cockerham 1984) using *FSTAT* ver. 2.9.3.2 (Goudet 2001). Their associated significance was computed

and tested using global tests implemented in *FSTAT* ver. 2.9.3.2 (Goudet 2001). Significance levels were adjusted for multiple tests using Bonferroni's standard correction (Rice 1989). In addition, we assessed relationships between populations with a Factorial Correspondence Analyses (FCA) based on individual genotypes and using the FCA procedure in *GENETIX* v. 4.05.2 (Belkhir et al. 2004). Finally, the population structure was also investigated using the individual-based approach implemented in the *STRUCTURE* software (Pritchard et al. 2000). Based on the Bayesian cluster approach, this method allowed the inference of both the number, *K*, of genetic clusters and the admixture coefficient of individuals to be assigned to the inferred clusters. Initially, we replicated 15 independent runs for each value of *K* (with *K* varying from 1 to 9) with a total of 1,000,000 iterations and a burn-in of 100,000. To determine the number of genetic clusters from *STRUCTURE* analyses, we used the *STRUCTURE HARVESTER* program (Earl and Vonholdt 2012) to compare the mean likelihood and variance per *K* values calculated from the 15 independent runs (Evanno et al. 2005). The results gave a Delta *K* value per tested *K* value allowing the determination of the most likely number of inferred clusters. Subsequent runs were performed to test for the presence of genetic sub-structure within each cluster when *K* > 1 was initially inferred. These subsequent runs used the same conditions as above (Fig. 2).

## Results

### Population structure and diversity

Based on microsatellite variation, genetic diversity (*H<sub>e</sub>*) ranged from 0 to 0.82 (Table 2) and allelic richness (*A<sub>r</sub>*) ranged from 1 to 3.86. No linkage disequilibrium was detected (adjusted *p*-value threshold = 0.0004) and no loci deviated from the Hardy-Weinberg expectations (adjusted *p*-value threshold = 0.0006). Analyses of microsatellite loci for population structure resulted in the identification of three groups (Fig. 2). Pairwise *F<sub>st</sub>* values ranged from 0.104 to 0.909 (overall *F<sub>st</sub>* = 0.595) and many were significant after Bonferroni correction (Indicative adjusted nominal level (5%) for multiple comparisons was 0.005) (Table 3). These results were corroborated by a FCA procedure which identified the same three groups: one including individuals from St. Lucia and Grenadines, a second including individuals from French Guiana, and the last including individuals from both Montserrat and Saba. Bayesian clustering using *STRUCTURE* and the *STRUCTURE HARVESTER* programs, also supported population subdivision, giving the highest posterior probability for *K* = 2. Specifically, individuals from Montserrat-Saba-French Guiana were mainly allocated to the first genetic cluster (i.e., mean ± *sd* of individual admixture coefficients: 0.997 ± 0.002; 0.998 ± 0.001 and 0.996 ± 0.0001, respectively), whereas individuals from Saint Lucia-Grenadines were allocated mainly to the second genetic cluster (i.e., mean ± *sd* of individual admixture coefficients: 0.997 ± 0.005 and 0.976 ± 0.029, respectively). Subsequent analyses within each of these genetic clusters revealed further sub-structure separating

**Table 2.** Genetic diversity parameters for each locus. Key: Ar, allelic richness, He, expected heterozygosity, and Fis were computed for each population and loci using FSTAT ver. 2.9.3.2 software (Goudet 2001). No Fis values deviated from Hardy-Weinberg's expectations ( $P < 0.0006$  after Bonferroni adjustment). NA: not available.

Loci		Montserrat	Saba	Saint Lucia	Grenadines	Guiana	All
L2	Ar	1.72	1.00	1.00	1.00	1.84	2.98
	He	0.23	0.00	0.00	0.00	0.26	0.10
	Fis	-0.10	NA	NA	NA	-0.09	-0.10
L3	Ar	1.00	1.00	1.00	1.00	1.00	1.00
	He	0.00	0.00	0.00	0.00	0.00	0.00
	Fis	NA	NA	NA	NA	NA	NA
L5	Ar	1.94	1.91	1.00	1.00	2.00	1.91
	He	0.39	0.33	0.00	0.00	0.52	0.25
	Fis	-0.29	1.00	NA	NA	-0.09	0.21
L6	Ar	2.66	1.80	1.00	1.00	2.00	3.36
	He	0.53	0.20	0.00	0.00	0.52	0.25
	Fis	0.37	0.00	NA	NA	0.73	0.37
L8	Ar	1.00	1.00	1.00	1.00	1.84	1.18
	He	0.00	0.00	0.00	0.00	0.26	0.05
	Fis	NA	NA	NA	NA	-0.09	-0.09
L9	Ar	3.42	2.96	1.00	3.00	2.89	3.80
	He	0.66	0.72	0.00	0.75	0.61	0.55
	Fis	0.18	0.54	NA	0.33	-0.41	0.16
L13	Ar	1.00	1.00	1.00	2.00	1.00	1.99
	He	0.00	0.00	0.00	0.50	0.00	0.10
	Fis	NA	NA	NA	1.00	NA	1.00
L14	Ar	1.98	2.91	1.36	1.00	1.57	2.65
	He	0.45	0.68	0.09	0.00	0.14	0.27
	Fis	-0.43	0.02	0.00	NA	0.00	-0.10
L15	Ar	1.33	1.00	1.00	1.00	2.93	2.33
	He	0.08	0.00	0.00	0.00	0.68	0.15
	Fis	0.00	NA	NA	NA	0.16	0.08
L16	Ar	1.00	1.00	1.00	2.00	1.57	1.19
	He	0.00	0.00	0.00	0.25	0.14	0.08
	Fis	NA	NA	NA	0.00	0.00	0.00
L17	Ar	1.00	1.00	1.00	1.00	2.52	2.36
	He	0.00	0.00	0.00	0.00	0.49	0.10
	Fis	NA	NA	NA	NA	0.42	0.42
L18	Ar	2.41	1.00	1.00	1.00	2.00	1.81
	He	0.40	0.00	0.00	0.00	0.53	0.19
	Fis	0.45	NA	NA	NA	-0.25	0.10
L19	Ar	2.91	2.00	1.00	1.00	2.00	3.13
	He	0.67	0.53	0.00	0.00	0.52	0.34
	Fis	-0.13	0.06	NA	NA	-0.36	-0.14
L20	Ar	1.98	1.00	1.00	1.00	3.14	3.44
	He	0.46	0.00	0.00	0.00	0.66	0.22
	Fis	-0.47	NA	NA	NA	-0.09	-0.28
L23	Ar	1.00	1.80	1.00	1.00	3.86	3.00
	He	0.00	0.20	0.00	0.00	0.82	0.20
	Fis	NA	0.00	NA	NA	0.30	0.15
L24	Ar	1.00	1.00	1.00	1.00	1.00	1.00
	He	0.00	0.00	0.00	0.00	0.00	0.00
	Fis	NA	NA	NA	NA	NA	NA
All	Ar	1.71	1.46	1.02	1.25	2.07	2.32
	He	0.24	0.17	0.01	0.09	0.39	0.18
	Fis	-0.03	0.29	0.00	0.50	0.03	0.16

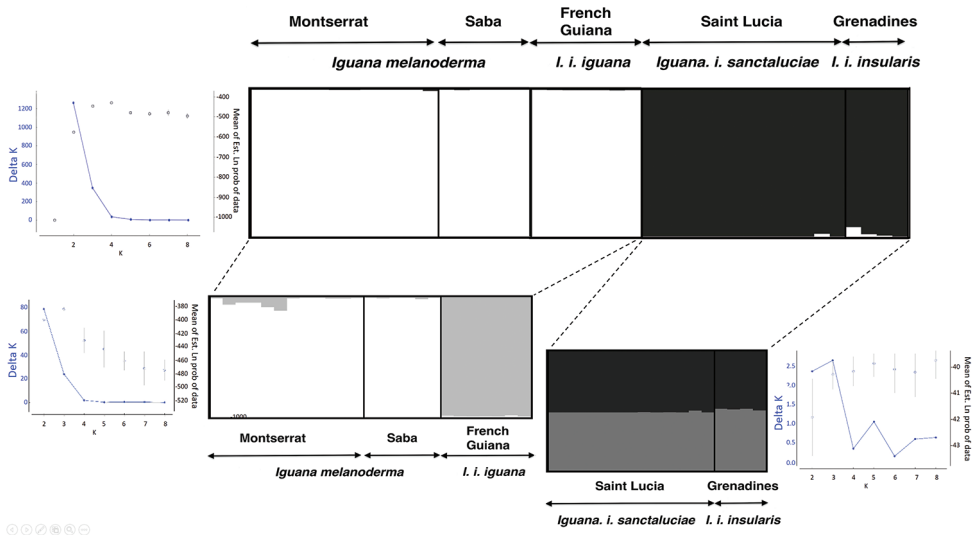


**Figure 2.** Hierarchical genetic structure of *Iguana* inferred by STRUCTURE and STRUCTURE HARVESTER. Bar plots show admixture coefficient of each analyzed individuals (represented by each vertical bar) for the inferred genetic clusters K (represented by a different color). The graphs show Delta K values (Evanno et al. 2005) as a function of K (number of clusters) and calculated from posterior probabilities of the data (i.e.,  $\ln [P(D|K)]$ ). The results inferred K = 2 genetic clusters when they were initially based on the overall sampling. A subsequent run, including individuals from Montserrat-Saba and French Guiana, revealed significant genetic substructure (i.e., K = 2) separating individuals from Montserrat-Saba and those from French Guiana. Independently, another subsequent run including only individuals from Saint Lucia and the Grenadines revealed no genetic substructure. The bar plots were produced using DISTRUCT 1.1 program (Rosenberg 2004) from the average of the 15 replicates. The names of the taxa are given according to Breuil et al. (2019) and to the conclusion of this work for Saba and Montserrat.

**Table 3.** Fst values for each pairwise population comparison (below the diagonal) and their significance levels (above the diagonal). The indicative adjusted nominal level (5%) for multiple comparisons is 0.005. Fst values that reveal a significant genetic differentiation are in bold.

	Montserrat	Saba	Saint Lucia	Grenadines	Guiana
Montserrat	–	0.01	0.005	0.005	0.005
Saba	0.104	–	0.005	0.035	0.005
Saint Lucia	<b>0.806</b>	<b>0.909</b>	–	0.005	0.005
Grenadines	<b>0.670</b>	0.777	<b>0.555</b>	–	0.005
Guiana	<b>0.392</b>	<b>0.467</b>	<b>0.738</b>	<b>0.529</b>	–

Montserrat-Saba and French Guiana individuals. In contrast, no genetic sub-structure was detected when considering individuals from Saint Lucia and the Grenadines (whatever the individuals, they showed similar inferences for genetic clusters) (Fig. 2).

**Phylogeny**

The ML tree based on ND4 sequences had the highest log likelihood of  $-2861.13$  (Fig. 3). The MP analysis, using the same data, generated 2 trees of length 302 (not shown). The consistency index was 0.659, the retention index was 0.892 and the composite index was 0.644 (0.588) for all sites and parsimony-informative sites (in parentheses). ND4 sequences from Montserrat and Saba specimens were placed in a well-supported monophyletic group (Fig. 3; ML BS = 98, MP BS = 97). The Montserrat and Saba sequences were closely related to GenBank sequence HM352501 from an *Iguana iguana* specimen from Venezuela (Sucre: Cumana). In the MJ network (Fig. 4, Table 4), four mutational steps separate HM352501 and “Hap\_4” (= HM352505 and MN590163 to 68) encompassed most of samples from Montserrat and Saba (nine in the present study and 13 from published studies). Only two ND4 haplotypes were found to characterise Montserrat and Saba iguanas represented by 24 specimens (9 from this study, 13 from GenBank consisting of 13 from Saba and 11 from Montserrat).

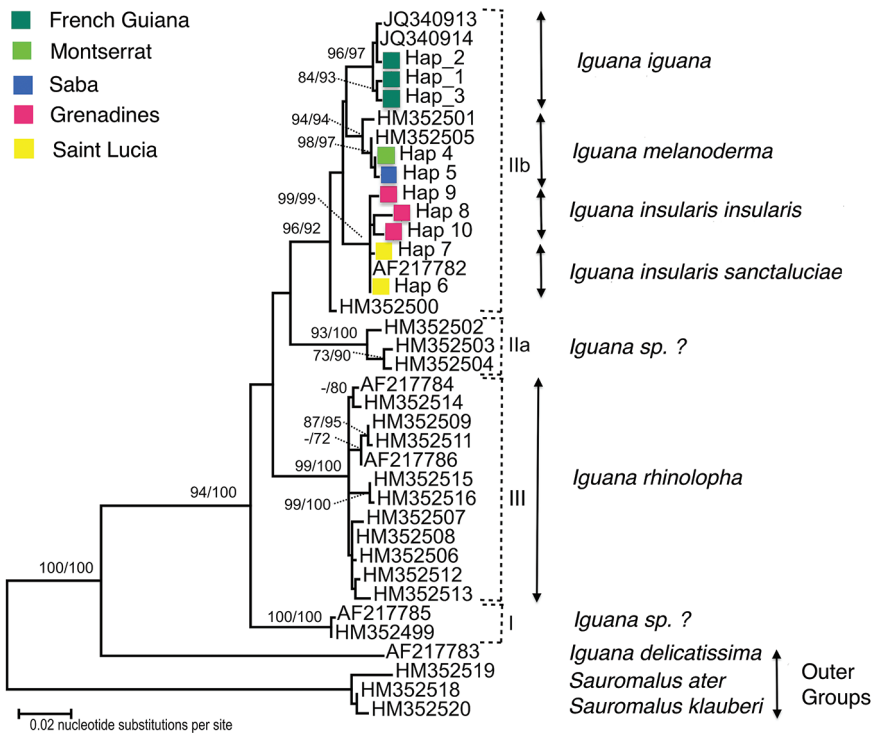


**Figure 3.** The Maximum Likelihood (ML) tree of the ND4 sequences of iguanas. The percentage of trees in which the associated taxa clustered is shown next to the branches, as bootstrap support (BS  $\geq 70$ ) for ML and Maximum Parsimony (MP) topologies respectively. Sequences amplified by the authors of this study were indicated by colored diamond-shaped marks. Marks are colored based on the sampling sites. Sequences from published studies were labelled by their NCBI GenBank access numbers (Fig. 4). The names of the taxa are classified according to the conclusions of this work. Roman numerals refer to clades identified by Stephen et al. (2013).

**Table 4.** Haplotypes used in MJ network. Sequences amplified by the authors of this study and corresponding haplotypes from published studies were labelled from “Hap\_1” to “Hap\_10”. HM352505 haplotype found in the 7 specimens from Montserrat and the 6 specimens from Saba corresponds to “Hap\_4”.

---

Origins of the specimens used for the network

BRA: Brazil  
 GRE: Grenadines  
 GUI: French Guiana  
 MON: Montserrat  
 STL: St. Lucia  
 SUR: Suriname  
 VEN: Venezuela  
 DEL: *Iguana delicatissima* (Anguilla, Dominica, St. Eustatius)

---

Hap_1:	2 [IGU78GUI, IGU79GUI]
Hap_2:	2 [IGU82GUI, JQ340914BRA]
Hap_3:	1 [IGU84GUI]
Hap_4:	22 [IGU88MON, IGU89MON, IGU92MON, IGU93MON, SABA01, SABA02, SABA03, SABA04, SABA07, HM352505_M1, HM352505_M2, HM352505_M3, HM352505_M4, HM352505_M5, HM352505_M6, HM352505_M7, HM352505_S1, HM352505_S2, HM352505_S3, HM352505_S4, HM352505_S5, HM352505_S6]
Hap_5:	2 [SABA05, SABA06]
Hap_6:	8 [IGU58STL, IGU63STL, AF217782_1, AF217782_2, AF217782_3, AF217782_4, AF217782_5, AF217782_6]
Hap_7:	1 [IGU65STL]
Hap_8:	1 [IGU73GRE]
Hap_9:	2 [IGU75GRE, IGU76GRE]
Hap_10:	1 [IGU77GRE]

1[JQ340913BRA]; 4[HM352500\_1SUR, HM352500\_2SUR, HM352500\_3SUR, HM352500\_4SUR]; 1[HM-352501VEN]; 7[AF217783\_1DEL, AF217783\_2DEL, AF217783\_3DEL, AF217783\_4DEL, AF217783\_5DEL, AF217783\_6DEL, AF217783\_7DEL]

---

The Saba-Montserrat-Venezuela populations formed a monophyletic group that is the sister group of the populations from French Guiana and Brazil, this group is, in turn, the sister group of the group of St. Lucia-Grenadines that was previously described as two endemic subspecies *Iguana iguana sanctaluciae* for the endemic population of St. Lucia and *Iguana iguana insularis* for the population of the Grenadines (Breuil et al. 2019).

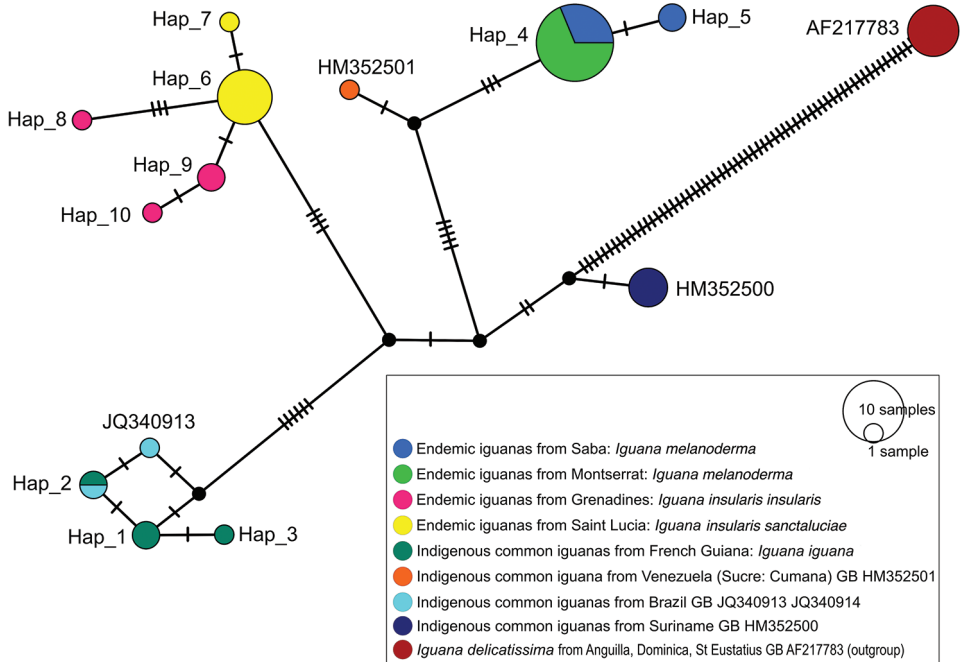


**Figure 4.** The Median-Joining (MJ) network of the ND4 sequences of iguanas. The sequences amplified by the authors of this study and the corresponding haplotypes from published studies were labelled from “Hap\_1” to “Hap\_10” (details in Table 4). Other sequences from published studies were labelled by their NCBI GenBank access number. Black circles are median vectors representing extinct or unsampled haplotypes. The remaining colored circles represent haplotypes as nodes in the networks. The circles are colored based on the sampling sites. The size of circles corresponds to the number of specimens with identical sequence. The number of mutational steps is indicated by hatch marks. The names of the taxa are classified according to the conclusions of this work.

From these genetic data and the following morphological data, it is clear that the endemic iguanas from Saba and Montserrat form a distinct evolutionary entity that we recognize as a new species which is formally describe below accompanied by a taxonomic analysis.

## Taxonomic analysis and description

### *Iguana melanoderma* sp. nov.

<http://zoobank.org/A4984EB3-7F03-412B-8A58-E0CAB36EC836>

Figures 5–7

**Diagnosis.** A species of *Iguana*, with a distinctive melanistic phenotype, with a black dewlap, huge tubercular nape scales, the absence of horns on the snout.

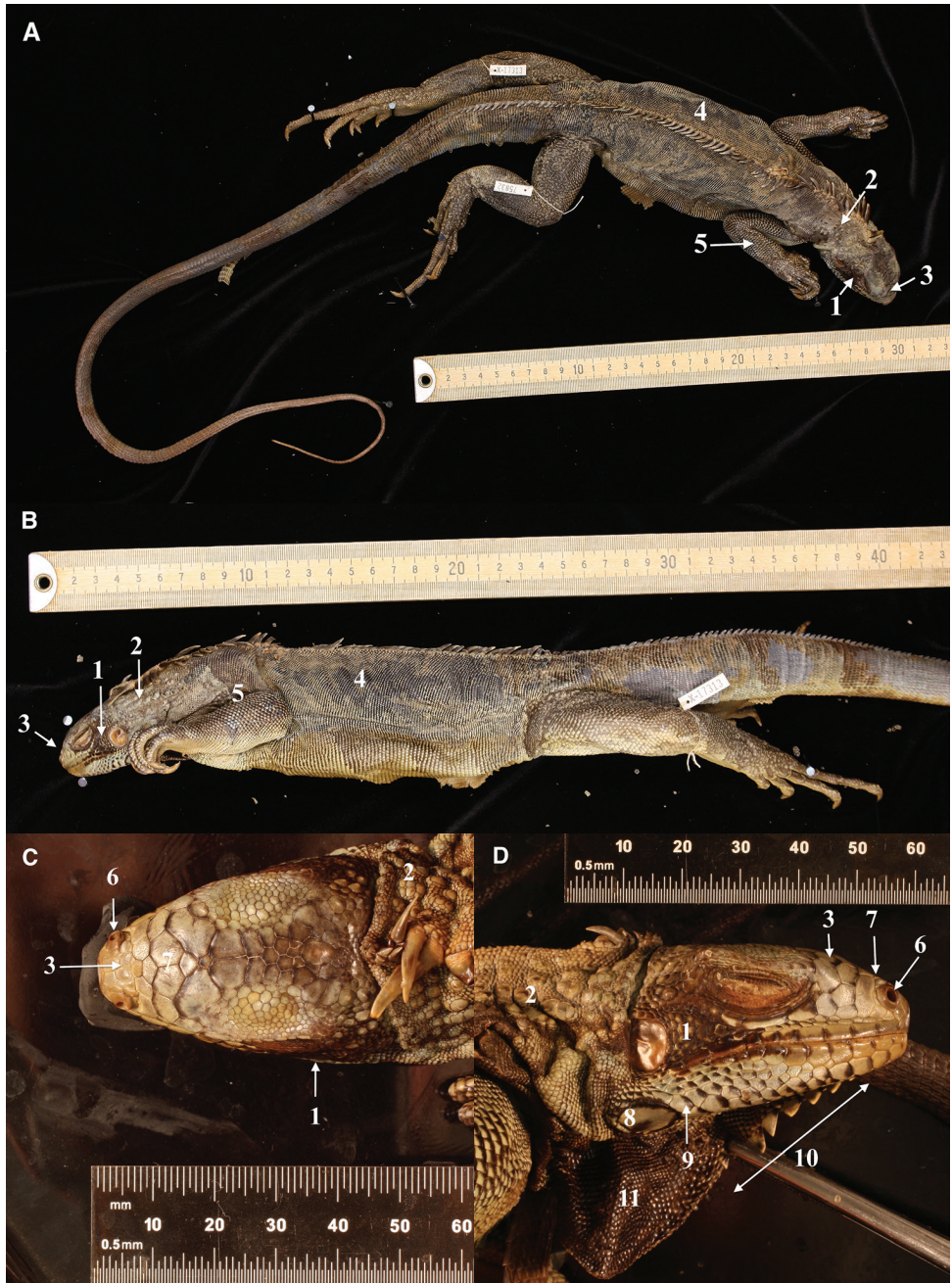


**Figure 5.** Holotype of *Iguana melanoderma* sp. nov. **A** Dorsal view **B** lateral view **C** dorsal view of the head **D** lateral view of the head. MCZ R-75832 from Saba, Windwardside. Museum of Comparative Zoology, Harvard University. President and Fellows of Harvard College. 1. Black patch between the tympanum and the subtympnic plate. 2. High number of aligned nape tubercles. 3. No horns on the stout. 4. Dorsal carpet pattern. 5. Black on the upper part of the forelimb. 6. Prominent nostrils. 7. Anterior part of the snout, not black. 8. Subtympnic plate with a dark posterior patch. 9. Black anterior edge of lower sublabial scales. 10. Fewer than 10 triangular gular spikes extended in the upper part of the lower dewlap. 11. Entirely black dewlap.

**Etymology.** The name was chosen to emphasize the most conspicuous feature of this new taxon, from *melano* meaning black and *derma* meaning skin.

Common local names are: Melanistic Lesser Antilles iguana, Saban Black iguana

**Type material. Choice of the holotype and the paratype.** The choice of our type specimens and the way we conducted the description of the type and the paratype attempt to best meet the criteria proposed by (Dubois 2009) for the case of *Conolophus marthae* described by Gentile and Snell (2009). We took into account the same kind of problems of sacrificing a specimen for museum collection and referencing an emblematic, iconic, large lizard that belongs to an endangered taxon.

- (1) The Saba and Montserrat populations survived for a long time in a period when the risk of extinction was lower than today. Nevertheless, the iguanas were hunted for food, killed by cats and dogs, and their habitats destroyed by livestock and natural events. Today, in Saba, the main risk for this small endemic population, which seems to be far from the carrying capacity of the island, is the arrival of invasive common iguanas from South and Central America that have a rapidly expanding population in Saint Maarten. In Montserrat, the same risk exists. Volcanic eruptions are also a major threat to these populations, as evidenced by the eruption of the Soufrière Hills in Montserrat in 1995 and the following years, which destroyed about a third of the island.

Hybridization with closely related lineages may in-fact be the greatest risk and could very likely lead to extinction of endemic lineages, as is the case for *Iguana delicatissima* in Guadeloupien Archipelago (Vuillaume et al. 2015). Moreover, the description of a new taxon may attract collectors and lead to unintended and undesirable consequences. This is of concern because on the Dutch island of Saint Maarten, both the legal and illegal pet trades are common. With the description of this new taxon, local authorities, such as the *Saba Conservation Foundation* and the NGO *Sea and Learn*, will have tools to protect the Saban Black Iguana from poaching on an island where the terrestrial protected area is less than 0.5 sq. km on the edge of this endemic iguana's range.

- (2) Lazell (1973) studied and collected iguanas in Saba and Montserrat in the 1960s. The vouchers are deposited at the Museum of Comparative Zoology (Harvard) with two other individuals collected in the seventies. Six vouchers for these two islands (Saba: MCZ R-75832, R-75833, R 133096; Montserrat: MCZ: R-61119, R-82310, R-126377) are present but unfortunately it is almost impossible to measure them properly due to their poor condition. In addition, some are young individuals, which do not have well developed diagnostic characteristics.
- (3) We have no precise idea of the size of the iguana population in Saba and Montserrat. Rough estimates based on density in some surveyed areas yield 100–300 adults and subadults for each island. In theory, it is always possible to catch a senile non-breeding male and prepare it in good conditions act as a voucher that will be available in a Museum collection for future study. But, for technical reasons, when the first author was in Saba in 2012, it was not possible to collect such an individual. Roadkill animals are often in poor conditions (broken, flattened, rotten) and in

most cases cannot be studied and preserved in a zoological reference collection. The same remarks apply to the Montserrat population.

- (4) Since diagnostic characteristics are mainly visible in adult individuals and are not measurements, we chose for the holotype of this new taxon specimen MCZ R-75032 from Saba collected by JD Lazell 6/23/63 on the Windward side of Saba. The paratype MCZ R-126377 is a head of an adult from Montserrat collected by JO Boos at Old Road Bluff 8/6/1970. These two samples are housed at the Museum of Comparative Zoology (MCZ, Harvard). They present the diagnostic characters as described by (Breuil 2013, 2016) and represent the populations of the two islands, respectively.

**Holotype** (Fig. 5). LESSER ANTILLES, SABA • ♀; Windward side; 23 June 1963; JD Lazell [leg.]; MCZ (R-75832).

This individual from Saba was not measured in detail because of the risk of spoiling the specimen. It is an adult female of approximately 26.3 cm SVL and a tail length of approximately 66.4 cm and a total length of 92.7 cm (measurements and photographs by Joseph Martinez, MCZ, Harvard).

**Description of the holotype.** The subtympenic plate is round, with a dark patch in the posterior part. The anterior, upper, and lower parts of the subtympenic plate are surrounded by black pigment. Most labial and sublabial scales have dark coloration on their anterior side. The lower labial scales, before the subtympenic plate, are arranged in a series of five pairs of scales of quite similar size and located one in front of the other. The tubercular nape scales are numerous, well developed, grey, and aligned in rows.

**Color pattern.** This specimen is partially discolored, with a slight carpet pattern, the stripes on the tail are almost invisible in the photographs, but according to (Lazell 1973) who captured this specimen, it had a conspicuous carpet pattern.

The dewlap is black in its lower part, and there are nine small, triangular yellowish gular spikes. The tympanum is brown. There is a conspicuous black spot between the eye and the tympanum. The snout and the top of the head are light, not black. The dorsal spikes are greenish and black.

**Paratype** (Fig. 6). LESSER ANTILLES, MONTSERRAT • ♂; Old Road Bluff; 6 Aug. 1970; JO Boos [leg.]; MCZ R-126377.

**Description of the paratype.** This individual is only a head of a small adult male based on the size of the dorsal spikes. This head presents the typical characteristics of this taxon: large grey scales on the tubercular nape, black spot between the eye and the tympanum, and labial and sublabial scales with black patches on the anterior part. There are five pairs of scales before the subtympenic plate almost completely black, a black dewlap, and a flat head with a light snout (photographs by Joseph Martinez, MCZ Harvard).

**Type locality.** On the Windward side of Saba for the holotype and on Old Road Bluff, west coast of Montserrat for the paratype (Figs 1, 11).

**Description of *Iguana melanoderma*.** *Iguana melanoderma* is distinguished from all other iguana lineages by the following combination of characteristics. This description is mainly based on adult iguanas observed in the field with the most developed diagnostic characteristics.

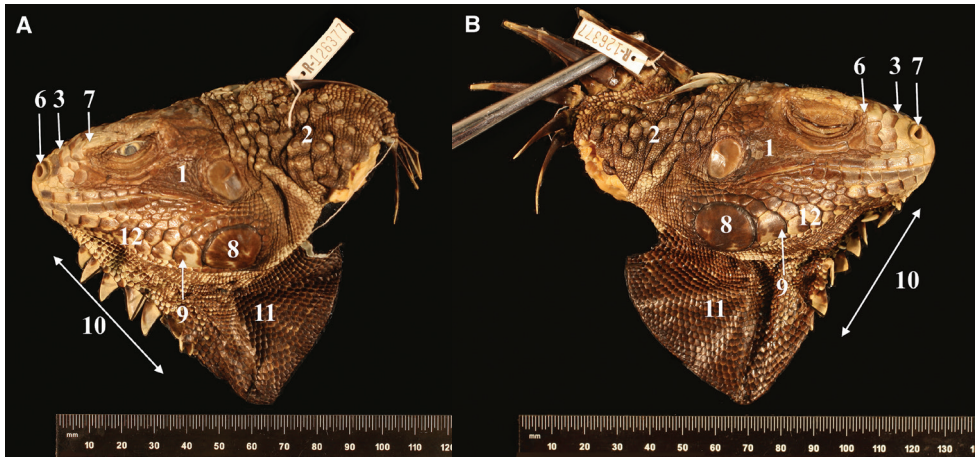


**Figure 6.** Paratype of *Iguana melanoderma* sp. nov. **A** Left side view of the head **B** right side view of the head. MCZ R 126377 from Montserrat, Old Road Bluff. Museum of Comparative Zoology, Harvard University. President and Fellows of Harvard College. 1. Black patch between the tympanum and the sub-tympanic plate. 2. High number of aligned nape tubercles. 3. No horns on the stout. 5. Black spot on the upper forelimb. 6. Prominent nostrils. 7. Anterior part of the snout, not black. 8. Subtympanic plate with a dark posterior patch. 9. Black anterior edge of lower sublateral scales. 10. Fewer than 10 triangular gular spikes extended in the upper part of the lower part of the dewlap. 11. Dewlap entirely black. 12. Lower sublateral scales arranged in pairs of nearly the same size.

*Iguana melanoderma* belongs to the Common Green Iguana phenotype (in contrast to the *Iguana delicatissima* phenotype) with its large subtympanic plate, the arrangement of sublateral scales, the rectangular shape of the dewlap, the shape and the distribution of the gular spikes, its flat head, its tubercular nape scales, and its banded tail (Breuil 2013, 2016). By the absence of horns on the snout, *Iguana melanoderma* can be distinguished from *Iguana rhinolopha* and *I. iguana insularis*, and from *I. iguana sanctaluciae* (Fig. 7).

The most distinctive morphological trait of this new taxon is its general color: adults from Saba and Montserrat iguanas are melanistic. There is a tendency for individuals to become blacker with age (Fig. 8).

There is always a black spot between the brown to grey-brown eye and the tympanum. In fully grown adults, the subtympanic plate is 2 to 2.5 times the height of the tympanum. Its color varies from light pink to dark pink with a proportion of black coloration ranging from hardly black to all black. The tympanum can be completely black. The labial and sublateral scales have the same coloring as the subtympanic plate. The lower labial scales, anterior to the subtympanic plate, are arranged in 3–5 pairs of scales of fairly similar size, one in front of the other, and do not form a mosaic of small scales. The head is usually black on the sides (tympanum, eye, subtympanic and posterior labial and sublateral parts), whereas the snout and the top of the head are light to dark grey, and in some individuals these parts are nearly entirely black.

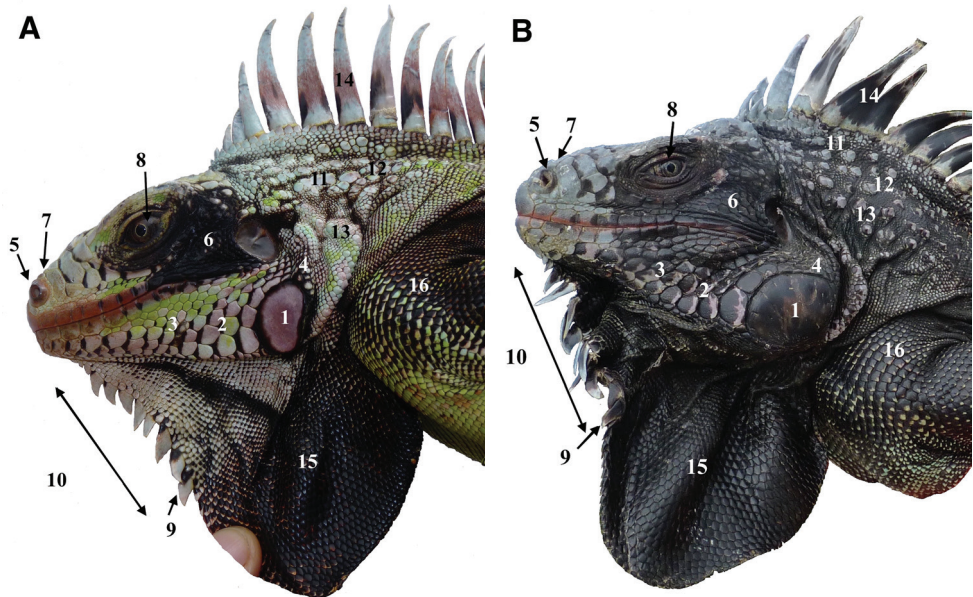


**Figure 7.** Comparison of morphological features of the head. **A** Young adult male. 1. Subtympnic plate with pink in the center. 2. Lower sublabial scales arranged in pairs of nearly identical size. 3. Black anterior edge of the lower sublabial scales. 4. Black border around the subtympnic plate. 5. Prominent nostrils. 6. Black spot between the eye and the tympanum. 7. Absence of horn and light snout. 8. Dark brown eye. 9. Triangular gular spikes. 10. Fewer than 10 gular spikes extended in the upper part of the lower dewlap. 11. High number of aligned nape tubercles. 12. Prominent light-grey tubercles. 13. Light greyish-green coloration on the neck. 14. High light-grey dorsal spines. 15. Dewlap half black. 16. Dorsal part of the limb with light-green scales becoming black with the extension of melanin from the anterior edge to the posterior edge of the scales. **B** Old male of *Iguana melanoderma* (Saba). 1. Large all-black subtympnic plate. 2. Extension of the black pigment on the sublabial scales. 3. Black coloration of the labial and upper sublabial scales. 4. Black coloration between the tympanum and the subtympnic plate. 6. Extension of the black spot around the eye and on the posterior labial and sublabial scales. 7. Snout turning dark grey. 9, 10. Gular spikes turning dark grey with extension of black patches. 12. Dark grey nape tubercles. 13. Black coloration on the neck. 14. Dorsal spikes turning black. 15. Dewlap completely black. 16. Black upper face of the limb.

The dewlap is completely black in adults, as in *Iguana iguana sanctaluciae* (Fig. 7). The gular spikes are light to dark grey with a variable portion of black. They are flat, triangular, quite small, and not exceed 10 in number. A variable percentage of the gular scales on the lower part of the dewlap are pentagonal or hexagonal, and do not overlap.

The dorsal parts of the limbs are more or less black, and the black is more developed in older individuals extending over the ventral face of the limb. Some specimens have entirely black head and legs whereas the body is dark green. This body coloration is the result of a black anterior part and a lighter posterior part of most scales while some others are black or dark green. The spikes of the dorsal crest range from light to dark grey; the central part can be black. Some individuals have entirely black dorsal and caudal crests.

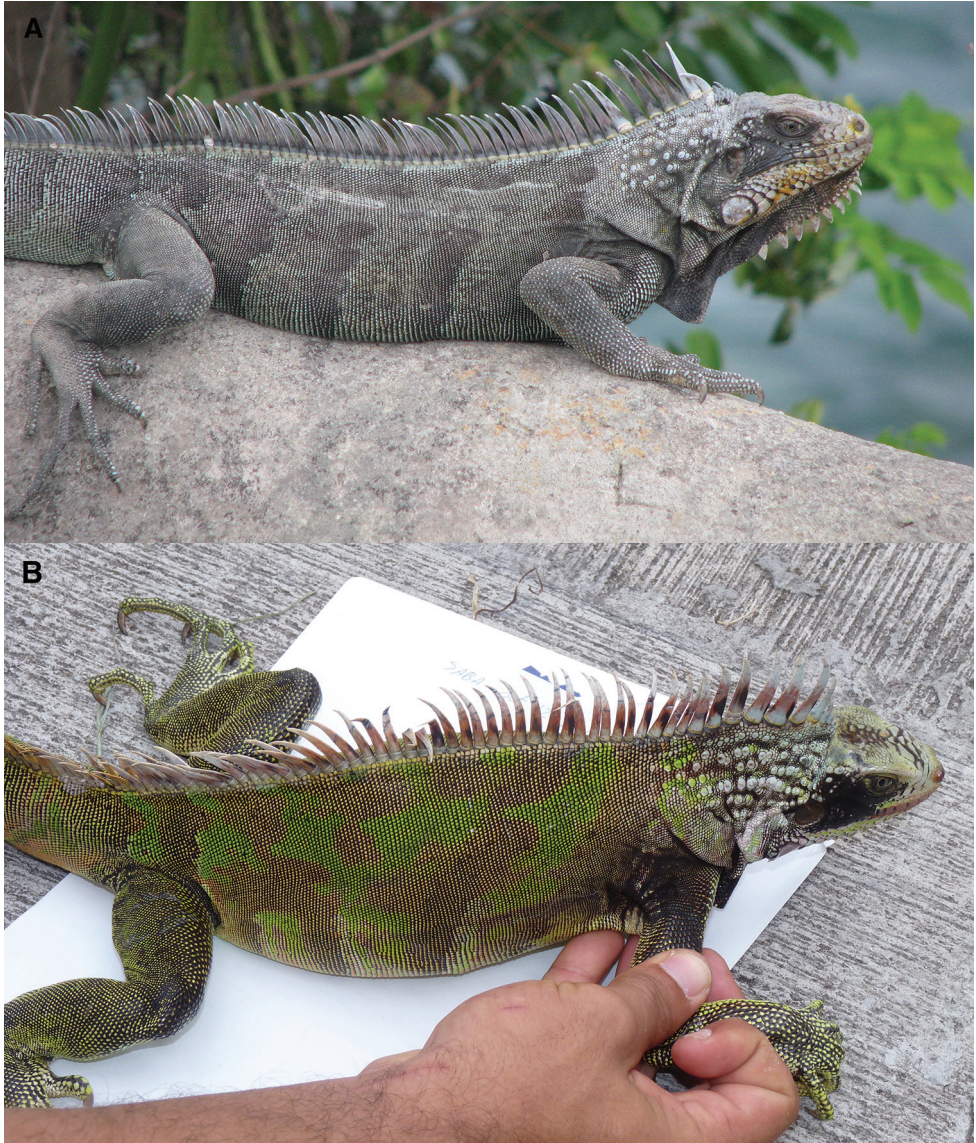


**Figure 8.** The dorsal carpet pattern of young adults *Iguana melanoderma*. **A** Montserrat **B** Saba. The dorsal coloration is formed by darker more or less interrupted dorso-ventral bands (brown, dark grey) on a lighter ground. This pattern disappears in old individuals. The black patch between the eye and the tympanum is already visible.

The nuptial coloration is present in both sexes, but more vivid and more developed in males than in females. Breeding adults sometimes become reddish-orange over the entire body (Powell et al. 2005) and the jowls are pinkish if not too melanistic. They never become as orange as *I. rhinolopha*. According to Lazell (1973), in melanistic individuals, the face, snout, and sometimes the sides are usually purple or brown.



**Figure 9. A** Old adult from Montserrat **B** old adult from Saba. In these old individuals the carpet pattern is absent. The head is almost entirely black, except for the top and the snout. The dewlap, neck, dorsal spikes, and forelimb are black. Dorsal and lateral coloring is more variable, ranging from entirely black to a mosaic of black, brown, and dark green scales.

The iguanas from Saba and Montserrat begin their lives with discontinuous light, medium and dark green dorsolateral bands and patches, some of which are underlined by white markings without black on the head and limbs. The black spot between the eye and the tympanum is present in one-year-old individuals, but it is very small and poorly developed. The proportion of the areas covered by these different green markings varies in hatchlings. In juveniles and subadults, this pattern then gradually changes to an ornate arrangement, called a carpet pattern by Lazell (1973) which consists of interrupted bands and patches, green and brown or grey and green, according to the

skin shade (Fig. 9). This highly disruptive carpet pattern may be the mark of an ancient adaptation to crypsis. A light carpet pattern, with brown and green, is also sometimes present in adults. With age, the individuals become darker, causing the carpet pattern to fade. The granular scales on the body are green, but at their periphery they are black, and a varying proportion of these scales are completely black. The details and chronology of these ontogenetic transformations are unknown.

There are no nasal horns. The tubercular nape scales are numerous, prominent, ranging from light to dark grey, and are often aligned in many rows. The cheek scales usually do not overlap.

Montserrat iguanas are similar to those of Saba. Overall, they appear less melanistic, but some individuals are as black as those of Saba. The head appears to be flatter and more elongated in Montserrat than in Saba, but more data are needed to assess putative morphological divergence between the two populations.

**Biology.** In Saba, *Iguana melanoderma* lives on cliffs (Fig. 10), in trees and bushes, in shrublands, and deciduous woodlands. One of the most striking facts about Saba is that these iguanas live in a foggy and cool environment up to about 500 m a.s.l. They sunbathe as soon as the sun rises (Figs 10, 11). The black coloration may be an adaptive trait to help rapidly raise their body temperature in these cool conditions (Breuil 2013, 2016). Hatchlings were observed in June and July.

In Montserrat, *Iguana melanoderma* have been reported in a variety of habitats, mostly in coastal residential areas. In 1995, before the eruption of the Soufrière Hills, iguanas could be seen in the then capital, Plymouth, along the seawall defenses just above high tide (M. Morton, personal observation). Blankenship (1990) reported a preference for ghauts (streams), and the majority of records to date are from locations near ghauts or rivers (J. Dawson, SL Adams, pers. comm., E. Corry, pers. obs.).

In Montserrat, there are far fewer records from mesic forest (Hamilton et al. 2008) from the Centre. The highest elevation for iguana sightings has been cited as ca. 400 m a.s.l. (G. Garcia pers. comm). However, this may reflect a bias towards areas where people spend the most time. Fewer people visit the forests, and far fewer people travel to the east of the island after the eruption. That being said, Daltry (1995) reported a negative association between iguana sightings and the elevation of the study plot ( $P < 0.0023$ ).

According to Blankenship (1990), Montserrat iguanas breed from late February, when nest digging begins, until the emergence of hatchlings in July and August. Clutch sizes range from 15 to 30 (Blankenship 1990). Observations after 1995, i.e., after the start of the last eruptions cycle of the Soufrière Hills, indicate that nesting has continued at these times of the year; egg-laying was recorded in March and April (E. Corry, M. Morton, personal observations). In April 2008, one female was observed nesting in sand at Iles Bay, an area of recent lahar deposits at the mouth of the Belham River, as well as higher up in this now subterranean stream (E. Corry; M. Morton, personal observations). This is consistent with Blankenship (1990), who stated that they nest in loose soil.

**Distribution.** The volcanic island of Montserrat is 102 km<sup>2</sup>. In 1995, the dormant volcano of the Soufrière Hills became active. Catastrophic eruptions in 1997 rendered two thirds of the south of the island uninhabitable and led to the creation of an exclusion



**Figure 10.** *Iguana melanoderma* sunbathing at dawn on the Windward coast of Saba.



**Figure 11.** A basking *Iguana melanoderma* optimizing after different trials its warming by a curved position when the sun is low on the horizon on the Windward coast of Saba.

zone (Fig. 12A). There are three major mountain ranges with natural vegetation restricted to small areas on the tops of two. The highest point before the eruption was Chances Peak, which reached 914 m a.s.l. The subsequent lava dome naturally rises and falls periodically; its maximum height was 1050 m a.s.l. in 2015. According to Lazell (1973), in the 1960s, iguanas were locally abundant in southern Montserrat and were present

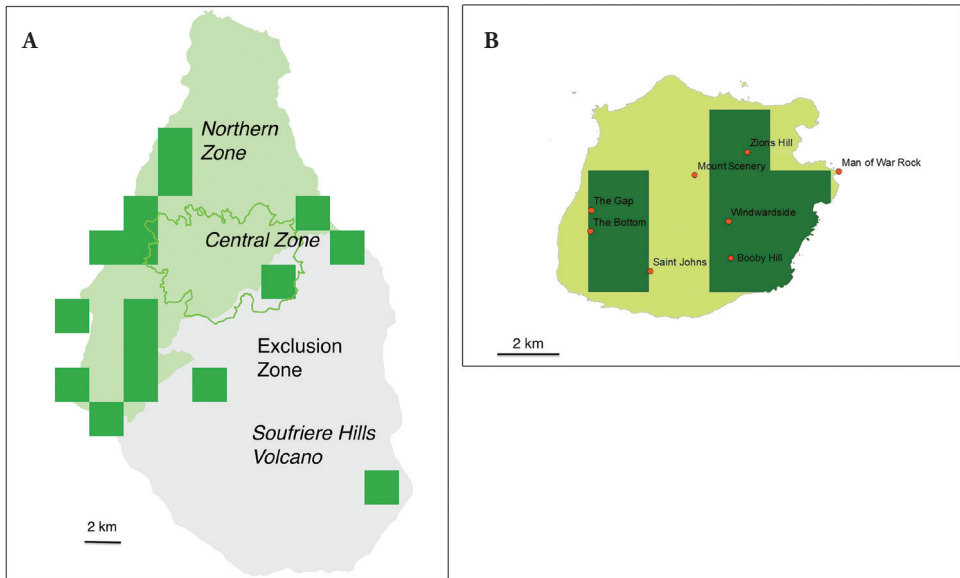


**Figure 12.** Distribution of *Iguana melanoderma* in Montserrat and Saba. Each square is 2 km along a side.

throughout the lowlands of the island. Steadman et al. (1984) reported that the species occurs in scattered areas around the island, and is locally common in some places along the southern coast. According to Reitz (1994), the iguana was not common on the island.

The island of Saba is about 13 km<sup>2</sup> and rises to an altitude of 877 m a.s.l. on Mt Scenery. This peak forms the summit of a dormant 400 ka-year-old volcano (Roobol and Smith 2004). Saba is surrounded by steep cliffs on all sides. There is no permanent beach for the laying of iguana eggs as in Martinique around Mt Pelée. Much of the central highlands of the island, above 400–500 m, are covered with dense primary and secondary rainforests. Rain and moisture from the surrounding clouds bring humidity to the forest. This pristine habitat thus seems to be incompatible for a permanent presence with the thermal and solar needs of iguanas, even in the canopy where clouds and mist are often present.

The superposition of the geological map (Roobol and Smith 2004) and the current vegetation shows that the rainforest is developing on the andesite lava of the recent central volcano. On the pelean volcanic domes on the periphery of Mount Scenery, patches of xeric vegetation are found, as on Lower and Upper Hell's Gate, Level, and Great Hill. Some hills, such as Old Booby, have little tree vegetation; overgrazing by goats is responsible for this. Some of the cliffs are made of volcanic tuff which is a poorly consolidated material that cannot withstand heavy tropical rains and where trees cannot grow. The vegetation and the climatic conditions, temperature and sun, therefore seem to restrict the distribution of iguanas and thus their numbers.

As such, the Saban Black Iguana is mainly present on the Windward side, from sea level to about 500 m a.s.l. (hilltop at the Level 514 m) (Fig. 12B). The main concentration is found on the slopes of Lower and Upper Hell's Gate, and on the cliffs of Booby

Hill. The total range of this taxon is about 5–6 km<sup>2</sup>. There are also some iguanas at The Bottom. This locality is located west of Windwardside village, but not in the shadow of Mt Scenery. For Lazell (1973), in the 1960s, Saba iguanas were common everywhere, even at 800 m a.s.l. in the rainforest of Mt Scenery.

## Discussion

### Morphological remarks

In the US Virgin Islands (St. Thomas, St. Croix, St. John) and the British Virgin Islands (BVI: Tortola) as well as on the coastal islands of Venezuela, and on the coast in the vicinity of Cumana, there are also melanistic iguanas (Lazell 1973; MacLean 1982; Buurt 2005; Falcón et al. 2018), but we found no morphological and color differences from the melanistic iguanas of Saba-Montserrat. Thus, as a hypothesis, we consider here that these melanistic iguanas belong to the same lineage as *I. melanoderma* (see below).

### Distribution remarks

Such a discontinuous distribution of this new species is puzzling. It can be explained by: [1] the natural dispersal from northern Venezuela (mainland and coastal islands) where iguanas with the same melanistic phenotype are found, as in Margarita, Los Roques and La Blanquilla, [2] human dispersion by pre-Columbian Indians, [3] recent dispersal by Modern Man, [4] convergent evolution, [5] the regression of a wider distribution area, or [6] a combination of the previous hypotheses.

To successfully colonize an island, iguanas must first arrive on that island by natural or human means, occupy an available ecological niche, or if not, be able to successfully compete with the local species. Based on what we know about the competition between *Iguana delicatissima* and *Iguana iguana* (Breuil 2013, 2016; Vuillaume et al. 2015), it is likely that *Iguana melanoderma* first became established in Montserrat-Saba and prevented the subsequent establishment of *Iguana delicatissima*. We found no evidence of mitochondrial introgression with *I. delicatissima* in this new taxon, whereas we discovered mitochondrial introgression with *I. delicatissima* in *Iguana iguana sanctaluciaae* (Breuil et al. 2019). Vuillaume et al. (2005) found no evidence of introgression with microsatellites in the Saba population. The possibility of nuclear introgression should be investigated in Montserrat to test the hypothesis of an ancient presence of *I. delicatissima*.

The first iguanas were collected in Saba by F. Laglois in 1879 (Garman 1887) and were housed at the MCZ (Harvard), but they no longer appear to be present according to the database of this museum. The first mention of iguanas in Montserrat seems to be recent, as this species is not mentioned by Dunn (1934) or by Barbour (1937), although herpetologists, such as Garman (1887), visited the island from where he described the endemic species *Anolis lividus*. This does not mean, however, that there

were no iguanas on this island at that time. The first mention of iguanas in Montserrat was probably published by Underwood (1962).

Saba and Montserrat are separated by 150 km. Between the two is the Christopher Bank or St. Kitts Bank (St. Eustatius, St. Kitts, Nevis) which was inhabited in historical times by *Iguana delicatissima* perhaps with the exception of St. Kitts (Lazell 1973). Nowadays, only a small population of *Iguana delicatissima* is present in St. Eustatius (Van den Burg et al. 2018b) and St. Kitts and Nevis have no *Iguana delicatissima*. In this context, the presence of *Iguana melanoderma* in Saba and Montserrat appears to be an anomaly in respect to the historical distribution of *Iguana delicatissima*. This species has inhabited in historical times, with the exception of these two islands, all islands from Martinique to Anguilla. This can be explained if *Iguana delicatissima* extended its geographical range with the help of Amerindians after the arrival of *I. melanoderma* in Saba and Montserrat.

Steadman et al. (1984), Reitz (1994), and Pregill et al. (1994) reported the presence in two ceramic assemblages in Montserrat ( $\pm$  2500 years ago) of *Iguana* cf. *iguana* bones that were used with other vertebrates as food. In Montserrat, the iguana is believed to have been introduced by Amerindians (Young and Hilton 2008) while Underwood (1962) thought it was a recent introduction but at that time no archeozoological iguana remains were known. Edgar (2009) suggested that the population may be native to Montserrat but that further studies are needed.

In Saba, a pre-ceramic occupation dating from 3300 BP with dense midden deposits, mainly land crabs and birds, located at 400 m a.s.l., in the tropical forest, was studied by Hofman and Hoogland (2003), but did not reveal any iguana remains. For these authors, the use of these limited food resources and the nature of the tools suggest a temporary seasonal occupation. Other Amerindian sites on Saba are dated between 400 and 1400 AD, with a major occupation period between (800–1400 AD) (Hofman and Hoogland 2003). These latter coastal archeological sites contain *Iguana iguana* bones (Hofman and Hoogland 1991), but it appears that this attribution is based only on the fact that *Iguana iguana* is the species present today on this island.

The similarity in morphology and coloration of these two populations (Breuil 2013, 2016) and their genetic homogeneity with respect to the ND4-Leu sequence and microsatellites suggest that an introduction from Saba to Montserrat or vice versa during the Amerindian period is a viable hypothesis. Our results clearly show that this Montserrat iguana belongs to the same group as Saba. The iguana bones in the Saba and Montserrat refuse middens strongly indicate that, while the attribution of bones to *Iguana iguana* by Hofman and Hoogland (1991) is correct with respect to *delicatissima*, *Iguana* cf. *melanoderma* is associated with Amerindian artifacts. However, this does not exclude the possibility of natural and/or Amerindian introductions from the eastern coastal region of Venezuela.

According to Schmidt and Inger (1957): “The common iguana, *Iguana iguana*, is apparently a recent immigrant to the southern Lesser Antilles and the Virgin Islands from northern South America, and has driven out the native rock iguana (genus *Cyclura*...) from these islands”. Platenberg and Boulon (2006) suggested that this species

was introduced to the latter islands by the pre-Colombian Indians, possibly to replace the native rock iguana as a food source, although it may also have floated or rafted there. According to Mayer (2012), all *Iguana iguana* present in the Virgin Islands were introduced. Recent introductions of iguanas from the pet trade into the USVI may have occurred from different locations (Falcón et al. 2013). According to Falcón et al. (2018), haplotypes of Caribbean iguanas were found on the islands of Vieques (Puerto Rico Bank) and St. Croix (USVI). These authors also found that all individuals from St. Thomas (USVI) with the melanistic phenotype shared haplotypes found in iguanas native to two Caribbean Islands not mentioned in their study. These preliminary genetic data concerning the melanistic iguanas of the Virgin Islands and Puerto Rico Bank and their morphology, which is indistinguishable from the iguanas of Saba-Montserrat, suggest that these melanistic iguanas belong to *I. melanoderma*. Genetic studies with microsatellites for these populations are urgently needed to answer this question in view of the presence of invasive iguanas (*Iguana iguana iguana*, *Iguana rhinolopha*) on the Virgin Islands and Puerto Rico Bank.

The Pleistocene natural deposits of Marie-Galante do not contain the remains of *Iguana delicatissima* nor *Iguana iguana* while many other reptiles, now extinct, are present. *Iguana delicatissima* appears on this island with Amerindians artifacts that suggest human introduction (Grouard 2001; Bochaton et al. 2015). The current distribution of *I. delicatissima* is thus a mixture of natural colonization and Amerindian introductions as it is now demonstrated.

Based on our data and those of Stephen et al. (2013), we propose that the origin of these insular populations with the black phenotype results from a first colonization from coastal Venezuela (Cumana area) and the Venezuelan continental islands such as Margarita, Los Roques or La Blanquilla where melanistic iguanas are present to Saba or Montserrat. A pre-Columbian colonization from one of these two islands to the other may have followed, and a third colonization towards the Puerto Rico Bank and St. Croix Bank. The original differentiation leading to this black phenotype and genetic differentiation may have taken place in the Cumana region. The colonization of Saba-Montserrat and the Puerto Rico Bank, Virgin Islands, and St. Croix Bank, with little or no divergence, may be the consequence of multiple, diachronic, Amerindians or recent colonization events.

### Phylogeographic remarks

Stephen et al. (2013) suggested that there were two natural dispersal events in the Lesser Antilles. The older one gave birth to the population of St. Lucia which is the most differentiated and is now considered as a subspecies *I. iguana sanctaluciae* (Breuil et al. 2019), and the most recent event to the Saba-Montserrat population, less differentiated from the Venezuela population, considered here as *I. melanoderma*. The phylogeny of Stephen et al. (2013) proposed the existence of three lineages in the Common Green Iguana. The deepest and therefore the oldest is represented by the Curaçao population which, in this context, warrants a specific status. The intermediate lineage is represent-

ed by the Central American clade and the most recent is the South American lineage to which the insular populations of St. Lucia-Grenadines and Saba-Montserrat-Venezuela belong. Breuil (2013, 2016) proposed to consider the Central American iguana clade as *Iguana iguana rhinolopha* and the South America clade as *Iguana iguana iguana*. Breuil et al. (2019) upgraded these two subspecies to the species level.

The five differences ( $5/818 = 0,6\%$ ) between the haplotype (HM352505) of Saba-Montserrat and the haplotype of Venezuela (HM352501) suggest differentiation, with a genetic divergence, approximated by a molecular clock of 1.29 million years for every 1% sequence divergence, at the ND4-Leu Locus (Malone et al. 2000), of ka. However, if the dark coloration of *I. melanoderma* is an adaptation to the cold environment of Saba, we have no parsimonious explanation for the presence of melanistic iguanas in northeastern Venezuela, and on the St. Croix and Puerto Rico Banks, except a very recent diaspora in a context where this black coloration does not show any loss of fitness in a very safe and protective environment.

Hap\_4 (GB HM352505), the most common haplotype, is shared by these two insular populations, but Saba also has its own haplotype (Hap\_5) (Fig. 4). This most common haplotype is, according to Falcón et al. (2018), also present in the Puerto Rico Bank. This is a strong argument in favor of a recent diaspora of this melanistic iguana throughout the Caribbean Region. A similar situation was found in *Leptodactylus fallax* where no genetic differences were found between the Montserrat population and the Dominican population (Hedges and Heinicke 2007). These authors suggested that Amerindians were responsible for this distribution pattern even though it had been present in the past in St. Kitts, Martinique, and St. Lucia (Lescure 2000).

Montserrat consists of three major volcanic centers: to the north are the heavily eroded Silver Hills (ca. 2.6–1.2 Ma); in the center are the Centre Hills (ca. 950–550 ka), also extinct and crossed by deep erosive canyons; and to the south is the massif comprising the South Soufrière Hills (ca. 135–125 ka) and the Soufrière Hills (ca. 170 ky to present) (Harford et al. 2002). Based on geographical distance and age, Montserrat is a better candidate for first natural colonization by propagules from Venezuela. Montserrat is located 150 km southeast of Saba.

Saba's oldest rocks are about 400 ky years but most of the volcanic deposits were produced in the last 70,000 years and have increased the size of the island on the edge of Mt Scenery. The last eruption is dated to 280 years BP and covers Amerindian artifacts but underlies those of the European settlers who colonized the island in 1640. European settlers may have been attracted to the island because of the presence of grassland instead of tropical rainforest caused by an eruption shortly before European settlement (Roobol and Smith 2004). Under these conditions, a recent major bottleneck may have occurred in the iguana population.

A bottleneck hypothesis and/or founder effect to explain the low genetic diversity of these insular iguanas is congruent with the fact that of the 16 common microsatellite loci used in this study, 9 are monomorphic in Saba while 8 are monomorphic in Montserrat with twice as many individuals. For example, the *Iguana delicatissima* population of Petite Terre (Guadeloupien Archipelago) has 8/15 monomorphic microsatellite loci

and the Chancel Islet population 6/15. In both populations, serious bottlenecks have recently occurred (Breuil 2002; 2009). Indeed, this panel of microsatellite molecular markers revealed high polymorphism in all the other common iguana populations studied by Valette et al. (2013) and Vuillaume et al. (2015).

Results based on microsatellite markers revealed a higher level of genetic diversity in Montserrat iguanas than in Saba iguanas. Montserrat iguanas show a genetic signature close to that of iguanas from French Guiana (Fig. 2). However, this did not appear to be the result of hybridization between two populations as several alleles are also present in the Central and South American clade populations (unpublished data). This should be investigated in a further study of the Montserrat population to check for the presence of exotic iguanas.

### Taxonomic remarks

According to Miralles et al. (2017), in their review of the taxonomic revision of *Amblyrhynchus cristatus*, there is no objective definition of subspecies, but for these authors, the subspecies rank is useful to refer to distinct population-level units that have not attained independent evolutionary lineage status, and so do not meet the species criteria. These authors thus described five new subspecies of *Amblyrhynchus cristatus* based on morphology, mitochondrial DNA, and microsatellite clusters as we did in this study. Most of their subspecies live on a single island, while two of them live on two islands and one island has two subspecies.

Breuil et al. (2019) discussed the arguments for naming the St. Lucia and Grenadines populations as one subspecies or a new species with two subspecies. The choice was made to adopt the most conservative solution for this emblematic species. The difficulty lies mainly in the different concepts used to distinguish between the species and subspecies categories (Torstrom et al. 2014). Hybridization is known between the endemic iguanas of the Lesser Antilles and the two invasive lineages i.e., *Iguana iguana* and *Iguana rhinolopha* (Breuil 2013, 2016; Vuillaume et al. 2015) and now with the Curacao lineage in Saint Maarten (Van den Burg et al. 2018a, 2018b). In addition, hybridization has recently occurred between endemic *Cyclura nubila* and *Iguana iguana* (Moss et al. 2018). In this context, it is clear that there are no intrinsic barriers to the reproduction among all the clades of *Iguana* identified first by Malone et al. (2000) and their subsequent work (Stephen et al. 2013). We chose to recognize these melanistic iguanas at the species level, integrating the source population of Venezuela and making it fit the criterion of an independent evolutionary unit.

For example, *Cyclura nubila nubila* differs by less than 1% from the ND4 sequence of *C. nubila caymanensis*. The same level of divergence is also found between *C. cyclura cyclura* and *C. cyclura inornata* which are considered valid subspecies (Malone and Davis 2004). With 1.47 % (12/818) difference between the two haplotypes (JQ340913, JQ340914) from Brazil and the two haplotypes from Saba-Montserrat (HM352505) and Venezuela (HM352501), the differences are greater than in these *Cyclura* subspecies. Powell and Henderson (2005), Powell et al. (2005), Powell (2006), and Henderson and

Powell (2009) suggested that the Saba and Montserrat populations (and possibly the historical population on St. Croix) may warrant designation as a separate species from the Common Green Iguana found elsewhere. We follow their recommendations here.

According to Stephen et al. (2013), the Central American clade (Mexico to northern Panama) is distinct from the South American clade and suggests the presence of cryptic species. The difficulty with naming these two clades is that many authors, such as Lazell (1973) or Stephen et al. (2013) considered that the only morphological distinction between these two clades is “enlarged tubercle scales on the snout” (i.e., horns). Breuil (2013; 2016) demonstrated that there are many morphological differences between these clades and that, in addition, the horns of iguanas of the southern group of Lesser Antilles are different from the horns of *rhinolopha* from Central America. Even if some populations or some individuals in some Central American populations have only small or no horns at all, this does not change the taxonomic issue. The first Central American iguanas in Mexico were described as a full species, *Iguana rhinolopha*, which clearly belongs to the Central American clade. This name should therefore be used for the Central American clade from Mexico to northern Panama, called number III by Stephen et al. (2013) (Fig. 3).

Clade II of (Stephen et al. 2013) comprises subclade IIa, called north west of Andes, which contains iguanas from Columbia, Peru and Ecuador, whereas subclade IIb, called south east of Andes, includes iguanas from Venezuela, Suriname, Brazil, and the Lesser Antilles (Saba, Montserrat, St. Lucia). According to our results, in our working region, we have the choice to consider that we have one species (*Iguana iguana*) with three subspecies (*iguana*, *sanctaluciae*, *insularis*), and *Iguana melanoderma* as another species, with the following distribution:

- *Iguana iguana iguana* (French Guiana and Brazil);
- *Iguana iguana sanctaluciae* (St. Lucia);
- *Iguana iguana insularis* (St. Vincent and Grenadines);
- *Iguana melanoderma* (north-eastern Venezuela, Venezuelan coastal islands, Saba-Montserrat Puerto Rico Bank, Virgin Islands, St. Croix Bank).

According to Stephen et al. (2013), populations in Brazil, Suriname and Venezuela have the same unique PAC haplotype (JN811116) as the Saba-Montserrat iguanas (23 iguanas), which is different from the haplotypes found in clades IIb and III. The single PAC haplotype identified in Saint Lucia (also present in the Grenadines populations, unpublished results) is a synapomorphy of the iguanas of this southern group. So, we have now recognized one new species, *Iguana insularis*, with two subspecies:

- *Iguana insularis insularis* comb. nov. of the Grenada Bank (including the Grenadines);
- and *Iguana insularis sanctaluciae* comb. nov. from Saint Lucia.

Naming species and subspecies in the South American clade has not resolved phylogenetic relationships with continental iguanas. For example, the formation of the Isthmus of Panama which was previously thought to be 2.5 My old (Iturralde-Vinent

2006) may be more than 10 My older (Montes et al. 2015). This new dating challenges the age of the first colonization of Central America by ancestral iguanas. Our taxonomic proposal simply reflects the morphological and genetic originalities of the endemic insular horned iguanas of the southern Antilles and the melanistic iguanas of the northern Antilles, regardless of changes in the original natural distribution area. The characterization of all these insular endemic taxa provides a solid basis for conservation.

### Conservation implications

The description of *Iguana melanoderma*, with its morphological and genetic diagnostic characteristics, will enable conservationists to differentiate between endemic and exotic iguanas. For example, the IUCN Red List (Bock et al. 2018) considered the Common Green Iguana, *Iguana iguana*, to be of “Least Concern” but failed to differentiate between populations that do not have the same threat levels. With our taxonomic proposal, these endemic insular populations will be considered as a conservation unit with their own assessments.

As the range of invasive iguanas increases worldwide (Falcón et al. 2013), and mainly in the Caribbean (Powell et al. 2011; van den Burg et al. 2018a, 2018b), the probability of invasive iguanas arriving on Saba increases with trade, travel, and tourism on St. Maarten (Yokoyama 2012), another Dutch island 45 km north of Saba. It is thus necessary to conserve these original populations and to be able to differentiate them from invasive iguanas of different lineages.

The Saba Conservation Foundation (SCF) is responsible for nature management on the island for the local government and runs programs for the Saban Black Iguana by reducing defoliation by goats through the restriction of the number of free-ranging domestic animals (Powell et al. 2005). As a seed dispersing animal, this taxon contributes to the recolonization of landscapes after human, animal or natural destruction.

We found no evidence of genetic introgression in the Saban Black Iguana population; the samples studied for genetic analysis, collected in 2011, have all the characteristics of this new taxon. However, according to a photograph published in the book by Powell et al. (2005) (fig. 92), but not taken by these authors, invasive iguanas could be (or could have been) present in Saba, unless the locality of the photograph is in error.

Moreover, it is clear from the Google photographs of iguanas taken in the Virgin Islands that the invasive iguana (*Iguana rhinolopha*) is also present and hybridization is occurring as shown by the presence of intermediate phenotypes in these islands and by genetic data (Falcón et al. 2018). The same holds true for Margarita Island (Venezuela).

*Iguana iguana* is listed in CITES Appendix II, but export quotas exist for many countries for pet trade and products (leather, meat). No distinction is made between native and introduced populations, or between continental and insular populations (Powell and Henderson 2007). With regard to its endemism [1], the small size of these islands (Saba: 13 km<sup>2</sup>, Montserrat: 100 km<sup>2</sup>) [2], that this new taxon occupies less than half of Saba and occupied less than 10 % of Montserrat before the eruption of the Soufrière Hills in 1995 [3], that the total effective population of this species in Saba

and Montserrat could be around 400 adults [4], that there is a pressure on the biotope [5], that hunting is rare but present [6], that dogs and cats, as well as motor vehicles, kill iguanas [7], and that the invasive iguanas could arrive soon [8], this new taxon is, based on IUCN criteria, critically endangered on the islands of Saba and Montserrat.

Priority actions for the conservation of the species *Iguana melanoderma* are biosecurity [1], minimization of hunting [2], and habitat conservation [3]. The maritime and airport authorities of both islands must be vigilant about the movements of iguanas, or their sub-products, in either direction, even if the animals remain within the same nation's territory. Capacity-building and awareness-raising should strengthen the islands' biosecurity system and could enhance pride in this flagship species.

Key stakeholders in conservation efforts are the Dutch Caribbean Nature Alliance (DCNA), the Saba Conservation Foundation (SCF), the Montserrat National Trust (MNT) and the UK Overseas Territories Conservation Forum (UKOTCF).

The DCNA is already involved in the conservation of *Iguana delicatissima* on St Eustatius<sup>1</sup>. The MNT is implementing a project funded by the Darwin Initiative entitled "Adopt a Home for Wildlife", which can also be harnessed for iguana conservation. MNT and UKOTCF suggested the following priority actions for the native iguana: preparation of an inventory, including a survey of the geographical distribution and ecology of the taxon, assessment of conservation status and regular monitoring, as well as habitat mapping and assessment of conservation purposes. The listing of Fox's Bay Bird Sanctuary as a Ramsar Site was also recommended<sup>2</sup>.

In conclusion, the pioneering work of Malone et al. (2000) and her subsequent works (Malone and Davis 2004; Stephen et al. 2013), followed by those of Breuil (2013, 2016), Vuillaume et al. (2015), and Breuil et al. (2019) clearly demonstrated that there are morphological, mitochondrial, and nuclear divergences between what was considered to be a single species, *Iguana iguana*. Thus, different clades have been identified genetically and morphologically without naming them. These diagnosable insular entities are here considered to form two new species: *Iguana melanoderma* and *Iguana insularis*. Southeastern Andes populations are considered to be *Iguana iguana* and populations in the northern Isthmus of Panama are considered to be *Iguana rhinolopha*. Morphological, genetic, ecological, and ethological studies are needed to characterize and name all lineages not included in these four recognized species. Our work provides the tools for a better protection of these insular flagship species, mainly against alien iguanas.

## Acknowledgements

All Saba samples were collected by the Natural Reserve of St. Barthélemy in collaboration with the Saba National Park (2011). St. Lucia samples were provided by M. Morton (Durrell Wildlife Conservation Trust) and the Forestry Service of St. Lucia. All samples were collected with the authorization of the local nature conservation authorities. Special

---

1 <http://www.dcnanature.org/lesser-antillean-iguana/>

2 <http://www.ukotcf.org/CP/monserrat.htm>

thanks also offered to F. Catzefis (CNRS, Montpellier, France) and Benoît de Thoisy (Institut Pasteur, Cayenne, French Guiana), who provided samples from French Guiana.

Moreover, the NGO Sea and Learn on Saba, a mainly locally sponsored foundation, invited the first author in 2012 to present the first results of this study in 2012 with Karl Kestel and Julien Le Quellec (St. Barthélemy Nature Reserve). Samples from Montserrat were exported and imported under CITES permit No. EX16–37 19/4/2016.

The genetic study was part of BV's Master's degree. This project was funded by the Direction Régionale de l'Environnement et du Logement de Martinique, as well as by the Natural Reserve of St. Barthélemy for Saba and St. Lucia iguanas. These sponsors play no role in the design of this study, the collection and analysis of data, the decision to publish, or the preparation of the manuscript. The genetic analyses were initially conducted at Genindexe by BV in La Rochelle (France) and completed by David Schikorski in Genindexe-Labofarm (France), which also funded part of this study.

Pictures and measurements of the MCZ specimens were kindly provided by Joseph Martinez and Joe Rosado. Corentin Bochaton provided us with some data concerning these iguanas at the MCZ. We thank Catherine Stephen for the helpful discussions regarding the status of these iguanas.

We are indebted to Robert Powell and an anonymous referee for their thorough, in depth, and thoughtful reviews of the manuscript, as well as to the subject editor and the editor-in-chief for the publication of this work.

We thank Chris Austin for English improvement on the final version of this manuscript.

## References

- Bandelt HJ, Forster P, Rohlf A (1999) Median-joining networks for inferring intraspecific phylogenies. *Molecular Biology and Evolution* 16: 37–48. <https://doi.org/10.1093/oxford-journals.molbev.a026036>
- Barbour T (1937) Third list of Antillean reptiles and amphibians. *Bulletin of the Museum of Comparative Zoology* 82: 77–166.
- Blankenship JR (1990) The Wildlife of Montserrat including an annotated bird list for the island. Montserrat National Trust, Montserrat, West Indies.
- Bochaton C, Grouard S, Cornette R, Ineich I, Lenoble A, Tresset A, Bailon S (2015) Fossil and subfossil herpetofauna from Cadet 2 Cave (Marie-Galante, Guadeloupe Islands, F. W. I.): Evolution of an insular herpetofauna since the Late Pleistocene. *Comptes Rendus Palevol* 14: 101–110. <https://doi.org/10.1016/j.crpv.2014.10.005>
- Bock B, Malone CL, Knapp C, Aparicio J, Avila-Pires TCS, Cacciali P, Caicedo JR, Chaves G, Cisneros-Heredia DE, Gutiérrez-Cárdenas P, Lamar W, Moravec J, Perez P, Porras LW, Rivas G, Scott, N, Solórzano A, Sunyer J (2018) *Iguana iguana*. The IUCN Red List of Threatened Species 2018: e.T174481A1414646.
- Breuil M (2002) Histoire naturelle des Amphibiens et Reptiles terrestres de l'Archipel Guadeloupéen. Guadeloupe, Saint-Martin, Saint-Barthélemy. Patrimoines naturels, 54. Institut d'Écologie et de Gestion de la Biodiversité, Muséum National d'Histoire Naturelle, Paris, 339 pp.

- Breuil M (2009) The terrestrial herpetofauna of Martinique: Past, present, future. *Applied Herpetology* 6: 123–149. <https://doi.org/10.1163/157075408X386114>
- Breuil M (2013) Caractérisation morphologique de l'iguane commun *Iguana iguana* (Linnaeus, 1758), de l'iguane des Petites Antilles *Iguana delicatissima* Laurenti, 1768 et de leurs hybrides. *Bulletin de la Société Herpétologique de France* 147: 309–346.
- Breuil M (2016) Morphological characterization of the common iguana *Iguana iguana* (Linnaeus, 1758), of the Lesser Antillean Iguana *Iguana delicatissima* Laurenti, 1768 and of their hybrids. Same paper as Breuil (2013) translated into English by International Reptiles Conservation Foundation (IRCF).
- Breuil M, Guiougou F, Questel K, Ibéné B (2010) Modifications du peuplement herpétologique dans les Antilles françaises. Disparitions et espèces allochtones. 2e partie: Reptiles. *Le Courrier de la Nature* 251: 36–43.
- Breuil M, Vuillaume B, Schikorski D, Krauss U, Morton M, Haynes P, Daltry J, Gaymes G, Gaymes J, Bech N, Jelić M, Grandjean F (2019) A story of nasal horns: two new subspecies of *Iguana* Laurenti, 1768 (Squamata, Iguanidae) in Saint Lucia, St Vincent and the Grenadines, and Grenada (southern Lesser Antilles). *Zootaxa* 4608: 201–232. <https://doi.org/10.11646/zootaxa.4608.2.1>
- Daltry JC (1995) Report on the Findings of the Amphibians and Reptiles Team Part A: Species and Habitat Associations. Montserrat National Trust and Division of Forestry and Environment. Montserrat Biodiversity Project, Fauna and Flora International, Montserrat.
- Darriba D, Taboada GL, Doallo R, Posada D (2012) jModelTest 2: more models, new heuristics and parallel computing. *Nature Methods* 9: 772–772. <https://doi.org/10.1038/nmeth.2109>
- Dubois A (2009) Endangered species and endangered knowledge. *Zootaxa* 2201: 26–29. <https://doi.org/10.11646/zootaxa.2201.1.5>
- Dunn ER (1934) Notes on *Iguana*. *Copeia* 1934: 1–4. <https://doi.org/10.2307/1436422>
- Earl DA, Vonholdt BM (2012) STRUCTURE HARVESTER: a website and program for visualizing STRUCTURE output and implementing the Evanno method. *Conservation Genetics Resources* 4: 359–361. <https://doi.org/10.1007/s12686-011-9548-7>
- Edgar P (2009) The Amphibians and Reptiles of the UK Overseas Territories. Crown Dependencies and Sovereign Base Areas. Species Inventory and Overview of Conservation and Research Priorities. The Herpetological Conservation Trust, Bornemouth, UK.
- Evanno G, Regnaut S, Goudet J (2005) Detecting the number of clusters of individuals using the software STRUCTURE: a simulation study. *Molecular Ecology* 14: 2611–2620. <https://doi.org/10.1111/j.1365-294X.2005.02553.x>
- Falcón W, Ackerman JD, Recart W, Daehler CC (2013) Biology and Impacts of Pacific Island Invasive Species. 10. *Iguana iguana*, the Green Iguana (Squamata: Iguanidae). *Pacific Science* 67: 157–186. <https://doi.org/10.2984/67.2.2>
- Falcón W, De Jesus Villanueva C, Van den Burg MP, Malone CL (2018) Disentangling the Origin of Common Green Iguanas in the Virgin Islands. IUCN SSC Iguana Specialist Group Annual Meeting, Forth Worth Zoo, Texas.
- Garman S (1887) On West Indian reptiles in the Museum of Comparative Zoology, at Cambridge, Massachusetts. *Proceedings of the American Philosophical Society* 24: 278–286.

- Gentile G, Snell H (2009) *Conolophus marthae* sp. nov. (Squamata, Iguanidae), a new species of land iguana from the Galapagos Archipelago. *Zootaxa* 2201: 1–10. <https://doi.org/10.11646/zootaxa.2201.1.1>
- Goudet J (2001) FSTAT, a program to estimate and test gene diversities and fixation indices.
- Grouard S (2001) Subsistance, systèmes techniques et gestion territoriale en milieu insulaire antillais précolombien. Exploitation des Vertébrés et Crustacés aux époques Saladoïdes et Troumassoïdes de Guadeloupe (400 av. J.-C. à 1500 ap. J.-C.). PhD thesis, Muséum national d'Histoire naturelle, Paris.
- Hamilton M, Clubbe C, Robbins SK, Bárrios S (2008) Plants and habitats of the Centre Hills and Montserrat. In: Young RP (Ed) A biodiversity assessment of the Centre Hills, Montserrat. Durrell Conservation Monograph N°1 Jersey, Channel Islands, 40–55.
- Harford CL, Pringle MS, Sparks RSJ, Young SR (2002) The Volcanic evolution of Montserrat using <sup>40</sup>Ar/<sup>39</sup>Ar geochronology. In: Druitt TH, Kokeclar BP (Eds). The Eruption of Soufrière Hills Volcano, Montserrat, from 1995 to 1999. The Geological Society of London, London, 93–113. <https://doi.org/10.1144/GSL.MEM.2002.021.01.05>
- Hasegawa M, Kishino H, Yano TA (1985) Dating of the human ape splitting by a molecular clock of mitochondrial DNA. *Journal of Molecular Evolution* 22: 160–174. <https://doi.org/10.1007/BF02101694>
- Hedges SB, Heinicke MP (2007) Molecular phylogeny and biogeography of west Indian frogs of the genus *Leptodactylus* (Anura, Leptodactylidae). *Molecular Phylogenetics and Evolution* 44: 308–314. <https://doi.org/10.1016/j.ympev.2006.11.011>
- Henderson RW, Powell R (2009) Natural History of West Indian Reptiles and Amphibians. University Press of Florida, Miami, 496 pp.
- Hofman CL, Hoogland MLP (1991) The later prehistory of Saba, N.A.: the settlement site of Kelbey's Ridge (1300–1450 A.D.). In: Ayubi EN, Havisier JB (Eds) Proceedings of the 13<sup>th</sup> International Congress for Caribbean Archaeology Anthropological Institute of the Netherlands Antilles Archaeology, Anthropological Institute of the Netherlands Antilles, 477–492.
- Hofman CL, Hoogland MLP (2003) Plum Piece Evidence for Archaic Seasonal Occupation on Saba, Northern Lesser Antilles around 3300 BP. *Journal of Caribbean Archeology* 4: 12–27.
- Iturralde-Vinent MA (2006) Meso-Cenozoic Caribbean paleogeography: implications for the historical biogeography of the region. *International Geology Review* 48: 791–827. <https://doi.org/10.2747/0020-6814.48.9.791>
- Katoh K, Kuma K, Toh H, Miyata T (2005) MAFFT version 5: improvement in accuracy of multiple sequence alignment. *Nucleic Acids Research* 33: 511–518. <https://doi.org/10.1093/nar/gki198>
- Kumar S, Stecher G, Tamura K (2016) MEGA7: Molecular Evolutionary Genetics Analysis Version 7.0 for Bigger Datasets. *Molecular Biology and Evolution* 33: 1870–1874. <https://doi.org/10.1093/molbev/msw054>
- Lazell JD (1973) The Lizard Genus *Iguana* in the Lesser Antilles. *Bulletin of the Museum of Comparative Zoology* 145: 1–28.
- Leigh JW, Bryant D (2015) POPART: full-feature software for haplotype network construction. *Methods in Ecology and Evolution* 6: 1110–1116. <https://doi.org/10.1111/2041-210X.12410>

- Leighton GRM, Hugo PS, Roulin A, Amar A (2016) Just Google it: assessing the use of Google Images to describe geographical variation in visible traits of organisms. *Methods in Ecology and Evolution* 7: 1060–1070. <https://doi.org/10.1111/2041-210X.12562>
- Lescure J (2000) Répartition passée de *Leptodactylus fallax* Müller, 1923 et d'*Eleutherodactylus johnstonei* Barbour, 1914 (Anoures, Leptodactylidés). *Bulletin Société herpétologique de France* 94: 13–23.
- MacLean WP (1982) *Reptiles and Amphibians of the Virgin Islands*. MacMillan Caribbean, London, 54 pp.
- Malone CL, Davis SK (2004) Genetic contributions to Caribbean iguana conservation. In: Alberts AC, Carter RL, Hayes, WK, Martins EP (Eds) *Iguanas: Biology and Conservation*. University of California Press, Los Angeles, 45–57. <https://doi.org/10.1525/california/9780520238541.003.0004>
- Malone CL, Wheeler T, Taylor JF, Davis SK (2000) Phylogeography of the Caribbean rock iguana (*Cyclura*): Implications for conservation and insights on the biogeographic history of the West Indies. *Molecular Phylogenetics and Evolution* 17: 269–279. <https://doi.org/10.1006/mpev.2000.0836>
- Malone CL, Reynoso VH, Buckley L (2017) Never judge an iguana by its spines: Systematics of the Yucatan spiny tailed iguana, *Ctenosaura defensor* (Cope, 1866) *Molecular Phylogenetics and Evolution* 115: 27–39. <https://doi.org/10.1016/j.ympev.2017.07.010>
- Mayer GC (2012) Puerto Rico and the Virgin Islands. In: Powell R, Henderson RW (Eds) *Island Lists of West Indian Amphibians and Reptiles*. *Bulletin of the Florida Museum of Natural History* 51(2): 136–147.
- Miralles A, Macleod A, Rodríguez A, Ibáñez A, Jiménez-Uzategui G, Galo Quezada G, Vences M, Steinfartz S (2017) Shedding light on the Imps of Darkness: an integrative taxonomic revision of the Galápagos marine iguanas (genus *Amblyrhynchus*). *Zoological Journal of the Linnean Society* 181: 678–710. <https://doi.org/10.1093/zoolinlean/zlx007>
- Montes C, Cardona A, Jaramillo C, Pardo A, Silva JC, Valencia V, Ayala C, Pérez-Angel LC, Rodríguez-Parra LA, Ramirez V, Niño H (2015) Middle Miocene closure of the Central American Seaway. *Science* 346 (6231): 226–229. <https://doi.org/10.1126/science.aaa2815>
- Moss JB, Welch ME, Burton FJ, Vallee MV, Houlcroft EW, Laaser T, Gerber GP (2018) First evidence for crossbreeding between invasive *Iguana iguana* and the native rock iguana (Genus *Cyclura*) on Little Cayman Island. *Biological Invasions* 20: 817–823. <https://doi.org/10.1007/s10530-017-1602-2>
- Nei M, Kumar S (2000) *Molecular Evolution and Phylogenetics*. Oxford University Press, New York, 333 pp.
- Platenberg RJ, Boulon RHJ (2006) Conservation status of reptiles and amphibians in the US Virgin Islands. *Applied Herpetology* 3: 215–235. <https://doi.org/10.1163/157075406778116159>
- Powell R (2006) Conservation of the herpetofauna on the Dutch Windward Islands: St. Eustatius, Saba, and St. Maarten. *Applied Herpetology* 3: 293–306. <https://doi.org/10.1163/157075406778905090>
- Powell R, Henderson RW (2005) Conservation status of Lesser Antillean reptiles. *Iguana* 12: 62–77.

- Powell R, Henderson RW (2007) The St. Vincent herpetofauna. *Applied Herpetology* 4: 295–312. <https://doi.org/10.1163/157075407782424539>
- Powell R, Henderson RW, Farmer MC, Breuil M, Echternacht AC, Van Buurt G, Romagosa CM, Perry G (2011) Introduced amphibians and reptiles in the greater Caribbean: Patterns and conservation implications. In: Hailey A, Wilson BS, Horrocks JA (Eds) *Conservation of Caribbean Island Herpetofaunas vol. 2*. Brill, Leiden, 63–143. <https://doi.org/10.1163/ej.9789004183957.i-228.38>
- Powell R, Henderson RW, Parmalee JSJ (2005) The Reptiles and Amphibians of the Dutch Caribbean St. Eustatius, Saba and St. Maarten. STENAPA, St Eustatius, 192 pp.
- Pregill GK, Steadmann DW, Watters DR (1994) Late Quaternary vertebrate faunas of the Lesser Antilles : historical components of Caribbean biogeography. *Bulletin of the Carnegie Museum of Natural History* 30: 1–51.
- Pritchard JK, Stephens M, Donnelly P (2000) Inference of population structure using multilocus genotype data. *Genetics* 155: 945–959.
- Reitz EJ (1994) Archeology of Trants, Montserrat. Part 2. Vertebrate Fauna. *Annals of the Carnegie Museum of Natural History* 63(4): 297–317.
- Rice WR (1989) Analyzing tables of statistical tests. *Evolution* 43: 223–225. <https://doi.org/10.1111/j.1558-5646.1989.tb04220.x>
- Roobol MJ, Smith AL (2004) *Volcanology of Saba and St. Eustatius*. Koninklike Nederlandse Akademie van Wetenschappen. Royal Netherlands Academy of Arts and Sciences, Amsterdam, The Netherlands, 320 pp.
- Schmidt KP, Inger RF (1957) *Living Reptiles of the World*. Hanover House, New York, 287 pp.
- Steadman DW, Waters DR, Reitz EJ, Pregill GK (1984) Vertebrates from archeological sites on Montserrat, West Indies. *Annals of the Carnegie Museum of Natural History* 53: 1–29.
- Stephen CL, Reynoso VH, Collett WS, Hasbun CR, Breinholt JW (2013) Geographical structure and cryptic lineages within common green iguanas, *Iguana iguana*. *Journal of Biogeography* 40: 50–62. <https://doi.org/10.1111/j.1365-2699.2012.02780.x>
- Torstrom SM, Pangle KL, Swanson BJ (2014) Shedding subspecies: The influence of genetics on reptile subspecies taxonomy. *Molecular Phylogenetics and Evolution* 76: 134–143. <https://doi.org/10.1016/j.ympev.2014.03.011>
- Underwood G (1962) Reptiles of the Eastern Caribbean. *Caribbean Affairs (N.S.)* 1: 1–192.
- Valette V, Filipova L, Vuillaume B, Cherbonnel C, Risterucci AM, Delaunay C, Breuil M, Grandjean F (2013) Isolation and characterization of microsatellite loci from *Iguana delicatissima* (Reptilia: Iguanidae), new perspectives for investigation of hybridization events with *Iguana iguana*. *Conservation Genetics Resources* 5: 173–175. <https://doi.org/10.1007/s12686-012-9761-z>
- Van Buurt G (2005) *Field Guide to the Amphibians and Reptiles of Aruba, Curaçao and Bonaire*. Chimaira, Frankfurt, 137 pp.
- Van den Burg MP, Breuil M, Knapp CR (2018a) *Iguana delicatissima*. The IUCN Red List of Threatened Species 2018: e.T10800A122936983. <https://doi.org/10.2305/IUCN.UK.2018-1.RLTS.T10800A122936983.en>
- Van den Burg MP, Meirmans PG, van Wagensveld TP, Kluskens B, Madden H, Welch ME, Breeuwer JAJ (2018) The Lesser Antillean Iguana (*Iguana delicatissima*) on St. Eustatius: genetically depauperate and threatened by ongoing hybridization. *Journal of Heredity* 109: 426–437. <https://doi.org/10.1093/jhered/esy008>

- Vuillaume B, Valette V, Lepais O, Grandjean F, Breuil M (2015) Genetic evidence of hybridization between the endangered native species *Iguana delicatissima* and the invasive *Iguana iguana* (Reptilia, Iguanidae) in the Lesser Antilles: management implications. PLoS ONE 10. <https://doi.org/10.1371/journal.pone.0127575>
- Weir BS, Cockerham CC (1984) Estimating F-statistics for the analysis of populations structure Evolution 38: 1358–1370. <https://doi.org/10.1111/j.1558-5646.1984.tb05657.x>
- Yokoyama M (2012) Reptiles and Amphibians Introduced on St Martin, Lesser Antilles. IRCF Reptiles and Amphibians 19: 271–279.
- Young RP, Hilton GM (2008) Background to the Centre Hills biodiversity assessment. In: Young RP (Ed.) A biodiversity assessment of the Centre Hills. Montserrat. Durrell Conservation Monograph N°1 Jersey, Channel Islands, 30–39.



# A new species of *Cyrtodactylus* (Squamata, Gekkonidae) from Cambodia's Prey Lang Wildlife Sanctuary

Thy Neang<sup>1</sup>, Adam Henson<sup>2</sup>, Bryan L. Stuart<sup>3</sup>

**1** Wild Earth Allies, 77a Street Beton, Bayap Village, Sangkat Phnom Penh Thmei, Khan Sen Sok, Phnom Penh, Cambodia **2** Wild Earth Allies, 2 Wisconsin Circle, Suite 900, Chevy Chase, Maryland 20815, USA **3** North Carolina Museum of Natural Sciences, 11 West Jones Street, Raleigh, North Carolina 27601, USA

Corresponding author: Bryan L. Stuart ([bryan.stuart@naturalsciences.org](mailto:bryan.stuart@naturalsciences.org))

---

Academic editor: T. Ziegler | Received 21 November 2019 | Accepted 18 February 2020 | Published 13 April 2020

---

<http://zoobank.org/1D4D9F01-4F87-4E49-9113-4B0D72A273D6>

---

**Citation:** Neang T, Henson A, Stuart BL (2020) A new species of *Cyrtodactylus* (Squamata, Gekkonidae) from Cambodia's Prey Lang Wildlife Sanctuary. ZooKeys 926: 133–158. <https://doi.org/10.3897/zookeys.926.48671>

---

## Abstract

*Cyrtodactylus phnomchiensis* **sp. nov.** is described from Phnom Chi, an isolated mountain in Prey Lang Wildlife Sanctuary, Kampong Thom Province, Cambodia. The new species is recognized by having a unique combination of morphological characters, including snout-vent length 76.1–80.7 mm; paravertebral tubercles 31–36; ventral scales 45–54; enlarged femoral scales 0–8, without pores; enlarged precloacal scales 7–10, bearing pores 4–5 in males, pits 1–7 in females; the posterior border of nuchal loop unbroken and pointed, bordered anteriorly and posteriorly by a broad yellow or yellowish white band; and yellow spots on top of head. The new species also represents a divergent mitochondrial DNA lineage within the *C. irregularis* complex that is closely related to *C. zieglerei*, but the phylogenetic relationships among the new species and two divergent mitochondrial subclades within *C. zieglerei* are not resolved based on available sequence data. *Cyrtodactylus phnomchiensis* **sp. nov.** is the only member of the *C. irregularis* complex known to occur west of the Mekong River. The new species may be endemic to Phnom Chi, and likely faces imminent conservation threats.

## Keywords

*Cyrtodactylus irregularis*, *C. zieglerei*, Mekong River, Phnom Chi, *Sphenomorphus preylangensis*

## Introduction

Bent-toed Geckos of the genus *Cyrtodactylus* Gray are one of the most species-diverse genera of gekkonid lizards, with 292 recognized species (Uetz et al. 2020). Much of the diversity within *Cyrtodactylus* has been described only during the past decade and from mainland Southeast Asia (Brennan et al. 2017; Uetz et al. 2020), and many of these newly-recognized species are thought to be highly localized with extremely narrow geographic ranges (e.g., Nazarov et al. 2012; Luu et al. 2016; Grismer et al. 2017; Murdoch et al. 2019).

*Cyrtodactylus irregularis* (Smith, 1921) was originally described from the Langbian Plateau near Da Lat, southern Vietnam. For nearly a century, *C. irregularis* was treated as a single, geographically widespread, but morphologically variable species. Recent taxonomic studies on variation in morphology and, usually, the mitochondrial cytochrome *c* oxidase subunit I (COI) gene (Brennan et al. 2017) have revealed that *C. irregularis* actually represents a complex of at least 19 species distributed in southern and central Vietnam, eastern Cambodia, and southern Laos (Nguyen et al. 2013, 2017; Pauwels et al. 2018). These include 18 named species from Vietnam recognized by Pauwels et al. (2018), as well as *C. buchardi* David, Teynie & Ohler, 2004 from southern Laos, a species that has been hypothesized to be a member of this complex (Ngo and Chan 2010; Nguyen et al. 2013, 2017) but that remains phylogenetically untested owing to lack of molecular data. The monophyly of the *C. irregularis* group has been demonstrated by phylogenetic analysis of the COI gene from most of the species in the complex (Nazarov et al. 2012; Nguyen et al. 2013, 2014, 2017; Luu et al. 2017; Schneider et al. 2014).

During field surveys by Wild Earth Allies in June–July 2019, five specimens of the *C. irregularis* complex were collected in Cambodia on the western side of the Mekong River at Phnom Chi (Mountain) in Prey Lang Wildlife Sanctuary, Kampong Thom Province. Herein, we investigate the taxonomic status of the Phnom Chi specimens through comparisons of morphological and mitochondrial DNA data with other members of the *C. irregularis* complex.

## Materials and methods

### Sampling

Field work was conducted both day and night to search microhabitats for amphibians and reptiles at Phnom Chi. Specimens were collected by hand and kept overnight in individual plastic or cloth bags for photographing the following day. Specimens were euthanized by cardiac injection of high concentration of tricaine methanesulfonate (MS-222) and fixed in 10% formalin after preserving liver tissue in 20% DMSO-salt saturated storage buffer. After a minimum of three days of formalin-fixation, the specimens were soaked in water for six hours to remove formalin, and transferred to 70% ethanol for permanent storage. Specimens were deposited in the herpetological collection at the Centre for Bio-

diversity Conservation, Royal University of Phnom Penh, Cambodia (CBC). Comparative data were taken from original species descriptions and the expanded descriptions of *C. irregularis* by Nazarov et al. (2008) and *C. buchardi* by Teynie and David (2010).

### Morphological analyses

Morphometric and meristic characters were measured and counted using a Nikon SMZ 645 dissecting microscope. Measurements were taken by hand with digital calipers to the nearest 0.1 mm (ratios calculated to 0.001). Measured characters were:

<b>AG</b>	Axilla-groin distance, measured from the posterior margin of forelimb at its insertion point on the body to the anterior margin of hind limb at its insertion point on the body;
<b>CrusL</b>	Crus length, measured from the knee to the base of the heel;
<b>EarDH</b>	Ear diameter in horizontal distance, measured as the horizontal distance between anterior and posterior margins of the ear opening;
<b>EarDV</b>	Ear diameter in vertical distance, measured as the vertical distance between dorsal and ventral margins of the ear opening;
<b>END</b>	Eye-nostril distance, measured from the anterior margin of eye to the posterior margin of nostril;
<b>ESD</b>	Eye-snout distance, measured from the anterior margin of eye to the tip of snout;
<b>EyeD</b>	Eye diameter, measured as the horizontal distance from the anterior to the posterior margins of the eyeball;
<b>Eye-EarD</b>	Eye-ear distance, measured from the posterior margin of eye to the anterior margin of ear opening;
<b>ForeL</b>	Forearm length, measured from the posterior margin of elbow while flexed 90° to the wrist inflection;
<b>HeadD</b>	Head depth, measured as the maximum depth of head from the occiput to the throat;
<b>HeadL</b>	Head length, measured from the tip of snout to the posterior margin of the retroarticular process of the lower jaw;
<b>HeadW</b>	Head width, measured as the maximum head width at the corners of the jaws;
<b>IOD</b>	Interorbital distance, measured as the shortest distance between the anterior corners of the eyes;
<b>IND</b>	Internarial distance, measured as the shortest distance between the nostrils;
<b>SVL</b>	Snout to vent length, measured from the tip of the snout to the vent;
<b>TaL</b>	Tail length, measured from the vent to the tip of the tail;
<b>TaW</b>	Tail width, measured at the base of the tail immediately posterior to the post-cloacal swelling.

Scale counts are reported in right and left (R, L) order. The presence, absence and/or numbers of the following characters were recorded:

<b>EFS</b>	Enlarged femoral scales;
<b>EPrecS</b>	Enlarged precloacal scales;
<b>FP</b>	Femoral pores;
<b>InL</b>	Infralabials, counted as the number of scales from the first lower labial scale immediately posterior to mental to the last scale below posterior edge of the eyeball;
<b>LDRT</b>	Longitudinal dorsal rows of enlarged tubercles, counted as the number of tubercles transversely across the dorsum between ventrolateral folds;
<b>PrecG</b>	Precloacal groove;
<b>PrecP</b>	Precloacal pores;
<b>PostPSR</b>	Post precloacal scale rows;
<b>PostSP</b>	Post cloacal spur;
<b>PVT</b>	Paravertebral tubercles, counted as the number of enlarged tubercles in a straight line between limb insertions left of the vertebral column;
<b>SDLF4</b>	Subdigital lamellae beneath fourth finger, counted as the number of both expanded proximal subdigital lamellae from the base to the largest scale on the digital inflection, and unmodified distal lamellae beneath fourth finger to the claw sheath;
<b>SDLT4</b>	Subdigital lamellae on fourth toe, counted as the number of expanded proximal subdigital lamellae from the base to the largest scale on digital inflection and unmodified distal subdigital lamellae beneath fourth toe to the claw sheath;
<b>SL</b>	Supralabials, counted as the number of scales from the first upper labial scale immediately posterior to rostral to the last scale below posterior edge of the eyeball;
<b>VS</b>	Ventral scales, counted as the number of scales transversely across the ventral surface at midbody between ventrolateral folds.

### Molecular analyses

Total genomic DNA was extracted from preserved liver tissue of two Phnom Chi specimens (CBC 03003–04) using the DNeasy Blood and Tissue Kit (Qiagen). A 658 bp fragment of mitochondrial (mt) DNA that encodes part of the COI gene was amplified in a 25 ul reaction by the polymerase chain reaction (PCR; 35 cycles of 95° 30s, 53 °C 40s, 72° 90s) and sequenced using the primers VF1d and VR1d (Ivanova et al. 2006). PCR products were cleaned using ExoSAP-IT (Applied Biosystems) and sequenced in both directions by direct double strand cycle sequencing using the Big-Dye Terminator version 3.1 Cycle Sequencing Kit on a 3130 DNA Analyzer (Applied Biosystems). Sequences were edited with Sequencher version 5.4.6 (Gene Codes) and deposited in GenBank under accession numbers MT066405–MT066406.

All available *Cyrtodactylus* COI sequences ( $n = 453$ ), and the outgroup *Hemidactylus frenatus* (GenBank accession GQ245970), were downloaded from GenBank on 1 October 2019. The downloaded sequences were aligned and visually inspected in Sequencher to ensure that insertion-deletions did not disrupt the coding region. Preliminary phylogenetic analysis (not shown) was performed on the alignment under the parsimony criterion using a heuristic search with equal weighting of nucleotide substitutions in PAUP\* version 4.0a165 (Swofford 2003). Those *Cyrtodactylus* sequences that clustered in the clades around the Phnom Chi samples (= *C. irregularis* group) in a strict consensus of the equally most parsimonious trees were retained in the alignment. Exemplar sequences of other major clades were also retained to represent known phylogenetic diversity within *Cyrtodactylus*, including *C. auribalteatus* (GenBank accession AP018116), *C. badenensis* (KF929505), *C. chanhomeae* (MF169908), *C. condorensis* (MF169910), *C. interdigitalis* (MF169919), *C. intermedius* (MF169920), *C. jellesmae* (MF169923), *C. peguensis* (AP018114), *C. russelli* (MF169938), and *C. thirakhupti* (AP018115).

The resulting pruned COI alignment contained 270 taxa and 717 characters, with no insertion-deletions. The alignment was partitioned by codon position, and the best-fit partitioning scheme and models of sequence evolution were selected using PartitionFinder 2 (Lanfear et al. 2017). Two partitions were selected, with the first and second codon positions merged into a single partition under the model TVM+I+G, and the third codon position under the model GTR+G. Four independent partitioned Bayesian analyses were performed using MrBayes 3.2.7a (Ronquist et al. 2012) on the Cyberinfrastructure for Phylogenetic Research (CIPRES) Science Gateway version 3.3 (Miller et al. 2010). In each analysis, four chains were run for 20 million generations using the default priors, the chain temperature was set to 0.1, trees were sampled every 4,000 generations, and the first 25% of trees were discarded as 'burn-in'. The resulting trace plots were viewed using Tracer v.1.7 (Rambaut et al. 2018). A 50% majority-rule consensus of the post burn-in trees was constructed to calculate the posterior probabilities of nodes. Nodes with posterior probabilities  $\geq 0.95$  were considered to be statistically supported. Uncorrected pairwise distances were calculated using PAUP\* version 4.0a165 (Swofford 2003).

## Results

### Morphological analyses

The Phnom Chi specimens could not be referred to any other named members of the *C. irregularis* complex owing to having a unique combination of morphological characters. These characters included body size such as having a relatively long body and tibia; scalation, such as the number of subdigital lamellae under the fourth finger and fourth toe, number of longitudinal dorsal and paravertebral rows of tubercles, number of ventral scales, number of enlarged precloacal scales and associated pores (in males) and pits (in females), absence of pores in their enlarged femoral scales, and size of the median subcaudal scale rows from other species in the complex; and pattern and col-

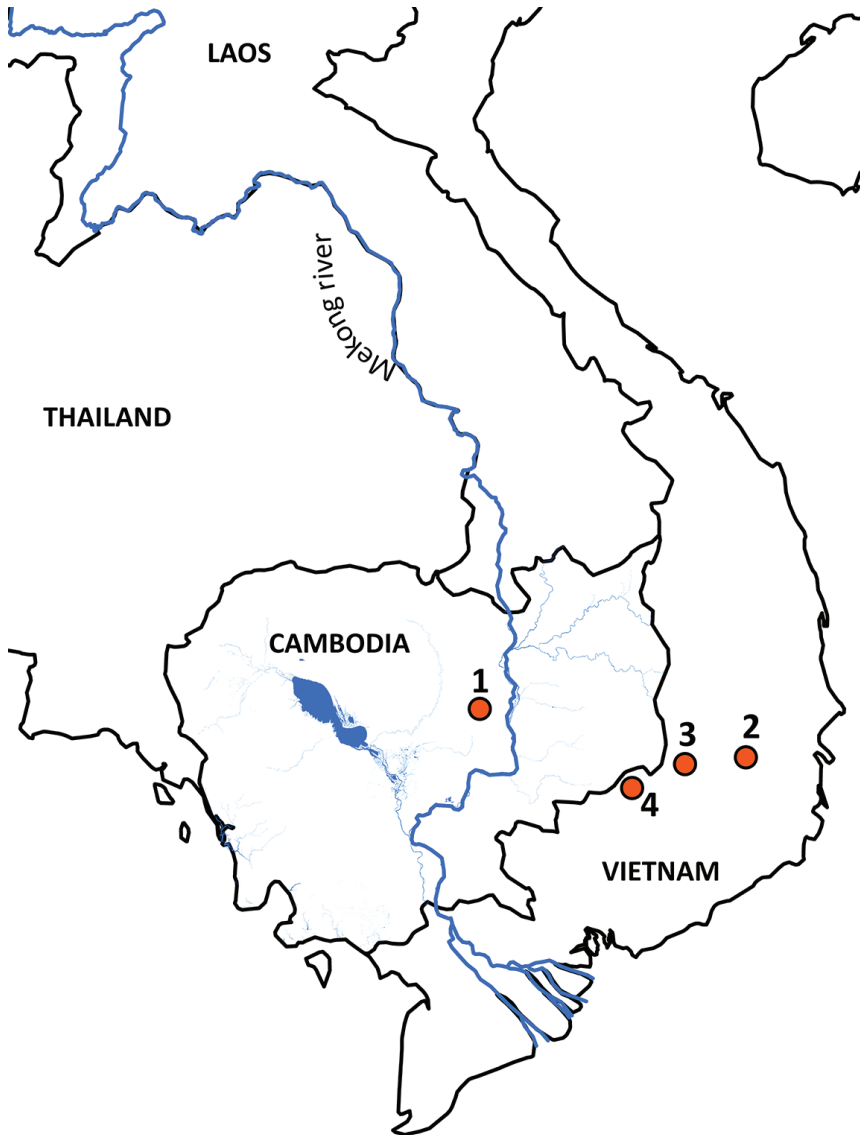


**Figure 1.** Map illustrating (1) the type locality of *Cyrtodactylus phnomchiensis* sp. nov. at Prey Lang Wildlife Sanctuary, Kampong Thom Province, Cambodia; (2) the type locality of *C. zieglerei* at Chu Yang Sin National Park, Dak Lak Province, Vietnam (Nazarov et al. 2008); (3) the second known locality of *C. zieglerei* at Nam Nung Nature Reserve, Dak Nong Province, Vietnam (Nguyen et al. 2013); and (4) the type locality of *C. bugiamapensis* at Bu Gia Map National Park, Binh Phuoc Province, Vietnam (Nazarov et al. 2012).

oration, including an unbroken nuchal loop bordered anteriorly and posteriorly by a broad yellow or yellowish white band, three or four dark brown body bands, and two or three yellowish white or light brown body bands, about half the width of the brown body bands, and yellow spots on top of the head.

## Molecular analyses

The standard deviation of split frequencies among the four Bayesian runs was 0.006260 and the Estimated Sample Sizes (ESS) of parameters were  $\geq 1,606$ , indicating that the four runs were sufficiently sampled and had converged. The Phnom Chi specimens represented a distinct mitochondrial lineage that did not match any other named species (Fig. 2). The Phnom Chi lineage was recovered with strong support (Bayesian posterior probability 1.00) to be phylogenetically nested within a clade containing two mitochondrial subclades of *C. zieglerei* (subclades Z1 and Z2; Fig. 2), but the relationships among the Phnom Chi lineage and the two subclades of *C. zieglerei* were unresolved, rendering *C. zieglerei* non-monophyletic (Fig. 2). The clade containing the Phnom Chi lineage and the two subclades of *C. zieglerei* was recovered with strong support (Bayesian posterior probability 1.00) to be sister to *C. bugiamapensis* (Fig. 2).

The Phnom Chi samples had uncorrected *p*-distances in COI of 4.3–6.2% from *C. zieglerei* (all samples) and 7.0–8.6% from *C. bugiamapensis*. *Cyrtodactylus zieglerei* (all samples) had uncorrected *p*-distances of 6.7–8.5% from *C. bugiamapensis*. *Cyrtodactylus zieglerei* subclade Z1 had uncorrected *p*-distances of 4.7–5.2% from *C. zieglerei* subclade Z2.

## Species description

On the basis of their distinctiveness in morphology and mitochondrial DNA, including from *C. zieglerei* to which they are phylogenetically related (but exact relationship unresolved; Fig. 2), and further corroborated by their geographic distance to any other named members in the complex (and the only member known from west of the Mekong River), the Phnom Chi specimens are hypothesized to represent a distinct species, described herein as:

### *Cyrtodactylus phnomchiensis* sp. nov.

<http://zoobank.org/103B12F4-6D6F-4928-85A5-A927A81225FE>

Figures 3–6

**Holotype.** CBC 03012, adult male (Fig. 3), Cambodia, Kampong Thom Province, Sandan District, Phnom Chi, Prey Lang Wildlife Sanctuary, 12°56'11.6"N, 105°39'17.1"E, 237 m elevation, collected on 18 July 2019 by Thy Neang and En E.

**Paratypes.** All from Cambodia, Kampong Thom Province, Sandan District, Phnom Chi, Prey Lang Wildlife Sanctuary: CBC 03003, adult male, 12°56'09.2"N, 105°39'12.7"E, 269 m elevation, coll. 13 June 2019 by Thy Neang; CBC 03004, adult female, 12°56'09.7"N, 105°39'14.4"E, 271 m elevation, coll. 13 June 2019 by Thy Neang; CBC 03013, adult female, same data as holotype; CBC 03014, adult female, same data as holotype except 12°56'08.7"N, 105°39'12.6"E, 284 m elevation.

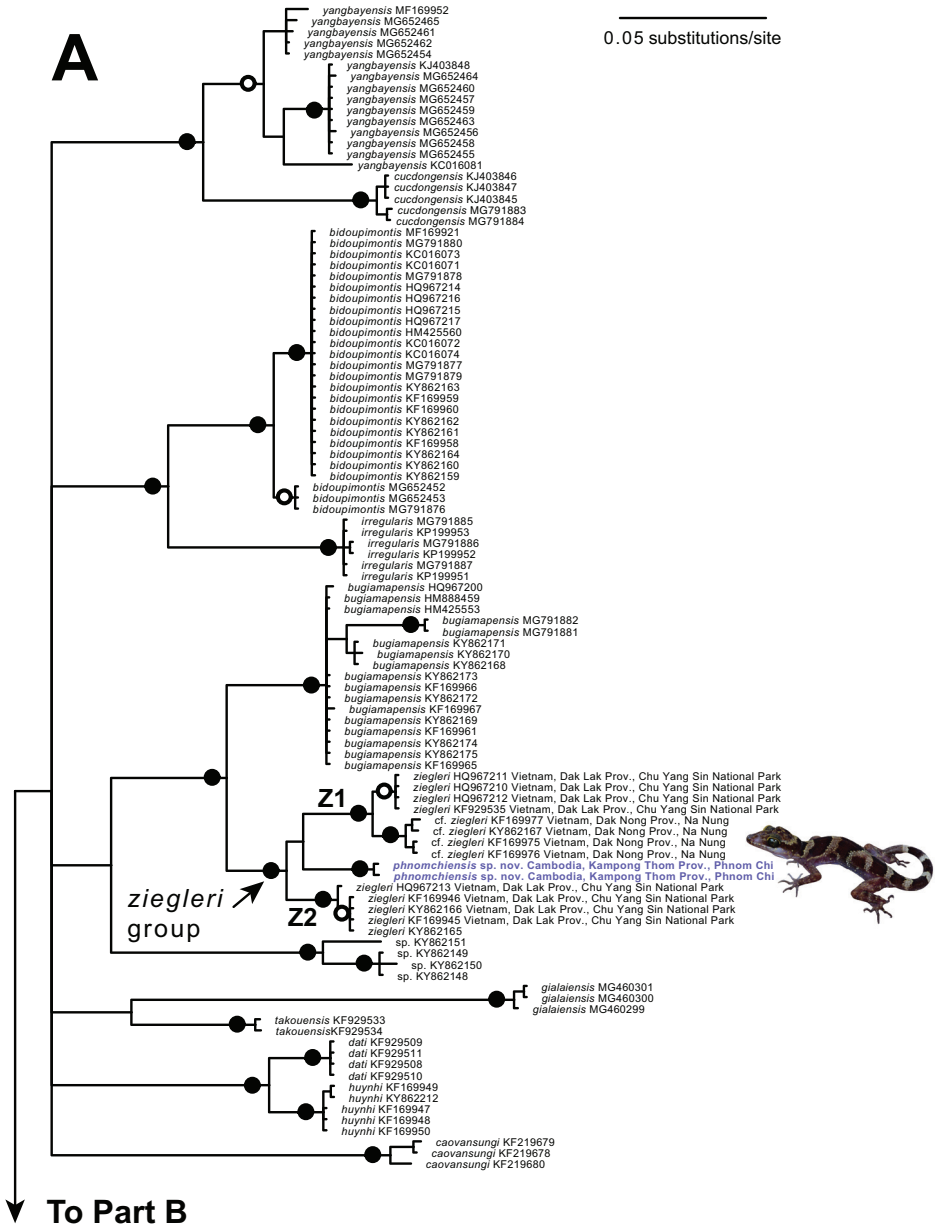


**Figure 2.** Upper (A) and lower (B) portions of a fifty percent majority-rule consensus phylogram resulting from partitioned Bayesian analysis of 717 aligned characters of the mitochondrial cytochrome *c* oxidase subunit I (COI) gene from geckos in the *Cyrtodactylus irregularis* group. The outgroup *Hemidactylus frenatus* (GenBank accession GQ245970) and exemplars of other *Cyrtodactylus* clades including *C. auribalteatus* (GenBank accession AP018116), *C. badenensis* (KF929505), *C. chanhomeae* (MF169908), *C. interdigitalis* (MF169919), *C. intermedius* (MF169920), *C. jellesmae* (MF169923), *C. peguensis* (AP018114), *C. russelli* (MF169938), and *C. thirakhupti* (AP018115) were also included in the analysis (not shown). Black circles at nodes indicate Bayesian posterior probabilities  $\geq 0.99$ , and open circles at nodes indicate Bayesian posterior probabilities  $\geq 0.95$ . Numbers at terminal tips are GenBank accession numbers.

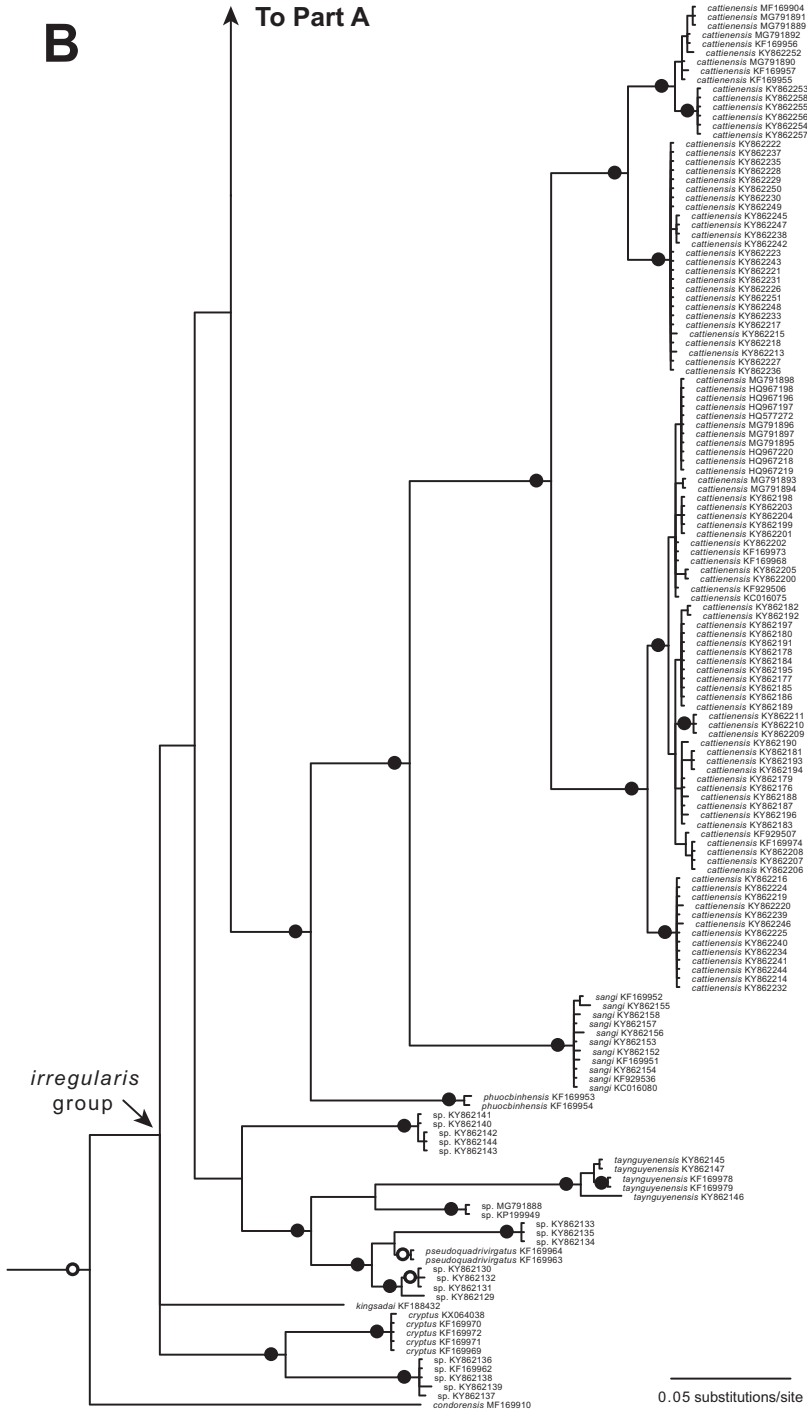
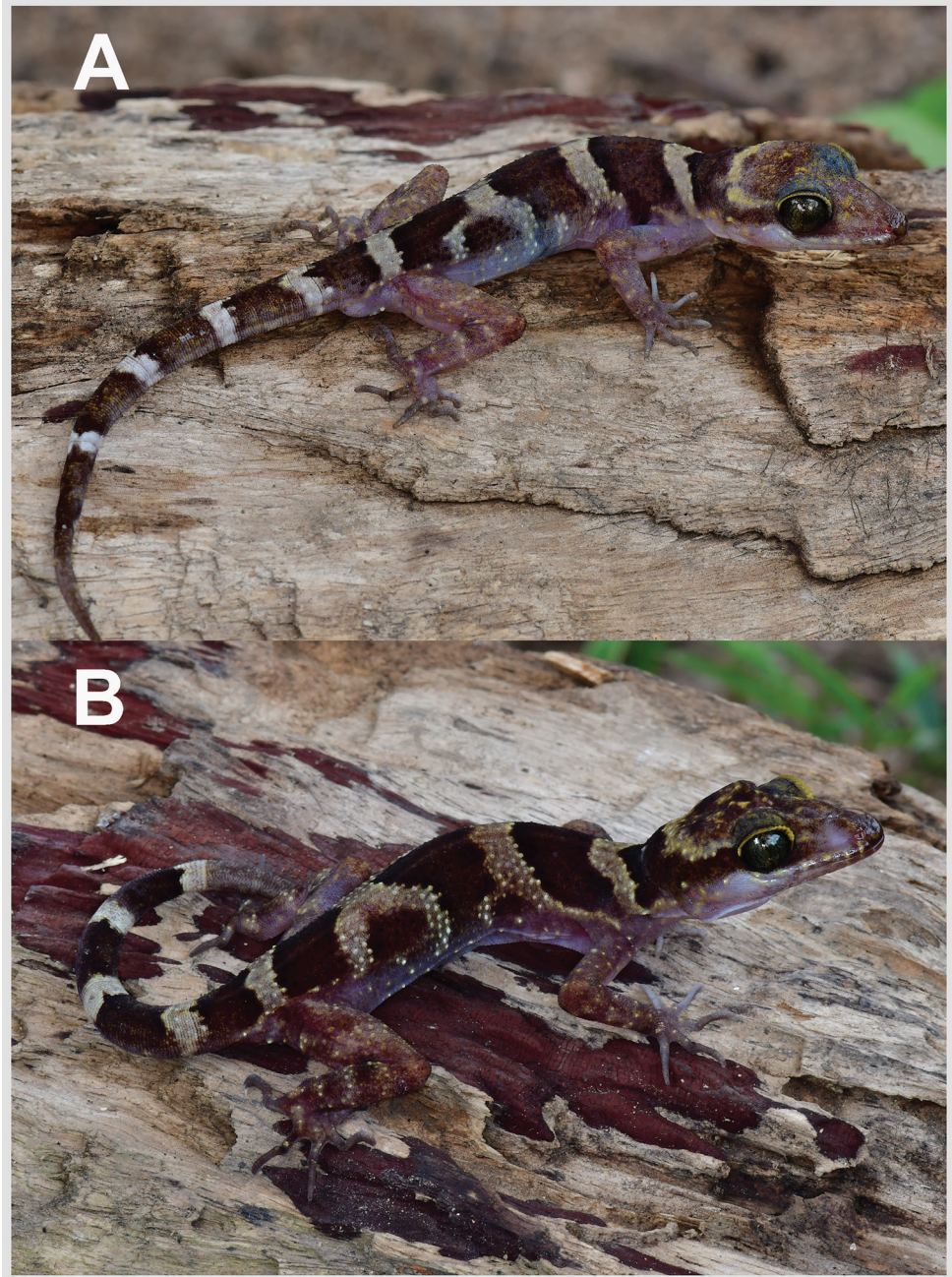


Figure 2. Continued.



**Figure 3.** *Cyrtodactylus phnomchiensis* sp. nov. in life. **A** Male holotype CBC 03012 and **B** female paratype CBC 03013.

**Etymology.** The specific epithet is taken from the type locality of Phnom Chi and the Latin suffix *-ensis* meaning “originating from.” The specific epithet is masculine in agreement with the gender of *Cyrtodactylus*.

**Diagnosis.** *Cyrtodactylus phnomchiensis* sp. nov. is distinguished from the 19 other named species in the *C. irregularis* group (Ngo and Chan 2010; Nguyen et al. 2013, 2017; Pauwels et al. 2018) by having the combination of SVL 76.1–80.7 mm; relatively long body, AG/SVL 0.451–0.481; relatively long tibia, CrusL/SVL 0.172–0.200; subdigital lamellae on fourth finger 18–20; subdigital lamellae on fourth toe 20–23; longitudinal dorsal rows of tubercles 18–20; paravertebral rows of tubercles 31–36; ventral scales 45–54; enlarged femoral scales 0–8, without pores; enlarged preloacal scales 7–10, bearing pores 4 or 5 in males, pits 1–7 in females; preloacal groove absent; median row of transverse subcaudal scales only slightly enlarged; posterior border of nuchal loop unbroken and pointed, bordered anteriorly and posteriorly by broad yellow or yellowish white band; dark brown body bands 3 or 4, the first intact, the second, third and fourth more irregular, alternating with two or three yellowish white or light brown body bands, about half the width of dark brown body bands; and yellow spots on top of head.

**Description of holotype.** Adult male with SVL 76.1 mm; head slightly elongate, HeadL 22.1 mm, about 30% of SVL, moderately widened, HeadW 14.1 mm, HeadW/HeadL 0.64, slightly depressed, HeadD 9.4 mm, HeadD/HeadL 0.43, distinct from neck, triangular in dorsal profile; snout rather elongated, rounded in rostral region, ESD 9.0 mm, slightly less than HeadD, ESD/HeadL 0.41, frontonasal region flattened, prefrontal region slightly concave, forming elongated medial rostral groove, canthus rostralis flattened, slightly angled between loreal region and rostral groove; lores posterior to nostrils depressed, anterior to orbit flattened; eye large, eyeball rounded, slightly protruding, EyeD 5.1 mm, shorter than the distance between eye and ear, Eye-EarD 5.7 mm, pupil vertical, covered by crenellate supraciliaries; ear opening oval, deeply sunk, rather small, elongated in oblique position, EarDV 1.2 mm, almost twice longer than its diameter in horizontal position, EarDH 0.7 mm; rostral large, subrectangular, height 1.9 mm, shorter than its width 3.6 mm, medially divided dorsally by a suture, reaching to about half way of rostral height, in contact with 1<sup>st</sup> SL and nostrils laterally, supranasals and internasal dorsally (Fig. 4); nostrils pieced at anterior angle of snout, directed lateroposteriorly, surrounded by rostral anteriorly, 1<sup>st</sup> SL ventrally, supranasals dorsally, and three small postnasal scales; internarial distance narrow, IND 2.9 mm; supranasals subrectangular, separated by intersupranasal, slightly smaller in size, in contact with rostral anteriorly, nostrils laterally, four small scales posteriorly; intersupranasal single, subpentagonal, slightly protruding rostral, in contact with two small scales posteriorly; interorbital rather narrow, IOD 5.5 mm, longer than EyeD, slightly shorter than Eye-EarD 5.7 mm; supralabials (12R, 13L), subrectangular anteriorly, circular shape posteriorly, anterior SL separated from small scales on loreal region by row of slightly enlarged scales; infralabials (9R, 9L), larger than SL, first InL bordered by mental anteriorly, first postmental ventrally, second InL bordered by second enlarged postmental, enlarged chin shield scale ventrally, 3–7<sup>th</sup> InL bordered by a row of slightly enlarged chin shield scales ventrally; mental large, triangular, width 3.3 mm in width, 2.3 mm in length, in contact with first InL laterally, two pairs postmentals posteriorly; the first pair largest, subrectangular, in broad contact medially, second pair enlarged, half the size of the first pair, separated by four smaller gular scales medially, in contact with smaller scales posteriorly (Fig. 4). Scales on frontonasal, prefrontal, loreal

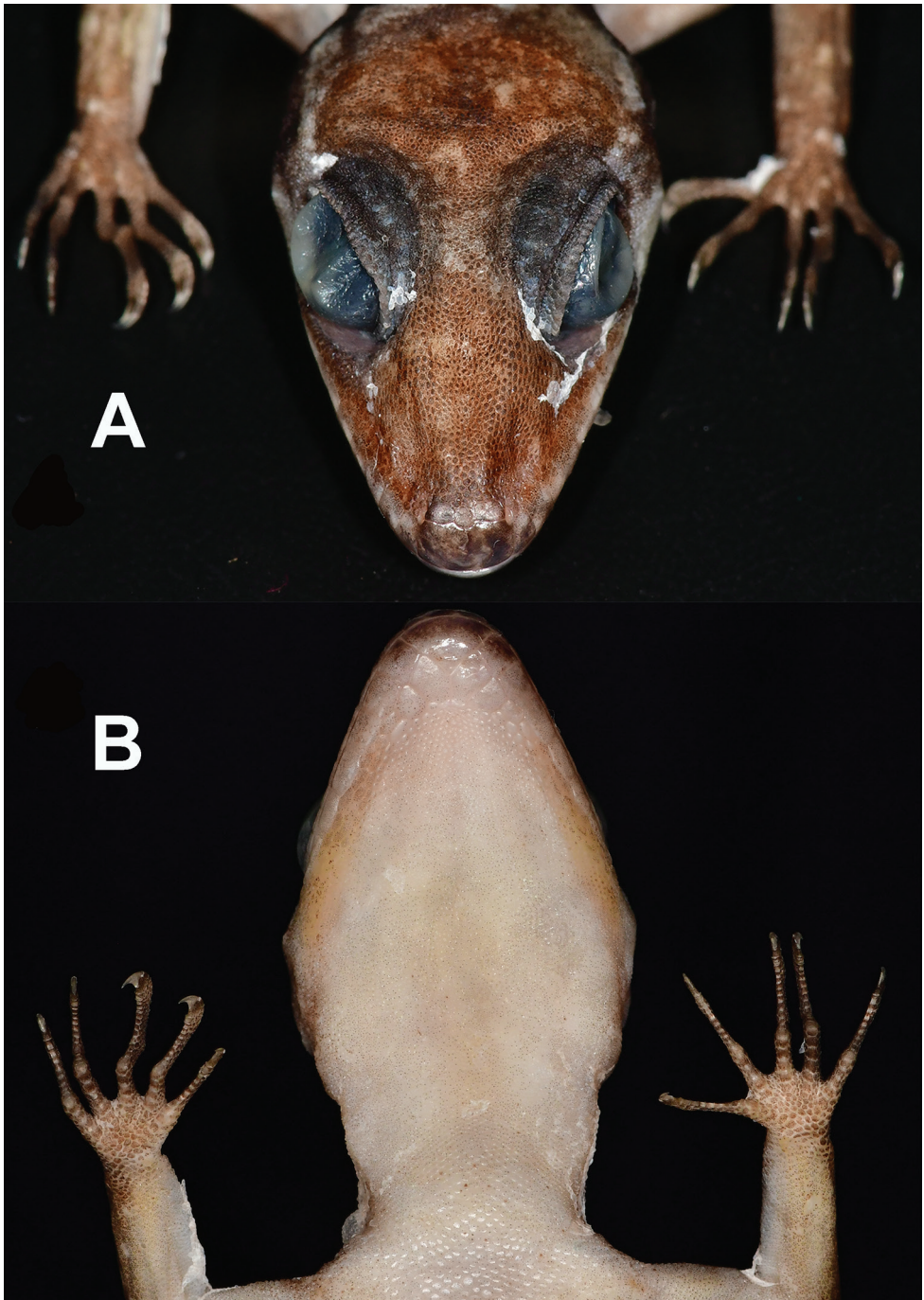


**Figure 4.** Head of male holotype CBC 03012 of *Cyrtodactylus phnomchiensis* sp. nov. in preservative. **A** Dorsal view illustrating the rostral, supranasal and internasalsupranasal scales **B** ventral view illustrating the mental and postmental scales.

regions small, almost homogenous, slightly larger than those on top of head; scales on occiput intermixed with scattered larger, more rounded, conical tubercles, more prominent tubercles on region between orbit and area above ear opening, a noticeably larger tubercle (compared to those surrounding) at the corner of jaw.

Body slightly slender, AG 36.6 mm, nearly half SVL, AG/SVL 0.481 with well-defined narrow vertebral furrow posteriorly; scales on dorsum small, mostly homogenous, granular, interspersed with larger, low, weakly keeled, irregularly arranged, tubercles; longitudinal dorsal rows of enlarged tubercles approximately 18; paravertebral tubercles 32; tubercles on nape within dark brown nuchal loop, anterior dorsal surface at level above shoulder smaller, more rounded, sparser than those on mid-dorsum and posterior dorsal surface, more prominent, being denser, weakly keeled, more regularly arranged on sacral and tail base region; tubercles on lateral body sparsely; ventral scales small, not imbricate, those near midline larger than lateral and dorsal scales; scales on throat and gular region the smallest; faint ventrolateral folds with few emerged tubercles; ventral scales at midbody between ventrolateral folds 47; preloacal region moderately enlarged, a few rows of enlarged preloacal non-pore bearing scales anterior to pore bearing preloacal scales; enlarged preloacal scales 7, in angular series, bearing 5 pores, terminal scale on each side poreless; post preloacal scale rows 3, the first row immediately posterior to enlarged preloacal pore-bearing scales with six scales in angular series, the second row with four scales in angular series, the third row with three scale in straight line, the medial scale largest; femoral scales slightly enlarged (8R, 8L), distal scales more than twice the size of proximal scales, all smaller than those of pore-bearing preloacal scales, separated from preloacal scales by diastema; preloacal groove absent; fully everted hemipenes thick, 5.9 mm in length, two penes at each sheath, two sockets posterior to hemipenal bases (Fig. 5).

Limbs rather slender; digits with strongly inflected interphalangeal joints; forelimbs bearing five relatively slender fingers, moderately bowed, ending with curved claws, ForeL/SVL 0.162; expanded proximal subdigital lamellae on fourth finger 6, unmodified distal subdigital lamellae on fourth finger 12, total subdigital lamellae on fourth finger 18; hind limbs bearing five relatively slender toes, strongly bent, ending with curved claws, CrusL/SVL 0.176; expanded proximal subdigital lamellae on fourth toe 7, unmodified distal subdigital lamellae on fourth toe 15, total subdigital lamellae on fourth toe 22; all digits lacking scansorial setae on ventral surface; scales on limbs small, interspersed with larger, low, conical, weakly keeled tubercles; scales on palmar and plantar surfaces small.

Tail moderately wide anteriorly, TaW 5.5 mm, segmented, cylindrical, becoming slender toward tip, regenerated posteriorly; dorsal caudal longitudinal tubercle rows at base of tail 8; 2 transverse rows of dorsal caudal tubercles at posterior margin of third band on tail, 22.7 mm from tail base; vertebral caudal surface with scattered bump at approximate intervals of 3 mm; subcaudal scale rows smooth, small, differing in size and irregular in shape, usually alternating between a single slightly enlarged and two smaller scales, 2 or 3 times larger than neighboring lateral caudal scales (Fig. 5).



**Figure 5.** Cloacal region of male holotype CBC 03012 of *Cyrtodactylus phnomchiensis* sp. nov. in preservative illustrating the enlarged precloacal scales, enlarged femoral scales, and not enlarged subcaudal scales.

**Color of holotype in life** (Fig. 3). Dorsal surface, nape, and tail yellowish white to light brown; top of head with yellowish spots; interorbital region, rostral and loreal regions lighter brown with scattered yellowish scales; eye ring yellowish; rostral, mental lighter brown; supralabials, corner of jaw, and region extending through dorsal margin of ear opening to shoulder yellowish; nuchal loop with large dark brown band, pointed, extending between posterior margins of eyes, bordered anteriorly by broad yellow band

along upper edge of dark brown nuchal loop, posteriorly by yellowish white band; three dorsal dark brown bands on body, the first more regular, the second and third bands irregular, interrupted by white irregular blotches; all dark brown bands ending near to mid-flank region, bordered below by lighter brown extending to lateral folds; dark brown body bands bordered by yellowish white or light brown bands about half the width of dark brown body bands, the last light brown band ending on tail base; anterior and posterior margins of body bands with darker brown coloration; dark brown bands 6 on regenerated tail, margins at tail base darker; white bands on tail 5, nearly encircling the tail except subcaudal scale row; subcaudal scales lighter brown than dorsal caudal scales; limbs lighter brown with orangish or yellowish on enlarged tubercles; ventral surfaces between ventrolateral folds, chin, throat, and limbs white with tiny black dots on tip of scales; ventral surfaces of fingers and toes dark brown. In preservative, all yellowish, yellowish white or orange coloration faded to white, cream, or light brown (Fig. 6).

**Variations.** Morphometric and meristic characters of the type series are presented in Table 1. The paratypes generally resemble the holotype (Fig. 6), except as follows. CBC 03003 has four enlarged post preloacal scale rows in an angular series, the last row with only a single enlarged scale. CBC 03004 and CBC 03014 have darker brown body bands. CBC 03003–03004 have a more pointed nuchal loop. CBC 03003 has more dense dark dots causing ventral surfaces to be darker brown. CBC 03003 has more slender, fully everted hemipenes. Females have enlarged preloacal scales with pits rather than pores.

**Distribution and natural history.** The new species is known only from the type locality at Phnom Chi in Prey Lang Wildlife Sanctuary, Kampong Thom Province, Sandan District, Cambodia. All individuals were found at night between 2001–2147 hr in evergreen-large dipterocarp dominated forest associated with rocky terrain (Fig. 7). The holotype CBC 03012 was found on a rock face following evening rain, paratypes CBC 03013–14 were on boulders following evening rain, paratype CBC 03003 was on leaf litter along a forest trail, and paratype CBC 03004 was on a rock wall at the entrance to a cave. Only five individuals were found during five-survey nights, suggesting the species is relatively uncommon. None were encountered during a brief survey by NT in the wet season of 2014 (Hayes et al. 2015). The new species is the only member of the *C. irregularis* complex known to occur west of the Mekong River (Nguyen et al. 2017; Pauwels et al. 2018).

**Comparisons.** *Cyrtodactylus phnomchiensis* sp. nov. is distinguishable from all 19 other members of the *C. irregularis* group by a unique combination of morphological characters (and in mitochondrial DNA; Fig. 2).

*Cyrtodactylus phnomchiensis* sp. nov. differs from *C. bidoupimontis* Nazarov, Poyarkov, Orlov, Phung, Nguyen, Hoang & Ziegler, 2012 by having ventral scales 45–54 (vs. 38–43 in *bidoupimontis*), preloacal pits in females 1–7 (vs. absent in *bidoupimontis*), dark brown body bands larger than yellowish white or light brown dorsal bands (vs. dark brown bands, when present, narrower than light yellow dorsal bands in *bidoupimontis*), and distinct large yellow band on anterior margin of dark brown nuchal loop (vs. narrow light margin in *bidoupimontis*), and yellow spots on top of head (vs. dark spots in *bidoupimontis*).

**Table 1.** Mensural, meristic and color pattern characters of *Cyrtodactylus phnomchiensis* sp. nov. Abbreviations defined in the text. All specimens have regenerated portions of tails (\*).

Voucher specimen	CBC 03012	CBC 03003	CBC 03004	CBC 03013	CBC 03014	Range
Type status	Holotype	Paratype	Paratype	Paratype	Paratype	
Sex	Male	Male	Female	Female	Female	
SVL	76.1	79.0	77.3	80.7	76.7	76.1–80.7
TaL*	75.1	56.9	66.6	79.1	64.6	56.9–79.1
TaW	5.5	4.4	5.3	5.6	5.7	4.4–5.7
TaW/SVL	0.072	0.056	0.069	0.069	0.074	0.056–0.74
ForeL	12.3	13.2	12.1	13.7	11.7	11.7–13.7
ForeL/SVL	0.162	0.167	0.157	0.170	0.153	0.153–0.170
CrusL	13.4	14.9	13.8	16.1	13.2	14.2–16.6
Crus/SVL	0.176	0.189	0.179	0.200	0.172	0.172–0.200
AG	36.6	36.1	35.3	36.4	35.4	35.3–36.6
AG/SVL	0.481	0.457	0.457	0.451	0.462	0.451–0.481
HeadL	22.1	23.5	22.2	23.6	23.4	22.1–23.6
HeadL/SVL	0.290	0.297	0.287	0.292	0.305	0.287–0.305
HeadW	14.1	14.5	13.7	15.2	13.7	13.7–15.2
HeadD	9.4	9.2	8.6	9.8	8.6	8.6–9.8
EyeD (eye diameter)	5.1	5.1	4.8	4.8	4.5	4.5–5.1
EyeD/SVL	0.067	0.065	0.062	0.059	0.059	0.059–0.067
Ear-EyeD (eye-ear distance)	5.7	6.1	6.0	6.5	5.7	5.7–6.5
ESD (eye-snout distance)	9.0	9.5	9.0	9.9	9.3	9.0–9.9
ESD/SVL	0.118	0.120	0.116	0.123	0.121	0.116–0.123
END (eye-nostril distance)	6.6	6.9	6.4	7.0	7.0	6.4–7.0
IO (interorbital distance)	5.5	4.8	5.0	5.7	5.2	4.8–5.7
IND (internarial distance)	2.9	2.8	2.6	2.9	2.7	2.6–2.9
EarDV (vertical)	1.2	1.3	1.2	1.3	1.3	1.2–1.3
EarDH (horizontal)	0.7	1.1	0.7	0.7	0.7	0.6–1.1
Intersupranasal scales	1	1	1	1	1	1
Supralabials (SL)	12R/13L	11R/11L	11R/11L	12R/12L	12R/13L	11–13
Infralabials (InL)	9R/9L	10R/9L	10R/10L	10R/9L	10R/10L	8–10
PVT	32	31	36	34	32	31–36
LDRT	18	20	20	20	19	18–20
VS	47	47	52	45	54	45–54
Median subcaudal scales slightly enlarged	yes	yes	yes	yes	yes	yes
SDLF4	18	20	18	19	19	18–20
SDLT4	22	23	20	21	21	20–23
EFS	8R8L	3R/3L	0	7R/6L	0	0–8
FP	0	0	0	0	0	0
EPrecS	7	9	7	10	9	7–10
PrecP	5	4	4	1	7	1–7
PrecG	0	0	0	0	0	0
PostPSR	3	4	3	3	3	3–4
PostSP	4	3	4	4	3	3–4
Number of dark brown body bands	3	3	4	3	3	3–4
Femoral and preloacal scales continuous	no	no	no	no	no	no
Yellowish spots on top of head	yes	yes	yes	yes	yes	yes

Voucher specimen	CBC 03012	CBC 03003	CBC 03004	CBC 03013	CBC 03014	Range
Posterior border of nuchal loop pointed	yes	yes	yes	yes	yes	yes
First body band complete	yes	yes	yes	yes	yes	yes
Second to fourth body bands more irregular	yes	yes	yes	yes	yes	yes
Yellowish white or light brown bands about half the width of dark brown body bands	yes	yes	yes	yes	yes	yes
Number of yellowish white or light brown body bands	2	2	3	2	2	2–3
Yellowish spot above ear opening	yes	yes	yes	yes	yes	yes
Enlarged tubercle at corner of jaw	yes	Yes	yes	yes	yes	yes

*Cyrtodactylus phnomchiensis* sp. nov. differs from *C. buchardi* by having SVL 76.1–80.7 mm (vs. 60–65 mm in *buchardi*), SDLF4 18–20 (vs. 14 in *buchardi*), SDLT4 20–23 (vs. 12–14 in *buchardi*), ventral scales 45–54 (vs. 30 in *buchardi*), LDRT 18–20 (vs. 25 in *buchardi*), preloacal pores in males 4–5 (vs. 9 in *buchardi*), and irregular dorsal body bands (vs. blotches in *buchardi*).

*Cyrtodactylus phnomchiensis* sp. nov. differs from *C. bugiamapensis* Nazarov, Poyarkov, Orlov, Phung, Nguyen, Hoang & Ziegler, 2012 by having LDRT 18–20 (vs. 20–24 in *bugiamapensis*), ventral scales 45–54 (vs. 36–46 in *bugiamapensis*), preloacal pores in males 4–5 (vs. 7–11 in *bugiamapensis*), SDLF4 18–20 (vs. 15–17 in *bugiamapensis*), SDLT4 20–23 (vs. 17–20 in *bugiamapensis*), CrusL/SVL in adult specimens 0.172–0.200 (vs. 0.144–0.157 in *bugiamapensis*), large nuchal loop bordered anteriorly and posteriorly by broad yellow bands (vs. narrow nuchal loop bordered by distinct narrow white lines in *bugiamapensis*), dark brown body bands 3–4 (vs. seven highly irregular dark blotches with light margins in *bugiamapensis*), and top of head with yellowish spots (vs. distinct dark brown spots in *bugiamapensis*).

*Cyrtodactylus phnomchiensis* sp. nov. differs from *C. caovansungi* Orlov, Nguyen, Nazarov, Ananjeva & Nguyen, 2007 by having SVL 76.1–80.7 mm (vs. 90.4–94.0 mm in *caovansungi*), ventral scales 45–54 (vs. 38–44 in *caovansungi*), femoral pores absent (vs. 6 in *caovansungi*), preloacal pores in males 4–5 (vs. 9 in *caovansungi*), SDLF4 18–20 (vs. 22 in *caovansungi*), and enlarged subcaudals absent (vs. present in *caovansungi*).

*Cyrtodactylus phnomchiensis* sp. nov. differs from *C. cattienensis* Geissler, Nazarov, Orlov, Böhme, Phung, Nguyen & Ziegler, 2009 by having SVL 76.1–80.7 mm (vs. 69.0 mm maximum in *cattienensis*), ventral scales 45–54 (vs. 28–42 in *cattienensis*), SDLF4 18–20 (vs. 12–16 in *cattienensis*), and SDLT4 20–23 (vs. 14–19 in *cattienensis*).

*Cyrtodactylus phnomchiensis* sp. nov. differs from *C. cucdongensis* Schneider, Phung, Le, Nguyen & Ziegler, 2014 by having SVL 76.1–80.7 mm (vs. 55.8–65.9 mm in *cucdongensis*), ventral scales 45–54 (vs. 35–44 in *cucdongensis*), SDLF4 18–20 (vs. 13–18 in *cucdongensis*), and SDLT4 20–23 (vs. 15–20 in *cucdongensis*).



**Figure 6.** Dorsal view of the type series of *Cyrtodactylus phnomchiensis* sp. nov. in preservative.

*Cyrtodactylus phnomchiensis* sp. nov. differs from *C. cryptus* Heidrich, Rösler, Vu, Böhme & Ziegler, 2007 by having precloacal pores in males 4–5 (vs. 9–11 in *cryptus*), and precloacal pits in females 1–7 (vs. absent in *cryptus*).

*Cyrtodactylus phnomchiensis* sp. nov. differs from *C. dati* Ngo, 2013 by having SVL 76.1–80.7 mm (vs. 70.1 mm maximum in *dati*), regenerated TaL 56.9–79.1 mm vs. (vs. 50.3 mm maximum, non-regenerated TaL in *dati*), femoral pores in both sexes absent (vs. present in *dati*), nuchal loop continuous (vs. broken in *dati*), and dark brown body bands (vs. irregular dark brown blotches on body in *dati*).

*Cyrtodactylus phnomchiensis* sp. nov. differs from *C. gialaiensis* Luu, Dung, Nguyen, Le & Ziegler, 2017 by having SVL 76.1–80.7 mm (vs. 62.8 mm maximum in *gialaiensis*), precloacal pores in males 4–5 (vs. 9–10 in *gialaiensis*), SDLF4 18–20 (vs. 14–15 in *gialaiensis*), and SDLT4 20–23 (vs. 15–17 in *gialaiensis*).

*Cyrtodactylus phnomchiensis* sp. nov. differs from *C. huynhi* Ngo & Bauer, 2008 by having SDLF4 18–20 (vs. 14–17 in *huynhi*), AGL/SVL 0.451–0.481 (vs. 0.370–0.428 in *huynhi*), ventral scales 45–54 (vs. 43–46 in *huynhi*), precloacal pores in males 4–5 (vs. 7–9 in *huynhi*), dark brown body bands 3–4 (vs. 5–6 in *huynhi*); femoral pores in both sexes absent (vs. 3–8 in *huynhi*), and nuchal loop bordered anteriorly and posteriorly by broad yellow bands (vs. narrow cream margin in *huynhi*).

*Cyrtodactylus phnomchiensis* sp. nov. differs from *C. irregularis* by lacking enlarged triangular tubercles at base of tail (vs. present in *irregularis*), CrusL/SVL 0.172–0.200 (vs. 0.138–0.156 in *irregularis*), LDRT 18–20 (vs. 22–24 in *irregularis*), paravertebral tubercles 31–36 (vs. 38–48 in *irregularis*); ventral scales 45–54 (vs. 38–45 in *irregularis*), SDLF4 18–20 (vs. 15–16 in *irregularis*), SDLT4 20–23 (vs. 18–20 in *irregularis*), dark brown body bands 3–4 (vs. 5–7, mostly as irregular blotches in *irregularis*), and yellowish spots on top of head (vs. distinct dark brown spots in *irregularis*).

*Cyrtodactylus phnomchiensis* sp. nov. differs from *C. kingsadai* Ziegler, Phung, Le & Nguyen, 2013 by having SVL 76.1–80.7 mm (vs. 83.0–94.0 mm in *kingsadai*), enlarged femoral scales 0–8 (vs. 9–12 in *kingsadai*), precloacal pore in males 4–5 (vs. 7–9 in *kingsadai*), and subcaudal scales not enlarged (vs. enlarged in *kingsadai*).

*Cyrtodactylus phnomchiensis* sp. nov. differs from *C. phuocbinhensis* Nguyen, Le, Tran, Orlov, Lathrop, MacCulloch, Le, Jin, Nguyen, Nguyen, Hoang, Che, Murphy & Zhang, 2013 by having SVL 76.1–80.7 mm (vs. 46.0–60.4 in *phuocbinhensis*); precloacal pits in females 1–7 (vs. absent in *phuocbinhensis*), top of head with yellow spots (vs. dark brown spots in *phuocbinhensis*), and dark brown body bands (vs. two dark brown longitudinal stripes or blotches in *phuocbinhensis*).

*Cyrtodactylus phnomchiensis* sp. nov. differs from *C. pseudoquadrivirgatus* Rösler, Vu, Nguyen, Ngo & Ziegler, 2008 by having yellow spots on top of head (vs. dark blotches on top of head in *pseudoquadrivirgatus*) and dark brown body bands (vs. highly irregular body blotches in *pseudoquadrivirgatus*).

*Cyrtodactylus phnomchiensis* sp. nov. differs from *C. sangi* Pauwels, Nazarov, Bobrov & Poyarkov, 2018 by having SVL 76.1–80.7 mm (vs. 56.3 mm maximum in *sangi*), paravertebral tubercles 31–36 (vs. 27–29 in *sangi*), ventral scales 45–54 (vs. 37 in *sangi*), precloacal pores in males 4–5 (vs. 7 in *sangi*), and first dark brown body band complete, second, third, and fourth more irregular (vs. highly irregular bands in *sangi*).



**Figure 7.** Habitat at Phnom Chi, the type locality of *Cyrtodactylus phnomchiensis* sp. nov.

*Cyrtodactylus phnomchiensis* sp. nov. differs from *C. takouensis* Ngo & Bauer, 2008 by having LDRT 18–20 (vs. 9–10 smooth tubercles in *takouensis*); ventral scales 45–54 (vs. 39–40 in *takouensis*), SDLF4 18–20 (vs. 16–17 in *takouensis*), SDLT4 20–23 (vs. 18–20 in *takouensis*), and dark brown canthal stripe absent (vs. present in *takouensis*).

*Cyrtodactylus phnomchiensis* sp. nov. differs from *C. taynguyenensis* Nguyen, Le, Tran, Orlov, Lathrop, MacCulloch, Le, Jin, Nguyen, Nguyen, Hoang, Che, Murphy & Zhang, 2013 by having supralabials 11–13 (vs. 8–9 in *taynguyenensis*), precloacal pits in females present (vs. absent in *taynguyenensis*), SDLF 18–20 (vs. 13–18 in *taynguyenensis*), top of head with yellow spots (vs. dark brown blotches in *taynguyenensis*), and dark brown body bands (vs. black irregular blotches margined by light brown in *taynguyenensis*).

*Cyrtodactylus phnomchiensis* sp. nov. differs from *C. yangbayensis* Ngo & Chan, 2010 by having SDLT4 20–23 (vs. 15–17 in *yangbayensis*) and lacking enlarged subcaudal scales (vs. present in *yangbayensis*).

*Cyrtodactylus phnomchiensis* sp. nov. is most closely related in mitochondrial DNA to *C. zieglerei* Nazarov, Orlov, Nguyen & Ho, 2008 (Fig. 2), but differs in morphology from *C. zieglerei* by having SVL 76.1–80.7 mm (vs. 84.6–93.0 mm in *zieglerei*), paravertebral tubercles 31–36 (vs. 38–46 in *zieglerei*), ventral scales 45–54 (vs. 33–45 in *zieglerei*), HeadL/SVL 0.287–0.305 (vs. 0.263–0.284 in *zieglerei*), ESD/SVL 0.116–0.123 (vs. 0.103–0.113 in *zieglerei*), CrusL/SVL 0.172–0.200 (vs. 0.140–0.168 in *zieglerei*), AG/SVL 0.451–0.481 (vs. 0.390–0.444 in *zieglerei*), eyeD/SVL 0.059–0.067 (vs. 0.053–0.057 in *zieglerei*), top of head with yellow spots (vs. dark brown spots in

*ziegleri*), large dark brown nuchal loop (vs. narrow in *ziegleri*), distinct, broad yellow band on anterior margin of dark brown nuchal loop (vs. absent in *ziegleri*), and dark brown body bands bordered by yellowish white or light brown bands about half the width of dark brown bands (vs. light yellow or light brown body bands about same width as dark brown body bands in *ziegleri*).

## Discussion

Mitochondrial DNA serves as a useful but imperfect tool for delimiting species within the *C. irregularis* complex (Nguyen et al. 2017; Pauwels et al. 2018). Two divergent mitochondrial lineages occur within *C. ziegleri*, with both lineages found at its type locality of Chu Yang Sin National Park, Dak Lak Province, and one lineage at Nam Nung Nature Reserve, Dak Nong Province, central Vietnam (Figs 1, 2; Nguyen et al. 2013, 2017; Ziegler et al. 2013; Schneider et al. 2014; Pauwels et al. 2018). Thus, from a matrilineal perspective, some individuals of *C. ziegleri* at Chu Yang Sin are more closely related to those at Nam Nung than to other individuals at Chu Yang Sin. Likewise, two divergent mitochondrial lineages occur within *C. cattienensis* (Fig. 2; Nazarov et al. 2012; Nguyen et al. 2013, 2014, 2017; Schneider et al. 2014; Pauwels et al. 2018), and both lineages of *C. cattienensis* can be found in sympatry at Ta Kou Mountain, Binh Thuan Province, southern Vietnam (Nguyen et al. 2017). The mitochondrial divergences within *C. ziegleri* and *C. cattienensis* are uncorroborated by divergences in morphology (or in one or two nuclear markers; Nguyen et al. 2017; Pauwels et al. 2018), and therefore these each continue to each be treated as single species that harbor considerable intraspecific mitochondrial DNA variation (Nguyen et al. 2017; Pauwels et al. 2018). The processes that resulted in the formation of these divergent mitochondrial lineages within *C. ziegleri* and *C. cattienensis* are unknown, but might be a consequence of a period of past separation of populations by geological or climatic events, the subsequent accumulation of mutations in the mitochondrial genome during isolation, and eventually recontact of these separated populations that today exhibit homogeneous morphology but persistent, divergent mitochondrial genomes (i.e., ancestral polymorphism). Similarly, Nguyen et al. (2017) preferred an explanation of allopatric divergence and subsequent migration into sympatry, rather than sympatric divergence, to explain the co-occurrence of the two mitochondrial lineages of *C. cattienensis* at Ta Kou Mountain. Importantly for this study, the divergent and unique mitochondrial lineage of *C. phnomchiensis* sp. nov. is corroborated by a divergence in morphology from *C. ziegleri* and all other members of the *C. irregularis* complex, and so we posit that *C. phnomchiensis* sp. nov. should be recognized as a distinct species.

Unfortunately, our phylogenetic analysis of the COI gene does not resolve the relationships among *C. phnomchiensis* sp. nov. and the two subclades of *C. ziegleri* (subclades Z1 and Z2; Fig. 2). This means that the resulting polytomy renders *C. ziegleri* as non-monophyletic in our analysis (Fig. 2). This polytomy could be a consequence of a near-simultaneous divergence among these three lineages (i.e., short internodes), but

is more likely to be a result of insufficient molecular data (Brennan et al. 2017). Unfortunately, most members of the *C. irregularis* complex have been represented by mitochondrial DNA in previous studies only with <700 bp of the COI gene (Brennan et al. 2017), and hence we were limited in our analyses by available comparative sequence data. Additional sequence data for members of this complex are needed. Specifically, additional mitochondrial data may resolve the polytomy found here among the two subclades of *C. ziegleri* and *C. phnomchiensis* sp. nov., and additional nuclear data can be used to test species boundaries that have been hypothesized from morphological and mitochondrial data (one or two nuclear markers have provided some, but limited, phylogenetic utility; Nguyen et al. 2017; Pauwels et al. 2018).

Phnom Chi consists of an isolated small rocky mountain (peak of 652 m elevation) and a few associated smaller hills, altogether encompassing an area of approximately 4,464 ha within the Prey Lang Wildlife Sanctuary in Kampong Thom and Kratie provinces, Cambodia. The base and lower elevations of Phnom Chi have dry and mixed deciduous forest, whereas upper elevations have large dipterocarp-dominated evergreen and semi-evergreen forest. The current habitat remains in relatively good condition, but this long-overlooked site needs urgent conservation attention. Local communities utilize Phnom Chi for resource extraction, notably the tapping of liquid resin from large dipterocarp trees on the mountain, and small-scale, illegal gold extraction around the base, in addition to forest burning during the dry season (possibly by resin tappers). A small pagoda at the base of the mountain and the scenic beauty of the area (Fig. 7) attracts local and domestic tourists, and will likely attract international tourists in the near future. A second species of lizard, the scincid *Sphenomorphus preylangensis* Grismer, Wood, Quah, Anuar, Poyarkov, Neang, Orlov, Thammachoti & Hun, 2019, was also recently described from Phnom Chi. Phnom Chi is the only feature with any significant topographic relief in Prey Lang Wildlife Sanctuary, other than some isolated limestone karst blocks in the northern section that have not yielded *Cyrtodactylus* during field surveys (TN, unpublished data). As such, *C. phnomchiensis* sp. nov. may be endemic to the immediate vicinity of Phnom Chi, and together with *S. preylangensis*, underscores the importance of the area for biodiversity conservation. Due to having a small area of occupancy, being relatively uncommon, and experiencing ongoing conservation threats, an assessment of *C. phnomchiensis* sp. nov. by the IUCN Red List of Threatened Species (IUCN 2020) is urgently warranted.

Species diversity of *Cyrtodactylus* in Cambodia is likely to be significantly underestimated. Recently, five species were described within the *C. intermedius* complex from the Cardamom Mountains of southwestern Cambodia (Murdoch et al. 2019), and an additional undescribed species in this complex has been reported from northern Cambodia near the Thai border (Geissler et al. 2019). The species diversity of the *C. irregularis* complex in Cambodia is even less known. Stuart et al. (2006) and Nazarov et al. (2008, 2012) referred to unstudied specimens in the *C. irregularis* complex from Mondolkiri and Ratanakiri Provinces in hilly eastern Cambodia, and those from Ratanakiri Province were later referred by Stuart et al. (2010) to *C. pseudoquadrivirgatus*. The rapid rate of taxonomic partitioning within the *C. irregularis* complex during

the past decade, underscored by the realization that many of these newly-recognized species have very narrow geographic ranges, suggests that re-evaluation of the species identities of the Mondolkiri and Ratanakiri specimens is needed.

## Acknowledgments

Wild Earth Allies is grateful to the General Department of Administration for Nature Conservation and Protection, Ministry of Environment of Cambodia, for providing permission to conduct research in Prey Lang Wildlife Sanctuary. Rangers of the Environmental Department of Kampong Thom Province, En E (Research Officer, Wild Earth Allies), and community members living at the foot of Phnom Chi assisted with field work. Field work was implemented with funding support from Wild Earth Allies. Sereivathana Tuy (Cambodia Director, Wild Earth Allies) provided technical support to the project. Hannah E. Som assisted with sequencing DNA and preparing figures. Thomas Ziegler and two anonymous reviewers improved the manuscript.

## References

- Brennan IG, Bauer AM, Ngo TV, Wang YY, Wang WZ, Zhang YP, Murphy RW (2017) Barcoding utility in a mega-diverse, cross-continental genus: keeping pace with *Cyrtodactylus* geckos. *Scientific Reports* 7: 5592. <https://doi.org/10.1038/s41598-017-05261-9>
- David P, Teynie A, Ohler A (2004) A new species of *Cyrtodactylus* Gray 1827 (Reptilia: Squamata: Gekkonidae) from southern Laos. *The Raffles Bulletin of Zoology* 52: 621–627.
- Geissler P, Nazarov R, Orlov NL, Böhme W, Phung TM, Nguyen TQ, Ziegler T (2009) A new species of the *Cyrtodactylus irregularis* complex (Squamata: Gekkonidae) from southern Vietnam. *Zootaxa* 2161: 20–32. <https://doi.org/10.11646/zootaxa.2161.1.2>
- Geissler P, Hartmann T, Ihlow F, Neang T, Seng R, Wagner P, Böhme W (2019) Herpetofauna of the Phnom Kulen National Park, northern Cambodia – An annotated checklist. *Cambodian Journal of Natural History* 2019(1): 40–63.
- Grismer LL, Wood Jr PL, Thura MK, Zin T, Quah ESH, Murdoch ML, Grismer MS, Aung Lin, Kyaw H, Lwin N (2017) Twelve new species of *Cyrtodactylus* Gray (Squamata: Gekkonidae) from isolated limestone habitats in east-central and southern Myanmar demonstrate high localized diversity and unprecedented microendemism. *Zoological Journal of the Linnean Society* 182(4): 862–959. <https://doi.org/10.1093/zoolinnean/zlx057>
- Grismer LL, Wood Jr PL, Quah ESH, Anuar S, Poyarkov NA, Neang T, Orlov NL, Tham-machoti P, Hun S (2019) Integrative taxonomy of the Asian skinks *Sphenomorphus stellatus* (Boulenger, 1900) and *S. praesignis* (Boulenger, 1900) with the resurrection of *S. annamiticus* (Boettger, 1901) and the description of a new species from Cambodia. *Zootaxa* 4683(3): 381–411. <https://doi.org/10.11646/zootaxa.4683.3.4>
- Hayes B, Eang HK, Neang T, Furey N, Chhin S, Holden J, Hun S, Phen S, La P, Simpson V (2015) Biodiversity assessment of Prey Lang: Kratie, Kampong Thom, Stung Treng

- and Preah Vihear Provinces. Conservation International, Winrock International, USAID, Phnom Penh, Cambodia, 124 pp.
- Heidrich A, Rösler H, Vu TN, Böhme W, Ziegler T (2007) Another new *Cyrtodactylus* (Squamata: Gekkonidae) from Phong Nha-Ke Bang National Park, central Truong Son, Vietnam. *Zootaxa* 1445(1): 35–48. <https://doi.org/10.11646/zootaxa.1445.1.3>
- IUCN (2020) The IUCN Red List of Threatened Species. Version 2019-3. <https://www.iucn-redlist.org>
- Ivanova NV, Dewaard JR, Hebert PDN (2006) An inexpensive, automation-friendly protocol for recovering high-quality DNA. *Molecular Ecology Notes* 6: 998–1002. <https://doi.org/10.1111/j.1471-8286.2006.01428.x>
- Lanfear R, Frandsen PB, Wright AM, Senfeld T, Calcott B (2017) PartitionFinder 2: new methods for selecting partitioned models of evolution for molecular and morphological phylogenetic analyses. *Molecular Biology and Evolution* 34(3): 772–773. <https://doi.org/10.1093/molbev/msw260>
- Luu VQ, Bonkowski M, Nguyen TQ, Le MD, Schneider N, Ngo HT, Ziegler T (2016) Evolution in karst massifs: cryptic diversity among bent-toed geckos along the Truong Son Range with descriptions of three new species and one new country record from Laos. *Zootaxa* 4107(2): 101–140. <https://doi.org/10.11646/zootaxa.4107.2.1>
- Luu VQ, Dung TV, Nguyen TQ, Le MD, Ziegler T (2017) A new species of the *Cyrtodactylus irregularis* complex (Squamata: Gekkonidae) from Gia Lai Province, Central Highlands of Vietnam. *Zootaxa* 4362(3): 385–404. <https://doi.org/10.11646/zootaxa.4362.3.4>
- Miller MA, Pfeiffer W, Schwartz T (2010) Creating the CIPRES Science Gateway for inference of large phylogenetic trees. *Proceedings of the Gateway Computing Environments Workshop (GCE)*: 1–8. <https://doi.org/10.1109/GCE.2010.5676129>
- Murdoch ML, Grismer LL, Wood Jr PL, Neang T, Poyarkov NA, Ngo TV, Nazarov RA, Aowphol A, Pauwels OSG, Nguyen HN, Grismer JL (2019) Six new species of the *Cyrtodactylus intermedius* complex (Squamata: Gekkonidae) from the Cardamom Mountains and associated highlands of Southeast Asia. *Zootaxa* 4554(1): 1–62. <https://doi.org/10.11646/zootaxa.4554.1.1>
- Nazarov RA, Orlov NL, Nguyen SN, Ho CT (2008) Taxonomy of naked-toes geckos *Cyrtodactylus irregularis* complex of South Vietnam and description of a new species from Chu Yang Sin Natural Park (Krong Bong District, Dac Lac Province, Vietnam). *Russian Journal of Herpetology* 15(2): 141–156.
- Nazarov R, Poyarkov NA, Orlov NL, Phung TM, Nguyen TT, Hoang DM, Ziegler T (2012) Two new cryptic species of the *Cyrtodactylus irregularis* complex (Squamata: Gekkonidae) from southern Vietnam. *Zootaxa* 3302(1): 1–24. <https://doi.org/10.11646/zootaxa.3302.1.1>
- Ngo TV (2013) *Cyrtodactylus dati*, a new forest dwelling Bent-toed Gecko (Squamata: Gekkonidae) from southern Vietnam. *Zootaxa* 3616(2): 151–164. <https://doi.org/10.11646/zootaxa.3616.2.4>
- Ngo TV, Bauer AM (2008) Descriptions of two new species of *Cyrtodactylus* Gray 1827 (Squamata: Gekkonidae) endemic to southern Vietnam. *Zootaxa* 1715(1): 27–42. <https://doi.org/10.11646/zootaxa.1715.1.2>

- Ngo TV, Chan OK (2010) A new species of *Cyrtodactylus* Gray, 1826 (Squamata: Gekkonidae) from Khanh Hoa Province, southern Vietnam. *Zootaxa* 2504(1): 47–60. <https://doi.org/10.11646/zootaxa.2504.1.4>
- Nguyen SN, Le TT, Tran TAD, Orlov NL, Lathrop A, MacCulloch RD, Le TT, Jin J, Nguyen LT, Nguyen TT, Hoang DD, Che J, Murphy RW, Zhang Y (2013) Phylogeny of the *Cyrtodactylus irregularis* species complex (Squamata: Gekkonidae) from Vietnam with the description of two new species. *Zootaxa* 3737(4): 399–414. <https://doi.org/10.11646/zootaxa.3737.4.4>
- Nguyen SN, Yang J, Le TT, Nguyen LT, Orlov NL, Hoang CV, Nguyen TQ, Jin J, Rao D, Hoang TN, Che J, Murphy RW, Zhang YP (2014) DNA barcoding of Vietnamese bent-toed geckos (Squamata: Gekkonidae: *Cyrtodactylus*) and the descriptions of a new species. *Zootaxa* 3784(1): 48–66. <https://doi.org/10.11646/zootaxa.3784.1.2>
- Nguyen SN, Zhou WW, Le TT, Tran TA, Jin J, Vo BD, Nguyen LT, Nguyen TT, Nguyen TQ, Hoang DD, Orlov NL, Che J, Murphy RW, Zhang YP (2017) Cytonuclear discordance, cryptic diversity, complex histories, and conservation needs in Vietnamese bent-toed geckos of the *Cyrtodactylus irregularis* species complex. *Russian Journal of Herpetology* 24(2): 133–154. <https://doi.org/10.30906/1026-2296-2019-24-2-133-154>
- Orlov NL, Nguyen TQ, Nazarov RA, Ananjeva NB, Nguyen SN (2007) A new species of the genus *Cyrtodactylus* Gray, 1827 and redescription of *Cyrtodactylus paradoxus* (Darevsky et Szczerbak, 1997) [Squamata: Sauria: Gekkonidae] from South Vietnam. *Russian Journal of Herpetology* 14(2): 145–152.
- Pauwels OSG, Nazarov RA, Bobrov VV, Poyarkov NA (2018) Taxonomic status of two populations of Bent-toed Geckos of the *Cyrtodactylus irregularis* complex (Squamata: Gekkonidae) with description of a new species from Nui Chua National Park, southern Vietnam. *Zootaxa* 4403(2): 307–335. <https://doi.org/10.11646/zootaxa.4403.2.5>
- Rambaut A, Drummond AJ, Xie D, Baele G, Suchard MA (2018) Posterior summarization in Bayesian phylogenetics using Tracer 1.7. *Systematic Biology* 67: 901–904. <https://doi.org/10.1093/sysbio/syy032>
- Ronquist F, Teslenko M, Van der Mark P, Ayres DL, Darling A, Höhna S, Larget B, Liu L, Suchard MA, Huelsenbeck JP (2012) MrBayes 3.2: efficient Bayesian phylogenetic inference and model choice across a large model space. *Systematic Biology* 61: 1–4. <https://doi.org/10.1093/sysbio/sys029>
- Rösler H, Vu TN, Nguyen TQ, Ngo TV, Ziegler T (2008) A new *Cyrtodactylus* (Squamata: Gekkonidae) from central Vietnam. *Hamadryad* 33(1): 48–63.
- Schneider N, Phung TM, Le MD, Nguyen TQ, Ziegler T (2014) A new *Cyrtodactylus* (Squamata: Gekkonidae) from Khanh Hoa Province, southern Vietnam. *Zootaxa* 3785(4): 518–532. <https://doi.org/10.11646/zootaxa.3785.4.2>
- Smith MA (1921) New or little-known reptiles and batrachians from southern Annam (Indo-China). *Proceedings of the Zoological Society of London* 1921: 423–440. <https://doi.org/10.1111/j.1096-3642.1921.tb03271.x>
- Stuart BL, Rowley JJJ, Neang T, Emmett DA, Som S (2010) Significant new records of amphibians and reptiles from Virachey National Park, northeastern Cambodia. *Cambodian Journal of Natural History* 2010(1): 38–47.

- Stuart BL, Sok K, Neang T (2006) A collection of amphibians and reptiles from hilly eastern Cambodia. *The Raffles Bulletin of Zoology* 54(1): 129–155.
- Swofford DL (2003) PAUP\*: Phylogenetic Analysis Using Parsimony \*(and Other Methods). Sinauer Associates, Sunderland, Massachusetts, USA.
- Teynie A, David P (2010) Voyages naturalists au Laos. Les reptiles. Revoir Editions, Chamalières, France, 315 pp.
- Uetz P (2020) The Reptile Database. <http://www.reptile-database.org> [Last accessed 13 February 2020]
- Ziegler T, Phung TM, Le MD, Nguyen TQ (2013) A new *Cyrtodactylus* (Squamata: Gekkonidae) from Phu Yen Province, southern Vietnam. *Zootaxa* 3686(4): 432–446. <https://doi.org/10.11646/zootaxa.3686.4.2>